Shining a Light on Copper Mediated Living Radical Polymerisation: Maximising End-group Fidelity

Athina Anastasaki

A thesis submitted in partial fulfilment of the requirements of the degree of
Doctor of Philosophy in Chemistry

Department of Chemistry

University of Warwick

July 2014

Table of Contents

Chapter 2: The Importance of Ligand Reactions in Cu(0)-mediated Living Radical Polymerisation of Acrylates

Chapter 3: Polymerisation of Long Chain Acrylates by Cu(0)-mediated Living Radical Polymerisation; High Fidelity End-group Incorporation and Modification

Chapter 4: High Molecular Weight Block Copolymers by Sequential Monomer Addition *via* Cu(0)-Mediated Living Radical Polymerisation (SET-LRP): An Optimised Approach

Chapter 5: Copper(II)/tertiary Amine Synergy in Photo-induced Living Radical Polymerisation; Accelerated Synthesis of ω-functional and α,ω-heterofunctional poly(acrylates)

Chapter 6: Expanding the Scope of the Photo-induced Living Radical Polymerisation of Acrylates in the Presence of $CuBr_2$ and Me_6-Tren

Chapter 7: Photo-induced Sequence-control *via* One Pot Living Radical Polymerisation of Acrylates

Chapter 8

List of Figures

List of Tables

List of Schemes

Abbreviations

AA	Acrylic acid
AIBN	Azobisisobutyronitrile
AN	Acrylonitrile
ARGET	Activators regenerated by electron transfer
ATRP	Atom transfer radical polymerisation
***n*BA**	Butyl acrylate
Bipy	2,2'-Bipyridyl
BiXANDLE	9,9´-bixanthene-9,9´-diol
BzMA	Benzyl methacrylate
CD	Compact disc
$CDCl_3$	Deuterated chloroform
CLRP	Controlled living radical polymerisation
CRP	Controlled radical polymerisation
CTA	Chain transfer agent
DC	Dissociation/combination
DCT	Degenerative chain transfer
DCTB	*trans*-2-[3-(4-*tert*-Butylphenyl)-2-methyl-2-propenylidene]malononitrile
DEGEEA	Di(ethylene glycol) ethyl ether acrylate
DMAC	Dimethylacetamide
DMF	Dimethylformamide
DMSO	Dimethylsulphoxide
DNA	Deoxyribonucleic acid
DP	Degree of polymerisation
DRI	Differential refractive index
EA	Ethyl acrylate
EBiB	Ethyl-2-bromoisobutyrate
EBP	Ethyl-2-bromopropionate
EGA	Ethylene glycol methyl ether acrylate
ESI-MS	Electrospray ionisation mass spectroscopy
EtOH	Ethanol

FRP	Free radical polymerisation
SI-ATRP	Surface initiated atom transfer radical polymerisation
GA	Glycidyl acrylate
GTP	Group transfer polymerisation
HEA	Hydroxyethyl acrylate
HPA	Hydroxypropyl acrylate
HR-ESI-MS	High-resolution electrospray ionisation mass spectroscopy
I	Initiator
ICAR ATRP	Initiators for continuous activator regeneration atom transfer radical polymerisation
ICP-MS	Inductively coupled plasma mass spectroscopy
Iniferter	Initiator-transfer agent-terminator
iOA	Isooctyl acrylate
IPA	Isopropyl alcohol
ISET	Inner sphere electron transfer
K_I	Rate constant of initiation
K_P	Rate constant of propagation
K_T	Rate constant of termination
LA	Lauryl acrylate
LCST	Low critical solution temperature
LRP	Living radical polymerisation
LS	Light scattering
$[M]_0$	Concentration of monomer at t = 0
$[M]_t$	Concentration of monomer at t = t
M_w	Molecular weight
MA	Methyl acrylate
MALDI	Matrix assisted laser desorption ionisation
MEK	Methyl ethyl ketone
Me_6-Tren	*N,N,N',N',N'',N''*-Hexamethyl-[tris(aminoethyl)amine]
MeCN	Acetonitrile
MeOH	Methanol
MS	Mass spectroscopy
MMA	Methyl methacrylate

NMR	Nuclear magnetic resonance
NMP	Nitroxide mediated polymerisation
ODA	Octadecyl acrylate
OSET	Outer sphere electron transfer
PC	Polycarbonate
PCRP	Photo-induced controlled radical polymerisation
PEG	Poly(ethylene glycol)
$PEGA_{480}$	Poly(ethylene glycol) methyl ether acrylate
PET	Poly(ethylene terephthalate)
PHC	Principle of halogen conservation
PMDETA	*N,N,N',N'',N''*-pentamethyldiethylenetriamine
PMMA	Poly(methyl methacrylate)
PMR	Principle of microscopic reversibility
PRE	Persistent radical effect
PTFE	Poly(tetrafluoroehtylene)
PS	Poly(styrene)
PVC	Poly(vinyl chloride)
RA	Reducing agent
RAFT	Reversible addition fragmentation chain transfer
RDRP	Reversible deactivation radical polymerisation
SA	Solketal acrylate
SARA ATRP	Supplemental activator and reducing agent atom transfer radical polymerisation
SEC	Size exclusion chromatography
SET-DT	Single electron transfer degenerative chain transfer
SET-LRP	Single electron transfer living radical polymerisation
St	Styrene
SFRP	Stable free radical polymerisation
***t*BA**	tert-Butyl acrylate
TEA	Triethylamine
TEMPO	(2,2,6,6-Tetramethyl-piperidin-1-yl)oxyl
TFE	2,2,2 Trifluoroethanol
TFP	2,2,3,3 Tetrafluoro-1-propanol

TMM- LRP	Transition metal mediated living radical polymerisation
ToF	Time of flight
Tol	Toluene
TPMA	Tris(2-pyridylmethyl)amine
Tren	Tris(2-aminoethyl)amine
VS	Viscometry
UV	Ultraviolet

Acknowledgements

It is going to be very difficult to acknowledge everyone but I will do my best and I want to apologise for the length of my acknowledgements because I will not stop unless I thank every single person!

Firstly, I would like to thank Professor David Haddleton for giving me the opportunity to pursue my PhD studies under his supervision. When I initially joined the group my knowledge and experience were very limited, if any. His quote "I don't care from what level you start, I care about what you become" encouraged me and made me smile the difficult days. I remember in my first year report in order to complete the "transferable skills folder" we had to answer the following question "Describe the personality of your supervisor". My answer was "I see my supervisor as a mummy chicken. He protects his students with his massive wings at the beginning when they cannot be independent and then he sets them free, allow them to fly by themselves and take great pleasure to watch them developing and progress". I cannot thank him enough for what he has done for me. Allowing me to work in multiple projects, participate in various international conferences, introducing and "advertising" me to famous chemists, correcting papers with the speed of the disproportionation of Cu(I)Br in water (pure water!!!) but more importantly I thank him for being a good person and a good supervisor alongside being a great scientist.

Also, I would like to thank Professor Virgil Percec, for allowing me to join his group as a visiting scholar during my PhD studies. I will never forget his phrases "What is the revolution today?" or "Any revolutionary results yet?" and "Maybe you need one more cup of coffee to start thinking". I gained a lot of experience under his guidance and I also had the chance to meet his amazing group!!! Olivier Moussodia, Shaodong Zhang, Na Zhang, Cecilie Roche, Pawaret (Kla) Leowanawat, Hao-Jun Sun, and David (I cannot find

surname, sorry!) you all made my stay very enjoyable. Special thanks go to Shampa Samanta for being so kind, helpful and supportive throughout my stay in the University of Pensylvania. I wish you all the best!

My first year has been very challenging, there were so many scientific things I did not know (and there still plenty!), the language was not Greek (this unfortunately did not change) and computer science was definitely not my strength. But I managed to write a thesis, so hopefully I ticked all the boxes. Also, I can now understand the various British ascents (ok some of them) and follow almost every conversation (only exception is when Paul and Jamie are talking about rugby terms and they are using unknown vocabulary that deny to translate!!!). Two people helped me a lot during my first year. Jasmin Menzel had to answer to at least 100 computer questions per day (how do we copy and paste is a representative example so that you can understand the level of my questions) together with chemistry related questions that it would be too embarrassing if I mention them. I know that I frustrated her a lot, especially when I was asking the same thing for the third time in one day so I apologise for that and I thank her for her patience (99% of the times) and her understanding. More importantly, she was and still is a friend who made my first year a lot more enjoyable and I am very happy that she is happy now. Although Jasmin was lucky enough to escape from me as she graduated at the end of my first year, Paul Wilson was not as lucky because we shared an office for my entire PhD (I am sad that he had to change office now but it is not his fault, he is just getting promoted too often!). Paul is the most relaxed, knowledgeable and polite person I know. He never complained (loudly!) about my numerous daily questions although I know I have really pushed his limits. I cannot thank him enough. He is a source of continuous inspiration and support in our lab and he is IRREPLACEABLE. And now I can admit that everytime he was telling me that I need one more experiment or one more characterisation to finish something off he was always right

and I knew he was right. He has an open invitation to visit me in Greece with his future Mrs Wilson (or more people if the Wilson family becomes bigger, also during my PhD corrections Mrs Wilson is not “future” any more so congratulations!!!) whenever he wants.

During my last two years Vasiliki Nikolaou joined the Haddleton team and my productivity increased. Doing experiments by yourself is always enjoyable but it can be challenging, especially when things are not working the way they should. She is my lab partner and I think we did a very good job together spending endless time to discuss scientific things and less scientific things too!!!(Some colleagues still think we were always talking about science when during our Greek conversation we were also using key words like “NMR” or “polymerisation” to mislead curious people! Can anyone guess what single electron transfer stands for??). I will never forget that for the one year that we were doing the multiblocks she had to stay until 12 (midnight) every day and I had to do the next addition at 6 in the morning!!! We both don’t want to hear about multiblocks anymore. I thank her for her patience, for being so supportive with everything and for making every day in the lab/office almost like holidays. She is a good friend and one day I will find the courage to tell her the only big secret I have not shared with yet!!!

I would also like to thank George Pappas (as a colleague and as a flatmate) for the endless carbohydrated food we have consumed together (although he claims he prefers healthy food) and for being such a good, quiet and clean flatmate. Much appreciated. Also, he is my personal “problem solving” person, from killing dangerous bags of unknown identity to put movies on my labtop. I am really happy that he joined our group!

Gabit Nurumbetov was also very very very helpful the last couple of months as he joined my early morning timetable although he was fasting (no food/water from 4:30 am to 9:30 pm). I thank him for his patience and assistance with the bloody images (and more) of my thesis but more importantly I thank him for his friendship and company. He is probably

one of the best people I know and he has promised to bring me horse meat from Kazakstan next time. Alrighty then!!!

Many people believe that I was spending all my time in the university and so I did not really have a life. If a life is defined as drinking 30 beers per day then no, I did not have a life, at least not very often! But my definition of life is different. Having good friends to share your day, your fears, your worries and your dreams, doing a job that does not feel like a job (I still cannot believe that someone is paying me to do what I love), having a partner that you love and you don't compromise, watching football matches and cooking every day delicious (at least for me!) meals…This is my life. Going out, having fun, drinking…Yes I do all these things as well, just not as often! We all have our priorities!

Back to science, there many people that I collaborated with in the lab the past 3 years and they have all been wonderful. Special thanks also go to Chris Waldron (my partner in crime, we travelled the world together, from USA to Saudi Arabia and he sorted out everything for me), Qiang Zhang (he has always been for me the example of the most efficient scientist), Antony Grice (my English teacher, now I can tell that the pen is on the table and not in the table, also Ant come back our GPC miss you every day), Alex Simula (for the fact that he is French, thus special), Fehaid Alsubaie ("your face looks ok today"), Mat Jones, Stacy Slavin, Kay McEwan, Chris Summers, Georgina Rayner, James Burns, Jamie Godfrey, Nuttapol Risangud , Nikos Engelis, Daniel Lester, Jenny Collins, Sam Lowe, Danielle Lloyds, Muxiu Li, Zaidong Li, Chongyu Zhu, Olivier Bertrand, Guanzhao Li, Yanzi Goo, but also people from Sebastian Perrier group; Sophie Larnaudie (for helping me cook 9 pizzas without burning them), Johannes Brendel (for being always so German and for not celebrating properly(=Greek way) even the world cup), Tammie Barlow, Ming Liang Koh, Liam Martin (for passing me the ball so many times), Junliang

Zhang (for his excellent cooking abilities), Ximo or Joaquin Sanchis-Martinez (who is a professional tennis player but decided to hide it and also because although he is very Spanish he is a very good person and I enjoyed our conversations, scientific and less scientific!) and Guillame Gody (for his one million explanations on RAFT, multiblocks *etc*. and for sharing his love for science with me! I also wish him to be an academic because we need him. Guillame together with Paul are the best chemists I know!). I would also like to thank Dan Phillips (Gibson group) for the scientific discussions and for always being a smily person in our corridor.

I would also like to thank Ivan, Lijiang, Phil and Ed for their help with NMR and mass spec facilities. They all made my lab life a lot easier. Special thanks go to Jason Noone (our IT person) for always fixing my laptop, even when I thought it was really dead and for explaining to me how computers work in a nice simple way!!! I understood almost 70% from what he taught me!

Thanks also go to Kat, Zion, and Bella for accepting me in their house, for treating me like I was a real member of their family and for making me feel "normal" again. I apologise for my behaviour and wish you all the best!

Aleksis, Alexandros, Dimitra, Zetta, Victoras and Matina (yes they are all Greek names!), although being far away, they definitely made my free (?) time a lot more enjoyable and supported me when I needed support. Alex thanks for being next to me, I did not expect that we would keep talking but I am glad we did and you are very important to me, despite being superficial from times to times! At least we share our love for food and this is deep enough!! Also, I would like to thank Alex's parents and especially his mother, Matina, for treating me like I am part of their family, even when things changed!

I would also like to thank my parents for raising me and giving me the opportunity to get proper education. Although we had and still have many arguments they are and will

always my family. I also thank my brother Konstantinos, my grandmothers Rena and Athina (that's how I got my name) and my uncle Dimitris. Every time I go back to Greece, they all make me feel like I never left.

Last but not at least, I would like to thank my partner (and my best friend) for being always next to me even when this was not possible, and for loving me unconditionally. I think we will always be in each other's life no matter what. Actually I don't think, I know!

Finally, although many people were next to me, doing a PhD is a personal case and I realised quite fast that I am the most important person in my life and I need to learn to like me and deal with me all the time. I even managed to overcome my biggest fear, named "Steve Armes". When I was trying to choose the best academic for my PhD studies I did an interview with both Professor Armes and Professor Haddleton. However, Professor Armes seemed very strict and demanding and the project seemed too challenging for me. I thought I would not be able to perform well enough to satisfy him. He scared me a lot. But I never stopped thinking that I want one day to feel good enough (scientific wise) and make this fear disappear. This is why Steve Armes became my external examiner for my PhD viva. And I survived. I would like to thank him and Sebastien Perrier for allowing me to learn things even during this last step of my PhD and for making my viva feel like a friendly, scientific conversation. It is now time to face my next fear!

Below you can find a famous Greek poem and one of my favourites. The main meaning is that we should enjoy the journey while travelling towards our destination. If we dedicate our spirit and soul towards a goal then no fear can stop us. We usually put burdens on our way because we are afraid to dare and claim our dreams. I started my PhD feeling very scared, as chemistry has never been my strength. But it was what I liked the most. So I took the risk and I don't regret. Even if I don't become a good chemist, I will definitely be a happy chemist.

And of course I don't forget the academics back in the University of Athens that taught me so many things and are still doing research despite the unfavored conditions. My thesis is dedicated to them and to all young Greek people that although they are in the middle of the financial crises, they don't lose their courage and they keep smiling and fighting!

Σα βγεις στον πηγαιμό για την Ιθάκη,
να εύχεσαι νάναι μακρύς ο δρόμος,
γεμάτος περιπέτειες, γεμάτος γνώσεις.
Τους Λαιστρυγόνας και τους Κύκλωπας,
τον θυμωμένο Ποσειδώνα μη φοβάσαι,
τέτοια στον δρόμο σου ποτέ σου δεν θα βρεις,
αν μέν' η σκέψις σου υψηλή, αν εκλεκτή
συγκίνησις το πνεύμα και το σώμα σου αγγίζει.
Τους Λαιστρυγόνας και τους Κύκλωπας,
τον άγριο Ποσειδώνα δεν θα συναντήσεις,
αν δεν τους κουβανείς μες στην ψυχή σου,
αν η ψυχή σου δεν τους στήνει εμπρός σου.

Να εύχεσαι νάναι μακρύς ο δρόμος.
Πολλά τα καλοκαιρινά πρωιά να είναι
που με τι ευχαρίστησι, με τι χαρά
θα μπαίνεις σε λιμένας πρωτοειδωμένους·
να σταματήσεις σ' εμπορεία Φοινικικά,
και τες καλές πραγμάτειες ν' αποκτήσεις,
σεντέφια και κοράλλια, κεχριμπάρια κ' έβενους,
και ηδονικά μυρωδικά κάθε λογής,
όσο μπορείς πιο άφθονα ηδονικά μυρωδικά·
σε πόλεις Αιγυπτιακές πολλές να πας,
να μάθεις και να μάθεις απ' τους σπουδασμένους.

Πάντα στον νου σου νάχεις την Ιθάκη.
Το φθάσιμον εκεί είν' ο προορισμός σου.
Αλλά μη βιάζεις το ταξείδι διόλου.
Καλλίτερα χρόνια πολλά να διαρκέσει·
και γέρος πια ν' αράξεις στο νησί,
πλούσιος με όσα κέρδισες στον δρόμο,
μη προσδοκώντας πλούτη να σε δώσει η Ιθάκη.

Η Ιθάκη σ' έδωσε τ' ωραίο ταξείδι.
Χωρίς αυτήν δεν θάβγαινες στον δρόμο.
Άλλα δεν έχει να σε δώσει πια.
Κι αν πτωχική την βρεις, η Ιθάκη δεν σε γέλασε.
Έτσι σοφός που έγινες, με τόση πείρα,
ήδη θα το κατάλαβες η Ιθάκες τι σημαίνουν.

As you set out for Ithaka
hope the voyage is a long one,
full of adventure, full of discovery.
Laistrygonians and Cyclops,
angry Poseidon—don't be afraid of them, you'll never
find things like that on your way, as long as you keep
your thoughts raised high, as long as a rare
excitement stirs your spirit and your body.
Laistrygonians and Cyclops,
wild Poseidon—you won't encounter them
unless you bring them along inside your soul,
unless your soul sets them up in front of you.

Hope the voyage is a long one.
May there be many a summer morning when,
with what pleasure, what joy,
you come into harbors seen for the first time;
may you stop at Phoenician trading stations
to buy fine things,
mother of pearl and coral, amber and ebony,
sensual perfume of every kind—
as many sensual perfumes as you can;
and may you visit many Egyptian cities
to gather stores of knowledge from their scholars.

Keep Ithaka always in your mind.
Arriving there is what you are destined for.
But do not hurry the journey at all.
Better if it lasts for years,
so you are old by the time you reach the island,
wealthy with all you have gained on the way,
not expecting Ithaka to make you rich.

Ithaka gave you the marvelous journey.
Without her you would not have set out.
She has nothing left to give you now.
And if you find her poor, Ithaka won't have fooled
you. Wise as you will have become, so full of
experience, you will have understood by then what
these Ithakas mean.

Κ.Π Καβαφης/C.P Kavafy

Declaration

Experimental work contained in this thesis is original research carried out by the author, unless otherwise stated, in the Department of Chemistry at the University of Warwick, October 2011 and July 2014. No material contained herein has been submitted for any other degree, or at any other institution.

Results from other authors are referenced in the usual manner throughout the text.

Date:

_____

Athina Anastasaki

Abstract

The objective of this thesis was to investigate Cu(0)-mediated living radical polymerisation and explore the potential and the limitations of this system with the ultimate goal to maximise the end-group fidelity and enable the synthesis of multiblock copolymers. Careful optimisation of the ligand and catalyst concentration was shown to be vital for preservation of end-group functionality, which can be exploited for post-polymerisation modifications. High molecular weight multiblock copolymers were obtained for the first time, although the weaknesses and limitations of the technique were also revealed and discussed.

At the same time, a new, novel polymerisation protocol was discovered, exploiting photo-activation in the presence of a cupric precursor $Cu^{II}(Me_6\text{-Tren})Br_2$ and an excess of an aliphatic tertiary amine ligand Me_6-Tren. For the first time under UV irradiation (λ ~ 360 nm) near-quantitative conversions and narrow dispersities for a range of targeted molecular weights were achieved while the scope of this technique was expanded to a range solvents and monomers. Significantly, temporal control is also observed during intermittent light and dark reactions and excellent end-group fidelity can be attained. This remarkable degree of control obtained during both homo and block copolymerisations motivated further investigation into the scope of the system in pursuit of acrylic multiblock copolymers with good sequential control over discrete block compositions, synthesised *via* a photo-mediated approach in a one-pot process without intermediate purification steps and in the absence of potentially costly additives such as photo-redox catalysts, initiators and dye sensitisers.

Both techniques utilised the multiblock copolymer synthesis as a tool not only to synthesise functional well-controlled materials but more importantly to enable

polymerisations with high end-group fidelity, whereby termination has been significantly suppressed.

Chapter 1

Introduction; From Free Radical Polymerisation to Frontiers in Macromolecular Chemistry

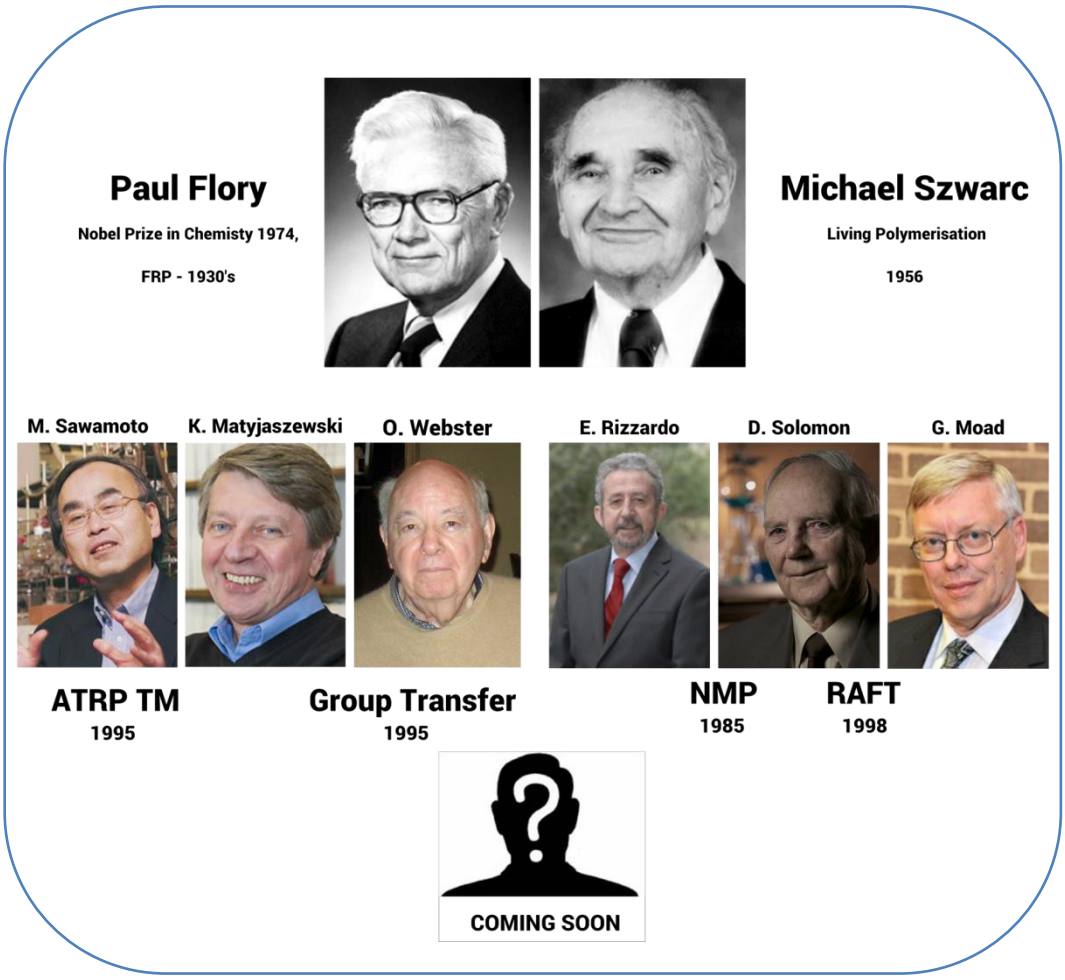

1.1 Where do you find Polymers?

The term "polymer" is derived (together with one million other words!) from the Greek and specifically from the words *πολύς* (*polys*, meaning "many, much") and *μέρος* (*meros*, meaning "part") and refers to a large molecule or macromolecule (another Greek word, *macro* means "long"), composed of many repeating units known as monomers (again Greek, *mono* means "one" and as mentioned *meros* means "part" so monomer means "one part").

There is often a general popular misconception that the word "polymer" is often used as a synonym for plastic; however the truth is that polymers are a large group of natural and synthetic materials, encompassing everything from shellac to Poly(Vinyl Chloride) (PVC). Plastics are simply one type of polymer. Natural polymers (biopolymers) include rubber and amber, while the range of synthetic polymers is wide and include materials such as nylons, silicones, bakelite, neoprene and polystyrene, *etc*. A plethora of synthetic polymers participate, and are indeed essential, in our everyday life and can be found in hundreds of different products.

Pantyhose and parachutes for example contain polyamides as the base material, commonly known as nylon (specifically Nylon 6.6). This is also the same type of polymer often used to make ropes, swimwear and boat sails. Non-stick cookware is made using polytetrafluoroethylene or PTFE. PTFE can resist temperatures of up to 260 ˚C which makes it ideal not only in the production of cooking products, but also as a cable insulator and sealant.

Despite their different look and feel, Styrofoam® cups, grocery store meat trays and disposable cutlery are all basically the same material. These items are all made from polystyrene, a plastic that is also used to make DVD cases, disposable razors and

refrigerator insulation. Probably the best known form of polystyrene is in foam. It's often seen as the base material for packing peanuts, Styrofoam® cups, takeout food containers, craft models and more.

Poly(ethylene terephthalate), or PET, is probably one of the best-known and one of the most widely used polymer in existence. From peanut butter jars to soft drink bottles to milk containers, PET can be found in pretty much any container in our refrigerator. This material is the most recyclable of all plastics, although not in the way that most people imagine. PET bottles collected for recycling never come back into the market as bottles. Instead, the bottles are separated according to color, then crushed and shredded. Subsequently, the pieces are melted and molded into other plastic products, which can include anything from toys to sleeping bag filler.

Figure 1.1: Polymers used in daily applications.

Polyurethanes are a quick-curing, highly elastic polymer used to make apparel that stretches. Spandex clothing fiber, like Lycra®, contains polyurethane linkages and is used in a number of clothing items, including bathing suits, exercise clothing, leggings, skinny jeans, socks and wetsuits. Even bra straps and disposable diapers are made using spandex containing polymers.

Polyolefins, also known as polyalkenes, are widely used in the construction industry. Everything from patio furniture, artificial grass and outdoor rugs to shower curtains and carpet backing contain polyolefin. Other common items that contain polyolefin include insulated socks, disposable hospital garments, rope and nets, woven sacks and bags, and once again disposable diapers.

Polycarbonate (PC) is a very versatile class of polymers. PC finds diverse application in computer cases, CDs, automotive and aircraft components, toys and riot shields. Polycarbonate has been used to make high-quality eyeglass lenses for years under the brand name Makrolon®. These lenses offer advantages over glass as they provide lighter and thinner materials with greater UV protection. They are also highly impact resistant, so you do not have to worry too much about cracks, however it is soft so it has poor resistance.

Most personal care and hair products also contain polymers. For example, polymers are used in hair conditioners to help flatten the hair strands and smooth out split ends. They're also added to shampoos as a thickener; without polymers, shampoos would be more like perfumed water than creamy soaps.

Finally, PVC is mostly known as the material used to make plumbing fittings and pipes, but has another function as well: It is used to make credit cards as PVC sheets can be strong while being thin. Thus to make a credit card, two or three layers are glued together. This includes a layer with the printed information on it, plus one or two clear

layers containing information. The same PVC material is used to make leather-like materials for clothing and shoes, as well as vinyl records, synthetic floor tiles and electrical wire insulation. Commercial signs and banners, like the ones at the storefront of a shop or restaurant, are also often made of PVC.

1.2 Free Radical Polymerisation

Many of the aforementioned polymers (*eg*. polystyrene) are made *via* free radical polymerisation, which consists of one of the most popular method of synthesising commercial polymers. Free radical polymerisation was first reported in the literature by Flory[1] in the 1930's. From an industrial stand-point, a major virtue of this type of polymerisation is that it can be carried out under relatively undemanding conditions and that it is tolerant towards impurities. High molecular weight polymers can be often produced without removal of the stabilisers present in commercial monomers, in the presence of trace amounts of oxygen, or in solvents that have not been rigorously dried or purified. Moreover, radical polymerisations are remarkable amongst chain polymerisation processes in that they can be conveniently conducted in many solvents, including aqueous media.

1.2.1 Sequence of events

Free radical polymerisation consists of three steps; initiation, propagation, and termination. The initiation step is considered to involve two reactions. The first is the production of free radicals by any one of a number of reactions. The usual case is the homolytic dissociation of an initiator species I to yield a pairs of radicals $R^{\cdot}$, where k_d is the rate constant for the initiator dissociation (Eq. 1.1).

The second part of initiation involves addition of one of these radicals to the first monomer molecule to produce a chain-initiating radical $M^{\cdot}$, where M represents a

monomer and k_i is the rate constant for the initiation step. The radical $R^{\cdot}$ is often referred to as an initiator radical or primary radical to distinguish it from the chain initiating species $M^{\cdot}$ (Eq. 1.2).

$$I \xrightarrow{k_d} 2R^{\bullet} \quad (1.1)$$

$$R^{\bullet} + M \xrightarrow{k_i} M^{\bullet} \quad (1.2)$$

$$M^{\bullet} + nM \xrightarrow{k_p} M_n^{\bullet} \quad (1.3)$$

Propagation consists of the growth of $M^{\cdot}$ by the successive addition of large numbers (hundreds and perhaps thousands) of monomer molecules. Each addition creates a new radical that has the same identity as the one previously, except that it is larger by one monomer unit. In general terms, this process can be described by Eq. 1.3, where k_p is the rate constant of propagation. Propagation with growth of the chain to high degrees of polymerisation takes place very rapidly. The value of k_p for most monomers is in the range 10^2-10^4 L mol^{-1} s^{-1}. Such rate constants are much higher than those usually encountered in step polymerisations[2].

At some point, the propagating polymer chain stops growing and terminates. Termination with the annihilation of the radical centers occurs by bimolecular reaction between radicals. Two radicals react with each other by combination (coupling) or, more rarely, by disproportionation, in which a hydrogen radical that is *beta* to one radical center is transferred to another radical center. This results in the formation of two polymer molecules - one saturated and one unsaturated (Eq. 1.4). Termination can also occur by both combination and disproportionation. The two different modes of termination can be represented by Eq. 1.4,

$$M_n^{\bullet} + M_m^{\bullet} \longrightarrow \underset{\text{Disproportionation}}{M_{n-1} = M_n} + \underset{\text{Combination}}{M_{m-1}M \text{ or } M_{n+m}} \quad (1.4)$$

where the particular mode of termination is not specified and $k_t = ak_{tc} + (1-a)k_{td,}$ where a and (1-a) are the fractions of termination by combination and disproportionation respectively. The propagation reaction would proceed indefinitely until the monomers in a reaction system were exhausted if it were not for the strong tendency towards termination. Typical termination rate constants are in the range of 10^6-10^8 L mol^{-1} s^{-1}, or an order of magnitude greater than the propagation rate constants. The much greater value of k_t compared to k_p does not prevent propagation, because the radical species are present in very low concentrations and also because the polymerisation rate is dependent on only the one-half power of k_t, as will be discussed in the next section.

1.2.2 Rate Expression/Kinetics

In order to obtain a kinetic expression for the rate of polymerisation, it is necessary to assume that k_p and k_t are independent of the size of the radical species. Small radicals are more reactive than propagating polymer radicals, but this effect is not important because the effect of the size vanishes at the dimer or trimer size.

Monomer disappears during initiation (Eq. 1.2), as well as *via* propagation (Eq. 1.3). The rate of monomer disappearance, which is synonymous with the rate of polymerisation, is given by Eq. 1.5, whereby R_i and R_p are the rates of initiation and propagation, respectively. However, the number of monomer molecules reacting in the initiation step is far less than the number consumed in the propagation step for a process producing high molecular weight polymer. To a very close approximation, the former can be neglected and the polymerisation rate is given simply by the rate of propagation (Eq. 1.6).

$$\frac{-d[\mathrm{M}]}{dt} = R_i + R_p \quad \textbf{(1.5)}$$

$$\frac{-d[\mathrm{M}]}{dt} = R_p \quad \textbf{(1.6)}$$

The rate of propagation and therefore the rate of polymerisation is the sum of many individual propagation steps.

Since the rate constants for all the propagation steps are the same, one can express the overall polymerisation rate by Eq. 1.7 and 1.8,

$$R_p = k_p[M^{\bullet}][M] \quad (1.7)$$

$$R_i = R_t = 2k_t[M^{\bullet}]^2 \quad (1.8)$$

where [M] is the monomer concentration and [M·] is the total concentration of all chain radicals, that is, all radicals of size M_1· and larger.

However, Eq. 1.7 is not directly usable as it contains a term for the concentration of radicals. The radical concentration is difficult to measure experimentally, since it is very low (~10^{-8} M), and is therefore desirable to eliminate [M·] from the equation. In order to do this, the steady-state assumption is invoked such that the concentration of radicals increases initially, but almost instantaneously reaches a constant, steady-state value. The rate of change of the concentration of radicals quickly becomes and remains zero during the majority of the polymerisation. This is equivalent to stating that the rates of initiation R_i and termination R_t of radicals are equal (Eq. 1.8). The right side of Eq. 1.8 represents the rate of termination. There is no specification as to whether termination is by combination or disproportionation, since both follow the same kinetic expression. The factor of 2 in the termination rate equation follows generally accepted convention for radicals been destroyed in pairs.

Rearrangement of Eq. 1.8 and substitution into Eq. 1.7 yields

$$[M^{\bullet}] = \left(\frac{R_i}{2k_t}\right)^{1/2} \quad (1.9)$$

$$R_p = k_p[M]\left(\frac{R_i}{2k_t}\right)^{1/2} \quad (1.10)$$

for the rate of polymerisation. Thus, Eq. 1.10 reveals the dependence of the polymerisation rate on the square root of the initiation rate.

The rate of producing radicals by thermal homolysis of an initiator R_d (Eq. 1.1) is given by Eq. 1.11, where [I] is the concentration of the initiator and *f* is the initiator efficiency. The initiator efficiency is defined as the fraction of the radicals produced in homolysis undergoing reactions that initiate polymer chains.

$$R_d = 2fk_d[I] \quad \textbf{(1.11)}$$

$$R_i = 2fk_d[I] \quad \textbf{(1.12)}$$

$$R_p = k_p[M]\left(\frac{fk_d[I]}{k_t}\right)^{1/2} \quad \textbf{(1.13)}$$

The initiation reaction is composed of two steps (Eq. 1.1 and 1.2). In most polymerisations the second step (the addition of the primary radical to monomer) is much faster than the first step. The homolysis of the initiator is the rate-determining step in the initiation sequence, and the rate of initiation is given by Eq 1.12 while substitution of Eq. 1.12 into Eq. 1.11 yields Eq. 1.13.

Although conventional free radical polymerisation, alongside Ziegler-Natta polymerisation[3], is still the most dominant polymerisation in the industrial field (due to its undemanding conditions and versatility) it also possess significant drawbacks. The most important disadvantage is its inability to regulate the molecular weight, the architecture and the topology of the resulting polymers.

1.3 Living Polymerisation

Living polymerisation was discovered by Szwarc[4-6] in 1956 when he reported the polymerisation of styrene *via* the use of anions in the presence of sodium naphthalene. The polymerisation was initiated by electron transfer to monomer and shown to be "*living*" as the chains generated kept growing by supplying the system with additional monomer.

Negligible termination or chain transfer was reported since the presence of the anions at both ends of the polymer chains eliminates bimolecular termination. However, in order to achieve such a highly living system, rigorously purified reagents are required which makes this process more difficult to commercialise. This led to the development of living radical polymerisation.

1.4 Living Radical Polymerisation

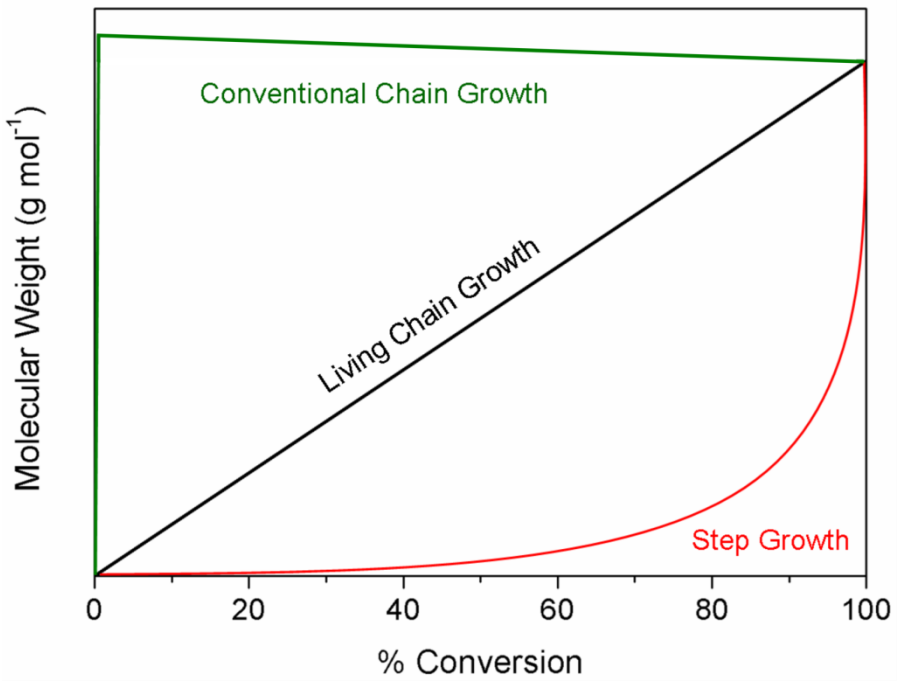

Figure 1.2: The evolution of molecular weight with increasing conversion for step and chain growth polymers.

Living radical polymerisation closely mimics anionic polymerisation but with less limitations based on reagent purity. For a long time, control of molecular architecture in a radical polymerisation was considered impossible at a similar level to that achieved for living ionic systems as two radicals would always terminate in a very fast, diffusion-controlled reaction[7, 8]. Although controlled living radical polymerisation (CLRP) cannot be realised in the purist's sense, when the concept of dynamic equilibrium was introduced to radical polymerisation[9-11], it revolutionised the field and gave access to polymers with precisely controlled molecular weight, relatively narrow dispersities and high end-group

functionality. Mediating species were introduced into the system that could reversibly deactivate/cap the propagating macroradicals, allowing all chains to grow at the same rate until all the monomer is consumed. Bimolecular termination still occurs in a radical polymerisation (although carefully optimised conditions may suppress it to minimal levels). However, the term "living" was still chosen as the system meets most of the experimental criteria for a living polymerisation as presented by Quirk and Lee[12].

1.4.1 Nitroxide Mediated Polymerisation

Various stable radicals such as (arylazo)oxy[13], substituted triphenyls[14], verdazyl[15], triazonilyn[16] and nitroxides[17] have been employed as the mediator or persistent radical (deactivator) for Stable Free Radical Polymerisation (SFRP). Nitroxides are generally more efficient than others and have been extensively studied. SFRP with nitroxides is called Nitroxide Mediated Polymerisation (NMP). NMP was patented by Solomon and Rizzardo in 1985[18] and is carried out by two methods that parallel those used in ATRP[19-21], which was developed a decade later. One method involves the thermal decomposition of an alkoxyamine such as 2,2,6,6-tetramethyl-1-(1-phenylethoxy)piperidine into a reactive radical and a stable radical (Scheme 1.1). The other method involves a mixture of a conventional radical initiator such as AIBN or benzoyl peroxide and the nitroxide radical. Nitroxide radicals are sufficiently stable (due to steric hindrance) that they can be stored at ambient temperature without decomposition and some are available for purchase from chemical vendors.

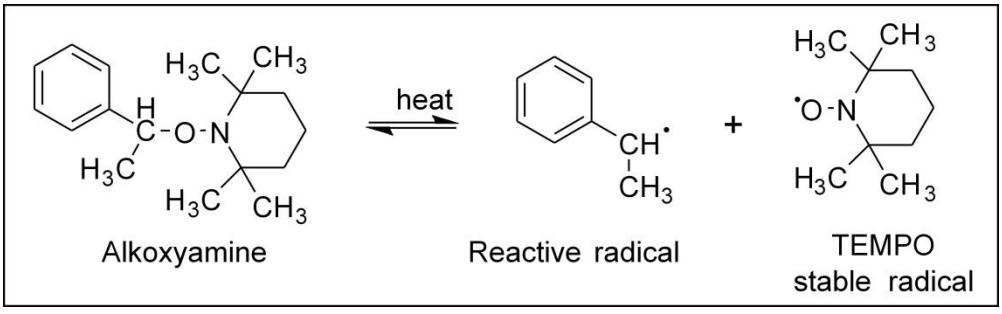

Scheme 1.1: TEMPO and reactive radical generation.

The reactive radical initiates polymerisation, while the stable radical mediates the reaction by reacting with propagating radicals to lower their effective concentration. The nitroxide radical, although unreactive with itself, reacts rapidly with the propagating radical to reduce the concentration of propagating radicals sufficiently such that conventional bimolecular termination is negligible. The propagating radical concentration is much lower than that of the dormant species, resulting in living radical polymerisation with control of target molecular weight and final dispersities.

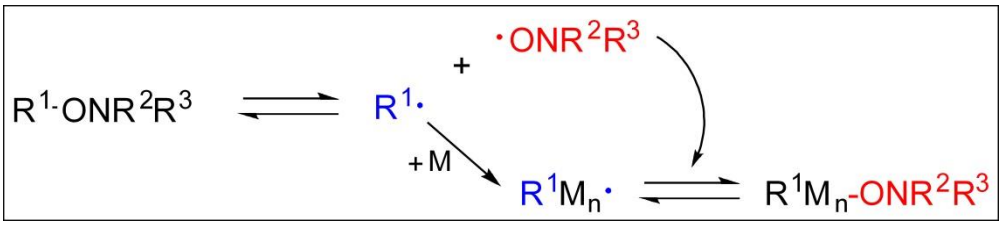

Scheme 1.2: Simplified mechanism for NMP.

However, only styrene and 4-vinylpyridine polymerisations proceeded with good control and the reaction times are reported to be quite long (1-3 days). Some improvements by using sterically hindered alicyclic nitroxides with a hydrogen on one of the α-carbons have led to faster polymerisation rates and extended NMP to other monomers (acrylates, acrylamides *etc.*). However, due to β-hydrogen abstraction by nitroxide, NMP has not been yet successfully extended to methacrylates[21], although some initial attempts have recently been performed[22].

1.4.2 Reversible Addition-Fragmentation Chain Transfer Polymerisation

Reversible Addition-Fragmentation chain transfer (RAFT) polymerisation was first reported in 1998[23] by Chiefari *et al.* who discovered that dithio-compounds could be used as very efficient chain transfer agents (CTA), ensuring a rapid exchange between the dormant and the living chains. The mechanism[24] is outlined in Scheme 1.3.

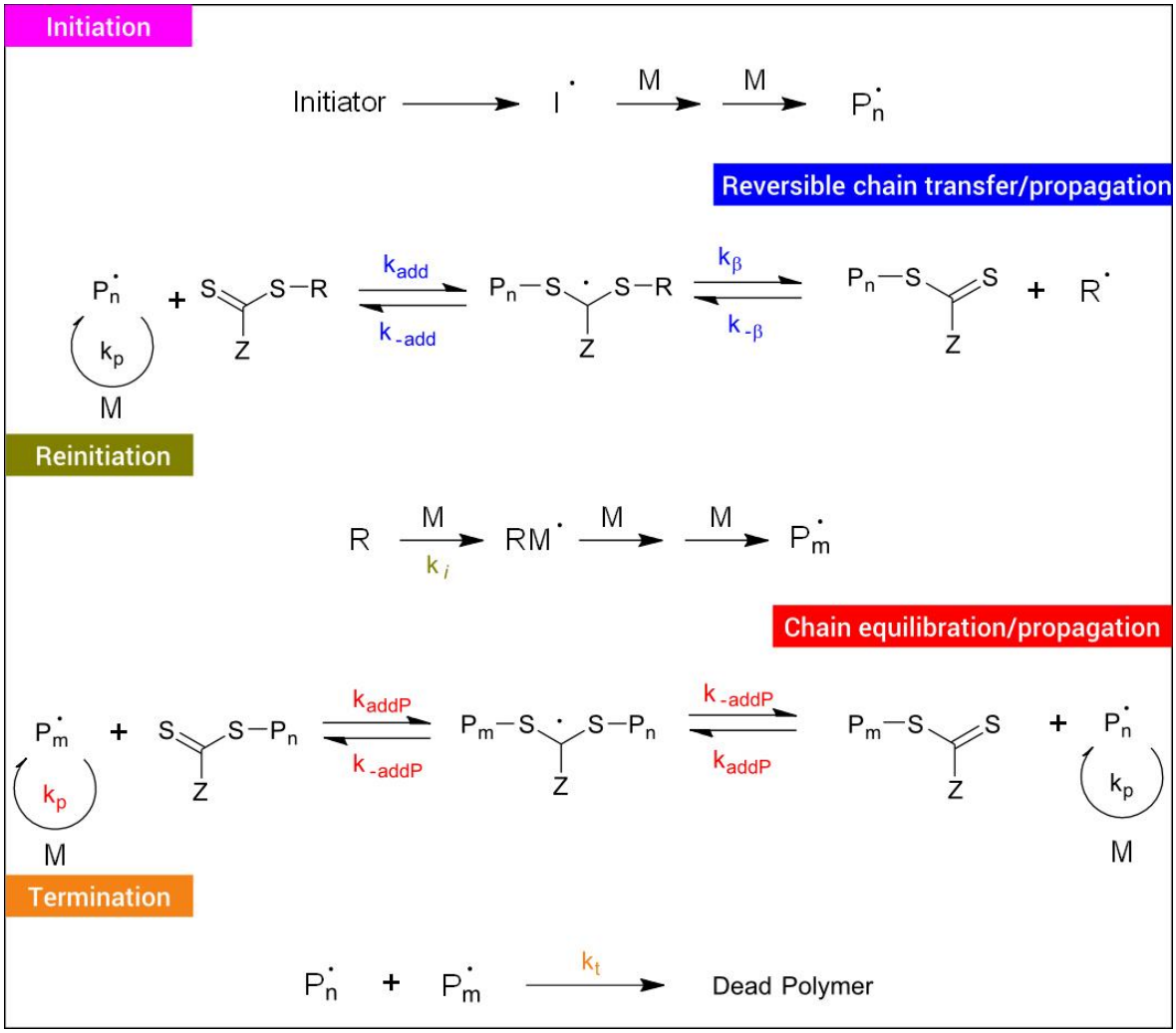

Scheme 1.3: Mechanism of RAFT polymerisation[24]

A significant advantage of RAFT is that it works with a wider range of monomers than NMP or ATRP (see next section) and that it does not produce polymers with copper or other metals present. However, many RAFT agents are not commercially available and therefore must be synthesised. Moreover, RAFT produces polymers with dithioester groups, which have some associated odour and colours (pink/red to yellow).

1.4.3 Atom Transfer Radical Polymerisation

Transition Metal Mediated Living Radical Polymerisation (TMMLRP) and Atom Transfer Radical Polymerisation (ATRP) was developed by Sawamoto[25] and Matyjaszewski[26] independently in 1995. ATRP, NMP and RAFT differ in the method of

radical generation. Radical generation in ATRP involves an organic halide undergoing a reversible redox process catalysed by a transition metal compound such as cuprous halide. ATRP is controlled by an equilibrium between propagating radicals and dormant species, predominately in the form of initiating alkyl halides/macromolecular species (P_nX). The dormant species periodically react with a rate constant of activation (k_{act}) with transition metal complexes in their lower oxidation state, Mt^m/L, acting as activators (Mt^m represents the transition metal species in oxidation state m and L is a ligand); to intermittently form growing radicals ($P_n^{\cdot}$), and deactivators-transition metal complexes in their higher oxidation state, coordinated with halide ligands $X\text{-}Mt^{m+1}$ (Scheme 1.4). The deactivator reacts with the propagating radical in a reverse reaction (k_{deact}) to re-form the dormant species and the activator.

As in all RDRP methods, termination will always occur. However, in ATRP the small amount of bimolecular termination present at the initial stage of the reaction is actually beneficial for the polymerisation as it provides further control over the molecular weight distribution. When radicals are terminating *via* any method other than the end-capping reaction with CuX_2, it results in a slight excess of deactivating species in the system, which provides more control over radical propagation by shifting the equilibrium towards the dormant species. This phenomenon is known as the Persistent Radical Effect (PRE)[27-29].

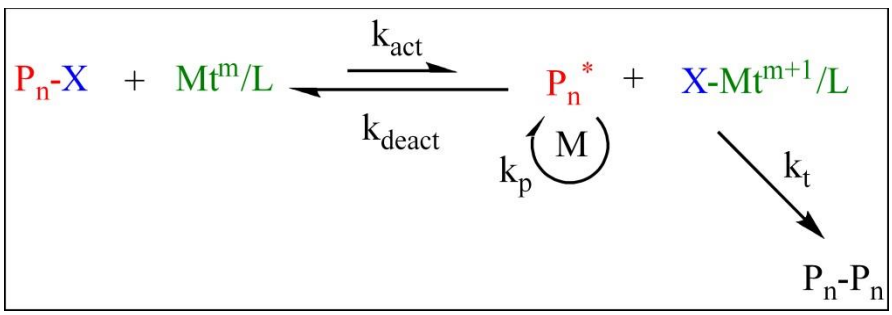

Scheme 1.4: ATRP equilibrium[30].

ATRP is typically described to proceed *via* an inner sphere mechanism, where the radical and the deactivating species are formed through the homolytic atom transfer of the halogen radical from the dormant species to the active species. Inner Sphere Electron Transfer (ISET) mechanism is more likely to happen in comparison with Outer Sphere Electron Transfer (OSET) as it is energetically favored[31].

Although copper has been the most often used transition metal, ATRP can be also be mediated by many other redox-active transition metals such as ruthenium[25, 32-39], iron[40-42], nickel[43-45], palladium[46] and molybdenum[47, 48]. For applications where lower amounts of metals are desirable, Activator Regenerated by Electron Transfer (ARGET-ATRP)[49, 50] and Initiators for Continuous Activator Regeneration (ICAR-ATRP)[51] have also been developed.

In ARGET-ATRP a small amount of catalyst is continuously regenerated by a reducing agent to account for unavoidable levels of radical termination. ARGET is a "green" procedure that uses ppm of the catalyst in the presence of appropriate reducing agents such as FDA-approved tin(II) 2-ethylhexanoate ($Sn(EH)_2$), glucose[49, 51], ascorbic acid[52], phenol[53], hydrazine, phenylhydrazine[49], excess inexpensive ligands[54] and nitrogen containing monomers[55] or metallic Cu (see next section). Since these reducing agents allow ATRP to be started with the oxidatively stable Cu(II) species, the reducing/reactivating cycle can also be employed to eliminate air, or other radical traps, in the system. For example, styrene was polymerised by the addition of 5 ppm of $CuCl_2$/Me_6-Tren and 500 ppm of $Sn(EH)_2$ to the reaction mixture, resulting in preparation of a polystyrene with M_n=12500 ($M_{n,th}$ = 12600) and $Đ$ = 1.28 without removal of inhibitors or deoxygenation[56]. An additional advantage of ARGET-ATRP is that catalyst-induced side reactions are diminished. Therefore it is possible to prepare copolymers with higher molecular weight while retaining chain-end functionality[57-59].

The initiators for continuous activator regeneration (ICAR) procedure could be considered as a "reverse" ARGET-ATRP process. In ICAR-ATRP a source of organic free radicals is employed to continuously regenerate the Cu(I) activator, which would otherwise be consumed in termination reactions, especially when catalysts are used in very low concentrations. With this technique controlled synthesis of polystyrene and poly(meth)acrylates ($Đ < 1.2$) can be conducted with catalyst concentrations between 5 and 50 ppm, levels at which removal or recycling of the catalyst complex could be avoided for some applications. The reaction is driven to completion with addition of low concentrations of standard free radical initiators[49]. The rate of ICAR ATRP is governed by the rate of decomposition of the added free radical initiator, as in RAFT, while the degree of control, the rate of the deactivation and molecular weight distributions are controlled by K_{ATRP}, as in ATRP[49, 59-62].

1.4.4 Single Electron Transfer Living Radical Polymerisation

In 2006 Percec and co-workers reported the LRP of functional monomers containing electron-withdrawing groups such as acrylates, methacrylates and vinyl chloride[63]. This process provides, at ambient temperature and below, an "ultrafast" synthesis of "ultrahigh" molecular weight polymers and occurs in polar media (such as DMSO, alcohols and water) in the presence of nitrogen-based ligands and alkyl halide initiators previously used in ATRP.

In a similar vein to ATRP, SET-LRP also involves an equilibrium between active (propagating macroradicals) and dormant (halide terminated polymer chains) species. However, the proposed activator is a Cu(0) species which acts as an electron donor and abstracts the halogen atom from the initiator *via* a heterolytic outer-sphere electron transfer (OSET) mechanism. The proposed mechanism[64] is presented in Scheme 1.5.

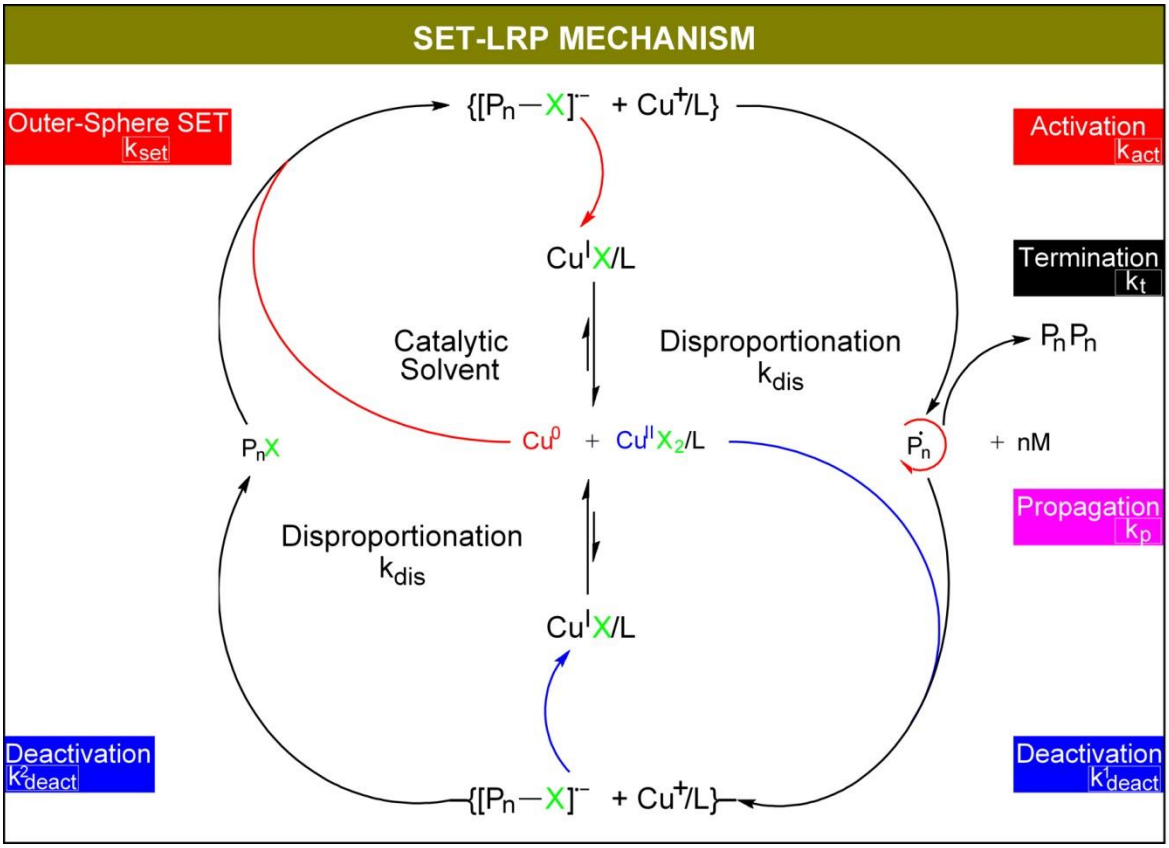

Scheme 1.5: Proposed mechanism for SET-LRP[64].

The key part in the SET-LRP mechanism is the disproportionation of the Cu(I)X species. The Cu(I) species generated during the formation of the radicals spontaneously disproportionate into extremely reactive atomic Cu(0) and Cu(II) species that will subsequently mediate the initiation and the reversible termination cycles. This disproportionation is integral to the mechanism, as it generates, by a self-regulated mechanism, *in situ*, the Cu(II) species that, in the case of VC for example, would not be accessible by a conventional PRE mechanism since the radical polymerisation of VC is dominated by chain transfer to monomer, rather than bimolecular termination. By this mechanism all Cu(I) are immediately consumed by disproportionation and the catalytically active Cu(0) species are continuously produced.

1.4.4.1 Monomer compatibility

A range of monomers have been reported using SET-LRP, including vinyl chloride[65], acrylates[64-80], methacrylates[65, 81-87], acrylamides[88-95], methacrylamides[96], and acrylonitrile[97]. Functional monomers have also been successfully polymerised including glycidyl acrylate, TMS acrylate[98] and solketal acrylate[99] resulting in polymers that could be further functionalised post-polymerisation or after self-assembly respectively. Recently, the scope of the reaction has been expanded to include semifluorinated[100] acrylates and methacrylates, presenting excellent control over the molecular weight distribution even at high conversion. Finally, sugar monomers[98, 101, 102] showed excellent compatibility with SET-LRP conditions, resulting in well-defined polymers with narrow dispersities, even at near-quantitative conversion. While the majority of monomers tested are acrylates, a larger diversity of vinyl monomers is expected to be compatible with SET-LRP.

1.4.4.2 Solvent compatibility

By far the most commonly used solvent for SET-LRP to date is DMSO. DMSO enhances the polarity of the medium, thereby aiding electron transfer[103, 104]. Moreover, DMSO has been reported to be a coordinating solvent that stabilises CuX_2[103] and thereby shifts the K_{dis} further to the right. DMSO is also suitable for solubilising a range of monomers and polymers. Additionally, DMSO possesses a high freezing point which aids in the freeze-pump-thaw process and therefore it is the preferred solvent in academic research laboratories.

Recently, H_2O[105] also showed excellent compatibility with SET-LRP. However, a different approach was introduced and copper wire was not the copper source. The key step in this process is to allow full disproportionation of CuBr/Me_6-Tren to Cu(0) powder and $CuBr_2$ prior to addition of both monomer and initiator. This provides an extremely powerful tool for the synthesis of functional water-soluble polymers with controlled chain

length and narrow molecular weight distributions ($Đ$ = 1.10), including acrylates and acrylamides. The polymerisations are performed at or below ambient temperature with very high conversions attained in minutes. Polymers have high chain-end fidelity and are capable of undergoing chain extension to full conversion or multiblock copolymerisation *via* iterative monomer addition after full conversion.

Alcohols, DMF and DMAC were also found to be compatible with SET-LRP, promoting the disproportionation of the *in situ* generated Cu(I)Br into Cu(0) and Cu(II)Br_2 in the presence of *N*-containing ligands. Finally, even when phosphate buffer[105], blood serum[106], and complex alcoholic media[107] were employed as the polymerisation medium, the polymerisation proceeded with unprecedented control and extraordinary tolerance towards unidentified chemical functionality, further demonstrating the versatility of this technique.

1.4.4.3 Catalyst compatibility

SET-LRP process has been initially reported to be activated, almost exclusively, by zero-valent copper or copper derivatives. However, the last two years several groups have extensively investigated alternative metallic catalytic sources, including iron (Fe)[108], nickel (Ni)[109], ytterbium (Yb)[110], lanthanum (La)[111, 112], gadolinium (Gd)[113], tin (Sn)[114], zinc (Zn)[115] and samarium (Sm)[116]. For instance, Fe is highly attractive as it is relatively inexpensive, non-toxic, abundant, environmentally-friendly, biocompatible and easy to separate. Polymerisation wise, methyl methacrylate (MMA), styrene (St) and acrylonitrile (AN) were successfully polymerised in the presence of Fe resulting in narrow molecular weight distributions and well-defined homo and block copolymers ($Đ$ ~ 1.1-1.3). These characteristics render it a good candidate for both biological and industrial applications as it could be a good alternative for additional applications where copper catalyst would be undesirable.

1.4.4.4 The Mechanistic debate

Undeniably, Cu(0)-mediated living radical polymerisation has attracted considerable interest over the last years due to its relative simplicity[64], mild conditions, tolerance to air[117-121], simple removal and reuse of unreacted solid Cu(0)[122] and relatively fast polymerisation rates[65] (for acrylates), allowing it to be used in various materials applications. The extremely high end-group fidelity has resulted in various well-defined complex polymers, including hyperbranched and dendritic structures[123], multiblock linear[99, 124, 125] and star copolymers[80, 99], functional polymers[126-129], functionalised surfaces[130, 131] and bioconjugates[82].

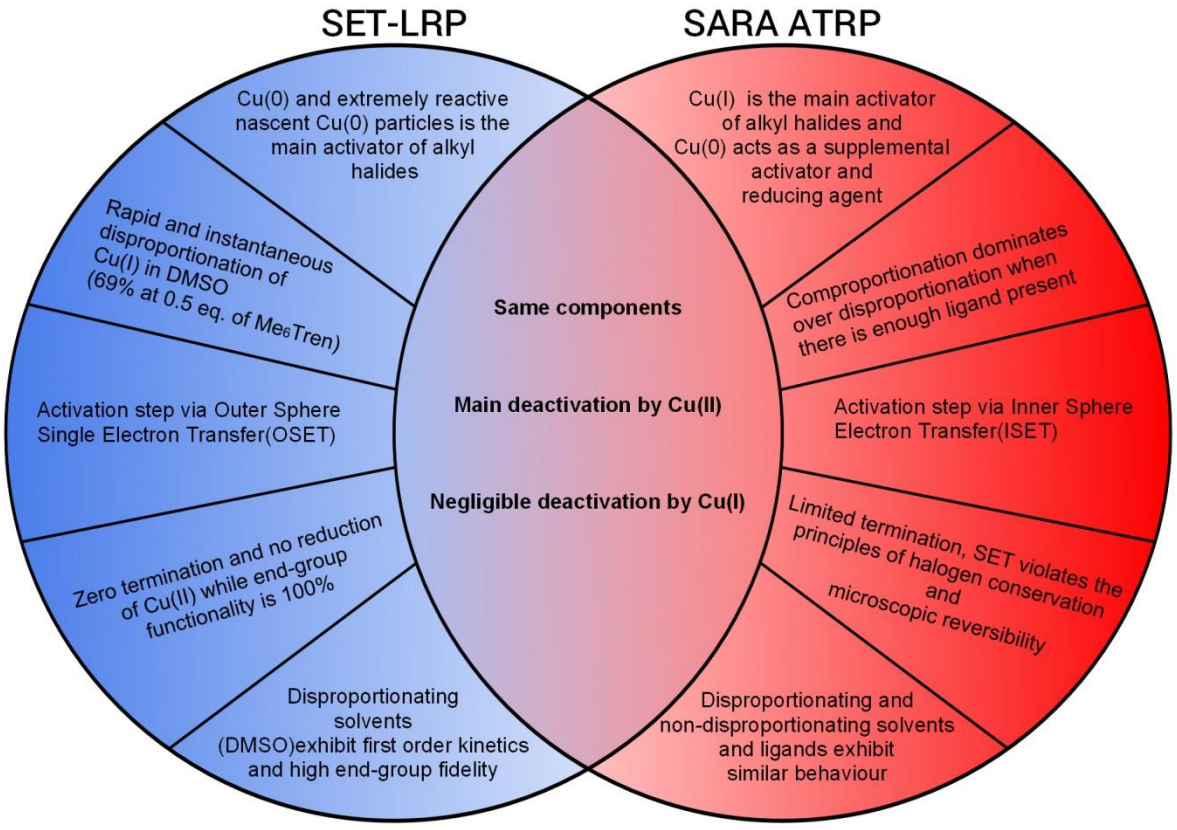

Figure 1.3: Comparison between SET-LRP and SARA-ATRP

Nevertheless, it is important to characterise reagents in the reaction mechanism and determine the effect of different parameters on the resulting polymer in order to optimise the reaction conditions and obtain the desired polymer structures. Interestingly, a debate is evident in the literature regarding the mechanism of reversible-deactivation radical

polymerisation in the presence of Cu(0). The two proposed models are SET-LRP[63], proposed by Percec and SARA-ATRP[132], proposed by Matyjaszewski. Both were proposed to explain the relatively rapid polymerisation of monomers such as methyl acrylate in polar solvents such as DMSO in the presence of metallic copper and ligands that form active Cu complexes.

On one side, Percec proposes that Cu(0)[63] or nascent Cu(0) particles[133, 134] is the major activator of alkyl halides. Moreover, no major activation occurs *via* Cu(I) complexes as the reaction ceases when the Cu(0) surface is removed from the reaction mixture, suggesting that the most active catalyst generated by disproportionation is not freely suspended in the reaction medium[133, 135]. Moreover, this activation event is suggested to occur *via* an OSET mechanism through a radical anion intermediate[63], suggesting much lower bond dissociation energies for the outer sphere single electron transfer process[136]. Percec claims that the crucial step in SET-LRP is the instantaneous disproportionation of the CuBr generated *in situ* by activation through Cu(0) wire or powder into nascent, extremely reactive Cu(0) nanoparticles and $CuBr_2$. This disproportionation has been visualised in protic, dipolar aprotic and non-polar solvents as well as protic, polar and non-polar monomers[137]. Particularly, in the case of DMSO, the disproportionation reaction occurs quite rapidly relative to polymerisation time scales and a maximum amount of disproportionation occurs in the presence of 0.5 equivalents of Me_6-Tren with respect to CuBr[138]. Thus, solvents that promote disproportionation due to the instability of Cu(I) are required for a well-controlled living polymerisation as non-disproportionating solvents (such as toluene, acetonitrile) exhibit two linear first order kinetic domains and a reduction in bromine chain-end functionality[139-141]. Finally, Percec reports "ultrafast" polymerisations, giving "ultrahigh" molecular weight polymers with zero termination and 100% chain-end functionality at 100% conversion[69, 141]. In order to illustrate his point, he

reported a continuous increase in $CuBr_2$ absorbance throughout the reaction, demonstrating no reduction of $CuBr_2$ concentration during the entire polymerisation process. In addition, the 100% chain-end functionality of the polymer observed from 10% to 95% monomer conversion indicated that, in this polymerisation, the bimolecular termination required to provide the persistent radical effect in ATRP was not responsible for the production of $CuBr_2$[142]. Therefore, disproportionation must be responsible for the accumulation of $CuBr_2$ during the polymerisation.

Conversely, Matyjaszewski, reports that Cu(I) is the major activator and Cu(0) will act as a supplemental activator of alkyl halides[143, 144] as Cu(0) is much less active than Cu(I) and 2000 m of Cu(0) wire, with diameter 0.25 mm would be required to match the activity of 1 mM Cu(I)/Me_6-Tren in DMSO[145]. Furthermore, Matyjaszewski interprets Percec's experiments[135] in a different way, highlighting that Cu(0) particles in solution represent only a small fraction (1%) of the surface area of the copper wire, and thus make a minimal contribution to the "nascent" Cu(0) in the reaction[146]. It is also shown that polymerisations in the presence of a non-disproportionating ligand (TPMA, which stabilises Cu(I) by accepting electron density into π^* orbitals) and a highly disproportionating ligand (Me_6-Tren) exhibit similar trends and both led to good control over the molecular weight distribution[144, 147], indicating that SARA ATRP operates in the presence of Cu(0) with both the aforementioned ligands. At the same time, the differences in kinetics between DMSO and MeCN are explained due to the higher K_{ATRP} in DMSO compared to less polar solvents[147]. Additionally, although relatively slow, comproportionation dominates over disproportionation under typical ATRP conditions and thus, Cu(I) is predominantly involved in the activation step rather than the disproportionation step[143, 148, 149]. Matyjaszewski also reports that the activation event, for both Cu(0) and Cu(I) occurs *via* an ISET mechanism as activation by Cu(I) *via* ISET is

10^{10} times faster than *via* OSET and approximately the same behaviour is observed for Cu(0)[31]. Another argument against SET-LRP is that it violates the "Principle of Halogen Conservation"[150] (PHC) and the "Principle of Microscopic Reversibility"[143] (PMR). Finally, limited amount of termination will always occur[150] and faster polymerisations with higher radical concentrations result in more dead chains[149] while the number of dead chains increase with polymerisation rate. In all cases, a build-up of Cu(II) species occurs due to loss of the Br end groups[142, 145, 150].

The majority of the data currently available indicate that at least in the case of DMSO, the contribution of Cu(I) species is greater than the contribution of Cu(0) as comproportionation appears to dominate over disproportionation. However, in the case of aqueous formulations where disproportionation is quantitative or near-quantitative[105], the existing literature is still quite limited[151]. Since the exact nature of the copper complexes is rather complicated, it is always wise to be open-minded and careful when making definitive assumptions and conclusions. After all, science is always progressing and yesterday's advances soon get replaced by current developments. Regardless of the mechanism, Cu(0)-mediated living radical polymerisation is undoubtedly considered a versatile technique that can be used to create well-controlled polymers with complex architectures.

1.4.5 External regulation; Utilising light as an external stimulus

Recently, considerable interest has been directed toward controlling the activation-deactivation equilibrium using various stimuli[152], including photochemical[153-155], pressure[156, 157] and electrochemical[158]. Processes that have the ability to turn "on" and "off" polymerisations simply by added reagents, an applied voltage, light or mechanical force are selected to further expand the scope of living radical polymerisation. In an ideal system, the propagating polymer chain should switch between an active and a dormant

state quickly, quantitatively, and fully reversible under external stimulation. In addition, the active state should show the qualities of a living polymerisation (in terms of minimal termination, low dispersity values and high end-group functionality), switching "on" and "off" should not compromise the polymerisation rate and finally the system should be tolerant to a large diversity of monomers and functional groups[152].

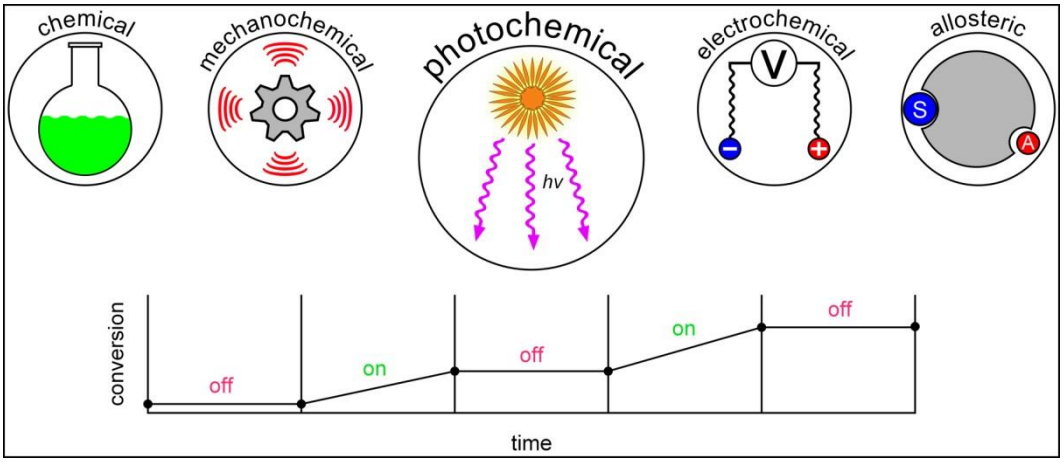

Figure 1.3: Temporally-controlled polymerisations can be regulated by a various stimuli to reversibly start and stop polymerisations.

Amongst all the external stimuli, light is perhaps one of the most popular, as it is a widely available, non-invasive and environmentally benign reagent that provides opportunities for both spatial and temporal control of polymerisation. Photolithography and photocuring are just some application examples arising from using light in order to mediate the polymerisation. However, many of the current traditional photochemical processes available lack the control desired to convey compositional and architectural design as only the initiation step is photo-controlled and all subsequent growth steps could not be photo-regulated[159-167]. In order to address this problem, three significant strategies have been employed, utilising light to control the monomer[155, 168], the polymer chain-end[169] or the catalyst[170].

Following the first strategy, Manners and co-workers[155, 168] reported an anionic photo-polymerisation that involves photo-excited monomers. Exposure of metal-containing

ferrocenophane monomers to Pyrex-filtered light from a mercury lamp (λ > 310 nm) or to bright sunlight in the presence of an anionic initiator leads to living polymerisations, in which the conversion and molecular weight of the resulting polymer can be controlled by the irradiation time. Photo-irradiation selectively weakens the iron–cyclopentadienyl bond in the monomer, allowing the use of moderately basic and highly functional-group-tolerant initiators. The polymerisation proceeds through attack of the initiator and propagating anion on the iron atom of the photo-excited monomer and, remarkably, the polymerisation rate decreases with increasing temperature. Block copolymer formation was also possible when the light source is alternately switched on and off in between sequential addition of different monomers, providing unprecedented, photo-controlled access to new types of functional polymers. However, the limitation of using only specialised, strained ferrocene monomers limits the potential of this specific system. Nevertheless, this strategy of photochemical monomer activation holds great promise and clearly defines the development of other monomers capable of activation as a future direction.

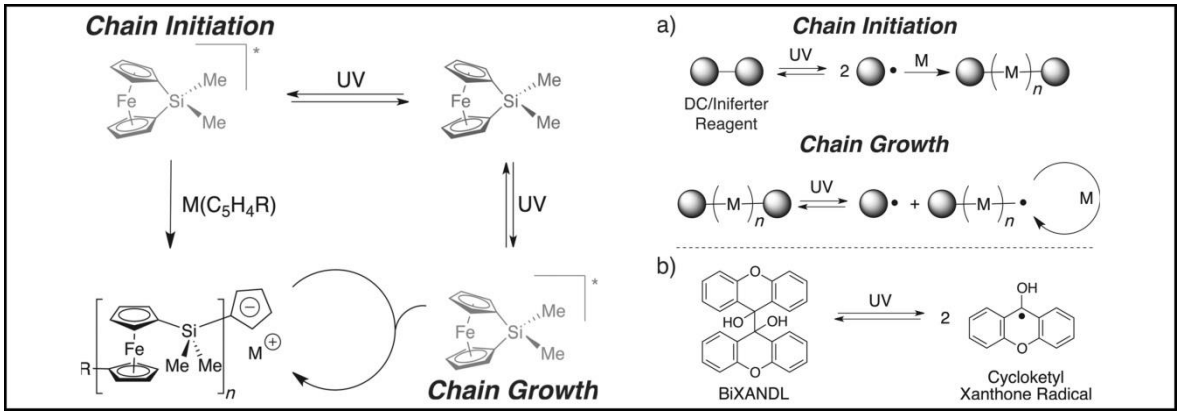

Scheme 1.6[152]: Strategy 1 (left); Monomer activation:anionic polymerisation of silicon-bridged ferrocenophanes mediated by monomer excitation with UV light and Strategy 2 (right); Chain-end activation: a) General mechanism for DC polymerisation and b) the DC reagent BiXANDL and its light-mediated fragmentation to give cycloketyl xanthone radicals.

Utilising light as an external stimulus in order to activate the polymer chain end (second strategy) includes light-sensitive alkoxyamines for NMP, which although

promising, have not led yet to a system that provides controlled polymerisations[161-163, 171]. Related to these alkoxyamine studies, preliminary works on the photolysis of organotellurium-functionalised polymers also holds considerable promise, although the dynamic nature of these systems has not yet been reported[172, 173]. Iniferter[174] (initiator-transfer agent-terminator) and Dissociation/Combination[175] (DC) polymerisations, pioneered by Otsu and Braun respectively, also belong in this strategy and involve homolytic cleavage of an initiator into two radical species upon exposure to UV light. The most successful system based on this concept is reported by Yang employing a new DC agent, 9,9´-bixanthene-9,9´-diol (BiXANDL)[169]. Upon photolysis, BiXANDL fragments into two cycloketyl xanthone radicals which are able to efficiently initiate the polymerisation as well as reversibly terminate the chain-end. However, moderate control over the molecular weight distributions ($Đ$ = 1.25-1.82) was observed and this system also lacks good thermal stability for the polymer chain end.

The third strategy (direct photo activation of a catalyst) is perhaps the most promising one for regulating controlled polymerisations with light as one only needs to control ppm levels of a catalytic species and not every monomer or every chain end. Hawker and co-workers were inspired by well-established organic photoredox catalysts[176] and reported an innovative and well-developed living polymerisation of methacrylates which is efficiently controlled by visible light[170]. The key component of this system is an Ir-based catalyst which undergoes excitation with a photon to afford an Ir^{III*} species. The excited catalyst is highly reducing and reacts with an alkyl bromide to give the desired alkyl radical, which initiates polymerisation. The resulting Ir^{IV} can then oxidise the alkyl radical chain-end back to the dormant alkyl bromide and the entire process can be repeated with an additional photon of light. The same technique was subsequently applied to acrylates[177]. Although in both cases relatively narrow molecular weight distributions were

obtained (*Đ*~1.19-1.39), the conversions were only moderate (50-70%) and the reaction times were relatively long (~12 h). Furthermore, iridium is a rather expensive catalyst to use, although low concentrations are usually required to obtain a well-defined polymer.

Yagci[178] and Matyjaszewski[179] have also successfully shown that traditional Cu-mediated polymerisation can benefit from UV or sunlight irradiation. In a lot less complicated system they utilised PMDETA and TPMA respectively which in the presence of $CuBr_2$ gave rise to narrow dispersity polymers (*Đ* = 1.1-1.3) although extremely long reaction times were required (> 20 h)[179] and the conversions was limited (50-80%). Finally, only homopolymers were obtained in both cases and rather simple monomers were utilised (MA and MMA).

Although these achievements in the photochemical field are already quite remarkable and promising, future challenges entail the exploration of a full range of polymerisable monomers while moving away from exotic metals (*e.g.* iridium) as well as the preparation of functional macromolecules (*e.g.* block copolymers) with external command of the final structure, architecture and sequence.

1.4.6 Multiblock copolymers: Towards "Sequence Control"?

Nature has always been an inexhaustible source of inspiration for synthetic polymer chemists. For instance, aminoacids form specific configurations (peptides, proteins *etc.*), forming monodisperse, complex structures to suit a pre-defined function. A rather ambitious target of polymer chemists is to try and replicate this precision over monomer sequence exhibited by natural polymers, having in mind potential applications, including nanomedicine and nanotechnology, whereby this high level of monomer sequence control will confer the potential of molecular targeting and recognition.

For cases where precise sequence control is strictly required, solid phase synthesis is perhaps the most popular method[180], although templated[181-183] and orthogonal

protection/deprotection strategies[184] can also be employed. However, the main drawback of the aforementioned techniques is that they are time-consuming as they require multiple purification steps which additionally compromise the yield of the final product. Conversely, the implementation of sequence control *via* chain growth polymerisation is challenging, given the reactive nature of the radical, and it always leads to a statistical mixture of products, compromising the integrity of the sequence. Although multiblock copolymers lack the control imposed by nature, they are still useful for specific applications. Moreover, careful optimisation of the polymerisation conditions can lead to rapid and quantitative synthesis (even 100% for every block), which increases their popularity. This has stimulated the development of polymerisation methods that focus on controlling the sequence of multiple discrete regions within the overall macromolecular structure.

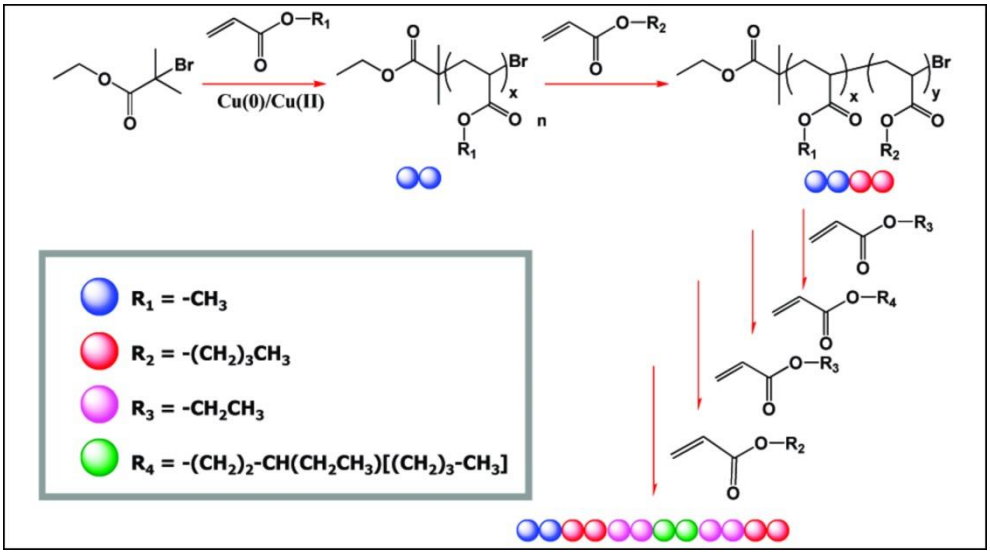

Scheme 1.7: Schematic representation of the synthesis of multiblock copolymers by sequential addition of monomers without intermediate purification as illustrated by Whittaker[124].

One of the first examples of a one-pot synthesis of multiblock copolymers *via* iterative monomer addition was reported by Whittaker and his co-workers in 2011[80, 124, 125]. Utilising Cu(0)-mediated living radical polymerisation they managed to synthesise high-

order multiblock copolymers comprising very short blocks. Although remarkable, this work reached its limitations when a decablock copolymer was targeted, whereby molecular weight distributions were found to gradually increase ($Đ$ ~ 1.7 for the final decablock copolymer), indicating significant termination events[125]. Moreover, higher molecular weight polymers were not reported. The same technique was subsequently employed for the synthesis of a number of multiblock glycopolymers which retained very narrow dispersity values[101], although quantitative conversion was not achieved in all cases[98].

More recently, and in parallel with our own experiments, Perrier and co-workers reported the synthesis of an icasoblock multiblock copolymer consisting of acrylamides both in aqueous and organic media[185-188]. However, the high temperature (~70 ˚C) that was utilised potentially limits the possibility of simultaneous biological applications while at the same time narrows the monomer pool to only acrylamides, as polymerisation of other monomers (*e.g.* acrylates) at these temperatures would result in unavoidable termination and side reactions[189, 190]. Moreover, the addition of external free radical initiator for each monomer addition potentially compromises the integrity of the multiblock copolymers, as it can lead to a small percentage of homopolymer.

Perhaps more importantly, multiblock copolymers, apart from forming functional domains, can also serve as a useful tool to explore and expand the potential as well as to identify the limitations of a given polymerisation system. Careful optimisation of the experimental conditions can provide useful guidelines for performing polymerisations with very high end-group fidelity, even at full monomer conversion, while keeping the dispersity values as low as possible. Of course, we should always remember that in a pseudo-living polymerisation system (such as SET, ATRP or RAFT) which involves radicals, termination will always happen. The challenge is to find the best way to suppress it. As John Maynard Keynes said "*In the very long run we are all dead*". Growing polymer

radicals will eventually die. We just do our best to make sure this will happen in a "*very, very long run*", on the timescales of the polymerisation reaction.

1.5 References

1. P. J. Flory, *J. Am. Chem. Soc.*, 1937, **59**, 241-253.
2. G. Odian, *Principles of Polymerization, 4th Edition*, John Wiley & Sons, 2004.
3. K. Soga and T. Shiono, *Prog. Polym. Sci.*, 1997, **22**, 1503-1546.
4. M. Szwarc, M. Levy and R. Milkovich, *J. Am. Chem. Soc.*, 1956, **78**, 2656-2657.
5. M. Szwarc, *J. Polym. Sci., Part A: Polym. Chem.*, 1998, **36**, v-xiii.
6. M. Szwarc, *J. Polym. Sci., Part A: Polym. Chem.*, 1998, **36**, IX-XV.
7. A. Goto and T. Fukuda, *Prog. Polym. Sci.*, 2004, **29**, 329-385.
8. K. Matyjaszewski and J. Xia, in *Handbook of Radical Polymerization*, John Wiley & Sons, 2002, pp. 523-628.
9. K. Matyjaszewski, S. Gaynor, D. Greszta, D. Mardare and T. Shigemoto, *J. Phys. Org. Chem.*, 1995, **8**, 306-315.
10. D. Greszta, D. Mardare and K. Matyjaszewski, *Macromolecules*, 1994, **27**, 638-644.
11. B. B. Wayland, G. Poszmik, S. L. Mukerjee and M. Fryd, *J. Am. Chem. Soc.*, 1994, **116**, 7943-7944.
12. R. P. Quirk and B. Lee, *Polym. Int.*, 1992, **27**, 359-367.
13. J. D. Druliner, *Macromolecules*, 1991, **24**, 6079-6082.
14. E. De León-Sáenz, G. Morales, R. Guerrero-Santos and Y. Gnanou, *Macromol. Chem. Phys.*, 2000, **201**, 74-83.
15. B. Yamada, Y. Nobukane and Y. Miura, *Polym. Bull.*, 1998, **41**, 539-544.
16. M. Steenbock, M. Klapper and K. Müllen, *Macromol. Chem. Phys.*, 1998, **199**, 763-769.
17. R. D. Puts and D. Y. Sogah, *Macromolecules*, 1996, **29**, 3323-3325.
18. Polymerization process and polymers produced thereby, US Patent **4581429**, 1986.
19. M. K. Georges, R. P. N. Veregin, P. M. Kazmaier and G. K. Hamer, *Macromolecules*, 1993, **26**, 2987-2988.
20. R. P. N. Veregin, M. K. Georges, P. M. Kazmaier and G. K. Hamer, *Macromolecules*, 1993, **26**, 5316-5320.
21. C. J. Hawker, A. W. Bosman and E. Harth, *Chem. Rev.*, 2001, **101**, 3661-3688.
22. Y. Guillaneuf, D. Gigmes, S. R. A. Marque, P. Astolfi, L. Greci, P. Tordo and D. Bertin, *Macromolecules*, 2007, **40**, 3108-3114.

23. J. Chiefari, Y. K. Chong, F. Ercole, J. Krstina, J. Jeffery, T. P. T. Le, R. T. A. Mayadunne, G. F. Meijs, C. L. Moad and G. Moad, *Macromolecules*, 1998, **31**, 5559-5562.
24. G. Moad, E. Rizzardo and S. H. Thang, *Aust. J. Chem.*, 2012, **65**, 985-1076.
25. M. Kato, M. Kamigaito, M. Sawamoto and T. Higashimura, *Macromolecules*, 1995, **28**, 1721-1723.
26. J.-S. Wang and K. Matyjaszewski, *J. Am. Chem. Soc.*, 1995, **117**, 5614-5615.
27. H. Fischer, *Macromolecules*, 1997, **30**, 5666-5672.
28. H. Fischer, *J. Polym. Sci., Part A: Polym. Chem.*, 1999, **37**, 1885-1901.
29. H. Fischer, *Chem. Rev.*, 2001, **101**, 3581-3610.
30. K. Matyjaszewski, *Macromolecules*, 2012, **45**, 4015-4039.
31. C. Y. Lin, M. L. Coote, A. Gennaro and K. Matyjaszewski, *J. Am. Chem. Soc.*, 2008, **130**, 12762-12774.
32. V. Percec, B. Barboiu, A. Neumann, J. C. Ronda and M. Zhao, *Macromolecules*, 1996, **29**, 3665-3668.
33. T. Ando, M. Kato, M. Kamigaito and M. Sawamoto, *Macromolecules*, 1996, **29**, 1070-1072.
34. T. Nishikawa, T. Ando, M. Kamigaito and M. Sawamoto, *Macromolecules*, 1997, **30**, 2244-2248.
35. T. Ando, M. Kamigaito and M. Sawamoto, *Tetrahedron*, 1997, **53**, 15445-15457.
36. J. Ueda, M. Matsuyama, M. Kamigaito and M. Sawamoto, *Macromolecules*, 1998, **31**, 557-562.
37. J. Ueda, M. Kamigaito and M. Sawamoto, *Macromolecules*, 1998, **31**, 6762-6768.
38. D. M. Haddleton, D. J. Duncalf, D. Kukulj and A. P. Radigue, *Macromolecules*, 1999, **32**, 4769-4775.
39. H. Takahashi, T. Ando, M. Kamigaito and M. Sawamoto, *Macromolecules*, 1999, **32**, 6461-6465.
40. T. Ando, M. Kamigaito and M. Sawamoto, *Macromolecules*, 1997, **30**, 4507-4510.
41. K. Matyjaszewski, M. Wei, J. Xia and N. E. McDermott, *Macromolecules*, 1997, **30**, 8161-8164.
42. R. K. O'Reilly, V. C. Gibson, A. J. P. White and D. J. Williams, *Polyhedron*, 2004, **23**, 2921-2928.
43. H. Uegaki, Y. Kotani, M. Kamigaito and M. Sawamoto, *Macromolecules*, 1997, **30**, 2249-2253.
44. H. Uegaki, Y. Kotani, M. Kamigaito and M. Sawamoto, *Macromolecules*, 1998, **31**, 6756-6761.

45. H. Uegaki, M. Kamigaito and M. Sawamoto, *J. Polym. Sci., Part A: Polym. Chem.*, 1999, **37**, 3003-3009.
46. P. Lecomte, I. Drapier, P. Dubois, P. Teyssié and R. Jérôme, *Macromolecules*, 1997, **30**, 7631-7633.
47. E. Le Grognec, J. Claverie and R. Poli, *J. Am. Chem. Soc.*, 2001, **123**, 9513-9524.
48. F. Stoffelbach, D. M. Haddleton and R. Poli, *Eur. Polym. J.*, 2003, **39**, 2099-2105.
49. K. Matyjaszewski, W. Jakubowski, K. Min, W. Tang, J. Huang, W. A. Braunecker and N. V. Tsarevsky, *Proc. Natl. Acad. Sci.*, 2006, **103**, 15309-15314.
50. A. de Vries, B. Klumperman, D. de Wet-Roos and R. D. Sanderson, *Macromol. Chem. Phys.*, 2001, **202**, 1645-1648.
51. W. Jakubowski and K. Matyjaszewski, *Angew. Chem., Int. Ed.*, 2006, **45**, 4482-4486.
52. K. Min, H. Gao and K. Matyjaszewski, *Macromolecules*, 2007, **40**, 1789-1791.
53. Y. Gnanou and G. Hizal, *J. Polym. Sci., Part A: Polym. Chem.*, 2004, **42**, 351-359.
54. Y. Kwak, A. J. D. Magenau and K. Matyjaszewski, *Macromolecules*, 2011, **44**, 811-819.
55. H. Dong and K. Matyjaszewski, *Macromolecules*, 2008, **41**, 6868-6870.
56. W. Jakubowski, K. Min and K. Matyjaszewski, *Macromolecules*, 2005, **39**, 39-45.
57. J. Pietrasik, H. Dong and K. Matyjaszewski, *Macromolecules*, 2006, **39**, 6384-6390.
58. H. Dong, W. Tang and K. Matyjaszewski, *Macromolecules*, 2007, **40**, 2974-2977.
59. L. Mueller, W. Jakubowski, W. Tang and K. Matyjaszewski, *Macromolecules*, 2007, **40**, 6464-6472.
60. W. Tang, N. V. Tsarevsky and K. Matyjaszewski, *J. Am. Chem. Soc.*, 2006, **128**, 1598-1604.
61. W. Tang and K. Matyjaszewski, *Macromol. Theory Simul.*, 2008, **17**, 359-375.
62. D. R. D'Hooge, D. Konkolewicz, M.-F. Reyniers, G. B. Marin and K. Matyjaszewski, *Macromol. Theory Simul.*, 2012, **21**, 52-69.
63. V. Percec, T. Guliashvili, J. S. Ladislaw, A. Wistrand, A. Stjerndahl, M. J. Sienkowska, M. J. Monteiro and S. Sahoo, *J. Am. Chem. Soc.*, 2006, **128**, 14156-14165.
64. B. M. Rosen and V. Percec, *Chem. Rev.*, 2009, **109**, 5069-5119.
65. V. Percec, T. Guliashvili, J. S. Ladislaw, A. Wistrand, A. Stjerndahl, M. J. Sienkowska, M. J. Monteiro and S. Sahoo, *J. Am. Chem. Soc.*, 2006, **128**, 14156-14165.
66. N. H. Nguyen, B. M. Rosen, G. Lligadas and V. Percec, *Macromolecules*, 2009, **42**, 2379-2386.
67. X. Jiang, B. M. Rosen and V. Percec, *J. Polym. Sci., Part A: Polym. Chem.*, 2010, **48**, 403-409.
68. G. Lligadas and V. Percec, *J. Polym. Sci., Part A: Polym. Chem.*, 2007, **45**, 4684-4695.

69. N. H. Nguyen, M. E. Levere and V. Percec, *J. Polym. Sci., Part A: Polym. Chem.*, 2012, **50**, 860-873.
70. S. Zhai, B. Wang, C. Feng, Y. Li, D. Yang, J. Hu, G. Lu and X. Huang, *J. Polym. Sci., Part A: Polym. Chem.*, 2010, **48**, 647-655.
71. X. Leng, N. H. Nguyen, B. van Beusekom, D. A. Wilson and V. Percec, *Polym. Chem.*, 2013, **4**, 2995-3004.
72. S. Zhai, J. Shang, D. Yang, S. Wang, J. Hu, G. Lu and X. Huang, *J. Polym. Sci., Part A: Polym. Chem.*, 2012, **50**, 811-820.
73. S. Zhai, X. Song, D. Yang, W. Chen, J. Hu, G. Lu and X. Huang, *J. Polym. Sci., Part A: Polym. Chem.*, 2011, **49**, 4055-4064.
74. A. Anastasaki, C. Waldron, V. Nikolaou, P. Wilson, R. McHale, T. Smith and D. M. Haddleton, *Polym. Chem.*, 2013, **4**, 4113-4119.
75. C. Boyer, A. Atme, C. Waldron, A. Anastasaki, P. Wilson, P. B. Zetterlund, D. Haddleton and M. R. Whittaker, *Polym. Chem.*, 2013, **4**, 106-112.
76. M. J. Monteiro, T. Guliashvili and V. Percec, *J. Polym. Sci., Part A: Polym. Chem.*, 2007, **45**, 1835-1847.
77. G. Lu, Y. Li, H. Gao, H. Guo, X. Zheng and X. Huang, *J. Polym. Sci., Part A: Polym. Chem.*, 2013, **51**, 1099-1106.
78. G. Lu, Y. Li, H. Guo, W. Du and X. Huang, *Polym. Chem.*, 2013, **4**, 3132-3139.
79. G. Lu, Y. Li, B. Dai, C. Xu and X. Huang, *J. Polym. Sci., Part A: Polym. Chem.*, 2013, **51**, 1880-1886.
80. C. Boyer, A. Derveaux, P. B. Zetterlund and M. R. Whittaker, *Polym. Chem.*, 2012, **3**, 117-123.
81. G. Chen, P. M. Wright, J. Geng, G. Mantovani and D. M. Haddleton, *Chem. Commun.*, 2008, **9**, 1097-1099.
82. M. W. Jones, M. I. Gibson, G. Mantovani and D. M. Haddleton, *Polym. Chem.*, 2011, **2**, 572-574.
83. S. Fleischmann and V. Percec, *J. Polym. Sci., Part A: Polym. Chem.*, 2010, **48**, 4884-4888.
84. S. Fleischmann and V. Percec, *J. Polym. Sci., Part A: Polym. Chem.*, 2010, **48**, 2236-2242.
85. N. H. Nguyen, X. Leng and V. Percec, *Polym. Chem.*, 2013, **4**, 2760-2766.
86. X. Song, Y. Zhang, D. Yang, L. Yuan, J. Hu, G. Lu and X. Huang, *J. Polym. Sci., Part A: Polym. Chem.*, 2011, **49**, 3328-3337.
87. Y. Deng, Y. Li, J. Dai, M. Lang and X. Huang, *J. Polym. Sci., Part A: Polym. Chem.*, 2011, **49**, 4747-4755.
88. N. H. Nguyen, B. M. Rosen and V. Percec, *J. Polym. Sci., Part A: Polym. Chem.*, 2010, **48**, 1752-1763.

89. X. Tang, X. Liang, Q. Yang, X. Fan, Z. Shen and Q. Zhou, *J. Polym. Sci., Part A: Polym. Chem.*, 2009, **47**, 4420-4427.
90. Y. Deng, J. Z. Zhang, Y. Li, J. Hu, D. Yang and X. Huang, *J. Polym. Sci., Part A: Polym. Chem.*, 2012, **50**, 4451-4458.
91. C. Feng, Y. Li, D. Yang, Y. Li, J. Hu, S. Zhai, G. Lu and X. Huang, *J. Polym. Sci., Part A: Polym. Chem.*, 2010, **48**, 15-23.
92. C. Feng, Z. Shen, Y. Li, L. Gu, Y. Zhang, G. Lu and X. Huang, *J. Polym. Sci., Part A: Polym. Chem.*, 2009, **47**, 1811-1824.
93. C. Feng, Z. Shen, D. Yang, Y. Li, J. Hu, G. Lu and X. Huang, *J. Polym. Sci., Part A: Polym. Chem.*, 2009, **47**, 4346-4357.
94. A. Ding, G. Lu, H. Guo, X. Zheng and X. Huang, *J. Polym. Sci., Part A: Polym. Chem.*, 2013, **51**, 1091-1098.
95. A. Anastasaki, A. J. Haddleton, Q. Zhang, A. Simula, M. Droesbeke, P. Wilson and D. M. Haddleton, *Macromol. Rapid Commun.*, 2014, **35**, 965-970.
96. N. H. Nguyen, C. Rodriguez-Emmenegger, E. Brynda, Z. Sedlakova and V. Percec, *Polym. Chem.*, 2013, **4**, 2424-2427.
97. X.-H. Liu, G.-B. Zhang, B.-X. Li, Y.-G. Bai and Y.-S. Li, *J. Polym. Sci., Part A: Polym. Chem.*, 2010, **48**, 5439-5445.
98. Q. Zhang, A. Anastasaki, G.-Z. Li, A. J. Haddleton, P. Wilson and D. M. Haddleton, *Polym. Chem.*, 2014, **5**, 3876-3883.
99. M. R. Whittaker, C. N. Urbani and M. J. Monteiro, *J. Polym. Sci., Part A: Polym. Chem.*, 2008, **46**, 6346-6357.
100. S. R. Samanta, R. Cai and V. Percec, *Polym. Chem.*, 2014, **5**, 5479-5491
101. Q. Zhang, J. Collins, A. Anastasaki, R. Wallis, D. A. Mitchell, C. R. Becer and D. M. Haddleton, *Angew. Chem., Int. Ed.*, 2013, **52**, 4435-4439.
102. Q. Zhang, P. Wilson, A. Anastasaki, R. McHale and D. M. Haddleton, *ACS Macro Lett.*, 2014, **3**, 491-495.
103. S. Monge, V. Darcos and D. M. Haddleton, *J. Polym. Sci., Part A: Polym. Chem.*, 2004, **42**, 6299-6308.
104. C. A. Bell, M. R. Whittaker, L. R. Gahan and M. J. Monteiro, *J. Polym. Sci., Part A: Polym. Chem.*, 2008, **46**, 146-154.
105. Q. Zhang, P. Wilson, Z. Li, R. McHale, J. Godfrey, A. Anastasaki, C. Waldron and D. M. Haddleton, *J. Am. Chem. Soc.*, 2013, **135**, 7355-7363.
106. Q. Zhang, Z. Li, P. Wilson and D. M. Haddleton, *Chem. Commun.*, 2013, **49**, 6608-6610.
107. C. Waldron, Q. Zhang, Z. Li, V. Nikolaou, G. Nurumbetov, J. Godfrey, R. McHale, G. Yilmaz, R. K. Randev, M. Girault, K. McEwan, D. M. Haddleton, M. Droesbeke, A. J.

Haddleton, P. Wilson, A. Simula, J. Collins, D. J. Lloyd, J. A. Burns, C. Summers, C. Houben, A. Anastasaki, M. Li, C. R. Becer, J. K. Kiviaho and N. Risangud, *Polym. Chem.*, 2014, **5**, 57-61.

108. L. Zhou, Z. Zhang, W. Wang, Z. Cheng, N. Zhou, J. Zhu, W. Zhang and X. Zhu, *J. Polym. Sci., Part A: Polym. Chem.*, 2012, **50**, 936-943.
109. X.-H. Liu, Y.-H. Yu, D. Jia, B.-W. Cheng, F.-J. Zhang, H.-N. Li, P. Chen and S. Xie, *J. Polym. Sci., Part A: Polym. Chem.*, 2013, **51**, 1559-1564.
110. D. Liu, J. Ma, H. Chen, P. Yin, N. Ji and G. Zong, *J. Polym. Sci., Part A: Polym. Chem.*, 2011, **49**, 5109-5115.
111. J. Zhang, Z. Hao and H. Chen, *J. Polym. Sci., Part A: Polym. Chem.*, 2013, **51**, 3323-3327.
112. Z. Hao, J. Zhang, H. Chen, D. Liu, D. Wang, H. Qu and J. Lang, *J. Polym. Sci., Part A: Polym. Chem.*, 2013, **51**, 4088-4094.
113. D. Liu, H. Chen, P. Yin, Z. Hao and L. Fan, *J. Polym. Sci., Part A: Polym. Chem.*, 2012, **50**, 4809-4813.
114. Z. Hao, H. Chen, D. Liu and L. Fan, *J. Polym. Sci., Part A: Polym. Chem.*, 2012, **50**, 4995-4999.
115. Y.-H. Yu, X.-H. Liu, D. Jia, B.-W. Cheng, F.-J. Zhang, H.-N. Li, P. Chen and S. Xie, *J. Polym. Sci., Part A: Polym. Chem.*, 2013, **51**, 1468-1474.
116. H. Chen, G. Zong, L. Chen, M. Zhang, C. Wang and R. Qu, *J. Polym. Sci., Part A: Polym. Chem.*, 2011, **49**, 2924-2930.
117. N. H. Nguyen, X. Leng, H.-J. Sun and V. Percec, *J. Polym. Sci., Part A: Polym. Chem.*, 2013, **51**, 3110-3122.
118. N. H. Nguyen and V. Percec, *J. Polym. Sci., Part A: Polym. Chem.*, 2011, **49**, 4756-4765.
119. S. Fleischmann and V. Percec, *J. Polym. Sci., Part A: Polym. Chem.*, 2010, **48**, 2243-2250.
120. S. Fleischmann, B. M. Rosen and V. Percec, *J. Polym. Sci., Part A: Polym. Chem.*, 2010, **48**, 1190-1196.
121. X. Jiang, B. M. Rosen and V. Percec, *J. Polym. Sci., Part A: Polym. Chem.*, 2010, **48**, 2716-2721.
122. N. Chan, M. F. Cunningham and R. A. Hutchinson, *Polym. Chem.*, 2012, **3**, 486-497.
123. B. M. Rosen, G. Lligadas, C. Hahn and V. Percec, *J. Polym. Sci., Part A: Polym. Chem.*, 2009, **47**, 3940-3948.
124. A. H. Soeriyadi, C. Boyer, F. Nyström, P. B. Zetterlund and M. R. Whittaker, *J. Am. Chem. Soc.*, 2011, **133**, 11128-11131.
125. C. Boyer, A. H. Soeriyadi, P. B. Zetterlund and M. R. Whittaker, *Macromolecules*, 2011, **44**, 8028-8033.

126. G. Lligadas, J. S. Ladislaw, T. Guliashvili and V. Percec, *J. Polym. Sci., Part A: Polym. Chem.*, 2008, **46**, 278-288.
127. S. L. Potisek, D. A. Davis, N. R. Sottos, S. R. White and J. S. Moore, *J. Am. Chem. Soc.*, 2007, **129**, 13808-13809.
128. S. Fleischmann and V. Percec, *J. Polym. Sci., Part A: Polym. Chem.*, 2010, **48**, 2251-2255.
129. J. A. Syrett, M. W. Jones and D. M. Haddleton, *Chem. Commun.*, 2010, **46**, 7181-7183.
130. S. Ding, J. A. Floyd and K. B. Walters, *J. Polym. Sci., Part A: Polym. Chem.*, 2009, **47**, 6552-6560.
131. J. O. Zoppe, Y. Habibi, O. J. Rojas, R. A. Venditti, L.-S. Johansson, K. Efimenko, M. Österberg and J. Laine, *Biomacromolecules*, 2010, **11**, 2683-2691.
132. D. Konkolewicz, Y. Wang, P. Krys, M. Zhong, A. A. Isse, A. Gennaro and K. Matyjaszewski, *Polym. Chem.*, 2014, **5**, 4396-4417.
133. G. Lligadas, B. M. Rosen, C. A. Bell, M. J. Monteiro and V. Percec, *Macromolecules*, 2008, **41**, 8365-8371.
134. N. H. Nguyen, H.-J. Sun, M. E. Levere, S. Fleischmann and V. Percec, *Polym. Chem.*, 2013, **4**, 1328-1332.
135. M. E. Levere, N. H. Nguyen, H.-J. Sun and V. Percec, *Polym. Chem.*, 2013, **4**, 686-694.
136. T. Guliashvili and V. Percec, *J. Polym. Sci., Part A: Polym. Chem.*, 2007, **45**, 1607-1618.
137. M. E. Levere, N. H. Nguyen, X. Leng and V. Percec, *Polym. Chem.*, 2013, **4**, 1635-1647.
138. B. M. Rosen, X. Jiang, C. J. Wilson, N. H. Nguyen, M. J. Monteiro and V. Percec, *J. Polym. Sci., Part A: Polym. Chem.*, 2009, **47**, 5606-5628.
139. N. H. Nguyen, M. E. Levere, J. Kulis, M. J. Monteiro and V. Percec, *Macromolecules*, 2012, **45**, 4606-4622.
140. N. H. Nguyen and V. Percec, *J. Polym. Sci., Part A: Polym. Chem.*, 2011, **49**, 4227-4240.
141. G. Lligadas and V. Percec, *J. Polym. Sci., Part A: Polym. Chem.*, 2008, **46**, 6880-6895.
142. M. E. Levere, N. H. Nguyen and V. Percec, *Macromolecules*, 2012, **45**, 8267-8274.
143. K. Matyjaszewski, N. V. Tsarevsky, W. A. Braunecker, H. Dong, J. Huang, W. Jakubowski, Y. Kwak, R. Nicolay, W. Tang and J. A. Yoon, *Macromolecules*, 2007, **40**, 7795-7806.
144. Y. Zhang, Y. Wang, C.-h. Peng, M. Zhong, W. Zhu, D. Konkolewicz and K. Matyjaszewski, *Macromolecules*, 2011, **45**, 78-86.
145. C.-H. Peng, M. Zhong, Y. Wang, Y. Kwak, Y. Zhang, W. Zhu, M. Tonge, J. Buback, S. Park, P. Krys, D. Konkolewicz, A. Gennaro and K. Matyjaszewski, *Macromolecules*, 2013, **46**, 3803-3815.
146. D. Konkolewicz, Y. Wang, M. Zhong, P. Krys, A. A. Isse, A. Gennaro and K. Matyjaszewski, *Macromolecules*, 2013, **46**, 8749-8772.

147. Y. Wang, Y. Kwak, J. Buback, M. Buback and K. Matyjaszewski, *ACS Macro Lett.*, 2012, **1**, 1367-1370.
148. Y. Wang, M. Zhong, W. Zhu, C.-H. Peng, Y. Zhang, D. Konkolewicz, N. Bortolamei, A. A. Isse, A. Gennaro and K. Matyjaszewski, *Macromolecules*, 2013, **46**, 3793-3802.
149. M. Zhong, Y. Wang, P. Krys, D. Konkolewicz and K. Matyjaszewski, *Macromolecules*, 2013, **46**, 3816-3827.
150. Y. Wang, M. Zhong, Y. Zhang, A. J. D. Magenau and K. Matyjaszewski, *Macromolecules*, 2012, **45**, 8929-8932.
151. D. Konkolewicz, P. Krys, J. R. Góis, P. V. Mendonça, M. Zhong, Y. Wang, A. Gennaro, A. A. Isse, M. Fantin and K. Matyjaszewski, *Macromolecules*, 2014, **47**, 560-570.
152. F. A. Leibfarth, K. M. Mattson, B. P. Fors, H. A. Collins and C. J. Hawker, *Angew. Chem., Int. Ed.*, 2013, **52**, 199-210.
153. J. Mosnáček and M. Ilčíková, *Macromolecules*, 2012, **45**, 5859-5865.
154. S. Yamago and Y. Nakamura, *Polymer*, 2013, **54**, 981-994.
155. M. Tanabe, G. W. M. Vandermeulen, W. Y. Chan, P. W. Cyr, L. Vanderark, D. A. Rider and I. Manners, *Nat. Mater.*, 2006, **5**, 467-470.
156. J. Rzayev and J. Penelle, *Angew. Chem., Int. Ed.*, 2004, **43**, 1691-1694.
157. J. Rzayev and J. Penelle, *Macromolecules*, 2002, **35**, 1489-1490.
158. A. J. D. Magenau, N. C. Strandwitz, A. Gennaro and K. Matyjaszewski, *Science*, 2011, **332**, 81-84.
159. Y. Kwak and K. Matyjaszewski, *Macromolecules*, 2010, **43**, 5180-5183.
160. J. C. Scaiano, T. J. Connolly, N. Mohtat and C. N. Pliva, *Can. J. Chem.*, 1997, **75**, 92-97.
161. A. Goto, J. C. Scaiano and L. Maretti, *Photochem. Photobiol. Sci.*, 2007, **6**, 833-835.
162. E. Yoshida, *Colloid Polym. Sci.*, 2010, **288**, 73-78.
163. Y. Guillaneuf, D. Bertin, D. Gigmes, D.-L. Versace, J. Lalevée and J.-P. Fouassier, *Macromolecules*, 2010, **43**, 2204-2212.
164. M. A. Tasdelen, Y. Y. Durmaz, B. Karagoz, N. Bicak and Y. Yagci, *J. Polym. Sci., Part A: Polym. Chem.*, 2008, **46**, 3387-3395.
165. S. Muthukrishnan, E. H. Pan, M. H. Stenzel, C. Barner-Kowollik, T. P. Davis, D. Lewis and L. Barner, *Macromolecules*, 2007, **40**, 2978-2980.
166. Y.-Z. You, C.-Y. Hong, R.-K. Bai, C.-Y. Pan and J. Wang, *Macromol. Chem. Phys.*, 2002, **203**, 477-483.
167. D.-C. Wu, C.-Y. Hong, C.-Y. Pan and W.-D. He, *Polym. Int.*, 2003, **52**, 98-103.
168. M. Tanabe and I. Manners, *J. Am. Chem. Soc.*, 2004, **126**, 11434-11435.
169. X. Zheng, M. Yue, P. Yang, Q. Li and W. Yang, *Polym. Chem.*, 2012, **3**, 1982-1986.
170. B. P. Fors and C. J. Hawker, *Angew. Chem., Int. Ed.*, 2012, **51**, 8850-8853.

171. D.-L. Versace, Y. Guillaneuf, D. Bertin, J. P. Fouassier, J. Lalevee and D. Gigmes, *Org. Biomol. Chem.*, 2011, **9**, 2892-2898.
172. S. Yamago, Y. Ukai, A. Matsumoto and Y. Nakamura, *J. Am. Chem. Soc.*, 2009, **131**, 2100-2101.
173. Y. Nakamura, T. Arima, S. Tomita and S. Yamago, *J. Am. Chem. Soc.*, 2012, **134**, 5536-5539.
174. T. Otsu, *J. Polym. Sci., Part A: Polym. Chem.*, 2000, **38**, 2121-2136.
175. A. Błedzki, D. Braun and K. Titzschkau, *Makromol. Chem.*, 1983, **184**, 745-754.
176. J. M. R. Narayanam and C. R. J. Stephenson, *Chem. Soc. Rev.*, 2011, **40**, 102-113.
177. N. J. Treat, B. P. Fors, J. W. Kramer, M. Christianson, C.-Y. Chiu, J. R. d. Alaniz and C. J. Hawker, *ACS Macro Lett.*, 2014, **3**, 580-584.
178. M. A. Tasdelen, M. Uygun and Y. Yagci, *Macromol. Rapid Commun.*, 2011, **32**, 58-62.
179. D. Konkolewicz, K. Schröder, J. Buback, S. Bernhard and K. Matyjaszewski, *ACS Macro Lett.*, 2012, **1**, 1219-1223.
180. R. B. Merrifield, *J. Am. Chem. Soc.*, 1963, **85**, 2149-2154.
181. Y. Hibi, M. Ouchi and M. Sawamoto, *Angew. Chem., Int. Ed.*, 2011, **50**, 7434-7437.
182. N. Badi and J.-F. Lutz, *Chem. Soc. Rev.*, 2009, **38**, 3383-3390.
183. J.-F. Lutz, M. Ouchi, D. R. Liu and M. Sawamoto, *Science*, 2013, **341**, 628-637
184. S. Pfeifer, Z. Zarafshani, N. Badi and J.-F. Lutz, *J. Am. Chem. Soc.*, 2009, **131**, 9195-9197.
185. G. Gody, T. Maschmeyer, P. B. Zetterlund and S. Perrier, *Nat. Commun.*, 2013, **4**, 2505-2513
186. G. Gody, T. Maschmeyer, P. B. Zetterlund and S. Perrier, *Macromolecules*, 2014, **47**, 639-649.
187. P. B. Zetterlund, G. Gody and S. Perrier, *Macromol. Theory Simul.*, 2014, **23**, 331-339.
188. G. Gody, T. Maschmeyer, P. B. Zetterlund and S. Perrier, *Macromolecules*, 2014, **47**, 3451-3460.
189. J. Chiefari, J. Jeffery, R. T. A. Mayadunne, G. Moad, E. Rizzardo and S. H. Thang, *Macromolecules*, 1999, **32**, 7700-7702.
190. M. C. Grady, W. J. Simonsick and R. A. Hutchinson, *Macromol. Symp.*, 2002, **182**, 149-168.

Chapter 2

The Importance of Ligand Reactions in Cu(0)-mediated Living Radical Polymerisation of Acrylates

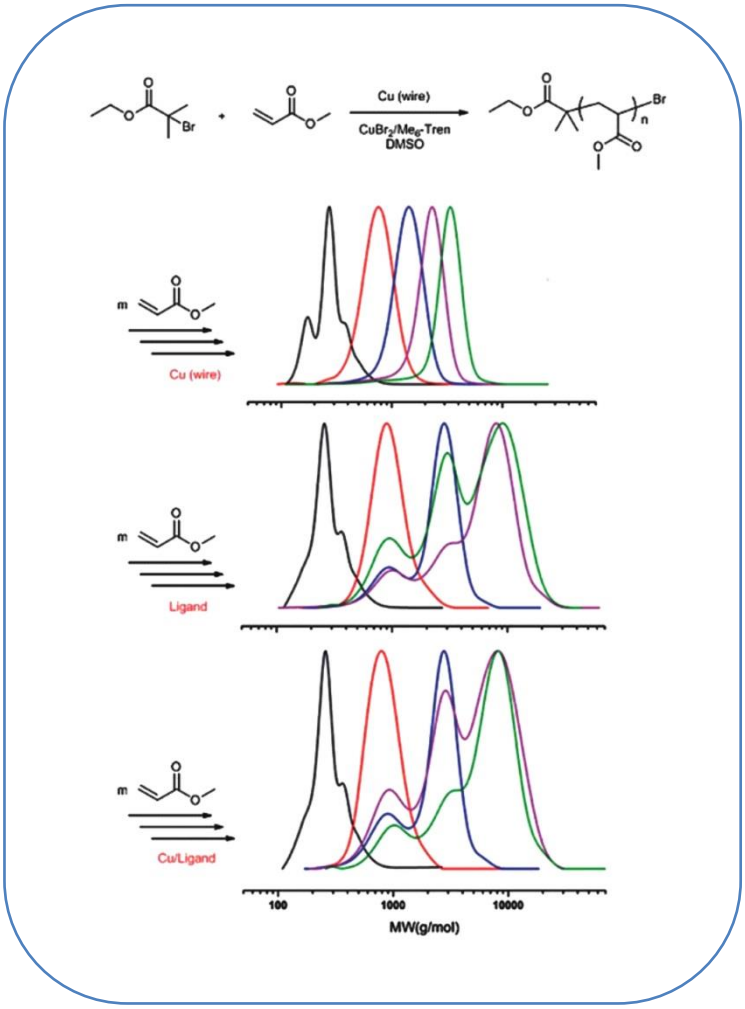

Ligand-mediated termination events occur during the homopolymerisation of methyl acrylate (MA) under SET-LRP (Cu(0)-mediated) conditions. Careful optimisation of [initiator]/[Me_6-Tren] ratios is required to reduce termination in order to achieve optimum polymerisation.

2.1 Introduction

Copper-mediated living radical polymerisations rely on the equilibrium between active and dormant growing polymer chains. In [$L_xCu(I)$] (L=donor ligand(s))-mediated processes (ATRP[1-3]) activation is achieved by a [$L_xCu(I)X$] complex (where X=Cl, Br, *etc*.). Control is subsequently inferred by the accumulation of deactivating [$L_xCu(II)X_2$] species arising from bimolecular radical–radical termination, thus invoking a persistent radical effect[4-6]. Alternatively, the Cu(0)-mediated reaction, SET-LRP (single electron transfer-living radical polymerisation) utilises Cu(0) as an activator with the proposed mechanism citing the disproportionation of *in situ* formed [$L_xCu(I)X$], to 'nascent' Cu(0) and [$L_xCu(II)X_2$] as a key step in the process[7-11]. Usually, [$L_xCu(I)$]-mediated reactions can be carried out in a range of solvents (both polar and non-polar) and require relatively large amounts of catalyst. Established ligands for these reactions include chelating pyridines (*e.g*. bpy, TPMA)[2, 12, 13], pyridine imines[14] and amines[15]. A spectrum of reactivity suggests that multi-dentate tertiary amine ligands (*e.g*. Me_6-Tren)[15] are highly suited for acrylate polymerisation and provide greater stabilisation of Cu(II) relative to Cu(I), whilst bidentate pyridine-imines ligands seem ideal for methacrylates giving stability to Cu(I) by accepting electron density into low-lying π^* orbitals *via* metal to ligand charge transfer[16].

Conversely, Cu(0)-mediated processes require polar/coordinating solvents[17-26] such as DMSO, DMF, alcohols, aqueous media or ionic liquids to facilitate disproportionation of [Cu(I)], which requires active ligands that stabilise [$L_xCu(II)X_2$](Me_6-Tren) in preference to [$L_xCu(I)X$] (pyridine imines)[27]. Under SET-LRP conditions, polymerisations can reach very high conversion, with minimal bimolecular termination and near-perfect terminal end-group (ω-bromo) functionality[28-31]. This level of livingness/control has recently been exemplified by *in situ* chain extension of acrylic polymers for the preparation

of linear[32, 33] and star[34] block co-polymers with highly ordered sequence control. Investigators reported the synthesis of decablock co-polymer using Cu(0) wire and sub-stoichiometric amounts of $CuBr_2$ and Me_6-Tren relative to initiator (0.05 and 0.18 eq. respectively) to activate the reaction and maintain a controlled catalytic cycle.

2.2 Results and Discussion

In our hands, polymerisation of methyl acrylate (MA), followed by *in situ* chain extension with additional aliquots of degassed MA was limited to only three extensions (Figure 2.1). Upon addition of a fourth aliquot of MA little or no consumption of monomer was observed by either ^{1}H NMR and SEC.

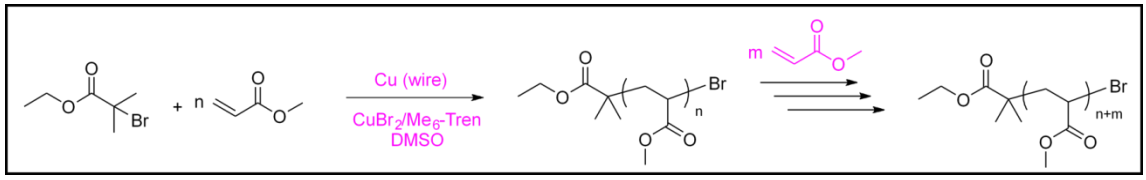

Scheme 2.1: Sequential addition of MA utilising [MA]:[EBiB]:[Me_6-Tren]:[$CuBr_2$]:[copper wire]=[3]:[1]:[0.18]:[0.05]:[5 cm]

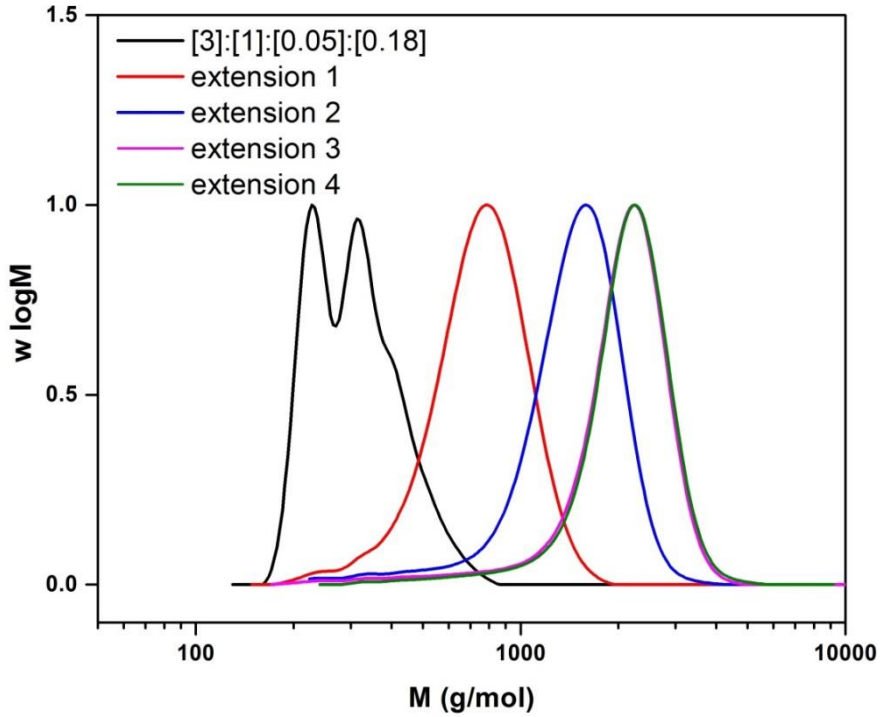

Figure 2.1: SEC of the pentablock homopolymer utilising [MA]:[EBiB]:[Me_6-Tren]:[$CuBr_2$]:[copper wire]=[3]:[1]:[0.18]:[0.05]:[5 cm]

This was attributed to either accumulated termination and/or an equilibrium shift towards the dormant chains. MALDI-ToF-MS analysis of the crude mixture revealed good ω-bromo end-group fidelity (Figure 2.2), suggesting minimal termination. Thus, the lack of conversion was likely due to a decrease in the rate of polymerisation.

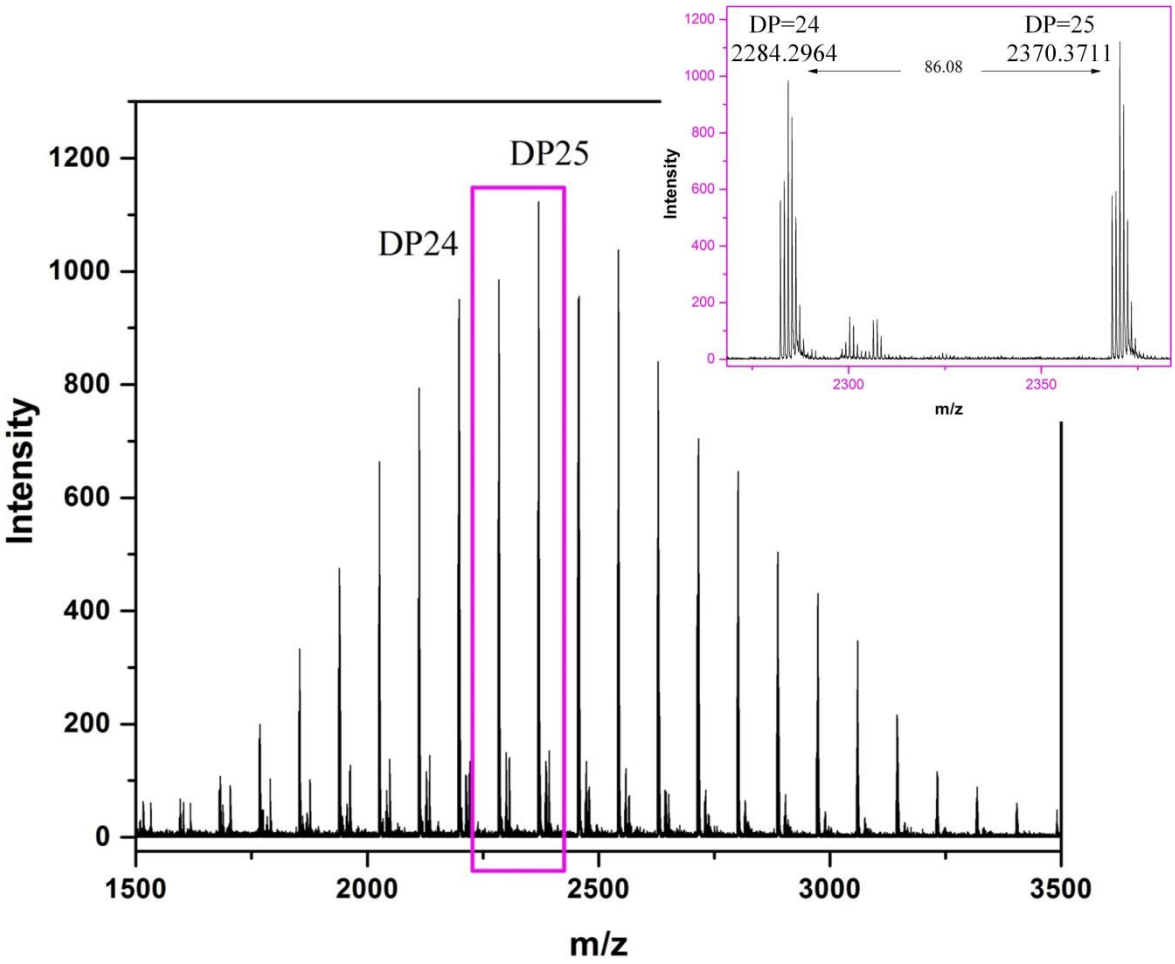

Figure 2.2: MALDI-ToF-MS analysis of the final pentablock copolymer utilising [MA]:[EBiB]:[Me_6-Tren]:[$CuBr_2$]:[copper wire]=[3]:[1]:[0.18]:[0.05]:[5 cm]

In order to circumvent this, a series of parallel experiments were performed in which each monomer addition was supplemented by the addition of a second variable, namely; Cu(0) wire (5 cm), Me_6-Tren or Cu(0) wire and Me_6-Tren concurrently.

Sequential addition of degassed MA, with Cu(0) wire resulted in successful chain extension beyond our previous limit. Four additions resulted in full conversion by ^{1}H NMR and a clear shift of the molecular weight distribution by SEC analysis. Furthermore, a rate

enhancement was observed in the presence of additional Cu(0). In previous experiments the rate of polymerisation was found to gradually decrease upon each monomer addition, with up to 24 h needed for the penta-block synthesis and 48 h for the final additions towards the decablock reported[32, 33]. However, in the presence of additional Cu(0), complete conversion was observed within 5 h upon each addition of monomer.

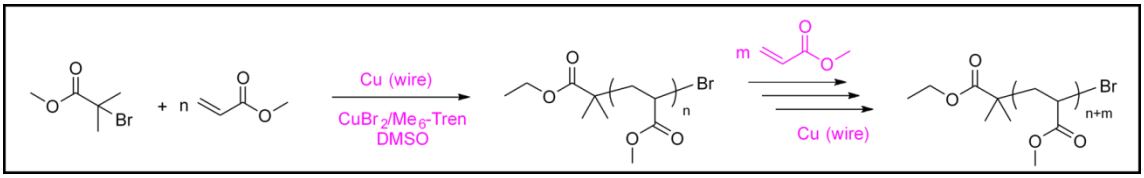

Scheme 2.2: Sequential addition of MA together with fresh activated copper wire utilising initial conditions [MA]:[EBiB]:[Me_6-Tren]:[$CuBr_2$]:[copper wire]=[3]:[1]:[0.18]:[0.05]:[5 cm]

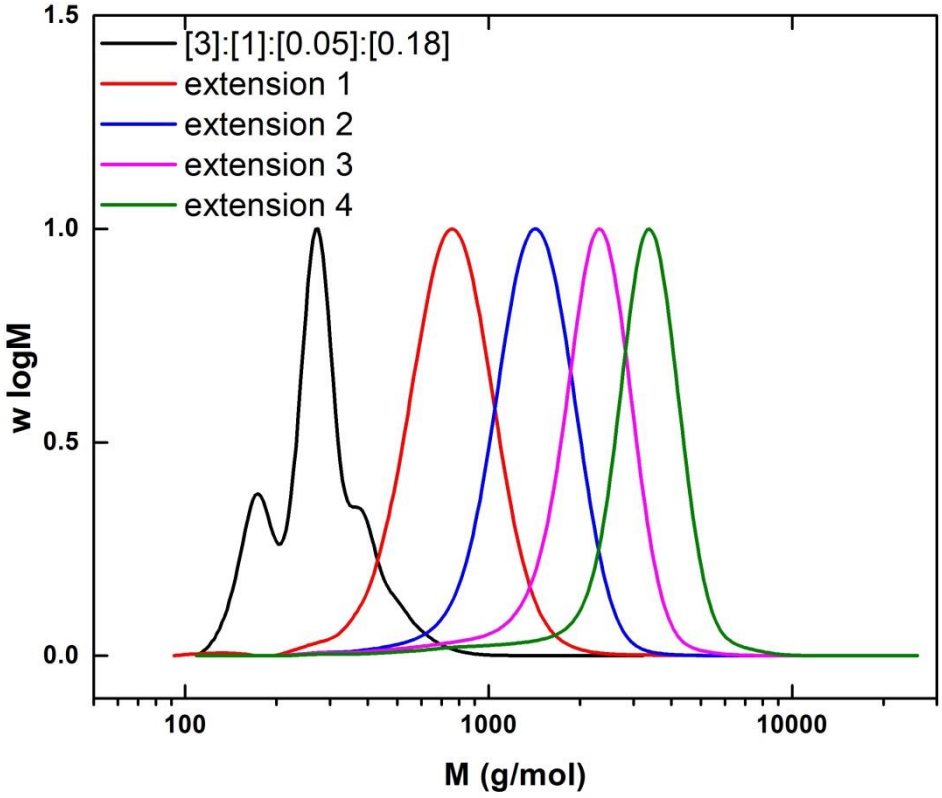

Figure 2.3: SEC of the pentablock homopolymer utilising [MA]:[EBiB]:[Me_6-Tren]:[$CuBr_2$]:[copper wire]=[3]:[1]:[0.18]:[0.05]:[5 cm]; copper wire upon every monomer addition.

The inclusion of Me_6-Tren with each monomer addition was less successful. Initially, chain extension occurred as desired, however, upon addition of the second, third and fourth aliquot of MA, significant low molecular weight tailing was observed with SEC

traces displaying multi-modal distributions indicative of termination on the addition of reagents (Figure 2.4).

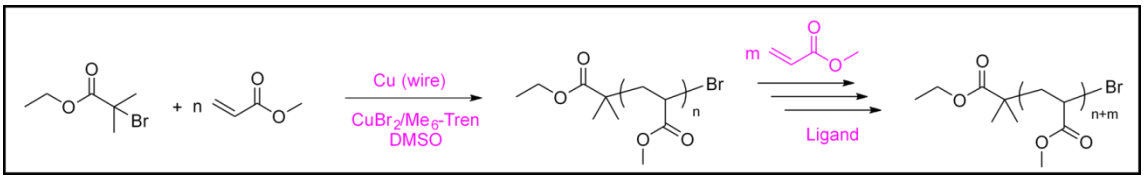

Scheme 2.3: Sequential addition of MA together with Me_6-Tren utilising initial conditions [MA]:[EBiB]:[Me_6-Tren]:[$CuBr_2$]:[copper wire]=[3]:[1]:[0.18]:[0.05]:[5 cm]

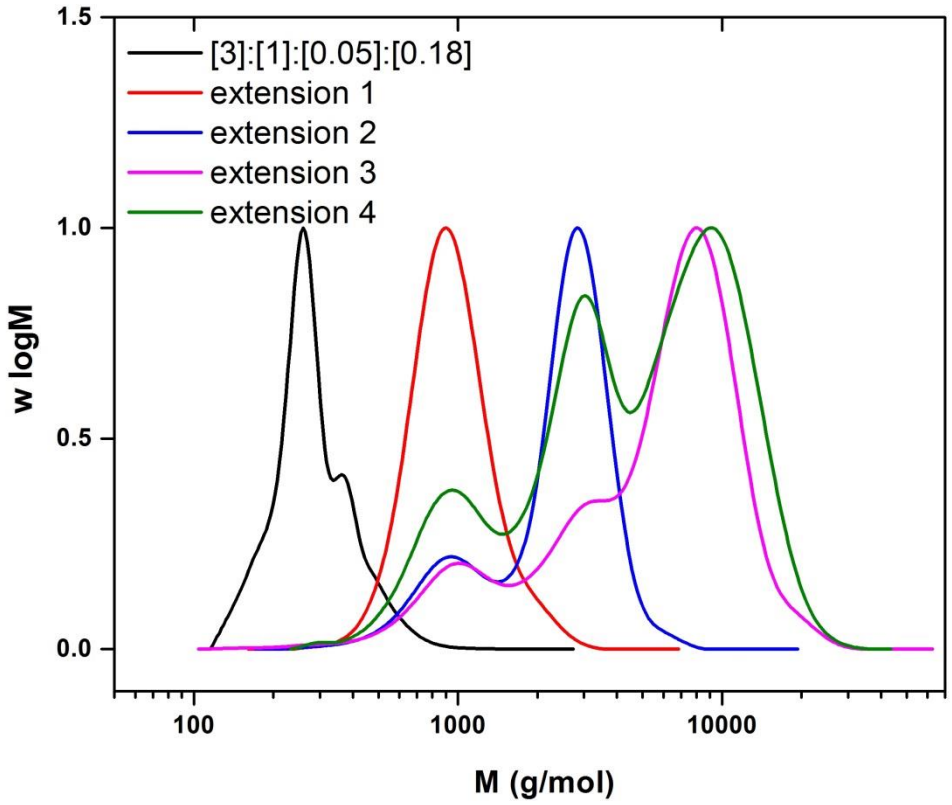

Figure 2.4: SEC of the pentablock homopolymer utilising [MA]:[EBiB]:[Me_6-Tren]:[$CuBr_2$]:[copper wire]=[3]:[1]:[0.18]:[0.05]:[5 cm]; Me_6-Tren upon every monomer addition.

Interestingly, near-identical observations were made when both Cu(0) wire and Me_6-Tren were added along with each aliquot of MA (Figure 2.5). It was hypothesised that the termination observed was associated with the increasing concentration of Me_6-Tren either *via* chain transfer to ligand or nucleophilic substitution of the secondary ω-bromine by uncomplexed ligand, resulting in quaternisation.

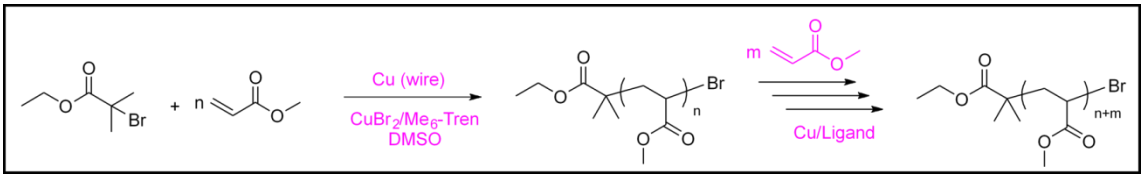

Scheme 2.4: Sequential addition of MA together with copper wire and Me_6-Tren utilising initial conditions [MA]:[EBiB]:[Me_6-Tren]:[$CuBr_2$]:[copper wire]=[3]:[1]:[0.18]:[0.05]:[5 cm]

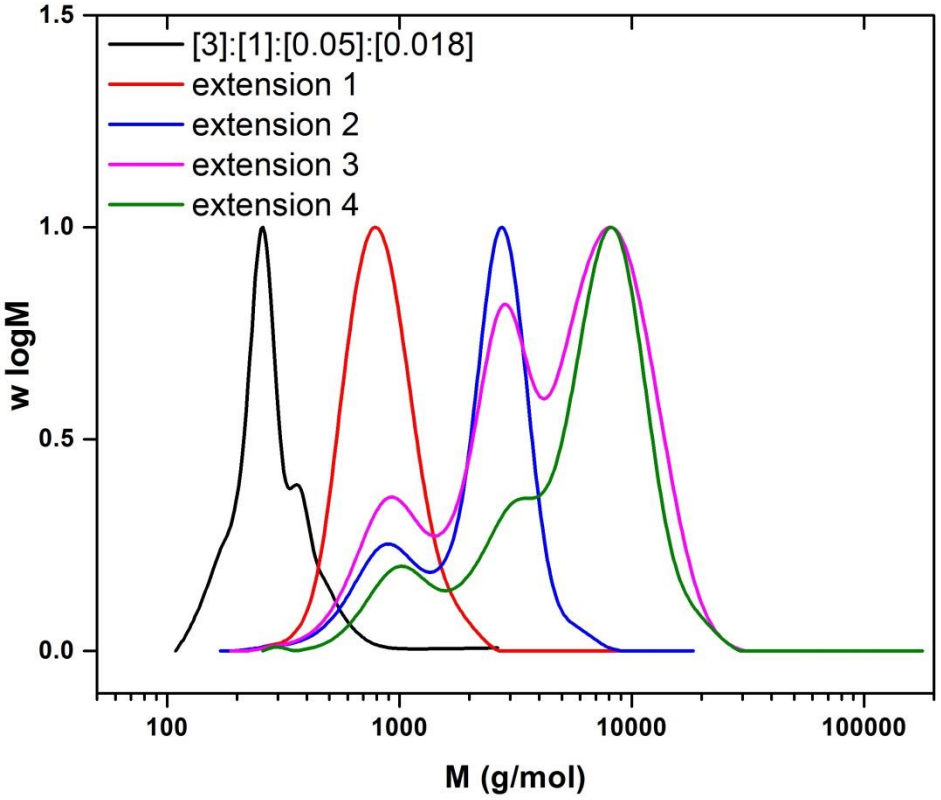

Figure 2.5: SEC of the pentablock homopolymer utilising [MA]:[EBiB]:[Me_6-Tren]:[$CuBr_2$]:[copper wire]=[3]:[1]:[0.18]:[0.05]:[5 cm]; Me_6-Tren /copper wire upon every monomer addition.

The feasibility of the quaternisation reaction was investigated using ethyl-2-bromopropionate (EBP) as a mimic for the poly(methyl acrylate) (PMA) ω-bromo chain end. EPB and Me_6-Tren (1 : 1) were dissolved in both d_6-DMSO and $CDCl_3$ and the reaction progress was monitored by ^1H and ^{13}C NMR. Within 30 minutes, significant evidence for quaternisation was seen in the form of additional peaks in both ^1H and ^{13}C NMR spectra (Figure 2.6), which became more intense over the timescale of a standard polymerisation (3 hours). A key shift was observed for the methine proton and methyl group which in EBP are found at 4.67 and 1.72 ppm respectively. However, upon

quaternisation the methine proton shifts to 5.02 ppm whilst retaining its coupling to the methyl group now found at 1.59 ppm. These shifts were mirrored in the ^{13}C NMR spectra whereby quaternisation shifted the *a*-carbon downfield from 40.8 to 66.3 ppm and the methyl carbon shifted from 13.5 to 12.5 ppm (Figure 2.6). Furthermore, precipitation was observed over time in DMSO, our solvent of choice for the polymerisation reactions.

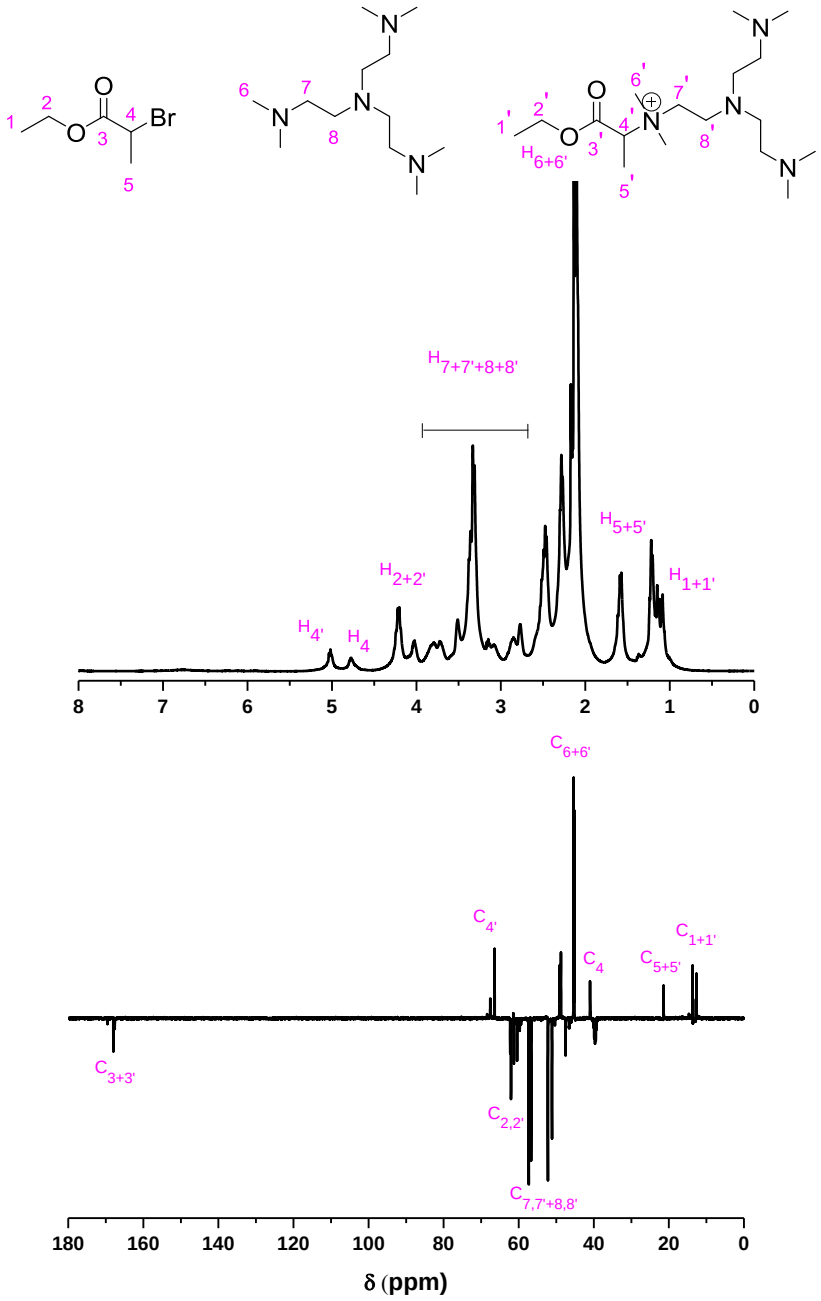

Figure 2.6: ^{1}H NMR (top) and ^{13}C NMR (bottom) of EBP from the proposed quaternisation reaction mixture.

HR-ESI-MS of the precipitate confirmed the presence of the quaternised product with a peak for $[C_{17}H_{39}N_4O_2]^+$ arising at *m/z* 331.3068, identical to the simulated data. No evidence for base-mediated elimination, forming ethyl acrylate, was observed at any point during the reaction.

In order to further investigate the proposed connection between ligand concentration and polymer dormancy under these conditions, a series of reactions were carried out with varying quantities of Me_6-Tren employed relative to the initiator. In all cases, 'controlled/living' characteristics were observed with close agreement between theoretical and observed molecular weight and narrow molecular weight distributions (Table 2.1). SEC analysis revealed narrow, symmetrical molecular weight distributions with dispersity indices ~1.10 (Figure 2.7). There was no indication of termination, either at low molecular weight due to chain transfer or quaternisation, or at high molecular weight due to bimolecular termination.

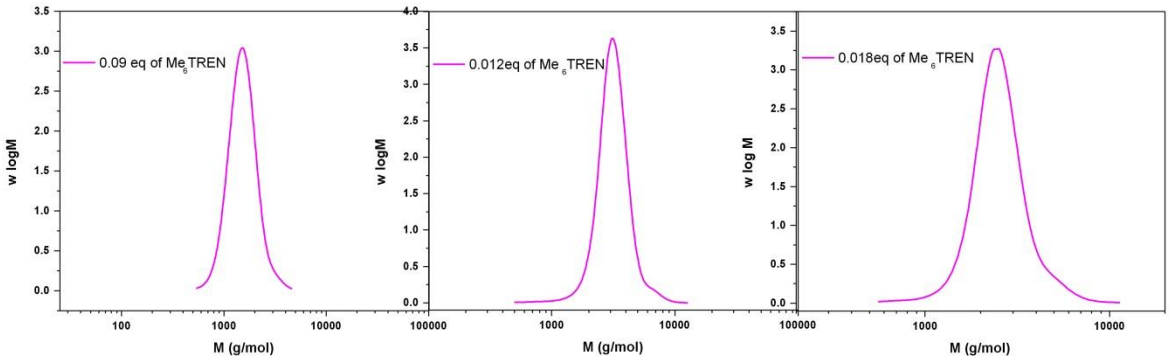

Figure 2.7: SEC traces employing different equivalents of Me_6-Tren.

Table 2.1: Hopolymerisations of MA with various ligand loadings

[M]:[I]:[Cu(II)]:[L]	Conv (%)	$M_{n,th}$ (g/mol)	$M_{n,SEC}$ (g/mol)	$Đ$
[20]:[1]:[0.05]:[0.09]	99	1900	1600	1.09
[35]:[1]:[0.05]:[0.12]	99	3200	3000	1.09
[35]:[1]:[0.05]:[0.18]	99	3200	2800	1.11

However, MALDI-TOF analysis of these polymers revealed two modes of termination in the presence of higher amounts of Me_6-Tren (0.18 eq. with respect to the initiator). Termination by radical chain transfer to Me_6-Tren results in "dead" polymer chains (Peak 2, Figure 2.8). The second type of termination arises due to ligand quaternisation at the ω-chain end, analogous to that observed with EBP (Peak 3, Figure 2.8). In both instances, termination results in loss of bromine from the growing polymer chains and thus further activation by the catalyst system and efficient chain extension is no longer possible. Peak 1 (Figure 2.8) consists of the dominant polymer distribution which corresponds to the ω-bromo-terminated poly(MA).

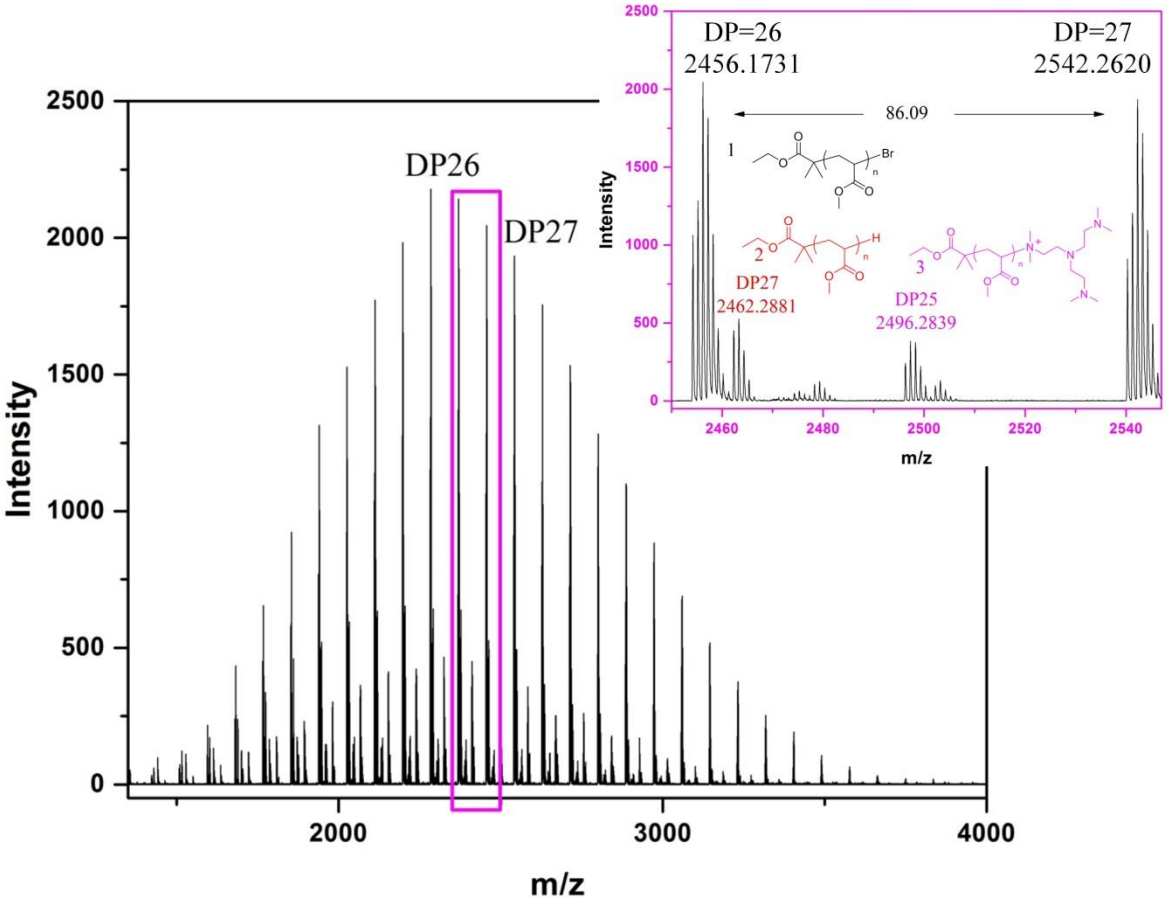

Figure 2.8: MALDI-ToF-MS of MA employing 0.18 eq of Me_6-Tren

When the amount of Me_6-Tren is reduced (0.12 eq.), MALDI-ToF-MS analysis revealed suppression of both modes of termination (Figure 2.9). Optimum polymerisation

conditions were obtained when 0.12 eq. Me_6-Tren was employed, as quaternisation was eliminated and termination by chain transfer was significantly reduced.

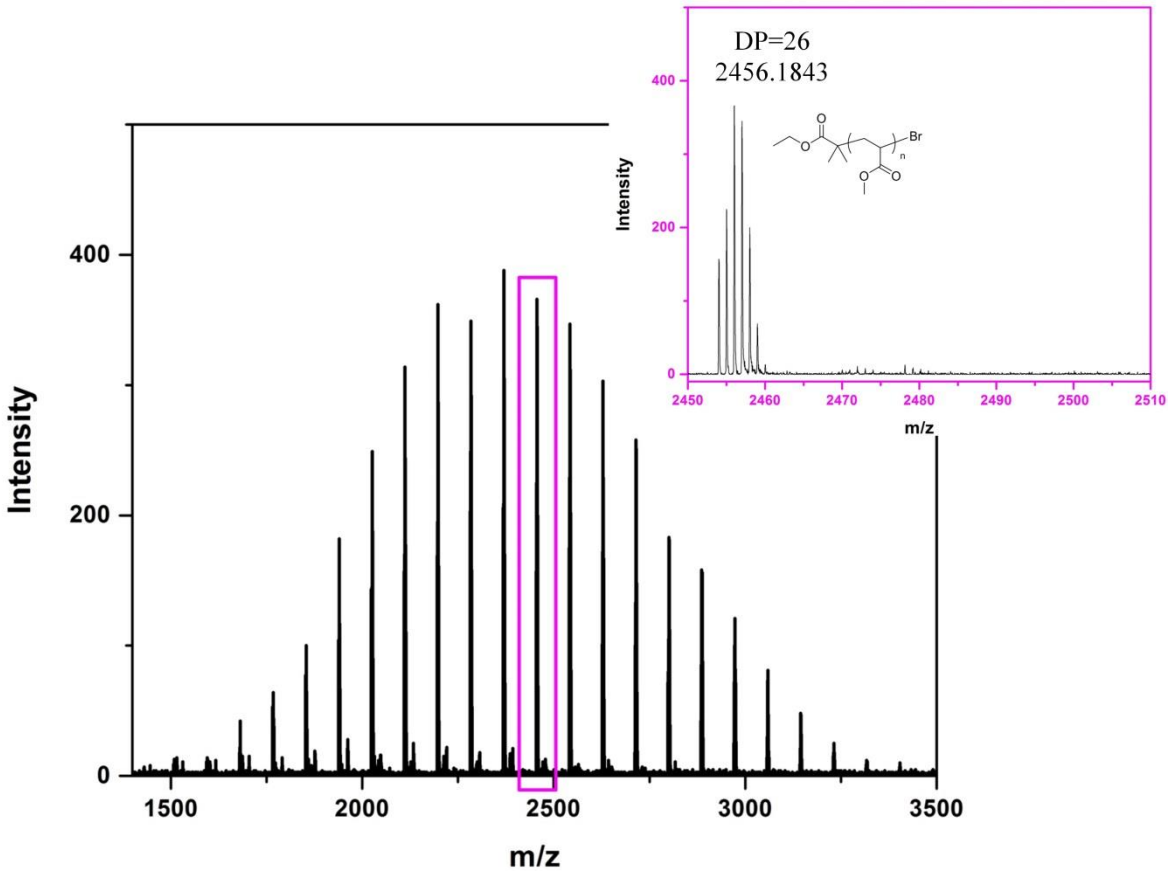

Figure 2.9: MALDI-ToF-MS of MA employing 0.12 eq of Me_6-Tren; Optimised conditions.

If the amount of Me_6-Tren is reduced further to 0.09 eq., chain transfer and quaternisation can be suppressed but this arises at the expense of increased bimolecular termination (Figure 2.10). Similar termination events were also observed when a bifunctional initiator was employed and methyl acrylate was replaced with butyl acrylate[35]. Again, optimum conditions suggest 0.12 eq. of ligand with respect to initiator in order to minimise termination. The different types of termination events are summarised in Figure 2.11.

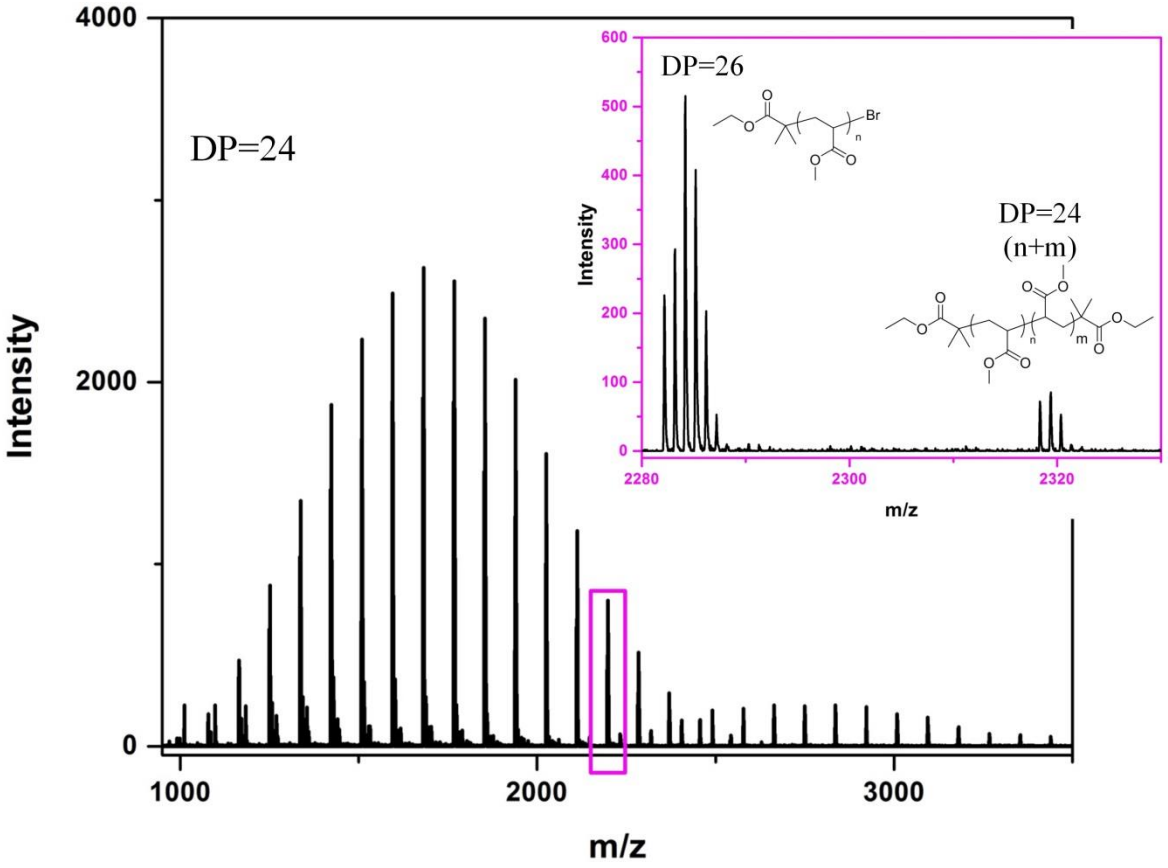

Figure 2.10: MALDI-ToF-MS of MA employing 0.09 eq of Me_6-Tren.

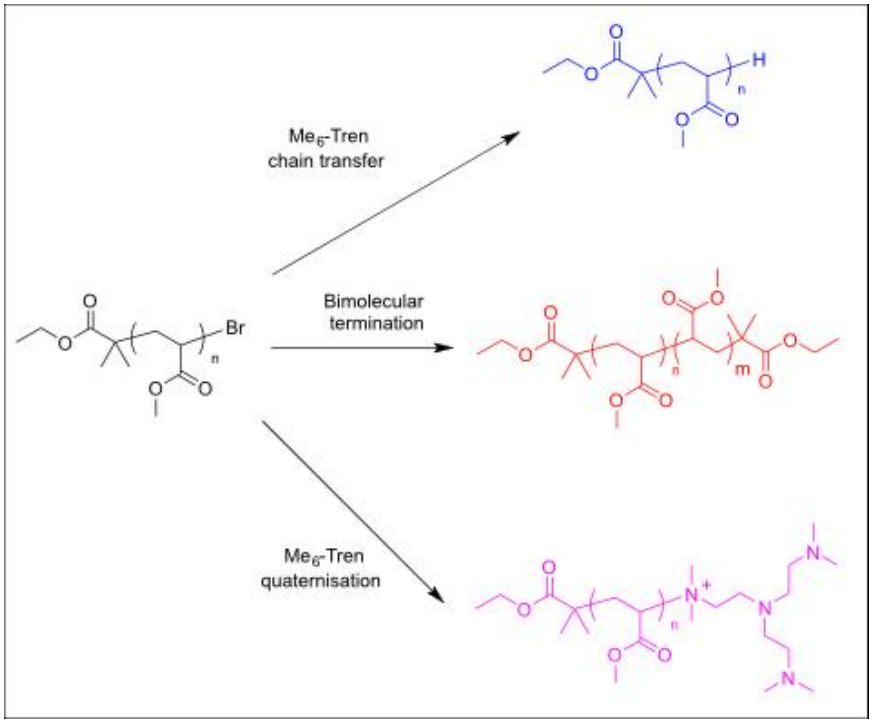

Figure 2.11: Different types of termination during a Cu(0)-mediated living radical polymerisation.

2.3 Conclusions

In summary, this investigation has shown that a relatively small change in ligand concentration can dramatically affect the end-group fidelity of polymer chains *via* this polymerisation methodology. Both mono- and bifunctional initiators have been employed in the synthesis of poly(acrylates). Despite the observation of symmetrical, narrow molecular weight distributions by SEC analysis, MALDI-ToF-MS analysis revealed additional peak distributions arising from two possible modes of ligand-dependent termination. It is very likely that these termination processes occur, to some extent, in all SET-LRP and ATRP polymerisations of acrylic monomers, especially with acrylates, where Me_6-Tren, and other tertiary amine-based ligands, are employed as the ligand. Fortunately, it has been shown that optimisation can suppress these termination reactions to afford very high end-group fidelity, the integrity of which is vital for *in situ* chain extension or ω-functionalisation.

2.4 Experimental

2.4.1 Materials

Methyl acrylate (MA), ethyl 2-bromopropionate and $CuBr_2$ were purchased from Aldrich and used as received. Me_6-Tren were synthesised according to previously reported literature. Cu(0) (gauge 0.25 mm) wire was purchased from Comax Engineered wires and was treated by immersion in conc. HCl prior to use. Solvents were purchased from Fisher Scientific and used as received.

2.4.2 Apparatus

^{1}H NMR spectra were recorded on a Bruker DPX-300, DPX-400 or DRX-500 spectrometers in $CDCl_3$ unless otherwise stated. Chemical shifts are given in ppm downfield from the internal standard tetramethylsilane. Size exclusion chromatography

(SEC) measurements were conducted using an Agilent 1260 SEC-MDS fitted with differential refractive index (DRI), light scattering (LS) and viscometry (VS) detectors equipped with 2 × PLgel 5 mm mixed-D columns (300 × 7.5 mm), 1 × PLgel 5 mm guard column (50 × 7.5 mm) and autosampler. Narrow linear poly (methyl methacrylate) standards in range of 200 to 1.0 × 10^6 g·mol^{-1} were used to calibrate the system. All samples were passed through 0.45 μm PTFE filter before analysis. The mobile phase was chloroform with 2% triethylamine eluent at a flow rate of 1.0 mL/min. SEC data was analysed using Cirrus v3.3 software with calibration curves produced using Varian Polymer laboratories Easi-Vials linear poly(methyl methacrylate) standards (200-4.7×10^5 g/mol).

2.4.3 General procedures

2.4.3.1 General procedure for the homopolymerisation of MA

Filtered MA (2 mL, 22.2 mmol, 35 eq), EBiB (94 μL, 0.6 mmol, 1 eq), $CuBr_2$ (6.7 mg, 30 μmol, 0.05 eq), Me_6-Tren (0.09-0.18 eq) and DMSO (2 mL) were deoxygenated by purging with nitrogen for 30 mins, during which time Cu(0) wire (5 cm) was immersed in conc. HCl. The Cu(0) wire was removed and thoroughly rinsed with acetone and water and then air dried. Polymerisation commenced upon addition of the Cu(0) wire to the degassed reaction mixture. Samples were taken periodically and conversions were measured using ^{1}H NMR and SEC analysis. Upon completion, the reaction mixture was diluted with THF then passed through an alumina column to remove traces of remaining copper and ligand. The filtrate was concentrated and the polymers were isolated by precipitation into MeOH/H_2O mixtures.

2.4.3.2 General procedure for *in situ* chain extension reactions

The general procedure for MA homopolymerisation was followed. Upon detection of >99% conversion a 1 : 1 mixture of degassed MA and DMSO was added to the reaction mixture *via* degassed syringe. Where necessary, additional ligand (0.18 eq) was added to the monomer/solvent mixture prior to degassing and additional Cu(0) wire (5 cm) was activated by immersion in conc. HCl. Samples were taken periodically and conversions were measured using ^{1}H NMR and SEC analysis.

2.4.3 General procedure for the quaternisation of EBP

EBP (1 eq) and Me_6-Tren (1 eq) were dissolved in d_6-DMSO and placed in an NMR tube. Reaction progress was followed by ^{1}H NMR and ^{13}C NMR; δ (^{1}H/^{13}C 400/100 MHz) Figure S3; υ (cm^{-1}) 2955, 2826, 1733, 1624, 1467, 1204, 1023, 1004, 762; HR-ESI-MS $C_{17}H_{39}N_4O_2^+$ found 331.3068, expected 331.3068.

2.5 References

1. P. De Paoli, A. A. Isse, N. Bortolamei and A. Gennaro, *Chem. Commun.*, 2011, **47**, 3580-3582.
2. J.-S. Wang and K. Matyjaszewski, *Macromolecules*, 1995, **28**, 7901-7910.
3. K. Matyjaszewski, *Macromolecules*, 2012, **45**, 4015-4039.
4. H. Fischer, *J. Polym. Sci., Part A: Polym. Chem.*, 1999, **37**, 1885-1901.
5. H. Fischer, *Macromolecules*, 1997, **30**, 5666-5672.
6. H. Fischer, *Chem. Rev.*, 2001, **101**, 3581-3610.
7. N. H. Nguyen, H.-J. Sun, M. E. Levere, S. Fleischmann and V. Percec, *Polym. Chem.*, 2013, **4**, 1328-1332.
8. M. E. Levere, N. H. Nguyen, X. Leng and V. Percec, *Polym. Chem.*, 2013, **4**, 1635-1647.
9. B. M. Rosen, X. Jiang, C. J. Wilson, N. H. Nguyen, M. J. Monteiro and V. Percec, *J. Polym. Sci., Part A: Polym. Chem.*, 2009, **47**, 5606-5628.
10. B. M. Rosen and V. Percec, *Chem. Rev.*, 2009, **109**, 5069-5119.

11. V. Percec, T. Guliashvili, J. S. Ladislaw, A. Wistrand, A. Stjerndahl, M. J. Sienkowska, M. J. Monteiro and S. Sahoo, *J. Am. Chem. Soc.*, 2006, **128**, 14156-14165.
12. J.-S. Wang and K. Matyjaszewski, *J. Am. Chem. Soc.*, 1995, **117**, 5614-5615.
13. J. Xia and K. Matyjaszewski, *Macromolecules*, 1999, **32**, 2434-2437.
14. D. M. Haddleton, A. J. Clark, M. C. Crossman, D. J. Duncalf, A. M. Heming, S. R. Morsley and A. J. Shooter, *Chem. Commun.*, 1997, **13**, 1173-1174.
15. J. Xia, S. G. Gaynor and K. Matyjaszewski, *Macromolecules*, 1998, **31**, 5958-5959.
16. W. Tang and K. Matyjaszewski, *Macromolecules*, 2006, **39**, 4953-4959.
17. V. Percec and C. Grigoras, *J. Polym. Sci., Part A: Polym. Chem.*, 2005, **43**, 5609-5619.
18. M. E. Levere, I. Willoughby, S. O'Donohue, A. de Cuendias, A. J. Grice, C. Fidge, C. R. Becer and D. M. Haddleton, *Polym. Chem.*, 2010, **1**, 1086-1094.
19. G. Lligadas, B. M. Rosen, M. J. Monteiro and V. Percec, *Macromolecules*, 2008, **41**, 8360-8364.
20. G. Lligadas and V. Percec, *J. Polym. Sci., Part A: Polym. Chem.*, 2008, **46**, 2745-2754.
21. G. Lligadas and V. Percec, *J. Polym. Sci., Part A: Polym. Chem.*, 2008, **46**, 6880-6895.
22. N. H. Nguyen, B. M. Rosen, X. Jiang, S. Fleischmann and V. Percec, *J. Polym. Sci., Part A: Polym. Chem.*, 2009, **47**, 5577-5590.
23. N. H. Nguyen and V. Percec, *J. Polym. Sci., Part A: Polym. Chem.*, 2011, **49**, 4227-4240.
24. X. Jiang, S. Fleischmann, N. H. Nguyen, B. M. Rosen and V. Percec, *J. Polym. Sci., Part A: Polym. Chem.*, 2009, **47**, 5591-5605.
25. N. H. Nguyen, J. Kulis, H.-J. Sun, Z. Jia, B. van Beusekom, M. E. Levere, D. A. Wilson, M. J. Monteiro and V. Percec, *Polym. Chem.*, 2013, **4**, 144-155.
26. E. Nicol, T. Derouineau, F. Puaud and A. Zaitsev, *J. Polym. Sci., Part A: Polym. Chem.*, 2012, **50**, 3885-3894.
27. S. Perrier, S. P. Armes, X. S. Wang, F. Malet and D. M. Haddleton, *J. Polym. Sci., Part A: Polym. Chem.*, 2001, **39**, 1696-1707.
28. M. E. Levere, N. H. Nguyen, H.-J. Sun and V. Percec, *Polym. Chem.*, 2013, **4**, 686-694.
29. N. H. Nguyen, M. E. Levere, J. Kulis, M. J. Monteiro and V. Percec, *Macromolecules*, 2012, **45**, 4606-4622.
30. N. H. Nguyen, M. E. Levere and V. Percec, *J. Polym. Sci., Part A: Polym. Chem.*, 2012, **50**, 860-873.
31. F. Nyström, A. H. Soeriyadi, C. Boyer, P. B. Zetterlund and M. R. Whittaker, *J. Polym. Sci., Part A: Polym. Chem.*, 2011, **49**, 5313-5321.
32. A. H. Soeriyadi, C. Boyer, F. Nyström, P. B. Zetterlund and M. R. Whittaker, *J. Am. Chem. Soc.*, 2011, **133**, 11128-11131.

33. C. Boyer, A. H. Soeriyadi, P. B. Zetterlund and M. R. Whittaker, *Macromolecules*, 2011, **44**, 8028-8033.
34. C. Boyer, A. Derveaux, P. B. Zetterlund and M. R. Whittaker, *Polym. Chem.*, 2012, **3**, 117-123.
35. A. Anastasaki, C. Waldron, P. Wilson, R. McHale and D. M. Haddleton, *Polym. Chem.*, 2013, **4**, 2672-2675.

Chapter 3

Polymerisation of Long Chain Acrylates by Cu(0)-mediated Living Radical Polymerisation; High Fidelity End-group Incorporation and Modification

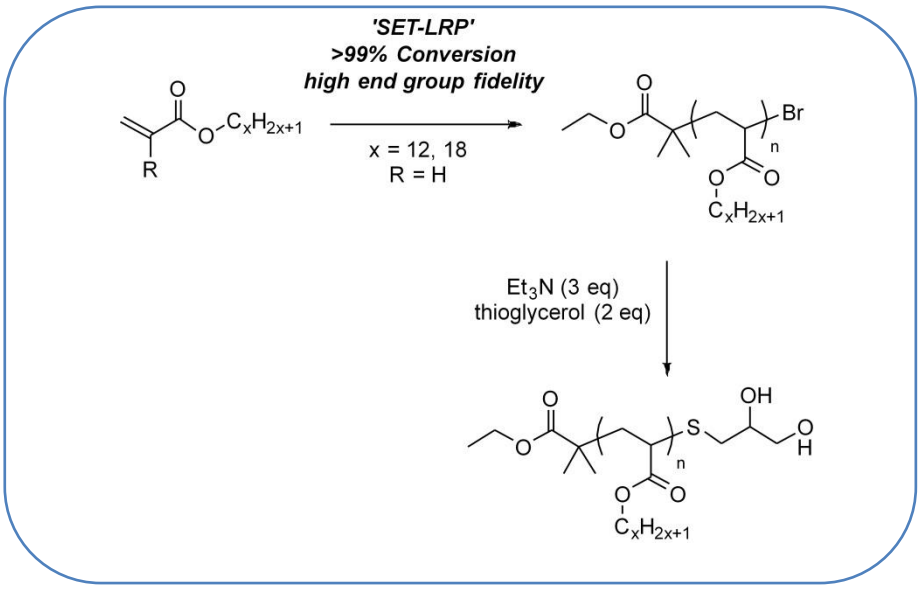

The Cu(0)-mediated polymerisation of lauryl (C_{12}) and stearyl(C_{18}) acrylate is reported under a range of reaction conditions. First-order kinetics, linear evolution of number-average molecular weight (M_n) with conversion and low dispersity (~1.10) are observed. The polymerisation of lauryl acrylate proceeds either homogeneously or in a self-generated biphasic system, depending on the solvent employed, with little deviation in overall polymerisation control. The near-quantitative retention of ω-bromo end groups is exploited via nucleophilic thio-bromine substitution with thioglycerol to yield highly hydrophobic polymers with polar head groups. Modification is spectroscopically confirmed by both NMR and MALDI-ToF-MS.

3.1 Introduction

Polymers composed of monomers containing long hydrophobic side chains have interesting materials properties. Lauryl (dodecyl) containing acrylic and methacrylic polymers in particular, are used in a variety of applications requiring high oil solubility[1-3]. To date, various controlled/living polymerisation techniques have been used for the radical polymerisation of these monomers, including Cu(I)-mediated polymerisation[3-5], reversible addition-fragmentation chain transfer polymerisation (RAFT)[6, 7], nitroxide-mediated polymerisation (NMP)[8] and single electron transfer degenerative chain transfer living radical polymerisation (SET-DTLRP)[9]. In regulating molecular weight (MW), dispersity (*Đ*) and end-group fidelity *etc*., such techniques promise added value with enhanced chemical functionality and an ability to tune physical properties of the final product, allowing greater diversity of application for long alkyl chain containing polymers.

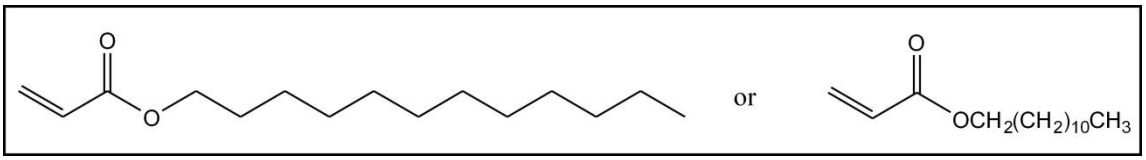

Scheme 3.1: Dodecyl or lauryl acrylate monomer

Cu(0)-mediated living radical polymerisation[10, 11] allows access to well-defined polymers at ambient temperatures with very low dispersities and excellent end-group fidelity. Typical dispersity values are in the range of 1.05-1.10 up to very high monomer conversion (>99%) with little quantifiable bimolecular termination observed for a variety of acrylates[12-15]. Careful optimisation of [initiator]/[ligand] (Me_6-Tren) ratios is therefore essential to suppress termination in order to achieve optimum polymerisation (See Chapter 2).

The solvent choice in SET-LRP has received significant attention[16, 17]. Percec and co-workers, in setting out the proposed mechanism of this Cu(0)-mediated polymerisation,

emphasise a necessity for polar solvents (*e.g.* DMSO, alcohols, water)[17-23], stipulating that such solvents promote disproportionation between two *in situ* generated Cu(I) species into Cu(0) and Cu(II) analogues (disproportionation equilibrium constants are reported to be as high as 10^6 in water[24, 25]). A particularly interesting aspect of this polarity requirement is a reported loss of control in SET-LRP of increasingly hydrophobic monomers[26], underlining how a delicate polarity balance is necessary in both promoting disproportionation, whilst retaining high solubility of the polymer and/or monomer. In the same report it was shown that control can be maintained in SET-LRP systems in which phase separation occurs during polymerisation. Thus, the SET-LRP of *n*-butyl acrylate (*n*BA) in DMSO was found to proceed in a self-generated biphasic system, attained at a certain critical MW of polymer *i.e.* the growing polymer chains precipitate out of the initially homogeneous solvent/monomer/catalyst mixture to create a bi-phasic system composed of a (partially) solvent-swollen polymer-rich layer with a lower density solvent/monomer/catalyst layer. Interestingly, and somewhat unexpectedly, the precipitated chains are seen to continue growing in a controlled/living fashion to higher monomer conversion, despite retention of the majority of the catalyst in the non-polymer/low polymer concentration containing phase. A significant advantage of such a bi-phasic system is an ability to separate *in situ* the copper catalyst from the final product. Given the success with *n*-butyl acrylate in DMSO we thought it would be interesting to extend this strategy to higher order alkyl acrylate monomers *e.g.* lauryl acrylate (LA), which to date have shown less control on phase separation from DMSO systems[26].

In this chapter, the Cu(0)-mediated (SET-LRP) polymerisation of lauryl acrylate in a range of higher "alkyl friendly" solvents and/or binary solvent mixtures (*e.g.* IPA, toluene–MeOH, toluene–DMSO) is presented. Polymerisation of lauryl acrylate in IPA results in phase separation in a fashion similar to that previously observed in the *n*BA–

DMSO system. Interestingly, controlled growth is retained following phase separation, with low dispersity values and high end-group (bromo) fidelity observed at high conversion. Such end groups are subsequently converted into thio functionality in a quantitative manner, underlining an ability to tailor these polymers for various applications. In furthering the investigation of such longer chain hydrophobic monomers, preliminary data on the SET-LRP of stearyl(octadecyl) acrylate are also presented.

3.2 Results and discussion

The Cu-mediated radical polymerisation of higher order acrylates such as lauryl acrylate (LA) has received little attention to date. Existing examples utilise [Cu(I)X/L_n] catalysts and success is limited to systems that efficiently solubilise the highly hydrophobic monomers and retain solubility throughout the polymerisation. In our previous work, the only example of Cu(0)-mediated polymerisation of LA, the reaction was uncontrolled, giving polymer with broad dispersities. This result was perhaps not unexpected considering our choice of solvent (DMSO), which is unable to fully solubilise the monomer prior to reaction as well as being a non-solvent for the polymer. Given that the Cu(0)-mediated polymerisation of *n*-butyl acrylate (*n*BA) was reported to proceed through a self-generated biphasic system with little or no loss of activity, it was postulated that a similar protocol could prove fruitful with the higher order acrylates.

Initially the solubility of LA in a number of SET-LRP compatible solvents was investigated. In common solvents such as DMSO, DMF and MeOH, solubility proved to be poor and restrictive. However, in IPA full dissolution of LA was attained. Thus, we anticipated that Cu(0)-mediated polymerisation of LA could be achieved in IPA with either retention of polymer solubility throughout the reaction, or the capacity of IPA to support a self-generating biphasic system.

Cu(0)-mediated homopolymerisation of LA in IPA was carried out with a range of targeted degrees of polymerisation (DP=10–50, $M_{n,th}$ = 2400–12000 g mol^{-1}, Table 3.1 and Figure 3.1). The reaction conditions chosen were: [M]/[I]/[$CuBr_2$]/[Me_6-Tren]/[Cu(0)]=[DP_n]/[1]/[0.05]/[0.12]/[5 cm wire]. In particular, attention was paid to the [Me_6-Tren] with a view to minimising potential side reactions at the propagating radical end.

Table 3.1: Data for the polymerisation of LA employing IPA as the solvent ([a] ^{1}H NMR, [b] $CHCl_3$ SEC analysis)

[LA]/[I]	Conv. (%)	$M_{n,th}$[a] (g/mol)	$M_{n,GPC}$[b] (g/mol)	Đ	Solvent
10	100	2400	2200	1.08	IPA
20	100	4800	4300	1.07	IPA
30	100	7200	6700	1.05	IPA
40	100	9600	8700	1.06	IPA
50	99	12000	10500	1.07	IPA

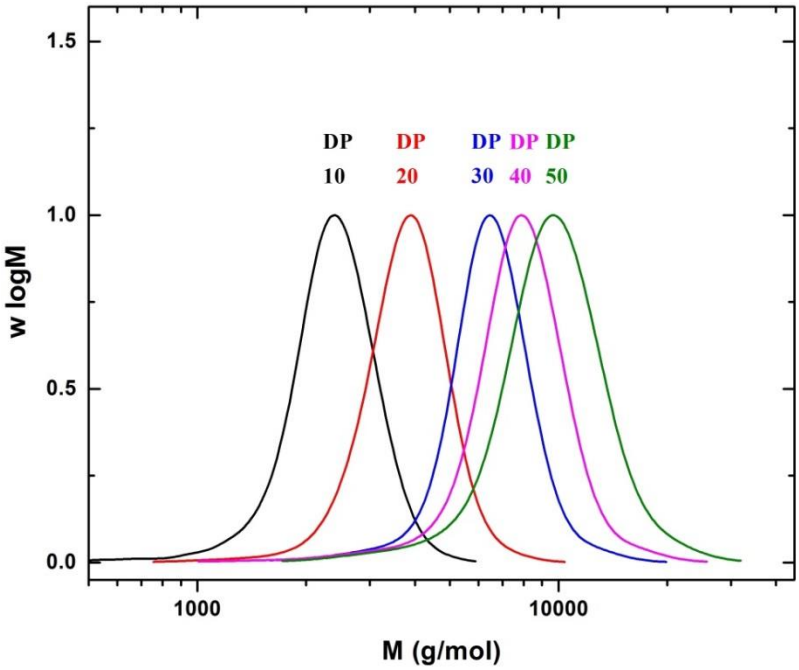

Figure 3.1: SEC analysis of poly(LA) with DP_n = 10-50 employing IPA as the solvent

Polymerisations proceeded relatively quickly at ambient temperature, attaining high conversion (>95%) in approximately 7 hours. SEC analysis revealed a linear increase in number-average molecular weight (M_n) with increasing conversion, excellent agreement with theoretical M_n and low dispersity (Table 3.1 and Figure 3.2).

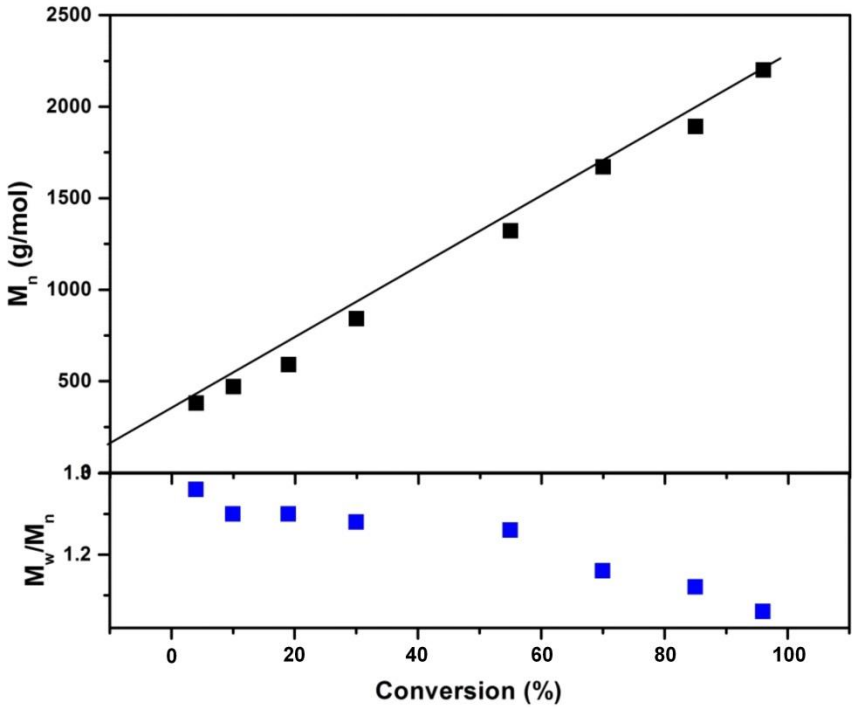

Figure 3.2: Kinetic data for the polymerisation of LA; Conversion *vs* M_n and conversion vs M_w/M_n.

Kinetic analysis revealed a largely first order dependence on both monomer and propagating radical for the majority of the polymerisation. A small, yet reproducible, deviation in linear first order kinetics was observed at 10 to 15% conversion as manifested by a distinct increase in polymerisation rate (Fig. 3.3). Previously, this has been attributed to the onset of heterogeneity, a phenomenon also observed under the current conditions when the polymerisation was complete and stirring ceased. The upper phase appears green whereas the lower phase was transparent/colourless with higher viscosity than the upper phase. A slight opaqueness was observed in the lower phase towards the interface (Fig. 3.4). On sampling, the upper phase showed no detectable polymer *via* either ^{1}H NMR or SEC. Careful sampling of the lower phase, from both the opaque and transparent regions,

revealed low dispersity polymer by both ^{1}H NMR and SEC analysis ($Đ$ <1.10). Both phases contained significant quantities of IPA (^{1}H NMR).

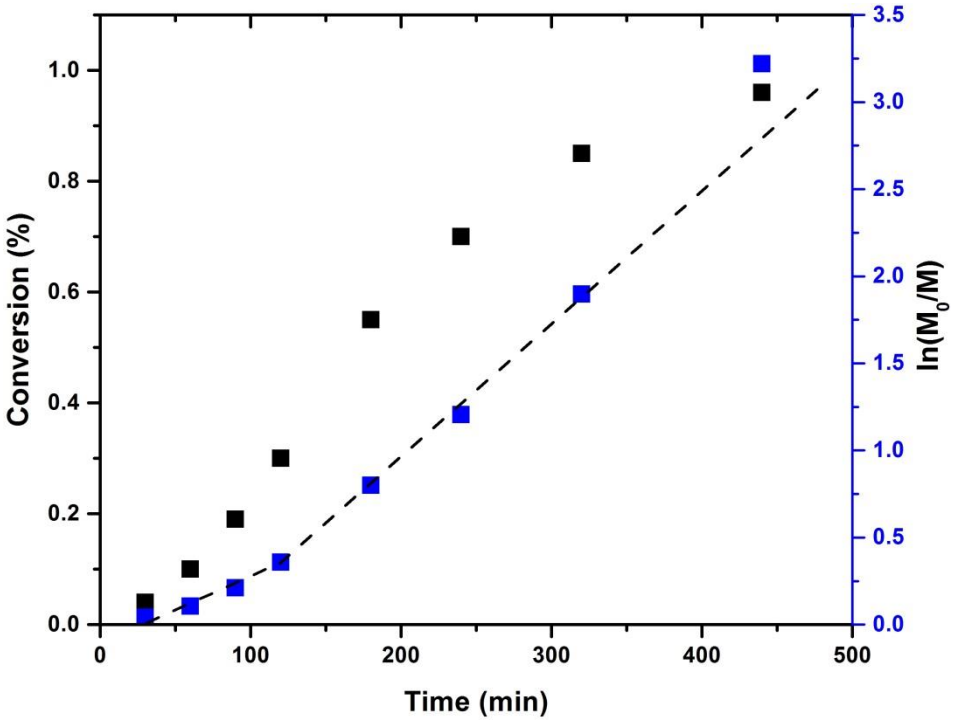

Figure 3.3: Kinetic data for the polymerisation of LA; Conversion *vs* time and ln(M_0/M) *vs* time

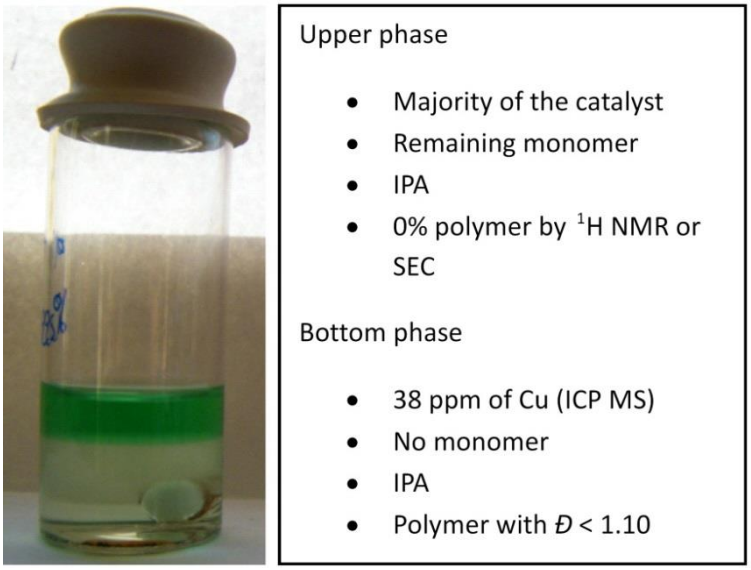

Figure 3.4: Poly(LA) self-generated bi-phasic system in IPA

Repeating the polymerisations in the absence of an external deactivator, $CuBr_2$, furnished near-identical results. The coloured nature of the polymer-free upper phase clearly suggests that the vast majority of the catalyst resided in this phase (the lower phase

remained colourless on exposure to air for one week). Verification of this was achieved by ICP-MS analysis on samples from both phases. As expected, the upper phase contained a significantly higher concentration of copper species than the lower (polymeric) phase. In the absence of externally added $CuBr_2$ the polymeric phase contained as little as 38 ppm Cu species whilst the upper phase contained approximately tenfold higher levels of Cu. The level of copper in the final polymer is thus lower than that observed upon phase separation of poly(*n*BA) from DMSO (~160 ppm) and significantly lower than polymers obtained *via* conventional ATRP. As such, it is evident that these reaction conditions allow access to well-defined, low catalyst-containing polymers without a requirement for purification *via* precipitation, column chromatography, dialysis *etc.*

To further explore the degree of control attained in this biphasic polymerisation, final polymer samples were analysed using MALDI-ToF-MS (Figure 3.5).

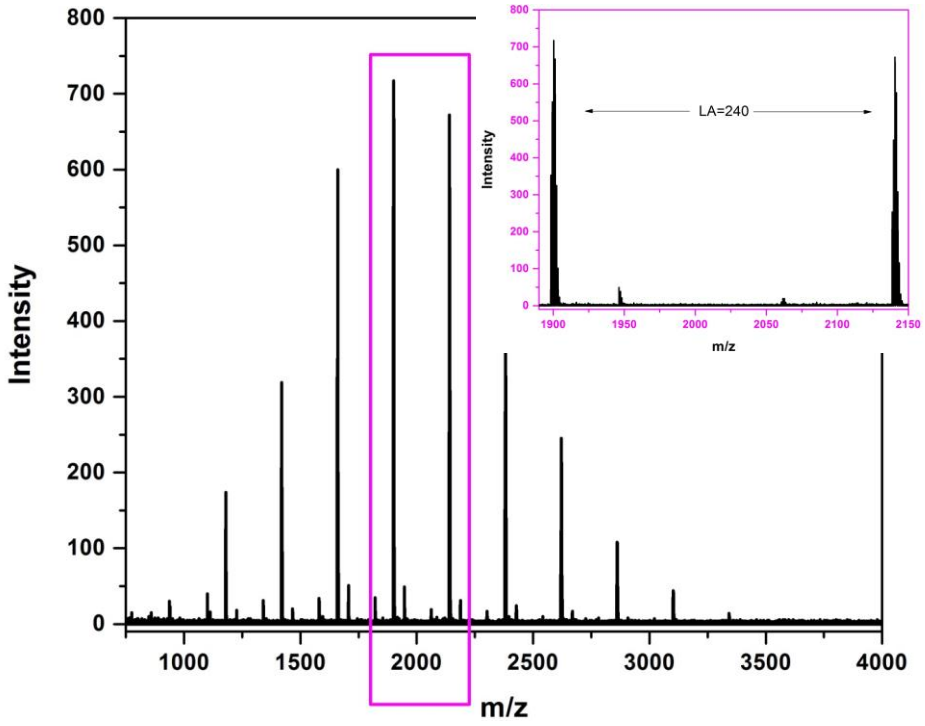

Figure 3.5: MALDI-ToF-MS of LA for the final polymer (100% conversion)

The dominant distribution corresponds to ω-bromo-terminated poly(LA), with the much smaller distribution corresponding to hydrogen-terminated polymer. Overall, this

analysis indicates high bromo end-group fidelity attained and an overall low instance of side reactions *i.e.* chain transfer *etc.*

Due to the excellent bromo end-group fidelity observed *via* MALDI-ToF-MS, post-polymerisation modification was investigated utilising a nucleophilic thio-bromine substitution as a route towards introducing new functionality to these polymers. The upper green phase, rich in the polymerisation catalyst, was carefully removed *via* syringe and thioglycerol, selected as a functional thiol, was added in the presence of triethylamine to the lower polymer-rich phase (Scheme 3.2). After stirring for two hours at ambient temperature, MALDI-ToF-MS analysis revealed a shift of the peaks corresponding to the bromo-terminated polymer to reveal a new thioglycerol functionalised polymer (Fig. 3.6). Both ^{1}H and ^{13}C NMR spectroscopy supports this transformation, as seen by the upfield shift of the methine proton and carbon at the ω-chain end from 4.02 ppm to 2.75 ppm and 42.8 ppm to 41 ppm respectively (Section 3.4.4, Figure 3.12 and Figure 3.13).

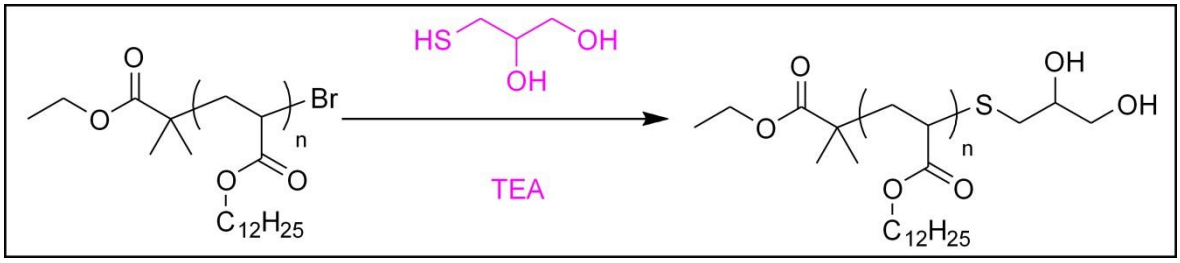

Scheme 3.2: General reaction scheme for thioglycerol modification

As a comparison with the bi-phasic lauryl acrylate-IPA system, a series of lauryl acrylate polymerisations were also carried out in a binary solvent system composed of toluene and methanol (4:1 *v/v*). Toluene was chosen to retain the polymer in solution whilst methanol, a polar solvent/co-ordinator, should promote disproportionation of Cu(I) to Cu(0) and Cu(II).

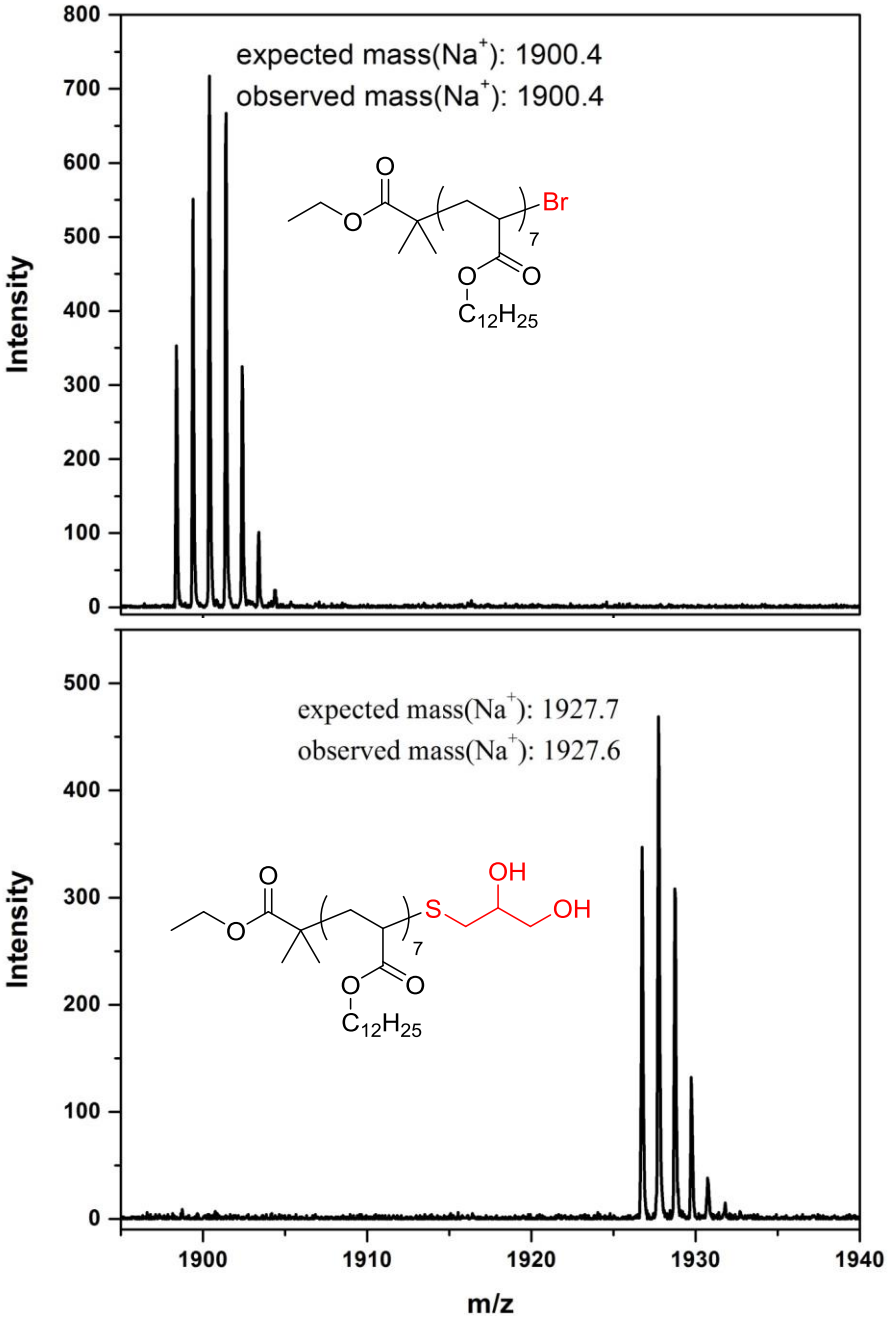

Figure 3.6: MALDI-ToF-MS confirmation of nucleophilic thio-bromine substitution of poly(LA) synthesised in IPA. Quantitative molecular weight shift upon reaction with thioglycerol.

Polymerisation of LA in this solvent mixture resulted in no observed phase separation. Interestingly this was inconsequential to overall polymerisation control, as M_n increased linearly with conversion (Figure 3.7) and low dispersity values (~1.10) with good correlation between theoretical and experimental M_n were observed (Table 3.2).

Table 3.2: Data obtained from the polymerisation of LA in toluene/MeOH ([a] ^{1}H NMR, [b] $CHCl_3$, SEC analysis)

[LA]/[I]	Conv. (%)	$M_{n,th}$[a] (g/mol)	$M_{n,GPC}$[b] (g/mol)	$Đ$	Solvent
10	98	2400	2400	1.10	Tol-MeOH
20	99	4800	4200	1.07	Tol-MeOH
30	98	7200	6800	1.09	Tol-MeOH
40	98	9600	9000	1.13	Tol-MeOH
50	99	12000	11000	1.14	Tol-MeOH

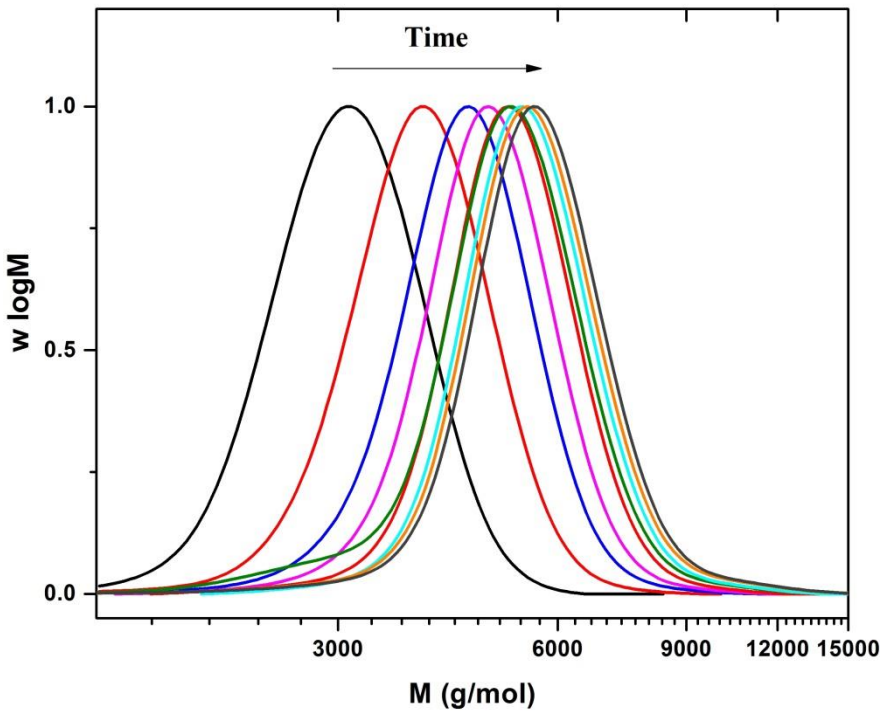

Figure 3.7: SEC data for the polymerisation of LA in toluene-MeOH (4:1 *v/v*); Evolution of molecular weight as a function of time.

Furthermore, polymerisations proceeded with the expected first order kinetics, exhibiting an increase in rate relative to IPA (Figure 3.8). Excellent end-group fidelity was also observd *via* MALDI-ToF-MS with analogous thiobromine substitutions achieved. Overall, both solvent systems exhibited little difference across a range of polymerisation

conditions, with symmetrical SEC chromatograms, low dispersities and near-quantitative conversion being achieved in all cases.

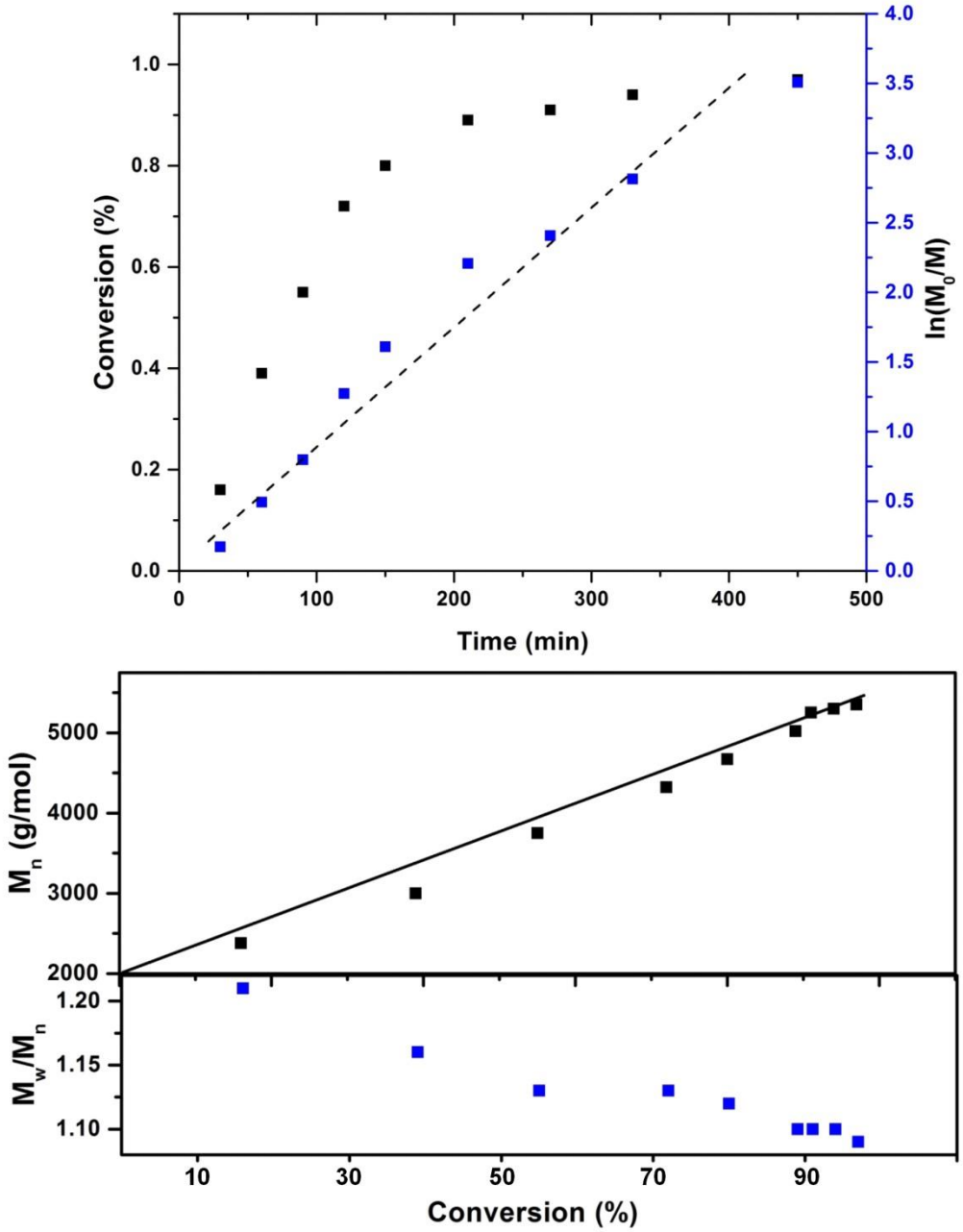

Figure 3.8: Kinetic data for the polymerisation of LA in Tol/MeOH (4:1 *v/v*) (top) and linear molecular weight evolution with conversion (bottom).

Subsequently, the Cu(0)-mediated polymerisation of stearyl acrylate (C_{18}) was also investigated (Scheme 3.3). Stearyl acrylate is insoluble in both IPA and the 4:1 toluene-MeOH mixture used previously. Thus, a mixture of toluene and IPA (4:1 *v/v*) was used to solubilise the monomer. Despite the increased hydrophobicity of the monomer,

living/controlled characteristics were again observed during polymerisation *i.e.* first order kinetics, linear increase in M_n *vs* conversion and low dispersity values (Figure 3.9).

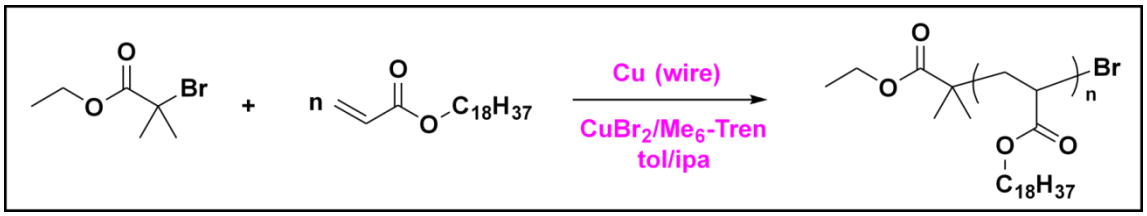

Scheme 3.3: Cu(0)-mediated living radical polymerisation of stearyl acrylate

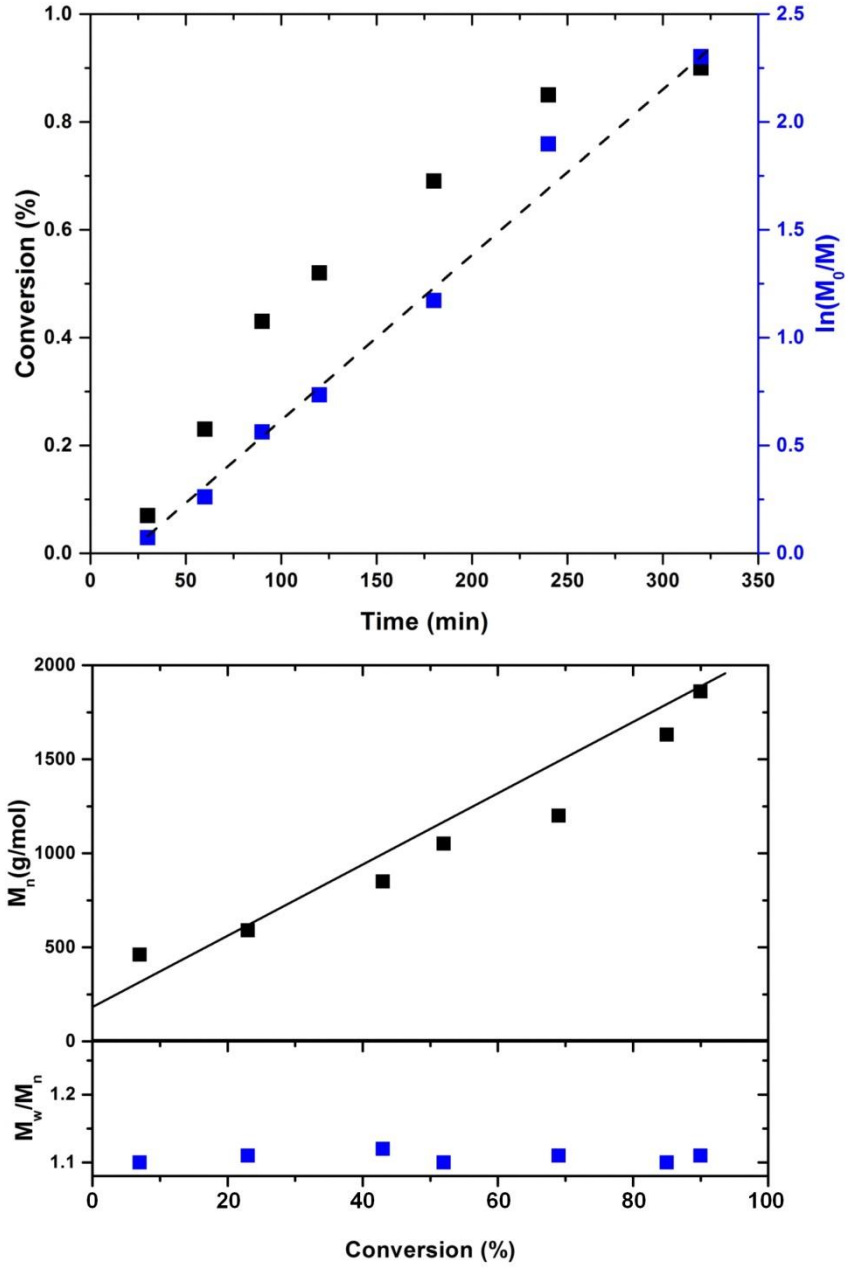

Figure 3.9: Kinetic data for the polymerisation of stearyl acrylate in Tol/IPA (4:1 *v/v*) (top) and linear molecular weight evolution with conversion (bottom).

MALDI-ToF-MS analysis revealed near-quantitative retention of bromo end-group fidelity. Despite the use of polar solvents in which poly(stearyl acrylate) was not fully soluble (acetone or MEK), thio-bromine substitution was again realised using thioglycerol, as seen from a near-quantitative shift in MALDI-ToF-MS (Figure 3.10). NMR spectroscopy again supports the occurrence of ω-chain end methine proton and carbon in ^{1}H and ^{13}C NMR respectively (4.10 ppm to 2.83 ppm and 43.5 ppm to 41 ppm).

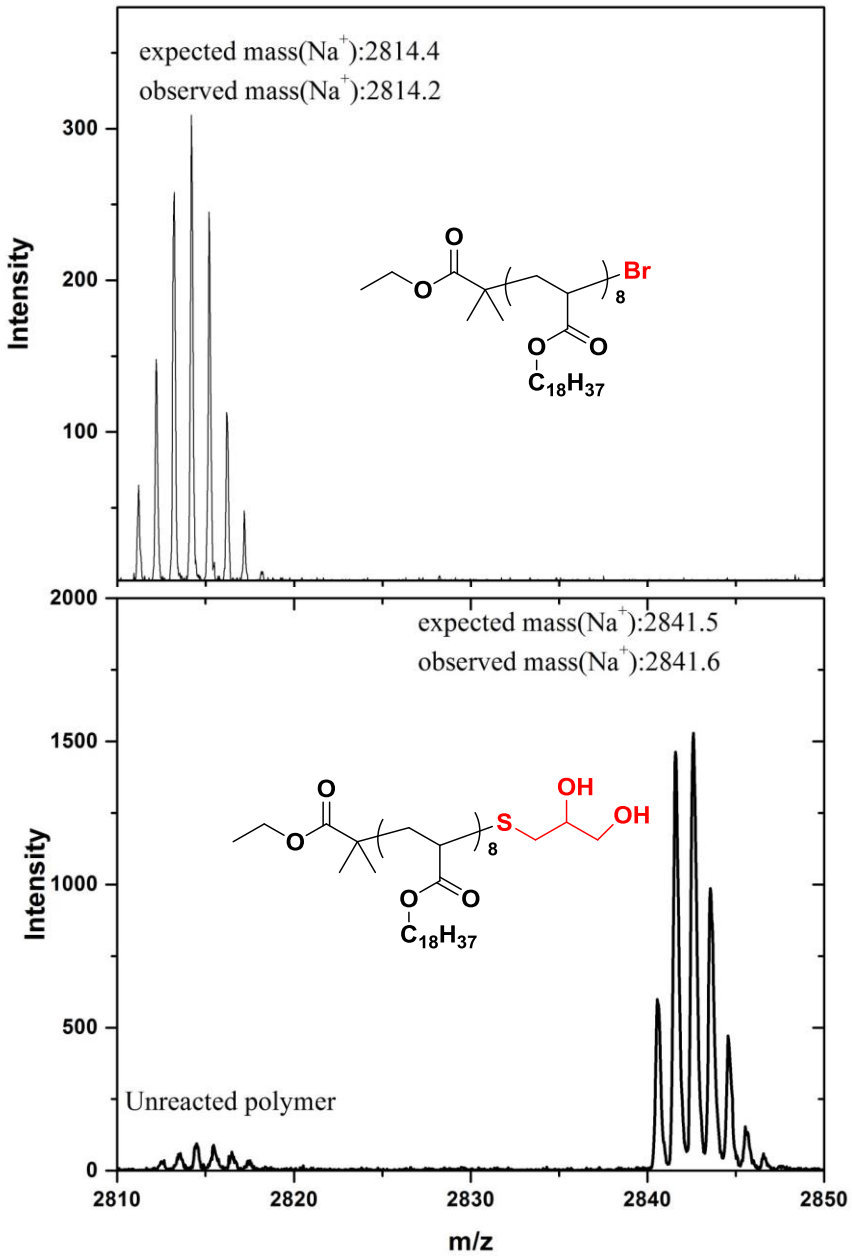

Figure 3.10: MALDI-ToF-MS confirmation of nucleophilic thio-bromine substitution of poly(stearyl acrylate) synthesised in Tol/IPA. Near-quantitative molecular weight shift upon reaction with thioglycerol.

3.3 Conclusions

In summary Cu(0)-mediated polymerisation has been used for the synthesis of long hydrocarbon chain (C_{12}-C_{18}) containing poly(acrylates). Poly(LA) has been synthesised in both toluene-MeOH and IPA with controlled polymerisation maintained to high conversions, resulting in polymers with narrow dispersity values (~1.10) and near-perfect end-group fidelity. When IPA is employed as the solvent poly(LA) undergoes phase separation during polymerisation, resulting in a highly pure polymer-rich layer containing very low levels of residual copper, as measured by ICP-MS. Polymerisation of stearyl acrylate requires a solvent system composed of toluene-IPA to ensure monomer solubility. This does not compromise the integrity of the final polymer with comparably narrow dispersity values obtained. The end-group fidelity of these poly(acrylates) has been further exemplified by quantitative nucleophilic thio-bromine substitution at the ω-chain end.

3.4 Experimental

3.4.1 Materials

Ethyl 2-bromoisobutyrate, copper(II) bromide, stearyl acrylate, 1-thioglycerol, hexylamine, triethylamine, isopropanol, toluene, methanol, acetone, methyl ethyl ketone, tetrahydrofuran and DMSO were purchased from Sigma Aldrich or Fisher Scientific and were all used as received. Lauryl acrylate was purchased from Sigma Aldrich and passed through a column of basic alumina in order to remove the inhibitors prior to use. Cu(0) wire (gauge 0.25 mm) was purchased from Comax Engineered wires and was treated by immersion in conc. HCl prior to use. Tris-(2-(dimethylamino) ethyl)amine (Me_6-Tren) was synthesised according to a literature procedure[27], degassed and stored in a fridge under nitrogen prior to use.

3.4.2 Apparatus

^{1}H and ^{13}C NMR spectra were recorded on Bruker DPX-300, DPX-400 or AV-600 spectrometers in $CDCl_3$ unless otherwise stated. Chemical shifts are given in ppm downfield from the internal standard tetramethylsilane. Size exclusion chromatography (SEC) measurements were conducted using an Agilent 1260 SEC-MDS fitted with differential refractive index (DRI), light scattering (LS) and viscometry (VS) detectors equipped with 2*PLgel 5 mm mixed-D columns (300*7.5 mm), 1*PLgel 5 mm guard column (50* 7.5 mm) and autosampler. Narrow linear poly(methyl methacrylate) standards in range of 200 to $1.0*10^6$ g mol^{-1} were used to calibrate the system. All samples were passed through 0.45 mm PTFE filter prior to analysis. The eluent was chloroform with 2% triethylamine at a flow rate of 1.0 mL min^{-1}. SEC data was analysed using Cirrus v3.3 software with calibration curves produced using Varian Polymer laboratories Easi-Vials linear poly(methyl methacrylate) standards (200–$4.7*10^5$ g mol^{-1}). MALDI-ToF-MS was conducted using a Bruker Daltonics Ultraflex II MALDI-ToF mass spectrometer, equipped with a nitrogen laser delivering 2 ns laser pulses at 337 nm with positive ion ToF detection performed using an accelerating voltage of 25 kV. Solutions in tetrahydrofuran (50 μL) of trans-2-[3-(4-tert-butylphenyl)-2-methyl- 2-propylidene] malonitrile (DCTB) as a matrix (saturated solution), sodium iodide as cationisation agent (1.0 mg mL^{-1}) and sample (1.0 mg mL^{-1}) were mixed, and 0.7 μL of the mixture was applied to the target plate. Spectra were recorded in reflector mode, calibrating with PEG-Me 1100 kDa.

3.4.3 General Procedures

Typical Cu(0)-mediated polymerisation procedure (SET-LRP)

Ethyl 2-bromoisobutyrate (EBiB, 0.089 mL, 0.61 mmol, 1.00 mol equiv.), lauryl acrylate (LA, 5 mL, 18.39 mmol, 30.0 mol equiv.), Me_6-Tren (0.019 mL, 0.07 mmol, 0.12 mol equiv.), $CuBr_2$ (6.8 mg, 0.03 mmol, 0.05 mol equiv.), IPA (5 mL) and a magnetic stir bar

were charged to a Schlenk tube with a rubber septum and the reaction mixture was degassed *via* bubbling with nitrogen for 20 min. A slight positive pressure of N_2 was applied and the pre-activated Cu(0) wire (5 cm) was then added under a nitrogen blanket. The Schlenk tube was then resealed and the polymerisation was allowed to proceed for 24 h at ambient temperature. Samples of the reaction mixture were carefully removed periodically for ^{1}H NMR, mass spectroscopy and SEC analysis. The samples for ^{1}H NMR spectroscopy were diluted in $CDCl_3$, while the SEC and mass spectroscopy samples were initially diluted with THF and then passed through a column of basic alumina to remove the copper salts. The lauryl acrylate polymer was precipitated in a mixture of cold methanol and water (4 : 1 *v/v*).

Typical thio-bromine substitution

The precipitated poly(lauryl acrylate) (1 g, 0.42 mmol, 1 mol equiv.), 1-thio glycerol (54 mL, 0.63 mmol, 1.5 eq.), triethylamine (87 mL, 0.63 mmol, 1.5 eq.), a stir bar and either acetone or methyl ethyl ketone were added in a flask and the reaction was stirred for 2 hours. Samples of the reaction were then removed for ^{1}H NMR and mass spectroscopy analysis. The sample for ^{1}H NMR was diluted with $CDCl_3$, while the sample for mass spectroscopy was diluted in THF.

3.4.4 Characterisation

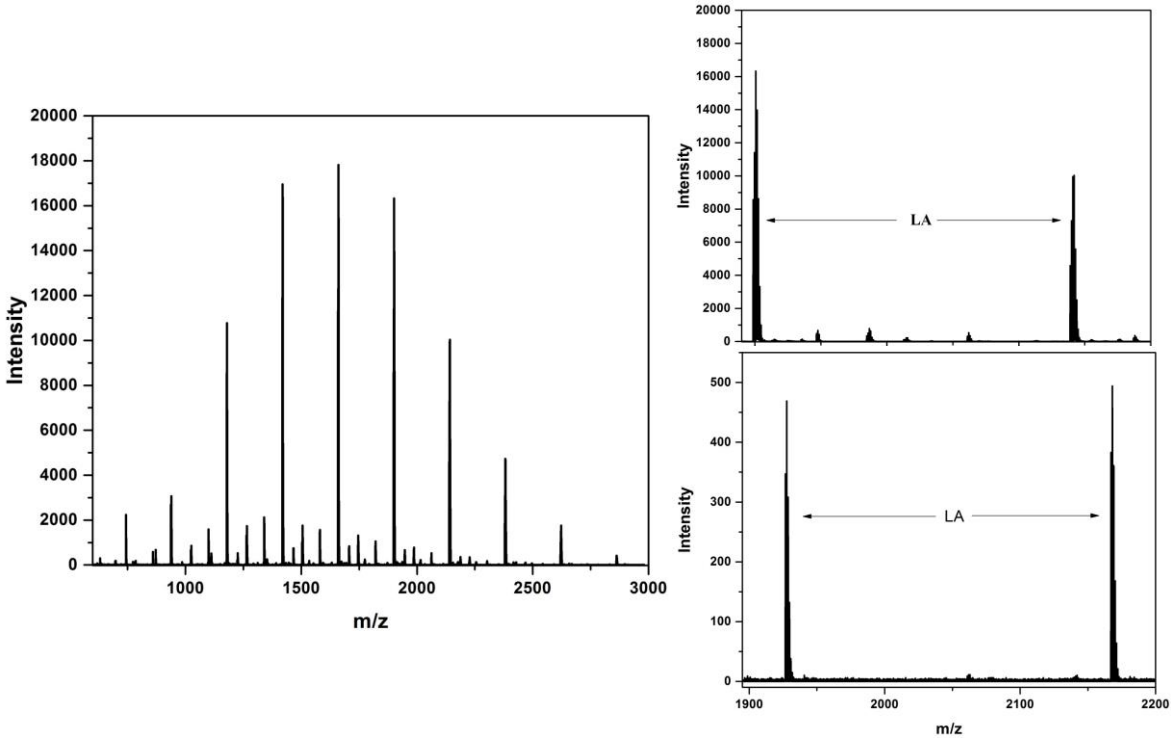

Figure 3.11: MALDI-ToF-MS confirmation of nucleophilic thio-bromine substitution of poly(LA) synthesised in Tol/MeOH. Quantitative molecular weight shift upon reaction with thioglycerol.

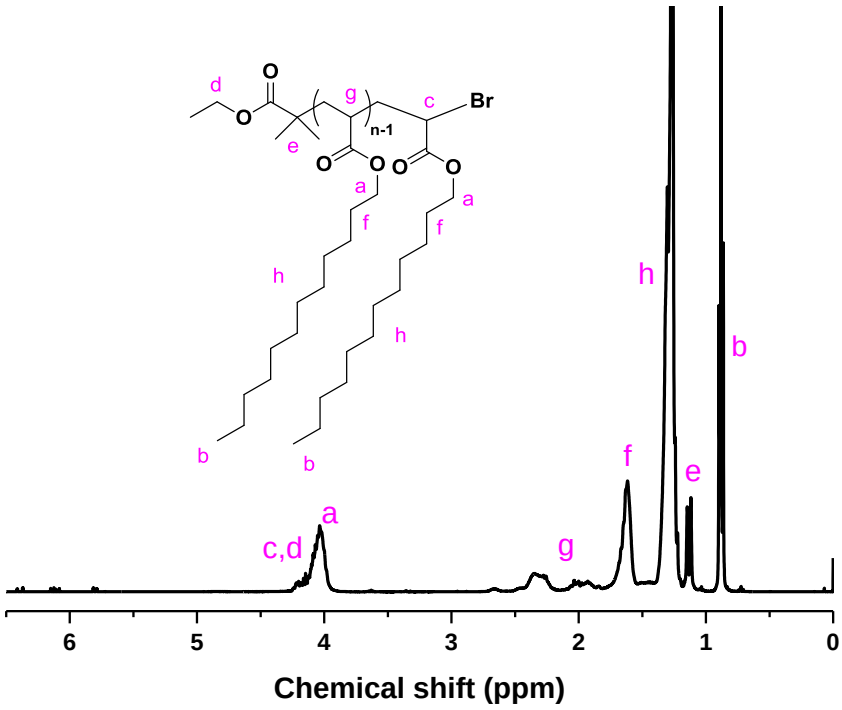

Figure 3.12: ^{1}H NMR of poly(LA) before the modification with thioglycerol.

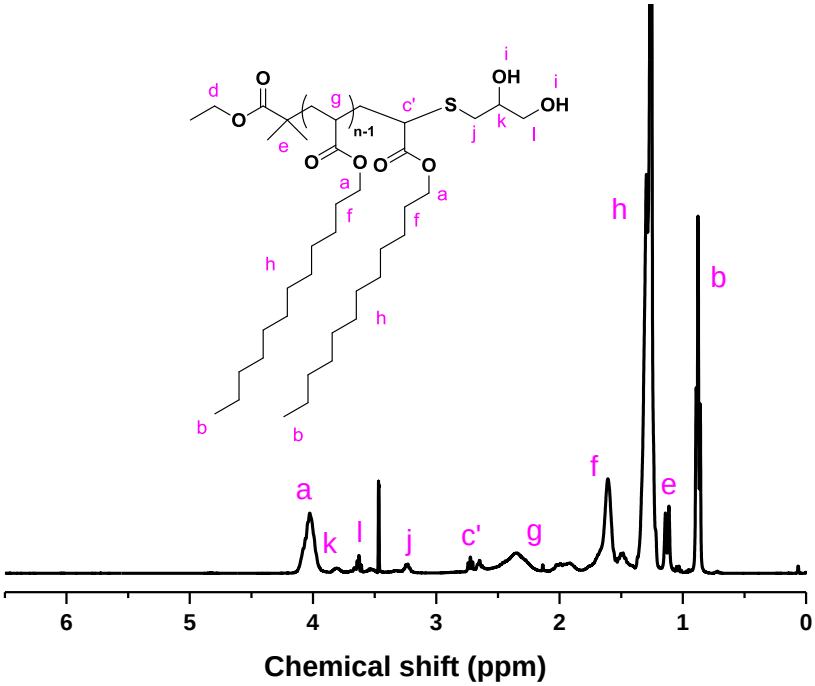

Figure 3.13: ^{1}H NMR of poly(LA) after modification with thioglycerol.

3.5 References

1. T. Çaykara and G. Birlik, *Macromol. Mater. Eng.*, 2005, **290**, 869-874.
2. Y. Ma, X. Zheng, F. Shi, Y. Li and S. Sun, *J. Appl. Polym. Sci.*, 2003, **88**, 1622-1626.
3. K. L. Beers and K. Matyjaszewski, *J. Macromol. Sci., Part A: Pure Appl.Chem.*, 2001, **38**, 731-739.
4. L. Liénafa, S. Monge and J.-J. Robin, *Eur. Polym. J.*, 2009, **45**, 1845-1850.
5. F. Dutertre, P.-Y. Pennarun, O. Colombani and E. Nicol, *Eur. Polym. J.*, 2011, **47**, 343-351.
6. A. Theis, A. Feldermann, N. Charton, T. P. Davis, M. H. Stenzel and C. Barner-Kowollik, *Polymer*, 2005, **46**, 6797-6809.
7. M. J. Nasrullah, A. Vora and D. C. Webster, *Macromol. Chem. Phys.*, 2011, **212**, 539-549.
8. K. Karaky, G. Clisson, G. Reiter and L. Billon, *Macromol. Chem. Phys.*, 2008, **209**, 715-722.
9. J. F. J. Coelho, E. Y. Carvalho, D. S. Marques, A. V. Popov, P. M. Goncalves and M. H. Gil, *Macromol. Chem. Phys.*, 2007, **208**, 1218-1227.
10. B. M. Rosen and V. Percec, *Chem. Rev.*, 2009, **109**, 5069-5119.
11. V. Percec, T. Guliashvili, J. S. Ladislaw, A. Wistrand, A. Stjerndahl, M. J. Sienkowska, M. J. Monteiro and S. Sahoo, *J. Am. Chem. Soc.*, 2006, **128**, 14156-14165.

12. X. Jiang, B. M. Rosen and V. Percec, *J. Polym. Sci., Part A: Polym. Chem.*, 2010, **48**, 2716-2721.
13. N. H. Nguyen, M. E. Levere and V. Percec, *J. Polym. Sci., Part A: Polym. Chem.*, 2012, **50**, 860-873.
14. M. E. Levere, N. H. Nguyen, H.-J. Sun and V. Percec, *Polym. Chem.*, 2013, **4**, 686-694.
15. F. Nyström, A. H. Soeriyadi, C. Boyer, P. B. Zetterlund and M. R. Whittaker, *J. Polym. Sci., Part A: Polym. Chem.*, 2011, **49**, 5313-5321.
16. G. Lligadas, B. M. Rosen, M. J. Monteiro and V. Percec, *Macromolecules*, 2008, **41**, 8360-8364.
17. X. Jiang, S. Fleischmann, N. H. Nguyen, B. M. Rosen and V. Percec, *J. Polym. Sci., Part A: Polym. Chem.*, 2009, **47**, 5591-5605.
18. V. Percec and C. Grigoras, *J. Polym. Sci., Part A: Polym. Chem.*, 2005, **43**, 5609-5619.
19. G. Lligadas and V. Percec, *J. Polym. Sci., Part A: Polym. Chem.*, 2008, **46**, 2745-2754.
20. N. H. Nguyen, B. M. Rosen, X. Jiang, S. Fleischmann and V. Percec, *J. Polym. Sci., Part A: Polym. Chem.*, 2009, **47**, 5577-5590.
21. N. H. Nguyen and V. Percec, *J. Polym. Sci., Part A: Polym. Chem.*, 2011, **49**, 4227-4240.
22. N. H. Nguyen, J. Kulis, H.-J. Sun, Z. Jia, B. van Beusekom, M. E. Levere, D. A. Wilson, M. J. Monteiro and V. Percec, *Polym. Chem.*, 2013, **4**, 144-155.
23. S. R. Samanta, M. E. Levere and V. Percec, *Polym. Chem.*, 2013, **4**, 3212-3224.
24. B. M. Rosen, X. Jiang, C. J. Wilson, N. H. Nguyen, M. J. Monteiro and V. Percec, *J. Polym. Sci., Part A: Polym. Chem.*, 2009, **47**, 5606-5628.
25. M. E. Levere, N. H. Nguyen, X. Leng and V. Percec, *Polym. Chem.*, 2013, **4**, 1635-1647.
26. C. Boyer, A. Atme, C. Waldron, A. Anastasaki, P. Wilson, P. B. Zetterlund, D. Haddleton and M. R. Whittaker, *Polym. Chem.*, 2013, **4**, 106-112.
27. M. Ciampolini and N. Nardi, *Inorg. Chem.*, 1966, **5**, 41-44.

Chapter 4

High Molecular Weight Block Copolymers by Sequential Monomer Addition *via* Cu(0)-Mediated Living Radical Polymerisation (SET-LRP): An Optimised Approach

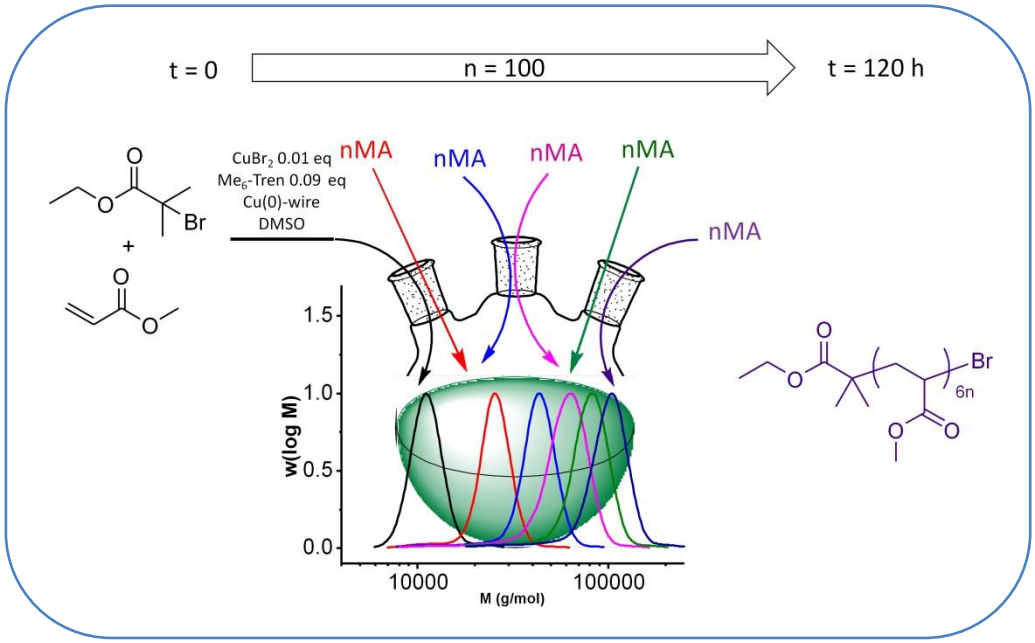

The synthesis of well-defined high molecular weight block copolymers by sequential in situ chain extensions via Cu(0)-mediated living radical polymerisation is reported. Optimal conditions for iterative high molecular weight block formation were determined using model homopolymer quasiblock systems, including methyl acrylate (MA), ethyl acrylate (EA), and n-butyl acrylate (nBA; each block $DP_n \approx 100$). The Đ after each chain extension was below 1.2, with good agreement between theoretical and experimental molecular weights, while the conversion of monomer incorporation into each distinct block was 95−100% (up to 6 blocks). To demonstrate this approach for true block copolymer materials, well-defined block polymers containing MA, ethylene glycol methyl ether acrylate (EGA), and tert-butyl acrylate (tBA) were prepared in high purity: diblock P(MA-b-EGA) and triblock P(MA-b-tBA-b-MA). These were prepared in high yields, on multigram scales, and with purification only required at the final step. To the best of our knowledge, this is the first time that high molecular weight block copolymers have been reported using this novel technique.

4.1 Introduction

Cu(0)-mediated living radical polymerisation has demonstrated, under carefully optimised conditions, to yield polymers with extremely high livingness, even at quantitative conversions and extending into post-polymerisation modifications. This high end-group fidelity offers a new synthetic tool to build complex macromolecules, such as multiblock copolymers. Block copolymers display a wide range of interesting and useful properties due to the fact that the combination of monomers with different physico-chemical properties, confined in block sequences, allows these systems to potentially undergo self-assembly and phase separation into higher ordered structures[1-8]. The synthesis of AB or ABA amphiphilic block copolymers of high molecular weight is of particular interest for the formation of micelles, vesicles, *etc.*, in solution, and various morphologies in the solid state. The morphology of these self-assembled constructs depends upon a well-controlled synthetic protocol allowing preordained molecular weights and volume fractions (ϕA/ϕB) to be obtained[9-12].

However, while there are many polymerisation techniques that have been used to produce block copolymers, a number of drawbacks exist. For example living anionic polymerisation[13] is extremely labour-intensive and the number of functional monomers that can be polymerised using this technique is limited. The development of controlled radical polymerisation (CRP) techniques such as ATRP[14, 15], NMP[16] and RAFT[17] has expanded this monomer library but experimental and synthetic limitations remain. The most significant limitation is the loss of 'livingness' – or end-group fidelity - as the polymerisation proceeds due to unwanted side reactions and termination events[18, 19]. This loss of 'livingness' of the chain end leads to an increase in $Đ$, which can be reflected in the structural dispersity of resulting higher order polymers.

Whittaker and coworkers initially exploited Cu(0)-mediated living radical polymerisation to prepare high-order multiblock copolymers *via* a continuous iterative process[20-22]. No purification steps were required during the polymerisation process and the investigators took advantage of the high end-group fidelity[23], even at high monomer conversions. Thus, hexablock, octablock and decablock copolymers were reported with a block molecular weight ranging from 500 to 2000 g/mol using [$CuBr_2$]:[Me_6-Tren]=[0.05]:[0.18] in DMSO at ambient temperature. Although remarkable, this work was limited to the synthesis of low molecular weight block copolymers: when slightly higher molecular weight multiblocks were attempted (2000 per block) the dispersity value increased to 1.7 for the final multiblock copolymer, showing significant termination. Thus, the optimisation of the approach to include the synthesis of higher molecular weight multiblock copolymers would represent a significant advance.

In this chapter, the extension of this Cu(0)-mediated technique to the synthesis of high molecular weight multiblock polymers, quasiblock homopolymers and true block copolymers is presented, with each block typically comprising more than 100 monomer units. Each block formation cycle was taken to quasi-full conversion (95-100%) and therefore, purification was only required at the final step. The potential scope of this technique was demonstrated by application to various monomers for which the dispersity values were kept low (1.1-1.2). The amount of Cu(II) and ligand employed was found to be crucial for optimal polymerisation conditions and differentiates this synthetic route from previously reported syntheses of lower molecular weight multiblock copolymers with much shorter block lengths.

4.2 Results and Discussion

Initial attempts to synthesise higher molecular weight polymers *via* sequential monomer addition were conducted using conditions previously reported by Whittaker ([$CuBr_2$]:[Me_6-Tren]=[0.05]:[0.18]), which allowed the successful iterative chain extension of the high order multiblock copolymers with short block lengths. In this approach, each iterative extension cycle was taken to almost full conversion before the addition of an aliquot of degassed monomer/DMSO solution. As a result, intermediate polymer purification was not necessary.

The polymerisations were initiated at 25 ˚C by EBiB in the presence of MA ($DP_{n.th}$=125), Me_6-Tren, $CuBr_2$ and Cu(0) wire (5cm) to generate the first block ([EBiB]:[$CuBr_2$]:[Me_6-Tren]=[1]:[0.05]:[0.18]). It is important to note that one ligand will complex to one $CuBr_2$ and therefore the ratio of free ligand is 0.13 (relative to initiator). High monomer conversion (>95%) at the end of the first chain extension cycle was confirmed *via* ^{1}H NMR. The evolution of the SEC molecular weight distributions of the iterative *in situ* chain extension cycles of methyl acrylate (MA) (2 chain extension cycles, each cycle generating a block length of M_n = 10,000 g/mol) reveals that the M_n of the model diblock PMA homopolymer is in reasonable agreement with the theoretical molecular weight ($M_{n,th}$). However the significant increase in dispersity could potentially reflect a loss of living chain ends.

Table 4.1: Diblock "hopolymer" of MA using [EBiB]:[MA]:[$CuBr_2$]:[Me_6-Tren]:[Cu(0) wire]=[1]:[125]:[0.05]:[0.18]:[5 cm] (black), and *in situ* chain extension with MA [125 eq] (red). DMSO 50% *v/v* used as solvent.

Cycle	Time (h)	Conversion (%)	$M_{n,th}$ (g/mol)	$M_{n,SEC}$ (g/mol)	$Đ$
1	24	98	10900	11000	1.05
2	24	95	21000	19000	1.24

This loss of livingness is manifested as a low molecular weight shoulder which we attribute to dead polymer chains formed during initial polymerisation (Figure 4.1).

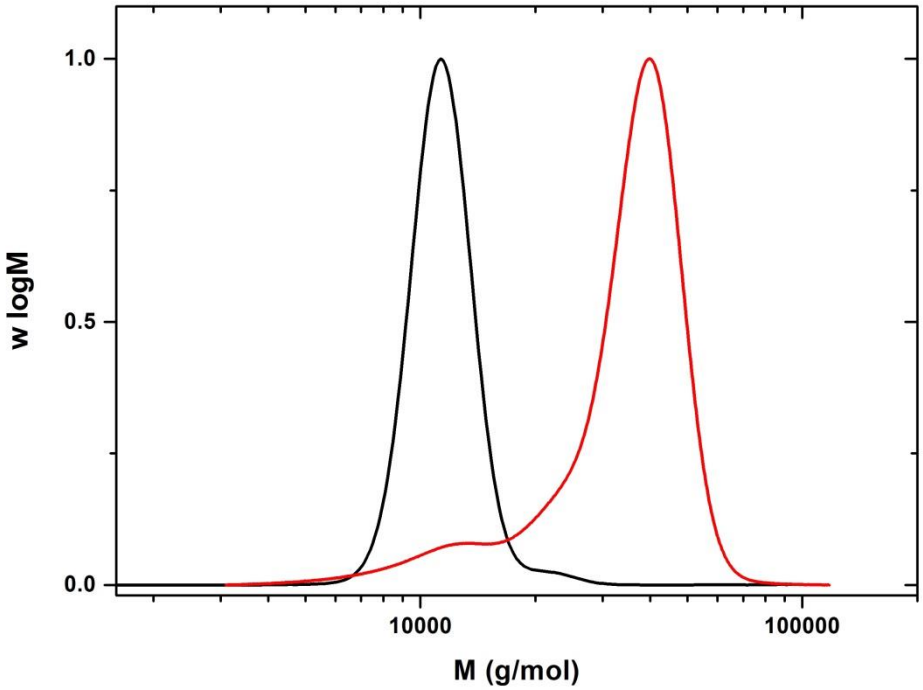

Figure 4.1: Diblock "hopolymer" of MA using [EBiB]:[MA]:[$CuBr_2$]:[Me_6-Tren]:[Cu(0) wire]=[1]:[125]:[0.05]:[0.18]:[5 cm] (black), and *in situ* chain extension with MA [125 eq] (red). DMSO 50% *v/v* used as solvent.

This is in contrast to results reported for lower molecular weight blocks where, after several chain extension cycles, no significant low molecular weight shoulder was observed[20, 22]. It has been previously demonstrated using these experimental conditions that the livingness is higher in the systems where shorter blocks are targeted (~500 g/mol) rather than larger blocks (~2 000 g/mol), in agreement with well-established theory[24]. It is not surprising then that, under the conditions described, non-ideal results have been obtained when higher molecular weight blocks of 10 kDa have been targeted.

In an effort to increase the livingness, the amount of deactivator was increased two fold with the addition of extra ligand to maintain a constant "free" ligand concentration ([EBiB]:[$CuBr_2$]:[Me_6-Tren] = [1]:[0.10]:[0.23]). Increasing the Cu(II) concentration to

improve the control in similar systems is widely demonstrated[21, 23, 25]. High conversion was confirmed *via* ^{1}H NMR in each of chain extension cycles 1-4. The livingness after the first chain extension was indeed improved: *Đ* decreased from 1.24 (Cu(II)=0.05 eq) to 1.09 (Cu(II)=0.010 eq). It should be noted that the livingness is not necessarily reflected in the dispersity values. However, there remains significant low molecular weight tailing as the chain extension cycles are repeated with the *Đ* of the final tetrablock increasing to 1.40 (Figure 4.2).

Table 4.2: Data obtained from the tetrablock "hopolymer" of MA using [EBiB]:[MA]:[$CuBr_2$]:[Me_6-Tren]:[Cu(0) wire]=[1]:[125]:[0.10]:[0.23]:[5 cm]

Cycle	Time (h)	Conversion (%)	$M_{n,th}$ (g/mol)	$M_{n,SEC}$ (g/mol)	*Đ*
1	24	95	10400	11600	1.05
2	24	95	20600	19000	1.09
3	24	94	30400	28200	1.25
4	48	93	40000	38800	1.40

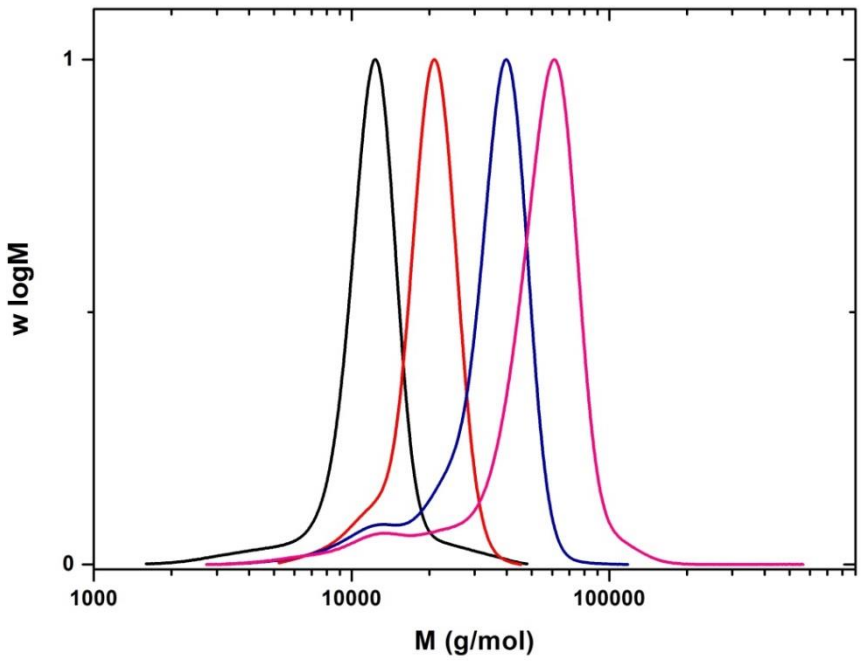

Figure 4.2: Molecular weight distributions for the synthesis and *in situ* chain extension of PMA. [MA]:[EBiB]:[$CuBr_2$]:[Me_6-Tren] = [125]:[1]:[0.1]:[0.23].

As highlighted in chapter 2, careful optimisation of [initiator]/[Me_6-Tren] ratios is crucial in order to achieve optimum polymerisation of acrylates[26]. Adventitious ligand-mediated side reactions were found to cause termination reactions if the ligand concentration was not optimised. Also, simply lowering the ligand concentration may lead to a prohibitive reduction in polymerisation rate[27]. Consequently, further optimisation of the [EBiB], [Cu(II)] and [ligand] was undertaken.

Percec *et al*. have reported excellent results for Cu(0)-mediated polymerisation in the absence of added Cu(II)[28-30]. Therefore we decided to reduce the [$CuBr_2$] from 0.05 eq to 0.01 eq and for comparison we conducted a reaction without adding $CuBr_2$. In the absence of [$CuBr_2$], using [Me_6-Tren] (0.18 eq) as ligand and activated Cu(0) wire, the EBiB initiated homopolymerisation of MA reached high conversion (99%) within 2 h with good agreement between theoretical and experimental M_n and $Đ$ = 1.05. Chain extension resulted in a well-defined block polymer (95% conversion, $Đ$ = 1.15) in 7.5 h. Additional chain extensions required longer times (24, 48, 100 h respectively), yielding a final pentablock copolymer with an overall final conversion of 94% and $Đ$ = 1.85 (Table 4.3 and Figure 4.3).

Table 4.3: Data obtained from the pentablock hopolymer of MA using [EBiB]:[MA]:[$CuBr_2$]:[Me_6-Tren]:[Cu(0) wire]=[1]:[125]:[-]:[0.18]:[5 cm]

Cycle	Time (h)	Conversion (%)	$M_{n,th}$ (g/mol)	$M_{n,SEC}$ (g/mol)	$Đ$
1	2	99	10600	9000	1.10
2	7.5	95	20400	17600	1.15
3	24	94	30300	30600	1.44
4	48	85	36600	42000	1.64
5	100	94	54600	50000	1.85

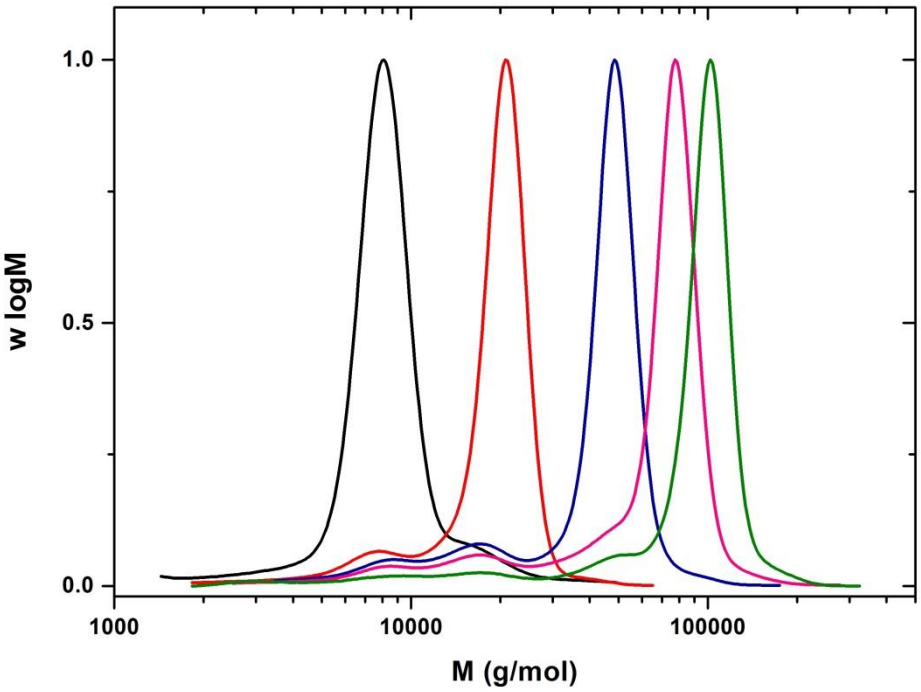

Figure 4.3: Molecular weight distributions for the synthesis and *in situ* chain extension of PMA. [EBiB]:[MA]:[$CuBr_2$]:[Me_6-Tren]:[Cu(0) wire]=[1]:[125]:[-]:[0.18]:[5 cm]

When a small amount of $CuBr_2$ (0.01 eq) was introduced at the beginning of the reaction, the chain extensions proceeded without a significant decrease in polymerisation rate and near-quantitative conversion (>99%) with $Đ$ = 1.78 (Figure 4.4 and Table 4.4). Under both sets of conditions, the initial inability to efficiently chain extend was remediated by an overall reduction in [$CuBr_2$]. However, the data were not ideal, with lower conversions for polymerisations in the absence of $CuBr_2$, and in both cases significant low molecular weight shoulders were observed, which compromised the dispersity values (Table 4.3 and 4.4).

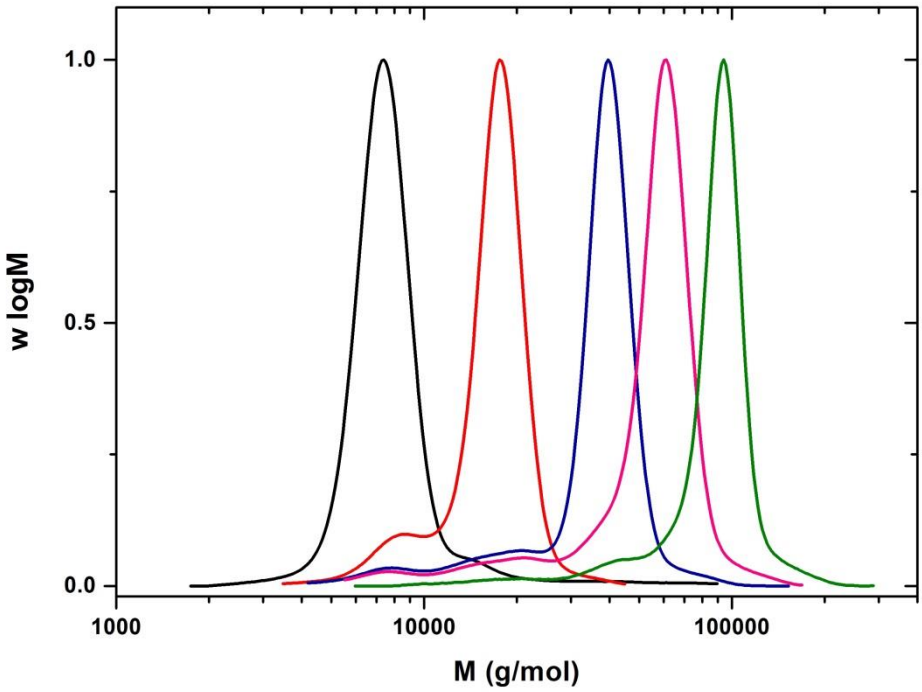

Figure 4.4: Molecular weight distributions for the synthesis and *in situ* chain extension of PMA. [EBiB]:[MA]:[$CuBr_2$]:[Me_6-Tren]:[Cu(0) wire]=[1]:[125]:[0.01]:[0.18]:[5 cm]

Table 4.4: Data obtained from the pentablock hopolymer of MA using [EBiB]:[MA]:[$CuBr_2$]:[Me_6-Tren]:[Cu(0) wire]=[1]:[125]:[0.01]:[0.18]:[5 cm]

Cycle	Time (h)	Conversion (%)	$M_{n,th}$ (g/mol)	$M_{n,SEC}$ (g/mol)	$Đ$
1	2	99	10900	8000	1.10
2	7.5	94	20200	16000	1.12
3	24	96	30900	29000	1.28
4	48	95	40800	40000	1.41
5	100	99	53000	49000	1.78

In consideration of our previous work[26], these experiments were repeated using a reduced Me_6-Tren concentration (0.09 eq). In the absence of $CuBr_2$, a significant reduction in the polymerisation rate was observed and the chain extension seldom reached >90% conversion.

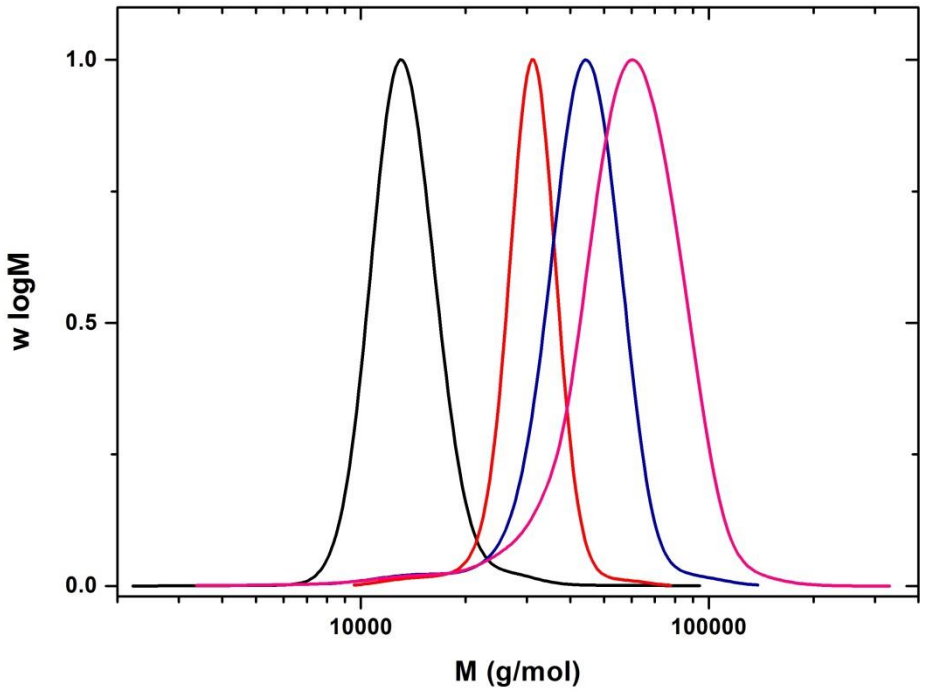

Figure 4.5: Molecular weight distributions for the synthesis and *in situ* chain extension of PMA. [EBiB]:[MA]:[$CuBr_2$]:[Me_6-Tren]:[Cu(0) wire]=[1]:[125]:[-]:[0.09]:[5 cm]

Table 4.5: Data obtained from the pentablock hopolymer of MA using [EBiB]:[MA]:[$CuBr_2$]:[Me_6-Tren]:[Cu(0) wire]=[1]:[125]:[-]:[0.09]:[5 cm]

Cycle	Time (h)	Conversion (%)	$M_{n,th}$ (g/mol)	$M_{n,SEC}$ (g/mol)	$Đ$
1	2	99	10800	13700	1.05
2	24	93	20000	30700	1.05
3	72	84	26000	40800	1.12
4	150	75	32300	53000	1.18

In contrast, when [EBiB]:[$CuBr_2$]:[Me_6-Tren] = [1]:[0.01]:[0.09] the homopolymerisation of MA reached 99% conversion in 2 h with a $Đ$ as low as 1.05, while the first chain extension was equally successful, furnishing a well-defined polymer (95%, $Đ$ = 1.06). A total of 5 iterative additions of degassed MA in DMSO were successfully carried out. Relatively good agreement between theoretical and experimental M_n was observed for each chain extension cycle (Figure 4.6 and Table 4.6) and the final polymer

had a dispersity value of 1.09 and 92% conversion. SEC analysis revealed symmetrical distributions for each chain extension without significant low molecular weight tailing (Figure 4.6).

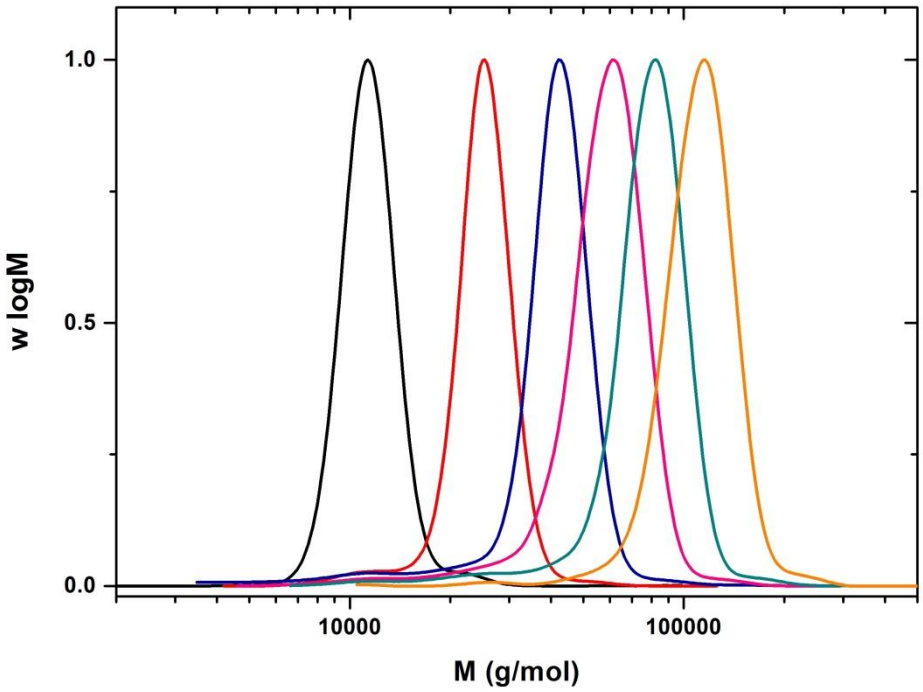

Figure 4.6: Molecular weight distributions for the synthesis and *in situ* chain extension of PMA. [EBiB]:[MA]:[$CuBr_2$]:[Me_6-Tren]:[Cu(0) wire]=[1]:[125]:[0.01]:[0.09]:[5 cm]

Table 4.6: Data obtained from the pentablock hopolymer of MA using [EBiB]:[MA]:[$CuBr_2$]:[Me_6-Tren]:[Cu(0) wire]=[1]:[125]:[0.01]:[0.09]:[5 cm]

Cycle	Time (h)	Conversion (%)	$M_{n,th}$ (g/mol)	$M_{n,SEC}$ (g/mol)	$Đ$
1	2	99	10800	11700	1.05
2	24	95	20500	24600	1.06
3	48	92	30000	38600	1.12
4	72	96	41000	50900	1.18
5	96	94	50600	67000	1.19
6	120	92	60000	105000	1.09

It is clear that both [Cu(II)] and [ligand] must be optimised w.r.t. [EBiB] to maximise livingness and polymerisation rate.

To demonstrate the versatility of this approach, well-defined P(MA-*b*-EGA) and P(MA-*b*-*t*BA-*b*-MA) were prepared. Polymers containing a PEG block are of wide interest due to the antifouling, temperature responsiveness and "stealth" properties the PEG component confers. For the purpose of self-assembly, preparation of amphiphilic block copolymers using *t*BA is well established, with amphiphilicity introduced post-polymerisation by facile removal of the *tert*-butyl protecting group to unmask a pH responsive, hydrophilic acrylic acid (AA) block[31-33].

P(MA-*b*-EGA): The PMA block was first synthesised using the optimised conditions ([MA]:[EBiB]:[$CuBr_2$]:[Me_6-Tren] = [100]:[1]:[0.01]:[0.09], 2h, 98%, $Đ$ = 1.07) and chain-extended by addition of degassed EGA in DMSO. A well-defined diblock copolymer, P(MA-*b*-EGA), with 94% conversion, $M_n \approx M_{n,th}$ and $Đ$ = 1.08 was achieved after 7 h (Figure 4.7 and Table 4.7). Subsequent chain extension with MA was unsuccessful, as no conversion was detected by ^{1}H NMR.

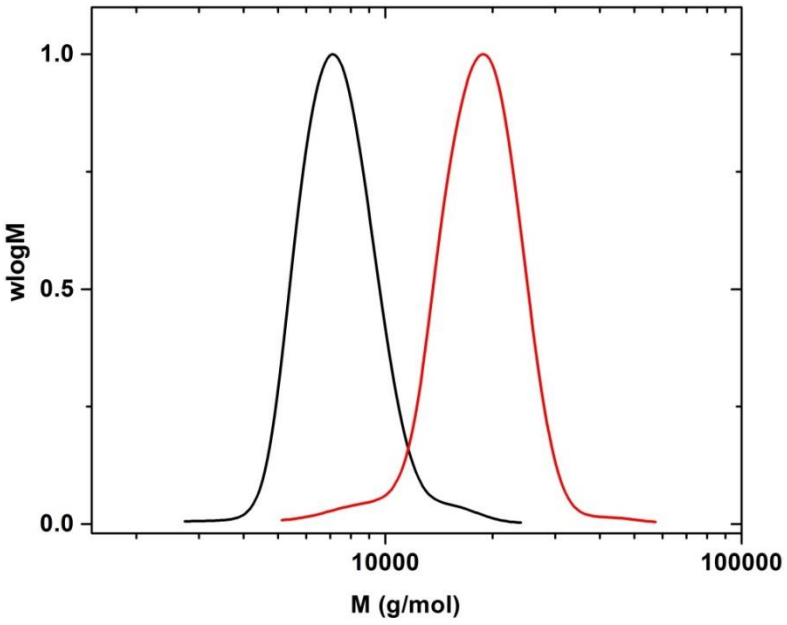

Figure 4.7: Molecular weight distributions for the synthesis and *in situ* chain extension of PMA with EGA. [EBiB]:[MA]:[$CuBr_2$]:[Me_6-Tren]:[Cu(0) wire]=[1]:[125]:[0.01]:[0.09]:[5 cm]

Table 4.7: Data obtained from the diblock copolymer of MA with EGA using [EBiB]:[MA]:[$CuBr_2$]:[Me_6-Tren]:[Cu(0) wire]=[1]:[100]:[0.01]:[0.09]:[5 cm]

Cycle	Time (h)	Conversion (%)	$M_{n,th}$ (g/mol)	$M_{n,GPC}$ (g/mol)	$Đ$
1	2	98	8600	8000	1.07
2	7	94	21600	19800	1.08

P(MA-*b*-*t*BA-*b*-MA): The MA block was synthesised as above (98%, $Đ$ = 1.05). The chain extension with *t*BA resulted in an extremely viscous gel-like mixture. However, upon dilution with degassed DMSO the viscosity was reduced, refuting the possibility of gel formation *via* potential cross-linking reactions. A well-defined diblock copolymer, P(MA-*b*-*t*BA), with 100% conversion, $M_n \approx M_{n,th}$ and $Đ$ = 1.05 was realised. The diblock was chain-extended to give P(MA-*b*-*t*BA-*b*-MA) with a final conversion of 100%. There was also excellent agreement between M_n and $M_{n,th}$ (Table 4.8) with narrow, symmetrical MWDs (Figure 4.8 and Table 4.8) indicating minimal termination in each chain extension cycle.

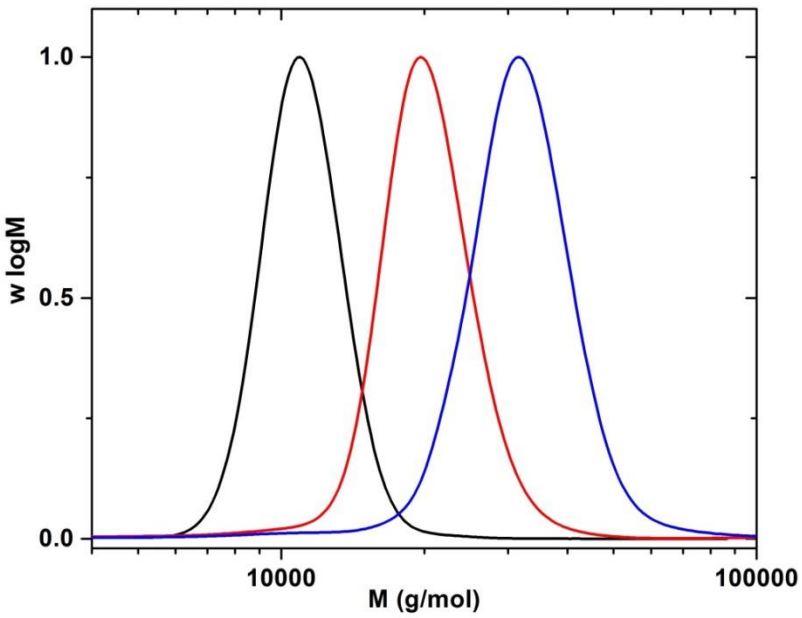

Figure 4.8: Molecular weight distributions for the synthesis and *in situ* chain extension of PMA with *t*BA and subsequently MA. [EBiB]:[MA]:[$CuBr_2$]:[Me_6-Tren]:[Cu(0) wire]=[1]:[125]:[0.01]:[0.09]:[5 cm].

Table 4.8: Data obtained from the triblock copolymer of poly(MA)-*b*-(*t*BA)-*b*-(MA) using [EBiB]:[MA]:[$CuBr_2$]:[Me_6-Tren]:[Cu(0) wire]=[1]:[100]:[0.01]:[0.09]:[5 cm]

Cycle	Time (h)	Conversion (%)	$M_{n,th}$ (g/mol)	$M_{n,SEC}$ (g/mol)	$Đ$
1	2	98	8600	9600	1.05
2	24	100	20100	20000	1.06
3	48	100	28700	33000	1.10

4.3 Conclusions

In summary, the successful synthesis of model block homopolymers and block copolymers of high molecular weight *via* Cu(0)-mediated living radical polymerisation at ambient temperature has been accomplished. No purification steps are required between the sequential monomer additions, while near-quantitative conversions and low dispersities are obtained after careful optimisation. The amounts of Cu(II) and ligand proved to be crucial for maintaining the balance between excellent control, livingness and high polymerisation rate. This work provides a facile route for accessing high molecular weight blocks and thus their associated applications, opening the path for well-defined copolymers in an extremely controlled and robust way. However, the hexablock copolymer that was achieved with MA could not be repeated when different monomers were utilised (EGA or *t*BA), revealing an important weakness of the system. Also, inconsistent results that are associated with large induction periods have been reported previously by our laboratory[34, 35]. Thus, a more versatile and tolerant method is required to be developed in order to further maximise the end-group fidelity.

4.4 Experimental

4.4.1 Materials

n-Butyl acrylate (*n*BA), *tert*-butyl acrylate (*t*BA), ethyl acrylate (EA), ethylene glycol methyl ether acrylate (EGA), methyl acrylate (MA), ethyl 2-bromopropionate and $CuBr_2$ were purchased from Aldrich and used as received. Me_6-Tren was synthesised according to previously reported literature. Cu(0) (gauge 0.25 mm) wire was purchased from Comax Engineered wires and was treated by immersion in conc. HCl prior to use. Solvents were purchased from Fisher Scientific and used as received.

4.4.2 Apparatus

^{1}H NMR spectra were recorded on a Bruker DPX-300, DPX-400 or DRX-500 spectrometers in $CDCl_3$ unless otherwise stated. Chemical shifts are given in ppm downfield from the internal standard tetramethylsilane. Size exclusion chromatography (SEC) measurements were conducted using an Agilent 1260 SEC-MDS fitted with differential refractive index (DRI), light scattering (LS) and viscometry (VS) detectors equipped with 2 × PLgel 5 mm mixed-D columns (300 × 7.5 mm), 1 × PLgel 5 mm guard column (50 × 7.5 mm) and autosampler. Narrow linear poly(methyl methacrylate) standards in range of 200 to 1.0×10^6 g·mol^{-1} were used to calibrate the system. All samples were passed through 0.45 μm PTFE filter before analysis. The mobile phase was chloroform with 2% triethylamine eluent at a flow rate of 1.0 mL/min. SEC data was analysed using Cirrus v3.3 software with calibration curves produced using Varian Polymer laboratories Easi-Vials linear poly(methyl methacrylate) standards (200-4.7×10^5 g/mol).

4.4.3 General procedure for the homopolymerisation of acrylates

Filtered monomer (2 mL, 100 eq), EBiB (1 eq), $CuBr_2$ (0.01 eq), Me_6-Tren (0.09 eq) and DMSO (2 mL) were deoxygentated by purging with nitrogen for 30 min, during which time, Cu(0) wire (5 cm) was immersed in conc. HCl. The Cu(0) wire was removed and thoroughly rinsed with acetone and water then dried. Polymerisation commenced upon addition of the Cu(0) wire to the degassed reaction mixture. Samples were taken periodically and conversions were measured using ^{1}H NMR and SEC analysis.

Chain extension/block copolymerisation - Upon detection of >99% conversion a 1 : 1 mixture of deoxygenated monomer and DMSO was added to the reaction mixture *via* deoxygenated syringe. Samples were taken periodically and conversions were measured using ^{1}H NMR and SEC analysis.

4.4.4 Characterisation

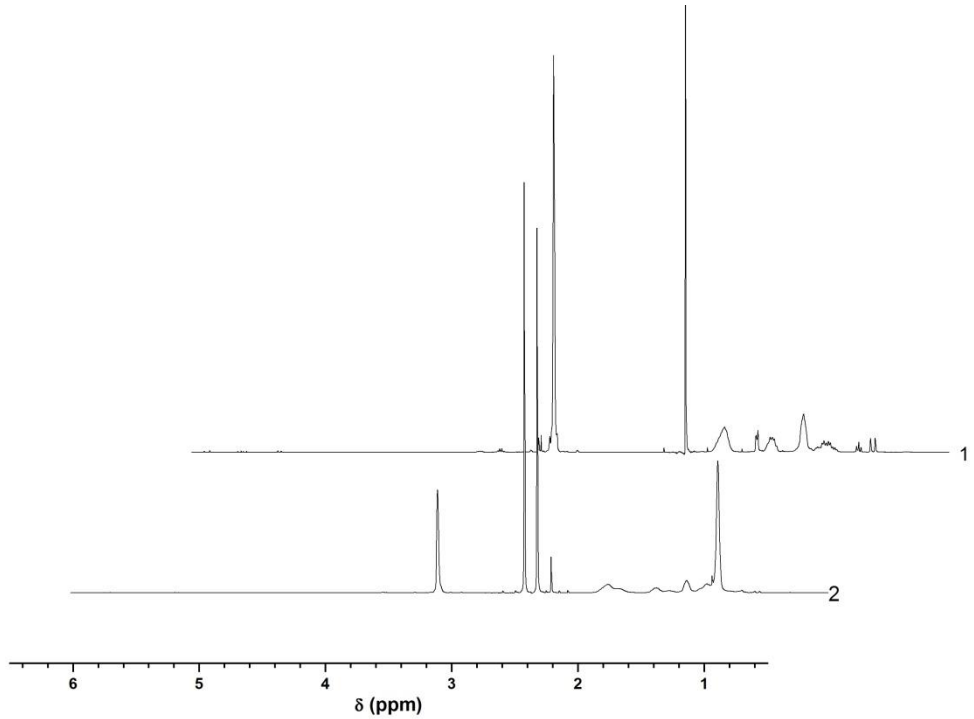

Figure 4.9: ^{1}H NMR for the synthesis and *in situ* chain extension of PMA with *t*BA [EBiB]:[MA]:[$CuBr_2$]:[Me_6-Tren]:[Cu(0) wire]=[1]:[125]:[0.01]:[0.09]:[5 cm].

4.5 References

1. J. Rodríguez-Hernández, F. Chécot, Y. Gnanou and S. Lecommandoux, *Prog. Polym. Sci.*, 2005, **30**, 691-724.
2. A. O. Moughton, M. A. Hillmyer and T. P. Lodge, *Macromolecules*, 2011, **45**, 2-19.
3. G. Pasparakis, N. Krasnogor, L. Cronin, B. G. Davis and C. Alexander, *Chem. Soc. Rev.*, 2010, **39**, 286-300.
4. R. C. Hayward and D. J. Pochan, *Macromolecules*, 2010, **43**, 3577-3584.
5. J. Gensel, I. Dewald, J. Erath, E. Betthausen, A. H. E. Muller and A. Fery, *Chem. Sci.*, 2013, **4**, 325-334.
6. Z. Zhu and S. A. Sukhishvili, *J. Mater. Chem.*, 2012, **22**, 7667-7671.
7. F. S. Bates, M. A. Hillmyer, T. P. Lodge, C. M. Bates, K. T. Delaney and G. H. Fredrickson, *Science*, 2012, **336**, 434-440.
8. J. C. Brendel, F. Liu, A. S. Lang, T. P. Russell and M. Thelakkat, *ACS Nano*, 2013, **7**, 6069-6078.
9. H. Cui, Z. Chen, S. Zhong, K. L. Wooley and D. J. Pochan, *Science*, 2007, **317**, 647-650.
10. D. E. Discher and A. Eisenberg, *Science*, 2002, **297**, 967-973.
11. I. W. Hamley, *Nanotechnology*, 2003, **14**, R39.
12. A.-C. Shi and B. Li, *Soft Matter*, 2013, **9**, 1398-1413.
13. N. Hadjichristidis, M. Pitsikalis, S. Pispas and H. Iatrou, *Chem. Rev.*, 2001, **101**, 3747-3792.
14. J.-S. Wang and K. Matyjaszewski, *J. Am. Chem. Soc.*, 1995, **117**, 5614-5615.
15. M. Kato, M. Kamigaito, M. Sawamoto and T. Higashimura, *Macromolecules*, 1995, **28**, 1721-1723.
16. C. J. Hawker, A. W. Bosman and E. Harth, *Chem. Rev.*, 2001, **101**, 3661-3688.
17. J. Chiefari, Y. K. Chong, F. Ercole, J. Krstina, J. Jeffery, T. P. T. Le, R. T. A. Mayadunne, G. F. Meijs, C. L. Moad, G. Moad, E. Rizzardo and S. H. Thang, *Macromolecules*, 1998, **31**, 5559-5562.
18. F. Schön, M. Hartenstein and A. H. E. Müller, *Macromolecules*, 2001, **34**, 5394-5397.
19. M. Zhong and K. Matyjaszewski, *Macromolecules*, 2011, **44**, 2668-2677.
20. A. H. Soeriyadi, C. Boyer, F. Nyström, P. B. Zetterlund and M. R. Whittaker, *J. Am. Chem. Soc.*, 2011, **133**, 11128-11131.
21. C. Boyer, A. Derveaux, P. B. Zetterlund and M. R. Whittaker, *Polym. Chem.*, 2012, **3**, 117-123.
22. C. Boyer, A. H. Soeriyadi, P. B. Zetterlund and M. R. Whittaker, *Macromolecules*, 2011, **44**, 8028-8033.

23. F. Nyström, A. H. Soeriyadi, C. Boyer, P. B. Zetterlund and M. R. Whittaker, *J. Polym. Sci., Part A: Polym. Chem.*, 2011, **49**, 5313-5321.
24. A. Goto and T. Fukuda, *Prog. Polym. Sci.*, 2004, **29**, 329-385.
25. M. R. Whittaker, C. N. Urbani and M. J. Monteiro, *J. Polym. Sci., Part A: Polym. Chem.*, 2008, **46**, 6346-6357.
26. A. Anastasaki, C. Waldron, P. Wilson, R. McHale and D. M. Haddleton, *Polym. Chem.*, 2013, **4**, 2672-2675.
27. N. H. Nguyen, X. Jiang, S. Fleischmann, B. M. Rosen and V. Percec, *J. Polym. Sci., Part A: Polym. Chem.*, 2009, **47**, 5629-5638.
28. M. E. Levere, N. H. Nguyen and V. Percec, *Macromolecules*, 2012, **45**, 8267-8274.
29. X. Jiang, B. M. Rosen and V. Percec, *J. Polym. Sci., Part A: Polym. Chem.*, 2010, **48**, 2716-2721.
30. G. Lligadas and V. Percec, *J. Polym. Sci., Part A: Polym. Chem.*, 2007, **45**, 4684-4695.
31. I. Astafieva, X. F. Zhong and A. Eisenberg, *Macromolecules*, 1993, **26**, 7339-7352.
32. K. A. Davis and K. Matyjaszewski, *Macromolecules*, 2000, **33**, 4039-4047.
33. Q. Ma and K. L. Wooley, *J. Polym. Sci., Part A: Polym. Chem.*, 2000, **38**, 4805-4820.
34. M. E. Levere, I. Willoughby, S. O'Donohue, A. de Cuendias, A. J. Grice, C. Fidge, C. R. Becer and D. M. Haddleton, *Polym. Chem.*, 2010, **1**, 1086-1094.
35. M. E. Levere, I. Willoughby, S. O'Donohue, P. M. Wright, A. J. Grice, C. Fidge, C. Remzi Becer and D. M. Haddleton, *J. Polym. Sci., Part A: Polym. Chem.*, 2011, **49**, 1753-1763.

Chapter 5

Copper(II)/tertiary Amine Synergy in Photo-induced Living Radical Polymerisation; Accelerated Synthesis of ω-functional and α,ω-heterofunctional Poly(acrylates)

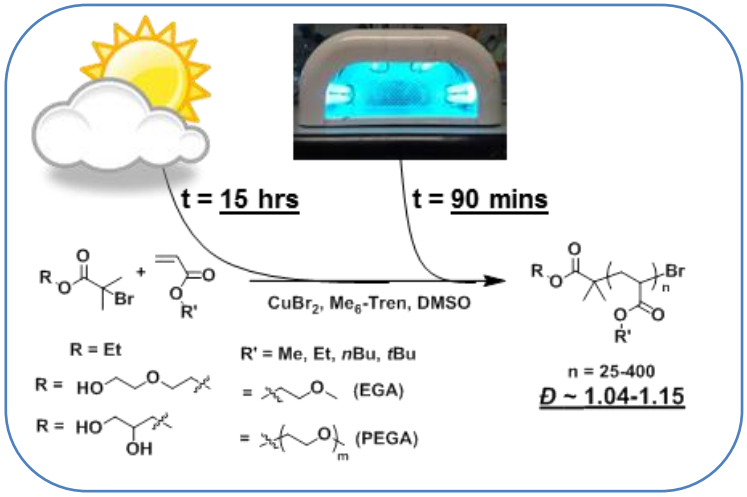

Photo-induced living radical polymerisation of acrylates, in the absence of conventional photo-initiators or dye sensitisers, has been realised in 'daylight' and is enhanced upon irradiation with UV radiation (λ_{max} ~ 360 nm). In the presence of low concentrations of copper(II) bromide and an aliphatic tertiary amine ligand (Me_6-Tren), near-quantitative monomer conversion (> 95%) is obtained within 80 minutes yielding poly(acrylates) with dispersities as low as 1.05 and excellent end-group fidelity (>99%). The versatility of the technique is demonstrated by polymerisation of methyl acrylate (MA) to a range of chain lengths (DP_n = 25-800), and a number of (meth)acrylate monomers including macromonomer poly(ethylene glycol) methyl ether acrylate ($PEGA_{480}$), tert-butyl acrylate (tBA) and methyl methacrylate (MMA), as well as styrene (Sty). Moreover, hydroxyl and vic-diol functional initiators are compatible with the polymerisation conditions, forming α,ω-heterofunctional poly(acrylates) with unparalleled efficiency and control. The control retained during polymerisation is confirmed by MALDI-ToF-MS and exemplified by in situ chain extension upon sequential monomer addition furnishing higher molecular weight polymers with an observed reduction in dispersity (Đ = 1.03). Similarly, efficient one-pot diblock copolymerisation by sequential addition of ethylene glycol methyl ether acrylate (EGA) and $PEGA_{480}$ to a poly(methyl) acrylate (PMA) macroinitiator without prior work-up or purification is also demonstrated. Minimal polymerisation in the absence of light confers temporal control and alludes to potential application at one of the frontiers of material chemistry whereby precise spatiotemporal control "on/off" control and resolution is desirable.

5.1 Introduction

When employing typical conditions of Cu-mediated living radical polymerisation, manipulation of the activation-deactivation equilibrium between active (P_n-·) and dormant species (P_n-X) maximises the control during polymerisation. Simply, this relies on selection of an appropriate Cu-ligand complex to optimise the overall rate of polymerisation and manage the concentration of the deactivation species which can accumulate through either the persistent radical effect (PRE)[1-3] or disproportionation mechanisms[4-9].

Recently, considerable interest has been directed towards controlling the activation-deactivation equilibrium using various stimuli[10], including photochemical[11, 12], pressure[13, 14], and electrochemical[15]. In an ideal synthesis such stimuli should result in lower activation energies for crucial steps such as initiation and repeated activations, allowing *in situ* generation of more active catalysts and thus faster CLRP under milder conditions. Many of these requirements are imparted by photo-mediated polymerisation with potential additional advantages over traditional thermal processes, including faster rates of polymerisation and spatial control over polymerisation. However, traditional photochemical processes lack the control desired to convey compositional and architectural design, a limitation that has been challenged in recent literature[16, 17].

Hawker and co-workers[18] recently showed that CLRP of methacrylates can be efficiently controlled using visible light, reaching relatively narrow dispersities (~1.25) and moderate conversions (~65%). Mechanistically, an activation-deactivation equilibrium was identified between an excited Ir^{III} photoredox catalytic complex (Ir^{III*}) and an Ir^{IV} complex, which act as the activator and deactivator, respectively. This was achieved by use of highly absorbing ligands in the photoactive complex *fac*-[$Ir(ppy)_3$] (ppy=2-pyridylphenyl)

(Scheme 3.1). Under irradiation, polymerisation of methyl methacrylate (MMA) was shown to proceed in a well-controlled manner up to 60% conversion ($Đ$ ~ 1.19-1.25), while reversible chain termination occurred upon removal of light, demonstrating a high degree of temporal control. The reversible termination was exemplified by block copolymerisation of the poly(MMA) macroinitiator with benzyl methacrylate (BzMA), while spatiotemporal control has recently been elaborated using surface-initiated CLRP in the presence of photomasks and density filters[19].

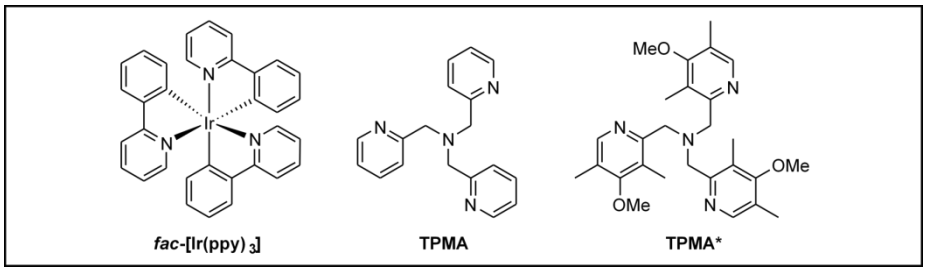

Scheme 5.1: Ir complex[18] and pyridine based ligands[20] reported to promote photo-mediated CLRP.

Traditional Cu-mediated polymerisation has also been shown to benefit from photo-irradiation. Yagci and co-workers have developed Cu-mediated, photo-induced controlled radical polymerisation (PCRP) systems both in the presence and absence of conventional photoinitiators or photosensitisers[17, 21-24]. In the absence of photosensitisers, it has been suggested that light induces polymerisation by *direct* reduction of $Cu^{II}(L)X_2$ to $Cu^{I}(L)X$[17, 21, 23]. The bulk polymerisation of MMA was performed using a $Cu^{II}(L)X_2$ complex (L = *N, N, N', N'', N''*-pentamethyldiethylenetriamine (PMDETA)), as a precatalyst. Upon irradiation, reduction of $Cu^{II}(L)X_2$ is proposed to proceed *via* homolysis furnishing $Cu^{I}(L)X$ and $X^{\cdot}$. The halide radical can either reoxidise the $Cu^{I}(L)X$ species or is quenched allowing the $Cu^{I}(L)X$ to activate a dormant chain. Interestingly, in the presence of MeOH as a co-solvent, polymerisation was aided by improved dissolution of the $Cu^{II}(L)X_2$ complex. Moreover, the $X^{\cdot}$ formed was shown to abstract $H^{\cdot}$ from MeOH,

forming HX and hydroxymethyl radicals which could act as reducing agents for the reduction of $Cu^{II}(L)X_2$ to $Cu^{I}(L)X$.

Matyjaszewski *et al.* recently reported visible/sunlight photo-induced ATRP using $Cu^{II}(TPMA)Br_2$ with subtle differences to the mechanism suggested by Yagci. They proposed the photo-reduction of $Cu^{II}(TPMA)Br_2$ to $Cu^{I}(TPMA)Br$ by ligand-to-metal charge transfer in the photo-excited state[20]. Polymerisation was then initiated by either $Cu^{I}(TPMA)Br$ or a bromine radical, both proposed products of the photo-reduction of the Cu^{II} complex, which was said to imply a hybrid mechanism somewhere between ICAR[25] and ARGET-ATRP[26]. Various wavelengths were investigated and well-controlled polymerisations were obtained using a modified TPMA ligand (*tris*((4-methoxy-3,5-dimethylpyridin-2-yl)amine), TPMA*) in sunlight and at λ_{max} = 392 nm. Reaction times were generally between 12-32 hours and optimum results were obtained in sunlight. Similar observations were made during the photo-mediated polymerisation of MMA at λ_{max} > 350 nm. Initiation from 2-bromopropionitrile in the presence of $Cu^{II}(TPMA)Br_2$ or $Cu^{II}(PMDETA)Br_2$ resulted in well-controlled polymerisation with conversions reaching 80%. Temporal control[20, 21, 27] by consecutive light and dark reactions has also been reported and readily translates into spatial resolution in light-induced surface-initiated ATRP (SI-ATRP)[28].

Herein a polymerisation protocol is presented exploiting photo-activation in the presence of a cupric precursor ($Cu^{II}(Me_6\text{-Tren})Br_2$) and an excess (with respect to $Cu^{II}(Me_6\text{-Tren})Br_2$) of *aliphatic* tertiary amine Me_6-Tren. For the first time, under UV irradiation (λ_{max} ~ 360 nm) near-quantitative conversions for a range of targeted molecular weights (DP_n = 25-400) has been achieved. Moreover, the breadth in scope of photo-induced polymerisation is also recognized, employing a variety of acrylate monomers as well as functional initiators, furnishing α,ω-heterofunctional poly(acrylates). The resulting

polymers are characterised by their narrow dispersities (*Đ*) and high end-group fidelities as exemplified by chain extension and block copolymerisation. Significantly, temporal control is also observed during intermittent light and dark reactions. An insight into the possible mechanism through a series of control experiments, with a view to gaining some clarity over the overall mechanism asserted in this photo-activated polymerisation in the presence of traditional Cu complexes is also discussed.

5.2 Results and Discussion

5.2.1 Photo-activated polymerisation of methyl acrylate (MA) in visible (*British*) light

Photo-induced controlled radical polymerisation (PCRP) was fortuitously observed whilst investigating Cu-mediated living radical polymerisation of methyl acrylate (MA) in a flow system[29], whereby the mixture in a pyrex syringe in the absence of copper(0) but in the presence of copper(II) gave slow but effective polymerisation.

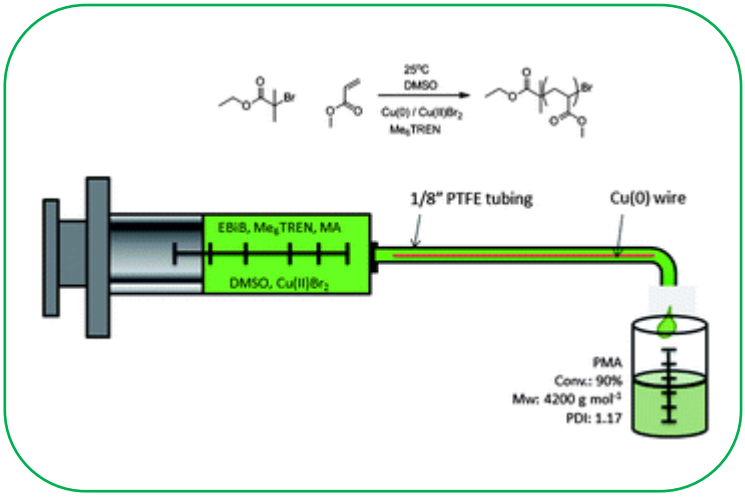

Scheme 5.2: Cu-mediated living radical polymerisation of methyl acrylate (MA) in a flow system

Deoxygenated mixtures containing [MA] : [EBiB] : [Me_6-Tren] : [$CuBr_2$] = [50] : [1] : [0.12] : [0.02] in DMSO (50 % *v/v*) were found to yield well defined PMA (M_n ~ 4500; *Đ* ~ 1.05) at quantitative conversion upon standing in a fume-hood for a period of 1

day in the absence of any known activators or apparent reducing agents. Kinetic investigations revealed quantitative conversion (~ 99%) within 15 h following an initial induction period of ~ 3 h. Following this induction period, a linear dependence of $\ln[M]_0/[M]_t$ *vs*. time indicated first order kinetics with respect to monomer concentration, while M_n increased linearly with time and $Đ$ values remained narrow (≤ 1.10) throughout the reaction (Figure 5.1).

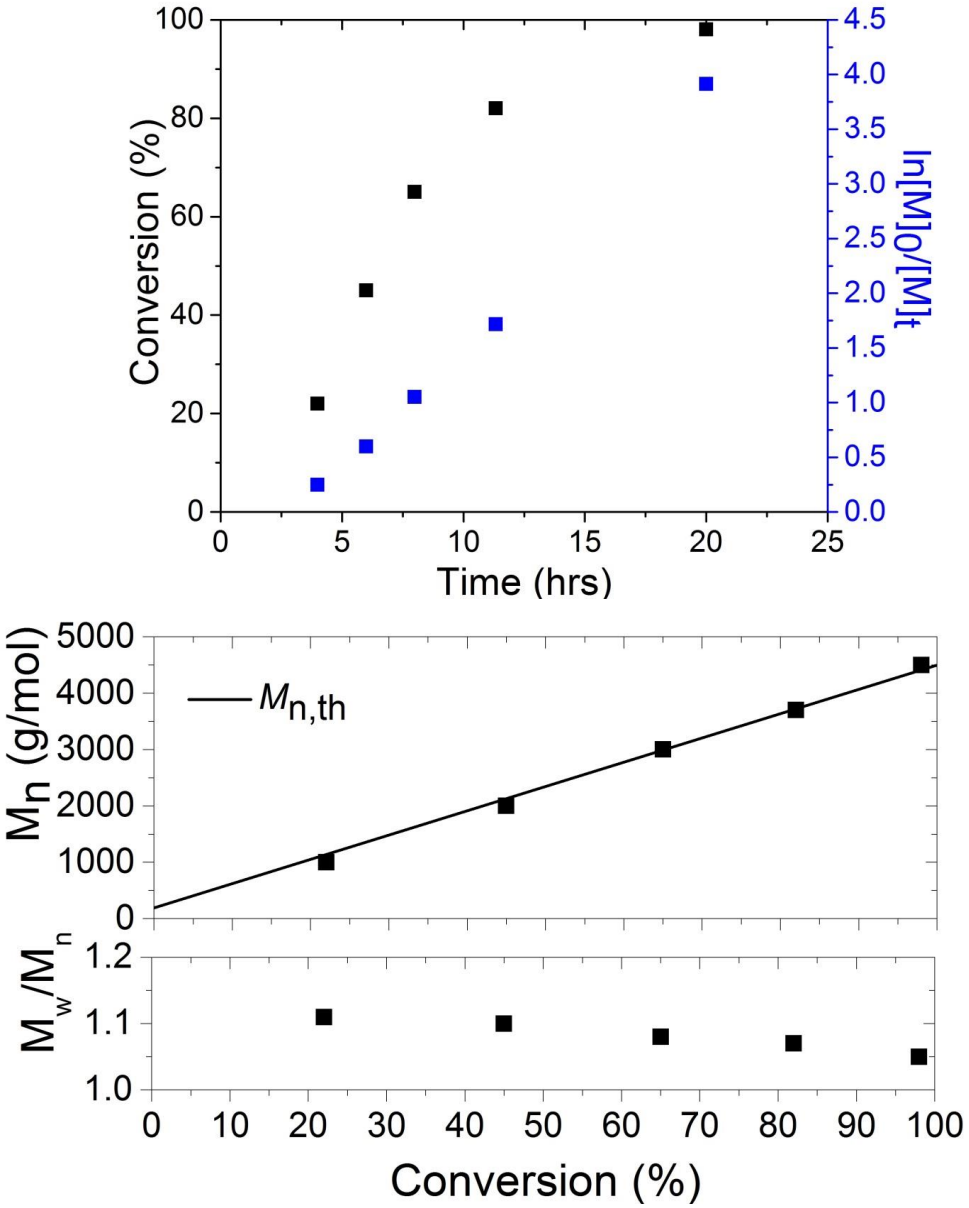

Figure 5.1: Kinetic and molecular weight/dispersity data of the polymerisation of MA in sunlight at ambient temperature.

Additionally, both MALDI-ToF-MS and ^{1}H-NMR (Figure 5.2) spectroscopic analyses confirmed living characteristics, with both techniques illustrating agreement between $M_{n,th}$ and $M_{n,exp}$ and excellent end-group fidelity.

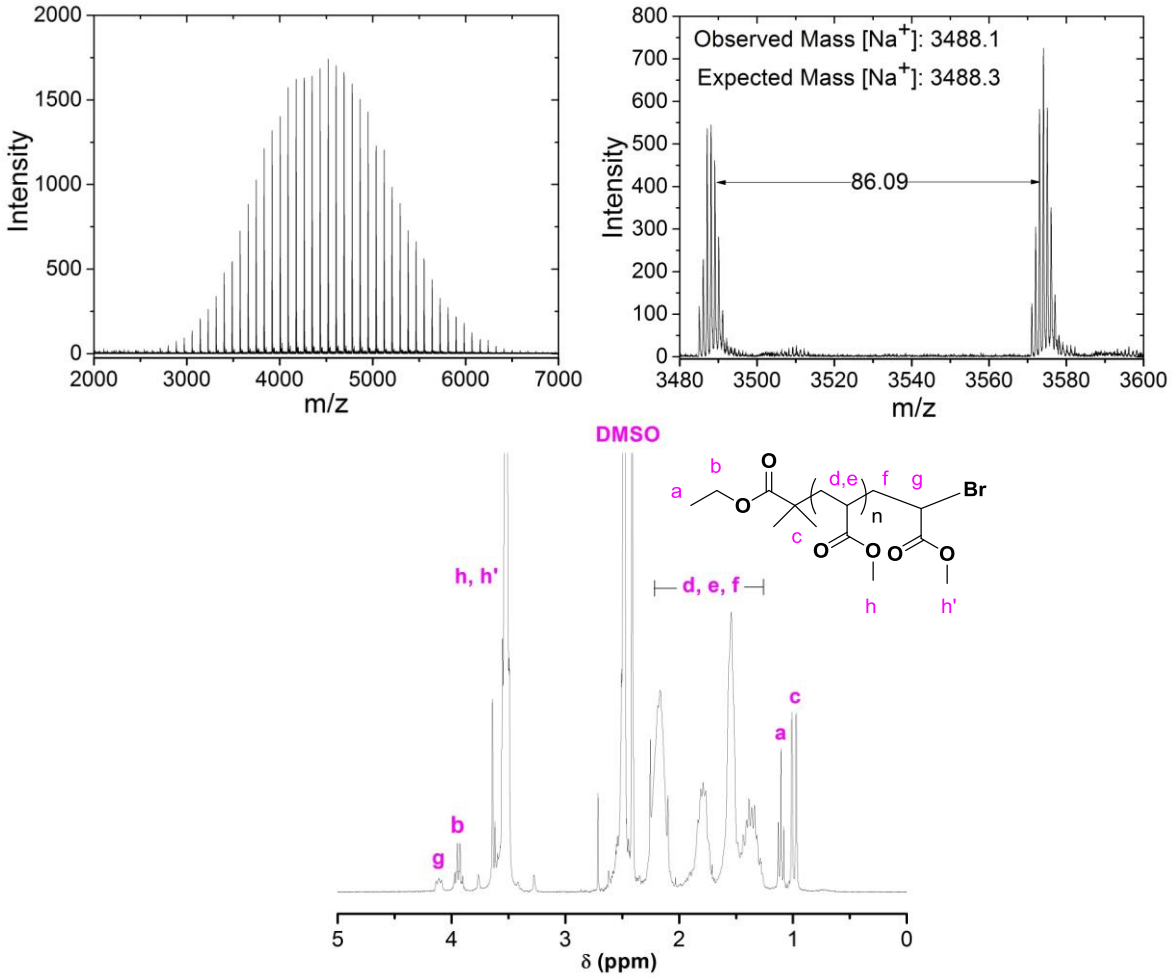

Figure 5.2: MALDI-ToF-MS and ^{1}H NMR ($CDCl_3$, 400 MHz) spectrum of final polymer obtained from the daylight experiment: [$CuBr_2$]/[Me_6-Tren]/[EBiB]/[MA] polymerisation mixture in DMSO (50:50 *v/v* monomer/solvent) at ambient temperature. Integrated ratio of g : c = 0.99 : 6.00.

Initially, we were perplexed by the degree of control associated with these polymerisations in the absence of established Cu-based activators such as Cu(0) or Cu(I). Previous research has described excess of tertiary amines adopting the role of a reducing agent for the reduction of $Cu^{II}(L)X_2$ to $Cu^{I}(L)X$ during Cu(I)-mediated polymerisation, as evidenced by a reduction of the intensity of the UV-Vis spectrum of $Cu^{II}(Me_6\text{-Tren})Br_2$[30-34]. However, there is limited evidence to support this claim and our own experiments

showed that this decrease in the UV-Vis absorption from the d^9 d-d transition in Cu(II) in DMSO is explained by the Cu(II) complex forming deep blue microcrystals on the side of the cuvette, thus reducing the concentration in solution, and not by a reduction to colourless d^{10} Cu(I). A change of solvent to isopropanol, which fully solubilises this complex, proved to show no loss in absorption and thus no reduction of $Cu^{II}(Me_6\text{-Tren})Br_2$[35].

We decided to repeat the polymerisation in a homemade 'black box' to eliminate this potential reduction by excess Me_6-Tren, present under the chosen reaction conditions. No polymerisation was observed over a period of 48 h, adding further evidence to the inability of Me_6-Tren to act as a reducing agent of $Cu^{II}(Me_6\text{-Tren})Br_2$ to $Cu^{I}(Me_6\text{-Tren})Br$ which might have acted as a source of activation if this report was reproducible. The lack of polymerisation also suggested that the presence of light was essential for polymerisation. We envisaged that light could either be generating radicals *via* C-X bond homolysis or auto-initiation of the alkyl halide initiator (EBiB), with control invoked by the presence of the $Cu^{II}(Me_6\text{-Tren})Br_2$, to reversibly terminate the propagating chains. This process would generate $Cu^{I}(Me_6\text{-Tren})Br$ which could either activate a dormant chain or disproportionate (to Cu(0) and $Cu^{II}(Me_6\text{-Tren})Br_2$), depending on the reaction conditions. Alternatively, the light could be directly reducing $Cu^{II}(Me_6\text{-Tren})Br_2$ to $Cu^{I}(Me_6\text{-Tren})Br$ as eloquently described by Yagci *et al.* for similar related complexes[17, 21, 23]. A series of control experiments were performed in order to probe these hypotheses.

5.2.2 Photo-activated polymerisation of methyl acrylate (MA) in UV light (λ_{max} ~ 360 nm).

The effect of wavelength was initially investigated by varying the light source to cover the UV/visible spectrum (Table 5.1). Optimal results were obtained from polymerisation under a UV lamp with λ_{max} ~ 360 nm.

Table 5.1: The effect on wavelength on the photo-mediated polymerisation of MA. [MA]:[EBiB]:[$CuBr_2$]:[Me_6-Tren] = [50]:[1]:[0.02]:[0.12]. DMSO solvent 50% *v/v*. [a] Determined by ^1H NMR. [b] Determined by $CHCl_3$ SEC. [c] Performed in duplicate with identical results.

Entry	Light	Time (h)	Conv.[a]	$M_{n,th}$	$M_{n,SEC}$[b]	$Đ$[b]
1[c]	Red L.E.D.	24	-	4500	-	-
2[c]	Green L.E.D.	24	-	4500	-	-
3	Blue L.E.D.	24	>99%	4500	3900	1.07
4	UV (λ_{max} ~ 360 nm)	1.7	96%	4500	4500	1.05

Applying the previous conditions ([MA] : [EBiB] : [Me_6-Tren] : [$CuBr_2$] = [50] : [1] : [0.12] : [0.02] in DMSO (50 % *v/v*), PMA was prepared in high conversion (96 %) within 80 minutes, including an initial induction period of 15 minutes (Figure 5.3). This represents a remarkable acceleration in the rate of polymerisation relative to the daylight reaction. Polymerisation control was retained as indicated by low $Đ$ values, which decreased as the reaction progressed (1.11 to 1.05, Figure 5.3). Kinetic analysis revealed a linear increase of $(\ln[M]_0/[M]_t)$ *vs*. time as well as a linear evolution of M_n with monomer conversion. Correlation between $M_{n,th}$ and $M_{n,exp}$ values further confirms the controlled/living character of the polymerisation.

Initially, prevailing thermal effects from the UV bulbs had to be investigated. The temperature of the reaction under UV irradiation was monitored with a thermocouple and found to fluctuate between 50-55 ^oC. To determine the effect of temperature we repeated polymerisations both under UV irradiation in a jacketed cell, with a steady flow of cold water to reduce the internal temperature, and under purely thermal conditions at 55 ^oC (no UV irradiation). After identical reaction times (80 min) the pure thermal reaction yielded no polymer whereas the jacketed reaction, under UV irradiation, gave almost identical results to the uncooled system (λ_{max} ~ 360 nm)[36].

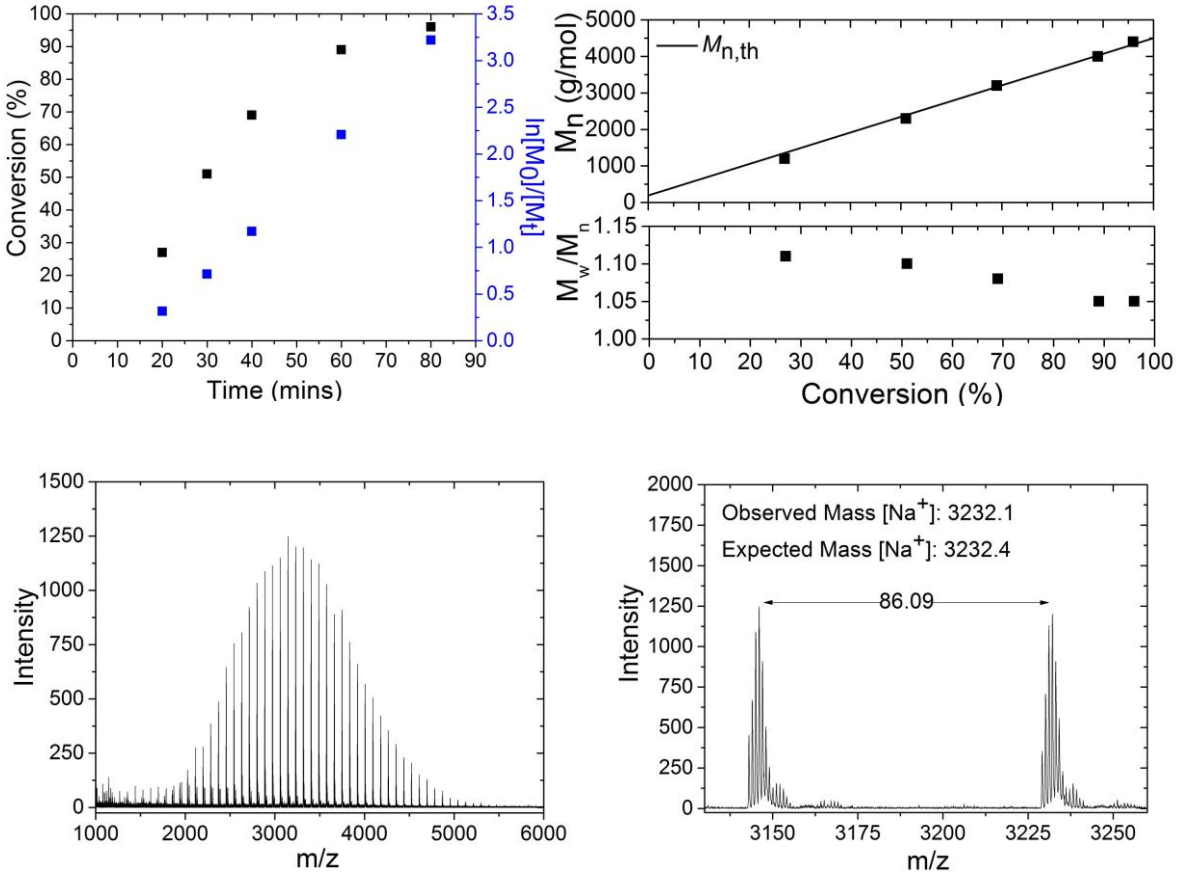

Figure 5.3: Kinetic and molecular weight and dispersity data of the polymerisation of MA under UV (λ_{max} ~360 nm) irradiation. MALDI-ToF-MS confirms high end-group fidelity.

Consequently, the remaining control experiments were performed under UV irradiation at λ_{max} ~ 360 nm without cooling (T ~ 50-55 ^{o}C). Polymerisations were systematically repeated in the absence of each single reagent to further elucidate key components in the polymerisation (Table 5.2). The most significant finding from these control experiments was that radicals are likely formed *via* a number of different mechanisms under UV exposure (Table 5.2, entries 1-7). Polymerisation of MA was possible under various conditions, proceeding in an uncontrolled manner ($Đ$ = 1.76-2.20) with variable conversions (10-61 %). Considered in the context of those experiments which yielded no polymer, it is evident that radicals can be produced separately by both uncomplexed Me_6-Tren (free ligand) and EBiB under UV irradiation, even in the absence of copper compounds, and that MA auto-initiation is also possible.

Table 5.2: A series of control experiments investigating photo-mediated polymerisation in the presence of UV light (λ_{max} ~ 360 nm), [L] = Me_6-Tren. [a] DMSO 50% *v/v* used as solvent. [b] Determined from ^{1}H NMR. [c] Determined from $CHCl_3$ SEC analysis. [d] Not reproducible when repeated in triplicate 0-12% conversion obtained.

Entry	[M]:[I]:[Cu^{II}]:[L][a]	Conv.[b] 90 min	M_n[c] g.mol^{-1}	*Đ*
1	[50]:[-]:[0.02]:[0.12]	12%	12600	1.65
2	[50]:[1]:[-]:[0.12]	61%	30000	1.76
3	[50]:[1]:[0.02]:[-]	-	-	-
4	[50]:[1]:[-]:[-]	38%	88000	2.2
5	[50]:[-]:[0.02]:[-]	-	-	-
6	[50]:[-]:[-]:[0.12]	45%	24000	1.79
7[d]	[50]:[-]:[-]:[-]	-	-	-
8	[50]:[1]:**[0.02]:[0.02]**	-	-	-
9	[50]:[1]:**[0.02]:[0.04]**	90%	4400	1.07
10	[50]:[1]:**[0.02]:[0.06]**	95%	5000	1.07
11	[50]:[1]:**[0.02]:[0.12]**	95%	4500	1.05

The [CuBr] : [Me_6-Tren] ratio was subsequently investigated (Table 5.2, entries 8-11). The initial reaction conditions ([MA] : [EBiB] : [Me_6-Tren] : [$CuBr_2$] = [50] : [1] : [0.12] : [0.02]), employed [$CuBr_2$] : [Me_6-Tren] = [1] : [6]. This could be reduced to [1] : [3] and [1] : [2] respectively with retention of both high conversion (90-95 %) and narrow dispersities (*Đ* = 1.07). However, when the relative stoichiometries were balanced ([$CuBr_2$] : [Me_6-Tren] = [1] : [1]) no polymerisation was observed. At this stoichiometry all of the ligand should be complexed to $CuBr_2$ to form $Cu^{II}(Me_6\text{-Tren})Br_2$, thus the lack of polymerisation implicates excess uncomplexed Me_6-Tren as being essential for photo-activation.

Whilst maintaining a [$CuBr_2$] : [Me_6-Tren] ratio of [1] : [6], the effect of the initial [$CuBr_2$] and [Me_6-Tren] loadings relative to initiator were investigated. Increasing the ratio ([EBiB] : [$CuBr_2$] : [Me_6-Tren] = [1] : [0.05] : [0.30]) resulted in a slight decrease in monomer conversion (85 %) but preservation of polymerisation control over the 90 minute

irradiation period. It was possible to decrease the [I] : [$CuBr_2$] : [Me_6-Tren] ratio to [1] : [0.005] : [0.03] without significant loss of control ($Đ$ = 1.12) or reaction rate (Table 5.3). However further reduction in [$CuBr_2$] to [0.001] relative to initiator was shown to compromise the polymerisation control (87%, $Đ$ = 1.42).

Table 5.3: Differing [$CuBr_2$], [Me_6-Tren] loadings relative to [EBiB] in UV (λ_{max} ~ 360 nm) and sunlight mediated polymerisation of MA

	[Cu][a]:[I]	Conv.[b]	$M_{n,th}$[c] g.mol^{-1}	$M_{n,SEC}$[d] g.mol^{-1}	$Đ$
UV 90 min	0.05	85	3900	4400	1.06
	0.02	96	4400	4500	1.05
	0.01	94	4300	4900	1.07
	0.005	92	4200	4700	1.12
	0.001	87	4000	4800	1.42
Daylight 15 h	0.05	~0%	-	-	-
	0.02	99%	4500	4500	1.05
	0.01	99%	4500	4200	1.07
	0.005	99%	4500	4000	1.11
	0.001	99%	4500	4000	2.39

5.2.3 Investigation into the scope of the photo-activated polymerisation.

In order to probe the potential of this technique in maintaining control for higher molecular weights a range of polymerisations were conducted, targeting degrees of polymerisation (DP_n) from 25 to 800 (Figure 5.4; also see Table 5.3). The ratio [$CuBr_2$] : [Me_6-Tren] = [1] : [6] was maintained for each polymerisation resulting in high conversions (≥ 93%) within 90 minutes, with a good correlation being observed between $M_{n,exp}$ and $M_{n,th}$ and dispersities remained very low ($Đ$ ~ 1.05, Table 5.3).

Table 5.4: Photo-mediated polymerisation of MA to range of DP_n. DMSO solvent 50% *v/v*. [a]Determined by ^1H NMR. [b]Determined by $CHCl_3$ SEC.

[MA]:[I]:[L]:[$CuBr_2$]	Conv.[a] (t = 90 min)	$M_{n,th}$ g.mol^{-1}	$M_{n,SEC}$[b] g.mol^{-1}	$Đ$
[25]:[1]:[0.12]:[0.02]	93%	2300	2300	1.10
[50] :[1]:[0.12]:[0.02]	96%	4500	4400	1.05
[100]:[1]:[0.12]:[0.02]	94%	8800	9000	1.04
[200]:[1]:[0.12]:[0.02]	94%	17400	17000	1.05
[400]:[1]:[0.12]:[0.02]	93%	34600	35000	1.04
[800]:[1]:[0.12]:[0.02]	92%	63500	46000	1.12

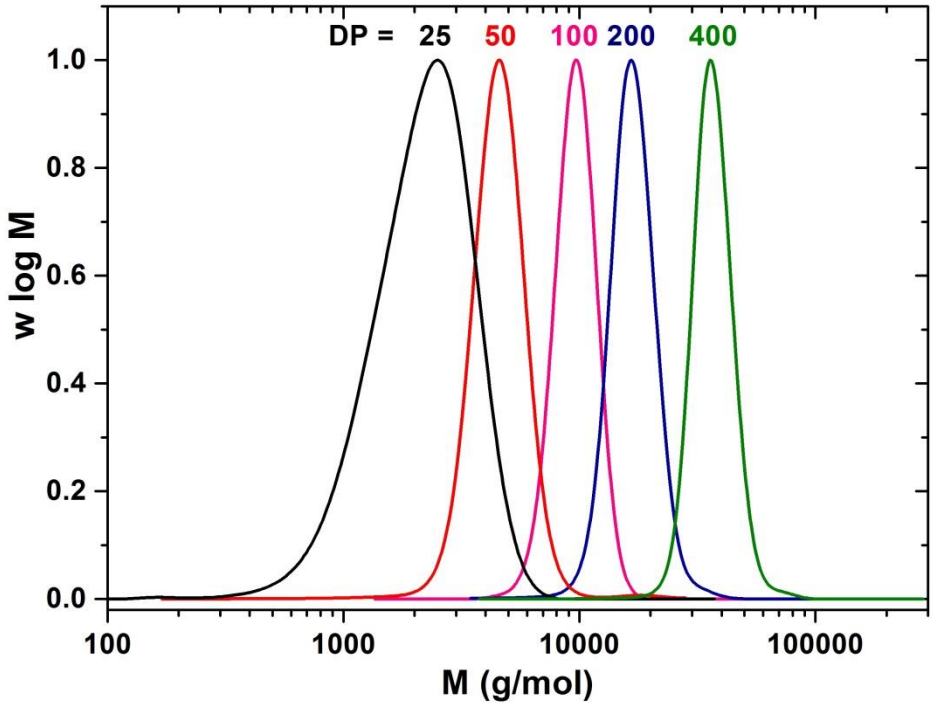

Figure 5.4: SEC analysis of PMA with various DP_n prepared by photo-mediated polymerisation in the presence of UV light (λ_{max} ~ 360 nm).

When extending the chain length to DP_n = 800, although polymerisation control was seemingly retained ($Đ$ = 1.12), $M_{n,exp}$ (46000) and $M_{n,th}$ (63500) were found to deviate considerably (Table 5.3).

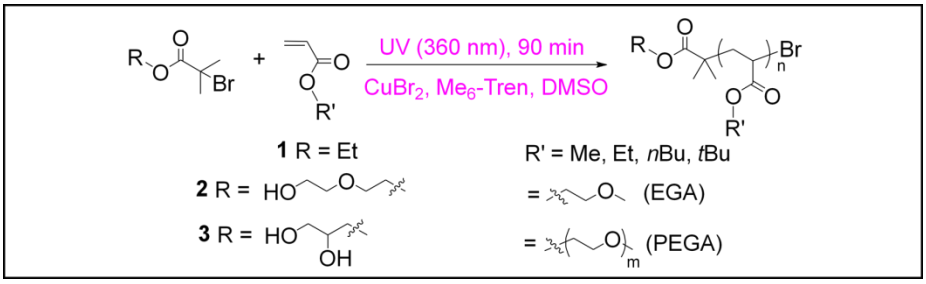

Scheme 5.3: Photo-mediated polymerisation of a variety of acrylate monomers.

The scope of the reaction was extended to a number of acrylate monomers including ethyl acrylate (EA) and *n*-butyl acrylate (*n*BA), protected/functional acrylates; *t*-butyl acrylate (*t*BA), as well as ethylene glycol acrylate (EGA) and poly(ethylene glycol) acrylate (M_n ~ 480, $PEGA_{480}$). Polymerisation of these acrylates reached high conversion (92-97%) and exhibited narrow dispersities ($Đ$ ~ 1.07-1.16, Table 5.5). The light-induced polymerisation of *n*BA in DMSO (Table 5.5, entry 2) was found to proceed *in situ* with phase-separation, as previously observed for a thermal process[37, 38]. Conversely, the polymerisation of *t*BA in DMSO was problematic, reproducibly furnishing no polymer within the 90 min reaction time. The choice of solvent in conventional Cu-mediated polymerisation is crucial when using increasingly hydrophobic monomers. A phase separation phenomenon has been reported during the Cu(0)-mediated polymerisation of hydrophobic acrylates[37, 38]. In the case of *tert*-butyl acrylate, an adverse effect on the polymerisation control, manifest as a broader dispersity relative to related butyl isomers[37], was reported when DMSO was used as solvent. In the case of the photo-activated reaction this was rectified by performing the polymerisation in DMF whereby high conversion (96%) and good control ($Đ$ = 1.10) was attained (Table 5.5 entry 3).

Table 5.5: Photo-mediated polymerisation of six acrylate monomers. [M]:[I]:[Cu^{II}]:[L] = [50]:[1]:[0.02]:[0.12] DMSO 50% *v/v* solvent. [a] Determined by ^{1}H NMR. [b] Determined by $CHCl_3$ SEC analysis (see SI). [c] DMF 50% *v/v* used as solvent. [d] DP_n=25 targeted for subsequent MALDI-ToF-MS analysis.

Entry	R	R'	Conv.[a]	$M_{n,th}$	$M_{n,SEC}$[b]	$Đ$
1	1	Et	97%	5200	5900	1.07
2	1	*n*Bu	97%	6600	6800	1.16
3[c]	1	*t*Bu	96%	6600	4500	1.10
4	1	EGA	97%	6700	6600	1.07
5	1	PEGA	92%	5000	6000	1.09
6[d]	2	Me	92%	2400	2400	1.11
7[d]	3	Me	93%	2400	2300	1.15

On expanding the technique to less activated monomers such as methyl methacrylate (MMA) and styrene (Sty), conversions were limited (78% and 40 % respectively) with an observable reduction in control ($Đ$ ~ 1.29-1.40, respectively). The lower conversions are consistent with relative rates of propagation (k_p), with acrylate > methacrylate > styrene. Furthermore, in the few reports of the polymerisation of styrene at ambient temperature, DMSO has been highlighted as a poor solvent, leading to a loss of control during the polymerisation[39, 40]. However, with a careful choice of solvent and catalyst system, relatively well-defined polymers can be obtained *via* traditional thermal polymerisation[39] suggesting that optimisation of this photo-activated process could furnish comparable results.

Hydoxy-functional[41] and *vic*-diol[42] functional initiators 2 and 3 (Scheme 5.3) were also tolerant of the irradiation conditions, resulting in the incorporation of α-functionality into well-defined PMA. Polymerisation from 2 (Table 5.5, entry 6) and 3 (Table 5.5, entry 7) gave high conversions (>90%) with dispersities of 1.11 and 1.15 respectively, indicative of a high degree of ω-chain end functionality to complement the α-functionality.

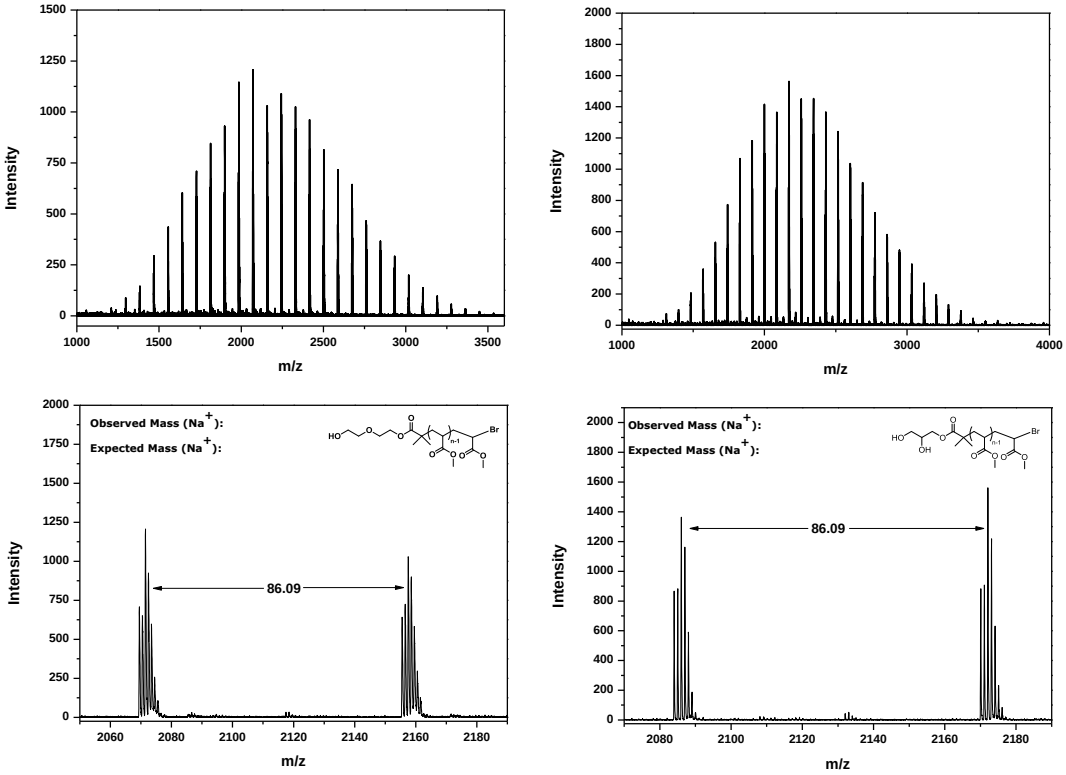

Figure 5.5: MALDI-ToF-MS reflectron mode spectrum of poly(methyl acrylate) obtained from photo-mediated polymerisation: [MA]:[2 or 3]:[$CuBr_2$]:[Me_6-Tren] = [25]:[1]:[0.02]:[0.12] in DMSO (50:50 *v/v* monomer/solvent).

The degree of control attained in the UV light-activated polymerisation from all three initiators was confirmed using MALDI-ToF-MS (Figure 5.5 and 5.6) and ^{1}H NMR spectroscopy for the lower DP_n polymers. MALDI-ToF-MS of PMA initiated from EBiB revealed a single distribution in linear mode corresponding to polymer chains initiated by the expected EBiB fragment and bromo-terminated. ^{1}H NMR confirmed a bromo-end functionality close to 100% fidelity on comparing signals corresponding to the -CH_3 groups of the isobutyrate group of EBiB (α-terminal; 2 singlets, 6H, 1.0 ppm) with the ω-terminal methine signal (triplet, 1H, 4.3 ppm, Figure 5.6).

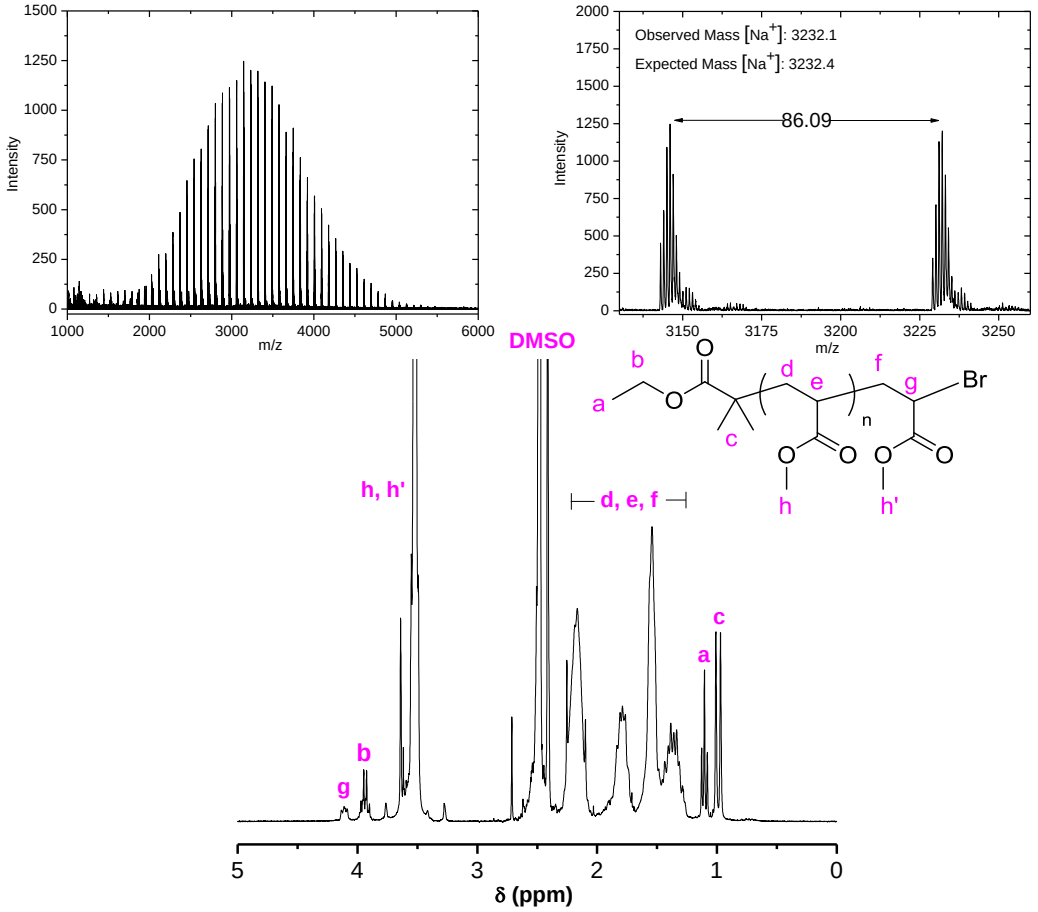

Figure 5.6: MALDI-ToF-MS and ^{1}H NMR ($CDCl_3$, 400 MHz) spectrum of final polymer obtained from the UV experiment: [$CuBr_2$]/[Me_6-Tren]/[EBiB]/[MA] polymerisation mixture in DMSO (50:50 *v*/*v* monomer/solvent) at ambient temperature. Integrated ratio of g : c = 0.99 : 6.00.

In situ chain extension verified these end-group analyses (Figure 5.7). Excellent control was observed with the molecular weight distribution shifting to higher molecular weight with an observable decrease in dispersity ($Đ$ ~ 1.03) upon addition of a second aliquot of MA (Figure 5; ~95% conversion attained within 90 minutes for the second MA block). Addition of a second acrylate monomer (EGA) resulted in a one-pot block copolymerisation as indicated by SEC and ^{1}H NMR (Figure 5.7), allowing access to a well-defined poly(MA)-*b*-(EGA) block copolymers without the need for a macroinitiator purification step. Amphiphilic block copolymers were also prepared using $PEGA_{480}$ as the comonomer with equal efficiency (Figure 5.7).

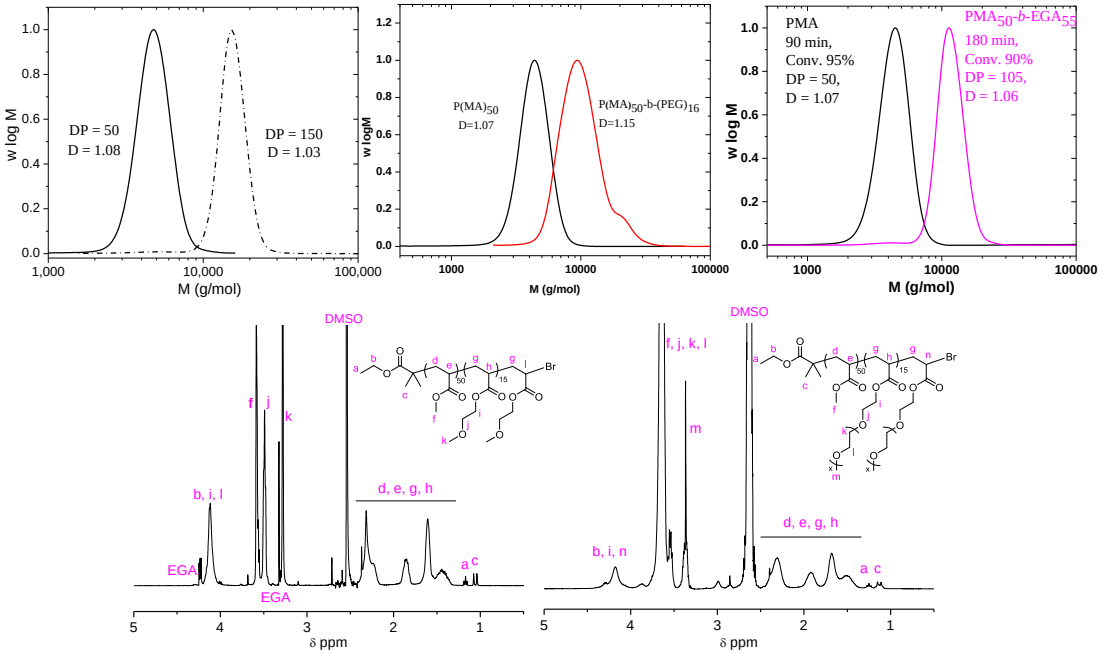

Figure 5.7: *In situ* chain extension and block copolymerisation from a pMA macroinitiator. SEC analysis p(MA)$_{50}$-*b*-p(MA)$_{100}$, p(MA)$_{50}$-*b*-p(PEG)$_{16}$ and p(MA)$_{50}$(EGA)$_{105}$ (top) and ^{1}H NMR analysis of the block copolymers respectively (bottom)

5.2.4 Synthesis of PMA with temporal control.

The possibility of "on/off" temporal control during polymerisation was investigated using intermittent light and dark exposure for alternating 20 minute periods. Approximately 30% monomer conversion was attained in the first period of UV irradiation (Figure 5.8). Confinement of the polymerisation mixture to a black box at this point resulted in near-complete discontinuation of polymerisation. On re-exposing the mixture after 40 minutes (20 minute dark reaction) the original polymerisation rate was restored. These cycles were repeated, equating to a total exposure time of 80 minutes and resulting in PMA (93%, M_n = 4900 g/mol, $Đ$ = 1.07, Figure 5.8) comparable to the standard polymerisation under uninterrupted UV irradiation. The kinetic profile of the polymerisation was also directly comparable, highlighting that the robust nature of this polymerisation protocol was unaffected by repeated "on/off" exposure.

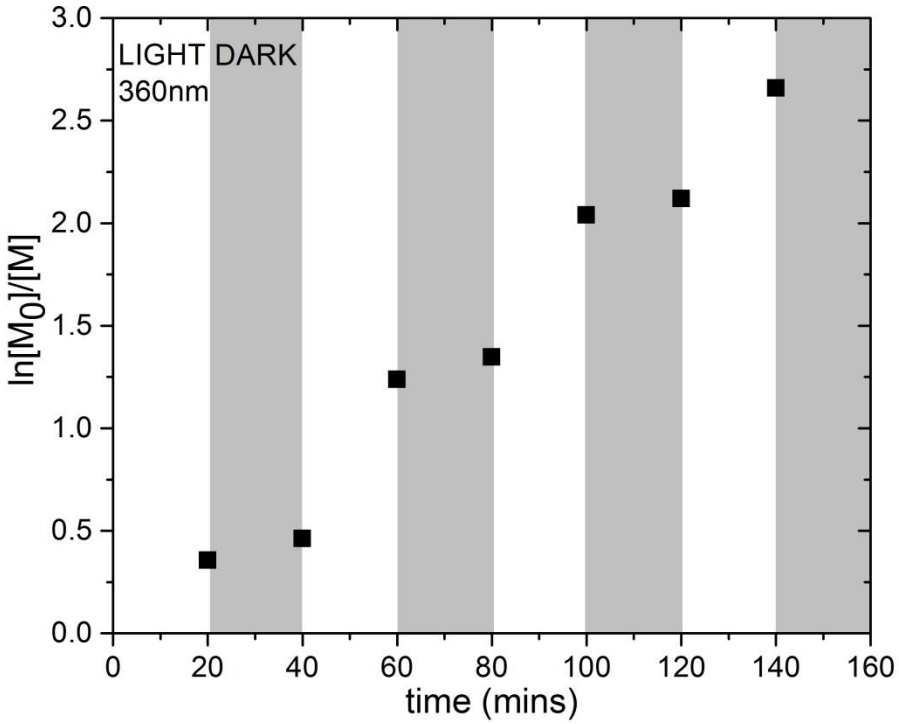

Figure 5.8 Evidence of temporal control *via* consecutive light (white area) and dark (shaded area) exposure obtained from the sequential light and dark exposure experiment; M_n = 4900 g/mol; $Đ$ = 1.07; 93% conversion [M]:[I]:[Cu^{II}]:[L] = [50]:[1]:[0.02]:[0.12] DMSO 50% *v/v* solvent.

Whilst temporal control presents positive implications for future applications, it also offers valuable mechanistic insight, underlining how the polymerisation requires photo-exposure at an appropriate wavelength for initiation and sustained reactivation/propagation in the presence of Me_6-Tren. This may imply direct involvement in the activation step or indirect involvement *via* continuous photo-regeneration of an active catalyst, which is required throughout the duration of the polymerisation.

5.2.5 The effect of the source and relative concentration of Cu on photo-activated polymerisation of MA.

A series of kinetic experiments were performed, initially varying the source of Cu followed by the overall loading of the $CuBr_2$ in the system. No appreciable difference, within error, was observed in the rate of reaction when the polymerisation was performed in the presence of CuBr, $CuBr_2$, $CuCl_2$ or Cu(0) (formed from the disproportionation of

$Cu^{I}(Me_6\text{-Tren})Br$ in H_2O according to a literature procedure[43]) present in [1] : [6] ratio with Me_6-Tren, in accordance with the standard polymerisation conditions (Figure 5.9).

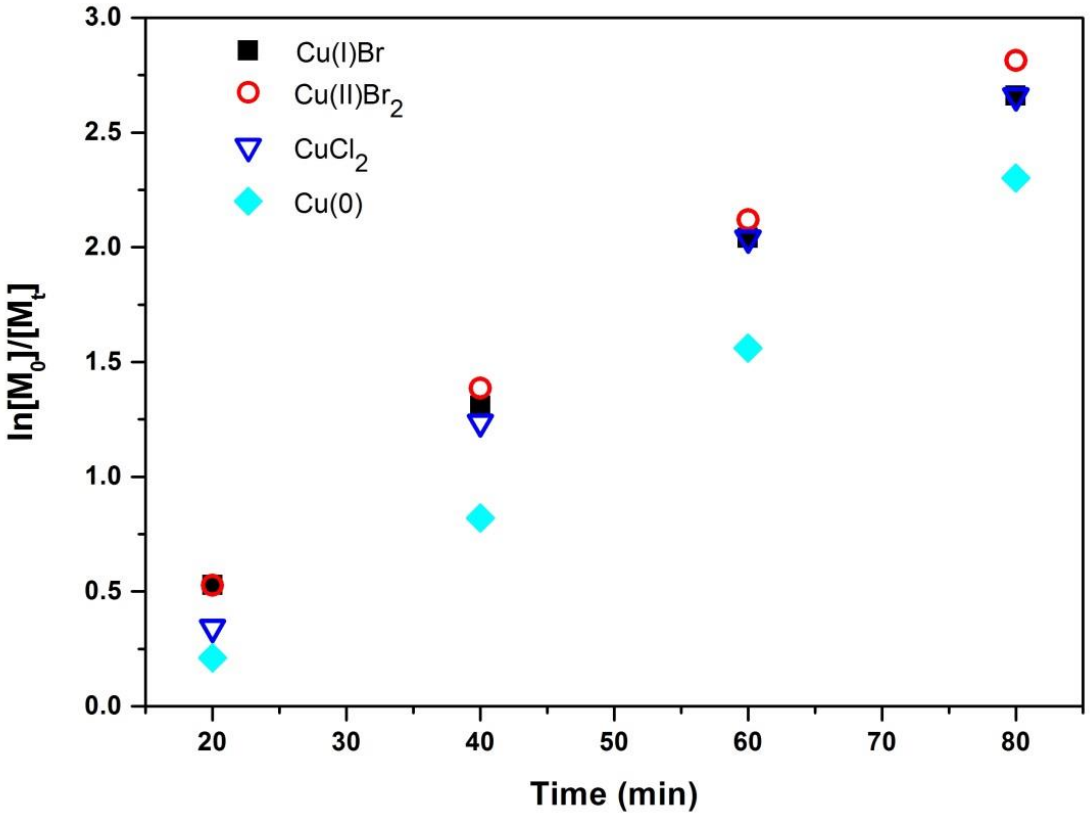

Figure 5.9: $\ln[M_0]/[M_t]$ vs time for the polymerisation of MA in 50%vol DMSO under UV irradiation (λ ~ 360 nm). Total irradiation time = 80 min;

■ [CuBr]/[Me_6-Tren]/[EBiB]/[MA] = 0.02:0.12:1:50, k_p = 0.0356 min^{-1}

○ [$CuBr_2$]/[Me_6-Tren]/[EBiB]/[MA]= 0.02:0.12:1:50, k_p = 0.0385 min^{-1}

▽ [$CuCl_2$]/[Me_6-Tren]/[EBiB]/[MA] = 0.02:0.12:1:50, k_p = 0.0388 min^{-1}

◆ [Cu(0)]/[Me_6-Tren]/[EBiB]/[MA] = 0.02:0.12:1:50, k_p = 0.0351 min^{-1}

The final polymers obtained exhibited good agreement between $M_{n,th}$ and $M_{n,exp}$ and narrow dispersities ($Đ$ ~ 1.07-1.18, Figure 5.10).

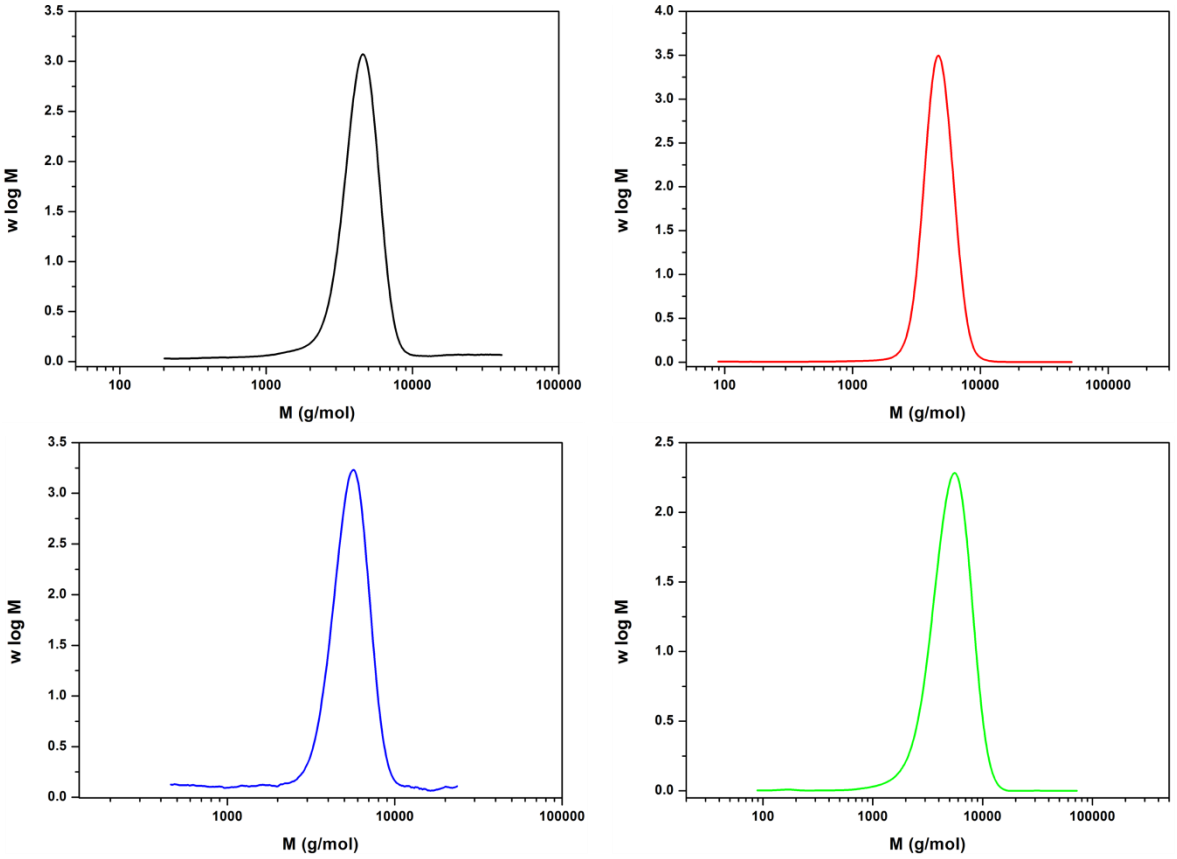

Figure 5.10: Molecular weight distribution of PMA from photo-mediated polymerisation in the presence of CuBr (black peak, M_n = 4000 g/mol; conversion 93%; $Đ$ =1.11), $CuBr_2$ (pink peak, M_n = 4400 g/mol; conversion 93%; $Đ$ =1.07), $CuCl_2$ (blue peak, M_n = 5000 g/mol; conversion 90%; $Đ$ =1.07), Cu(0) (green peak, M_n = 4700 g/mol; conversion 94%; $Đ$ =1.18) Total irradiation time = 80 min. DMSO (50:50 *v/v* monomer/solvent).

Modification of the standard conditions ([I] : [$CuBr_2$] : [Me_6-Tren] = [1] : [0.02] : [0.12]), imposing a gradual increase in [$CuBr_2$] ([0.02] - [0.08]) resulted in a steady reduction in the rate of polymerisation (Figure 5.11). There seemed to be two possible explanations for the observed reduction in rate. Increasing [$CuBr_2$] results in an increase of [Cu^{II}(Me_6-Tren)Br_2] deactivator, shifting the polymerisation equilibrium to the dormant chains. This coincides with a reduction in free [Me_6-Tren], which has been identified as an essential reagent in these photo-activated reactions. To investigate these hypotheses [Me_6-Tren] was increased, while maintaining the higher [$CuBr_2$], to reinstate [$CuBr_2$] : [Me_6-

Tren] = [1] : [6] (*i.e.* [I] : [$CuBr_2$] : [Me_6-Tren] = [1] : [0.08] : [0.48]). Under these conditions the rate of polymerisation increased, although the rate observed under the standard conditions ([I] : [$CuBr_2$] : [Me_6-Tren] = [1] : [0.02] : [0.12]) was not fully restored. This suggests that, whilst the free [Me_6-Tren] is vital, a high concentration of deactivator can still retard/deactivate polymerisation.

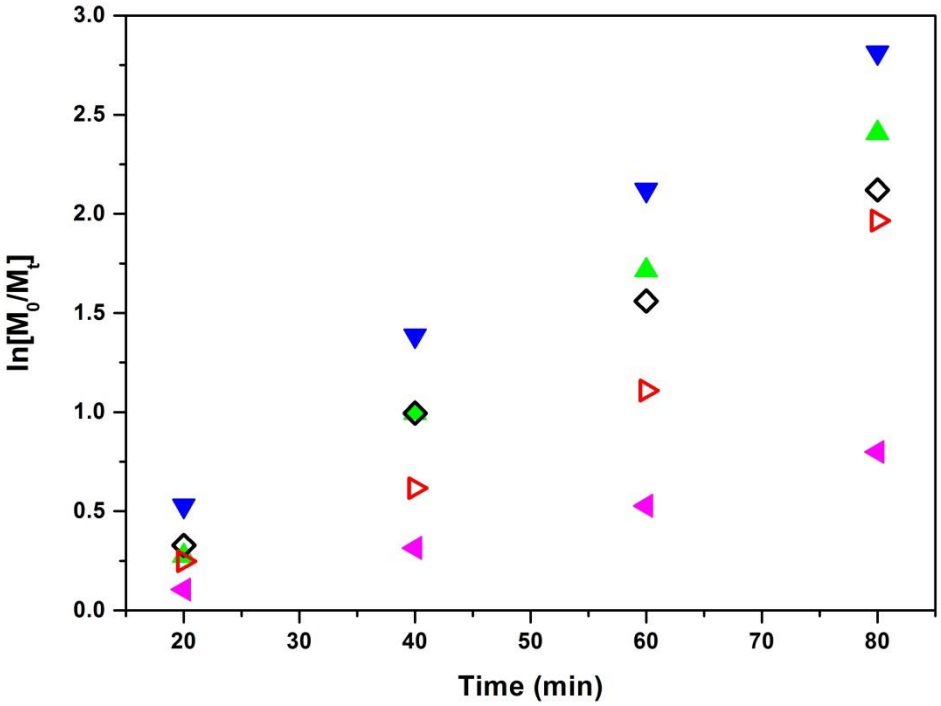

Figure 5.11: $\ln[M_0]/[M_t]$ *vs* time for the polymerisation of MA in 50% vol DMSO under UV irradiation (λ ~ 360 nm)

▲ [Cu(II)]/[Me_6-Tren]/[EBiB]/[MA] = **0.01:0.12**:1:50, k_p = 0.356 min^{-1}

▼ [Cu(II)]/[Me_6-Tren]/[EBiB]/[MA] = **0.02:0.12**:1:50, k_p = 0.0385 min^{-1}

◇ [Cu(II)]/[Me_6-Tren]/[EBiB]/[MA] = **0.04:0.12**:1:50, k_p = 0.0297 min^{-1}

◀ [Cu(II)]/[Me_6-Tren]/[EBiB]/[MA] = **0.08:0.12**:1:50, k_p = 0.0115 min^{-1}

▷ [Cu(II)]/[Me_6-Tren]/[EBiB]/[MA] = **0.08:0.48**:1:50, k_p = 0.0282 min^{-1}

5.2.6 The effect of ligand and solvent on photo-activated polymerisation of MA.

The polymerisation was screened in a selection of disproportionating and non-disproportionating solvents (Table 5.6). In solvents that promote disproportionation (DMF and MeOH), excellent control was retained ($Đ$ = 1.08 and 1.05 respectively), albeit with

conversions lower than those observed in DMSO (69% and 84% respectively). In non-disproportionating solvents, *e.g.* MeCN and toluene, conversions remained lower than those obtained with DMSO (67% and 62% respectively), and the dispersities were variable. Comparable control was exhibited by MeCN ($Đ$ = 1.06) whereas a significant drift was observed during polymerisation in toluene ($Đ$ = 1.54). This could be attributed to the poor solubility of the $Cu^{II}(Me_6\text{-Tren})Br_2$ complex in toluene, culminating in insufficient deactivation and free radical polymerisation, mirroring slightly the result of the controlled experiment performed in the absence of $CuBr_2$ (Table 5.2, entry 2).

Table 5.6: The effect of solvent and ligand on photo-mediated polymerisation of MA. [M]:[I]:[$CuBr_2$]:[L] = [50]:[1]:[0.02]:[0.12]. 90 min irradiation time. Solvents used in 50% *v/v*. [a] Determined by ^{1}H NMR. [b] Determined by $CHCl_3$ SEC.

Solvent	[L]	Conv.[a]	$M_{n,th}$	$M_{n,SEC}$[b]	$Đ$
DMSO	Me_6-Tren	96%	4400	4500	1.05
DMSO	Tren	96%	4400	4200	1.10
DMSO	PMDETA	48%	2200	1900	1.27
DMSO	Bipy	-	-	-	-
DMF	Me_6-Tren	69%	3100	3800	1.08
MeOH	Me_6-Tren	84%	3800	4500	1.05
MeCN	Me_6-Tren	67%	3000	3700	1.06
Tol.	Me_6-Tren	62%	2800	7800	1.54

A range of ligands were also explored in this photo-activated polymerisation, including aliphatic amino ligands *tris*(2-aminoethyl)amine (Tren) and *N*, *N*, *N*', *N*'', *N*''-pentamethyldiethylenetriamine (PMDETA) as well as bipyridine (bpy) (Table 5.6). The results indicate little difference between Me_6-Tren (96%, $Đ$ = 1.05) and Tren (96%, $Đ$ =

1.10), whereas a significantly reduced polymerisation rate and a drift in the dispersity was observed when PMDETA was employed as ligand over an identical irradiation time (90 min, 48%, $Đ$ = 1.27). Interestingly, no polymer was formed in the presence of bpy as ligand, reinforcing the implication that aliphatic amino-based ligands (C-NR_2 groups) are required.

5.2.7 Mechanistic insight – UV-*vis* spectroscopy

To further investigate the mechanism, a series of UV-*vis* spectroscopy experiments were performed to follow the polymerisation. A deoxygenated solution of [$CuBr_2$] : [Me_6-Tren] = [1] : [6] in DMSO (polymerisation ratio and concentration) revealed the characteristic absorbance at λ_{max} = 950 nm with an additional absorbance at λ = 750 nm, attributed to the d-d transitions of the d^9 Cu^{II} complex (Figure 5.12a).

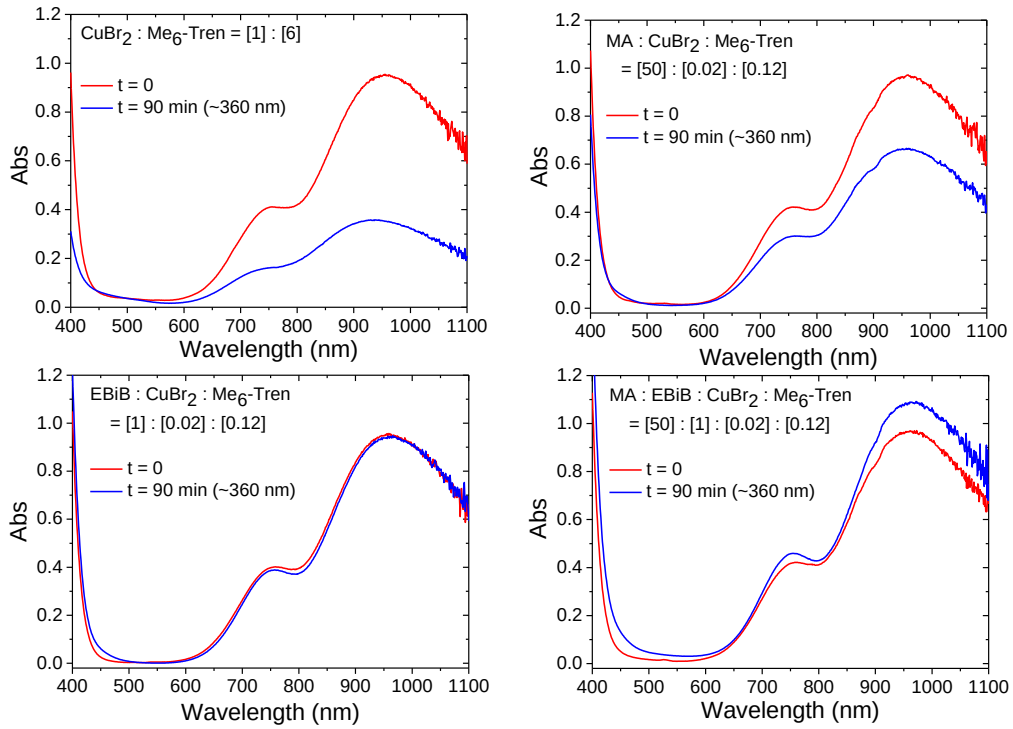

Figure 5.12. Monitoring the effect of UV irradiation on [$Cu^{II}(Me_6$-Tren)Br_2] as a function of time by UV-*vis* spectroscopy.

The mixture was subsequently exposed to UV irradiation for 90 minutes, to mimic polymerisation conditions, before re-measuring the absorbance spectrum. An approximate

75% reduction (of λ_{max}) in the characteristic absorbance was observed, suggesting a significant reduction in the [Cu^{II}(Me_6-Tren)Br_2] (Figure 5.12a). The absorbance continues to decrease over a period of 9 hours, however, but it never reaches zero. Continued irradiation over 70 hours results in no further reduction in the absorbance but does result in a significant deviation in the baseline signal at $\lambda \sim$ 450-600 nm (Figure 5.13).

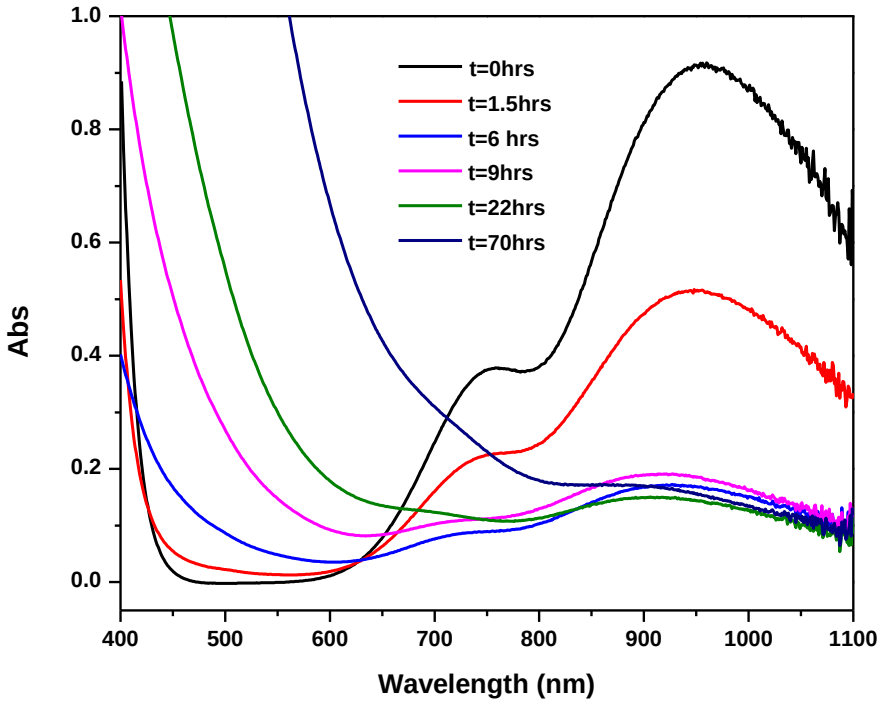

Figure 5.13: UV-vis spectra of [$CuBr_2$] : [Me_6-Tren] = [1] : [6] in DMSO, mimicking standard polymerisation conditions in the absence of initiator and monomer; monitoring the absorbance as a function of time during UV irradiation for a total of 70 h under at $\lambda_{max} \sim$ 360 nm. Reaction conditions: [$CuBr_2$]:[Me_6-Tren]:[DMSO]: [4.5 μmol] : [27.0 μmol] : [2ml].

In the presence of initiator ([EBiB] : [$CuBr_2$] : [Me_6-Tren] = [1] : [0.02] : [0.12]) no quantifiable change was observed in the absorbance spectrum after 90 minutes UV irradiation (Figure 5.12b). The presence of the initiator (in significant excess relative to Cu^{II}) could reoxidise Cu^{I}(Me_6-Tren)Br back to Cu^{II}(Me_6-Tren)Br_2 relatively quickly on the polymerisation timescale. Alternatively, photo-activated Me_6-Tren could activate the alkyl halide initiator, in preference to acting as a direct photo-reducing agent of Cu^{II}(Me_6-Tren)Br_2. Repeating the experiment in the presence of monomer, thus fully replicating the

polymerisation conditions, leads to a similar observation, perhaps supporting the latter hypothesis (Figure 5.12 d).

Whilst the reduction of $Cu^{II}(Me_6\text{-Tren})Br_2$ to $Cu^{I}(Me_6\text{-Tren})Br$ is not readily observed in the presence of initiator or under polymerisation conditions, the fact that rapid controlled polymerisation is observed underlines that sufficient active species are generated under these conditions. Indeed, the ability of this polymerisation to proceed in the presence of $Cu^{II}(Me_6\text{-Tren})Br_2$ is most likely a crucial factor in the success and overall control of this protocol, with deactivation expected to dominate over side reactions such as bimolecular termination and/or chain transfer *etc*. Upon generation of $Cu^{I}(Me_6\text{-Tren})Br$, either from reduction by photo-activated [Me_6-Tren]* or *via* deactivation of propagating chains, its lifetime is probably short on the polymerisation time scale. Under the reaction conditions, $Cu^{II}(Me_6\text{-Tren})Br_2$ can be regenerated either by disproportionation or oxidation of $Cu^{I}(Me_6\text{-Tren})Br$ by a oxidative intermediate (radical cation) of free Me_6-Tren (see proposed mechanism).

5.2.8 Proposed mechanism

The result of control, kinetic and UV-*vis* experiments provide a preliminary mechanistic insight and enables proposal of a potential mechanism for this photo-mediated process (Scheme 5.4).

In organic chemistry amines have been employed as outer-sphere electron donors and photoelectron donors in a number of synthetic transformations including reductive dehalogenation[44, 45] and cyclisation[46-48] reactions of alkyl halides, which are believed to proceed *via* a radical mechanism. More importantly, tertiary amines and their salts have been cited as organocatalysts for both thermal and photochemical CLRP[49-51]. With this in mind, we propose initial photo-activation occurs in free ligand (Me_6-Tren, Figure 5.14 and 5.15).

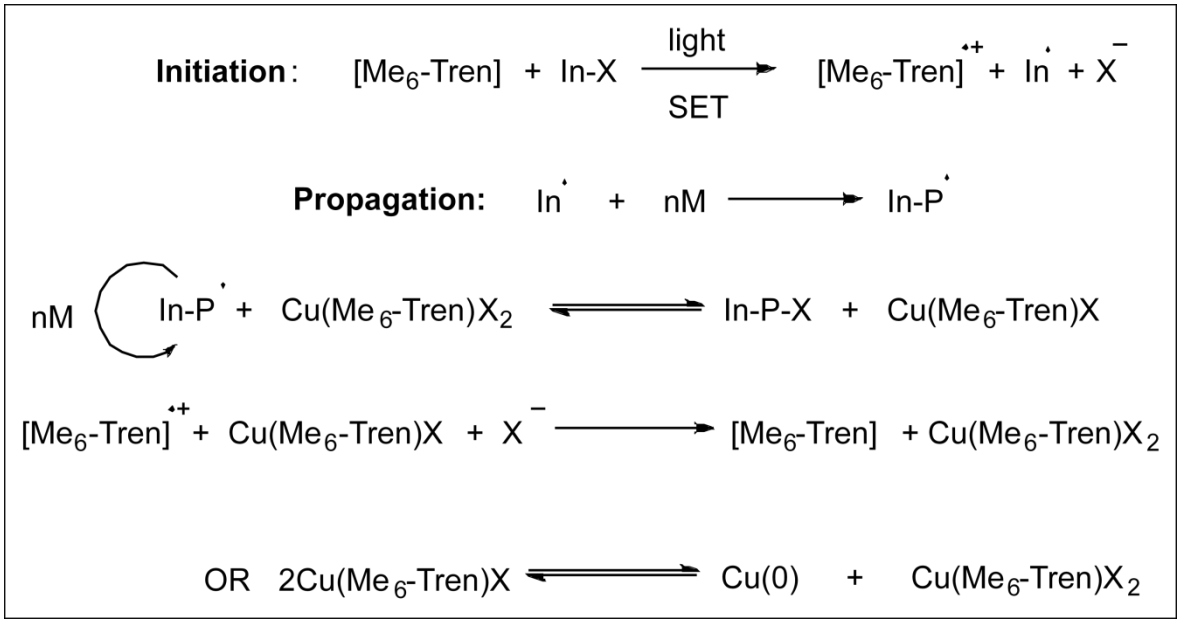

Scheme 5.4: Proposed mechanism for tertiary amine-mediated, photo-induced living polymerisation of acrylates.

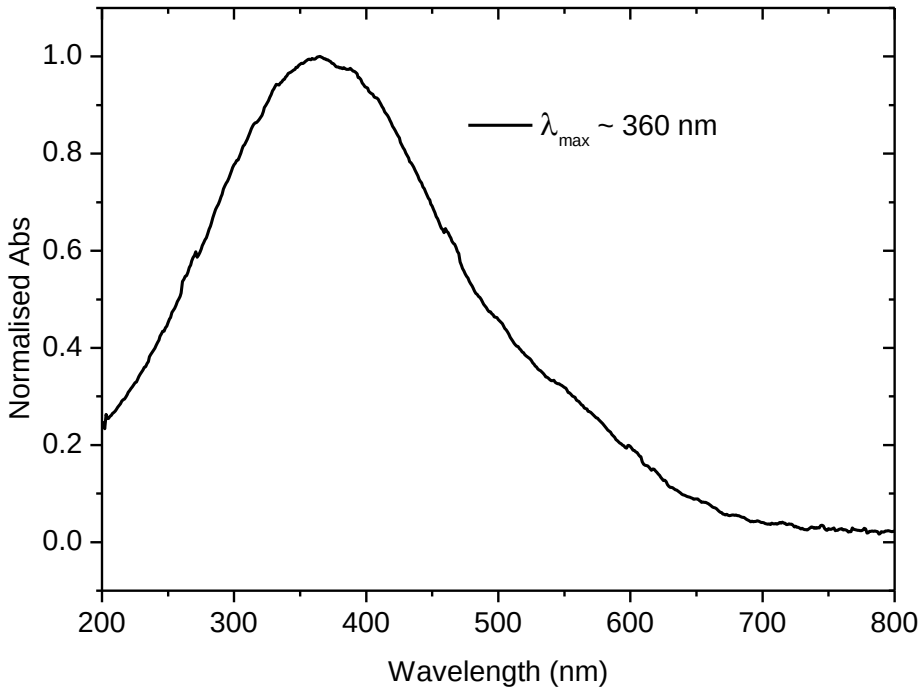

Figure 5.14: UV-*vis* spectrum of UV light source used throughout this investigation, λ_{max} ~ 360 nm.

Outer-sphere single electron transfer (OSET) then occurs from photo-excited [Me_6-Tren]* to the alkyl halide initiator, resulting in homolysis of the C-Br bond. This would furnish the required initiating radical and a Me_6-Tren radical-cation with a Br^- counterion. In the presence of an appropriate acrylate, polymerisation can then occur with excellent

control imposed by the presence of $Cu^{II}(Me_6\text{-Tren})Br_2$. Deactivation results in reduction of $Cu^{II}(Me_6\text{-Tren})Br_2$ to afford a dormant polymer chain (P_n-Br) and $Cu^{I}(Me_6\text{-Tren})Br$. Here the mechanism becomes complex due to the variable fate of the $Cu^{I}(Me_6\text{-Tren})Br$ complex. Oxidation back to $Cu^{II}(Me_6\text{-Tren})Br_2$ could occur upon interaction with the intermediate Me_6-Tren radical-cation. Likewise in non-disproportionating solvents $Cu^{I}(Me_6\text{-Tren})Br$ could activate a dormant polymer chain, leading to propagation and formation of $Cu^{II}(Me_6\text{-Tren})Br_2$. Conversely, in polar organic and aqueous solutions, disproportionation can occur resulting in the formation of Cu(0) and $Cu^{II}(Me_6\text{-Tren})Br_2$. Relative rates of reaction at this stage will be highly dependent upon the conditions, including solvent, temperature and catalyst loading.

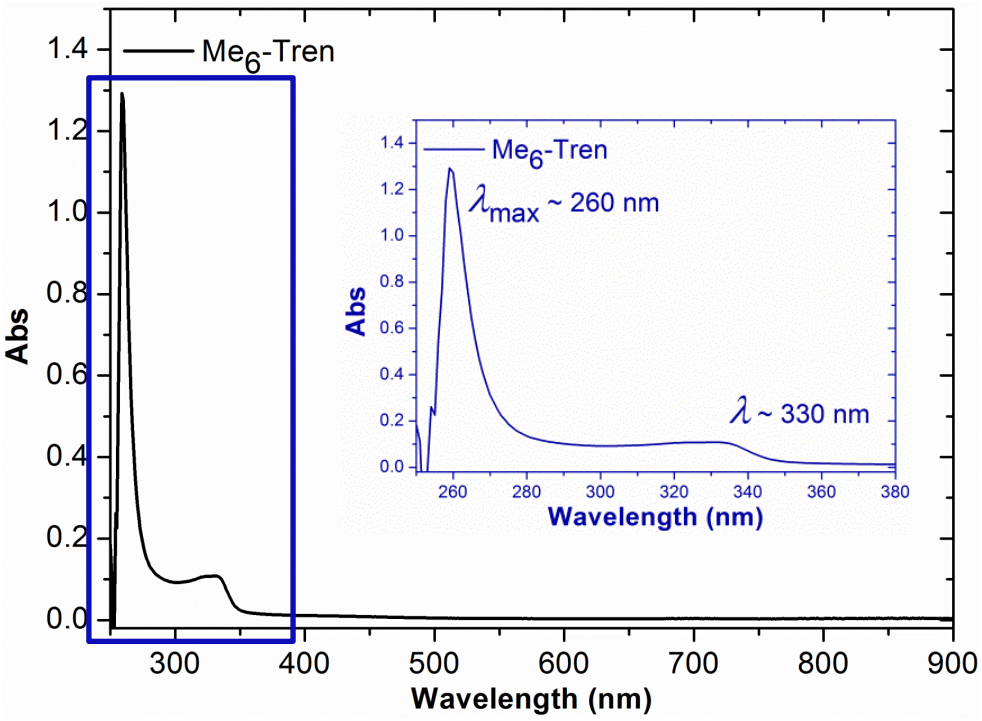

Figure 5.15: UV-*vis* spectra of [Me_6-Tren] in [DMSO] with DMSO used as a blank.

Nevertheless, from the data presented it is clear that, under UV irradiation (λ_{max} ~ 360 nm), a synergistic relationship exists between free amine (Me_6-Tren) and the cupric complex ($Cu^{II}(Me_6\text{-Tren})Br_2$) affording poly(acrylates) in unrivalled conversions, rates and end-group fidelity.

5.3 Conclusions

This chapter reports an efficacious photo-activated living polymerisation of acrylates mediated by $CuBr_2$ in the presence of aliphatic tertiary amine ligands. It is proposed that initial photo-activation occurs into free ligand, which acts as a photoelectron donor and promotes polymerisation *via* single electron transfer (SET) into the alkyl halide initiator. The ligands and transition metals used are routinely employed for thermal polymerisation and no added photo-activator is employed. An outstanding degree of control and end-group fidelity, as indicated by narrow dispersities, has been exemplified by chain extension and block copolymerisation *via* sequential monomer addition. The scope of the reaction has been expanded to include a variety of acrylates, including biologically relevant PEG acrylate monomers. Furthermore, *α*-hydroxy and *vic*-diol functionality is tolerated when incorporated into the alkyl halide initiator. Reaction rates are rapid and temporal control is possible during polymerisation *via* intermittent light and dark reactions.

5.4 Experimental

5.4.1 Materials

Methyl acrylate (MA), ethyl 2-bromoisobutyrate (EBiB), $CuBr_2$ and $CuCl_2$ were purchased from Aldrich and used as received. CuBr was treated with acetic acid, washed with EtOH, dried and stored under nitrogen prior to use. Cu(0) particles were prepared by disproportionation of Cu(Me_6-Tren)Br in water according to the literature procedure. Me_6-Tren, 2-bromo-2-methyl-propionic acid 2-(2-hydroxy-ethoxy)-ethyl ester (2) and 1,2-dihydroxypropane-3-oxy-(2-bromo-2-methylpropioyl) (3) were synthesised according to previously reported literature. Solvents were purchased from Fisher Scientific and used as received.

5.4.2 Apparatus

^{1}H and ^{13}C NMR spectra were recorded on Bruker DPX-300, DPX-400 or DRX-500 spectrometers in $CDCl_3$ unless otherwise stated. Chemical shifts are given in ppm downfield from the internal standard tetramethylsilane. Size exclusion chromatography (SEC) measurements were conducted using an Agilent 1260 SEC-MDS fitted with differential refractive index (DRI), light scattering (LS) and viscometry (VS) detectors equipped with 2 × PLgel 5 mm mixed-D columns (300 × 7.5 mm), 1 × PLgel 5 mm guard column (50 × 7.5 mm) and autosampler. Narrow linear poly(methyl methacrylate) standards in the range of 200 to 1.0×10^6 $g \cdot mol^{-1}$ were used to calibrate the system. All samples were passed through 0.45 μm PTFE filter before analysis. The mobile phase was chloroform with 2% triethylamine eluent at a flow rate of 1.0 mL/min. SEC data was analysed using Cirrus v3.3 software with calibration curves produced using Varian Polymer laboratories Easi-Vials linear poly(methyl methacrylate) standards (200-4.7×10^5 g/mol). High Resolution Mass Spectrometry (HR-MS) was conducted on a Bruker UHR-Q-ToF MaXis with electrospray ionisation. MALDI-ToF mass spectrometry was conducted using a Bruker Daltonics Ultraflex II MALDI-ToF mass spectrometer, equipped with a nitrogen laser delivering 2 ns laser pulses at 337 nm with positive ion ToF detection performed using an accelerating voltage of 25 kV. Solutions in tetrahydrofuran (50 μL) of trans-2-[3-(4-tert-butylphenyl)-2-methyl-2-propylidene] malonitrile (DCTB) as a matrix (saturated solution), sodium iodide as cationisation agent (1.0 mg/mL) and sample (1.0 mg/mL) were mixed, and 0.7 μL of the mixture was applied to the target plate. Spectra were recorded in reflector mode calibrating PEG-Me 1100 kDa. UV/Vis spectra were recorded on Agilent Technologies Cary 60 UV-Vis spectrophotometer in the range of 200-1100 nm using a cuvette with 10 mm path length. The source of UV light was a UV nail

gel curing lamp (available on ebay from a range of suppliers) (λ_{max} ~ 360 nm) equipped with four 9W bulbs (see below).

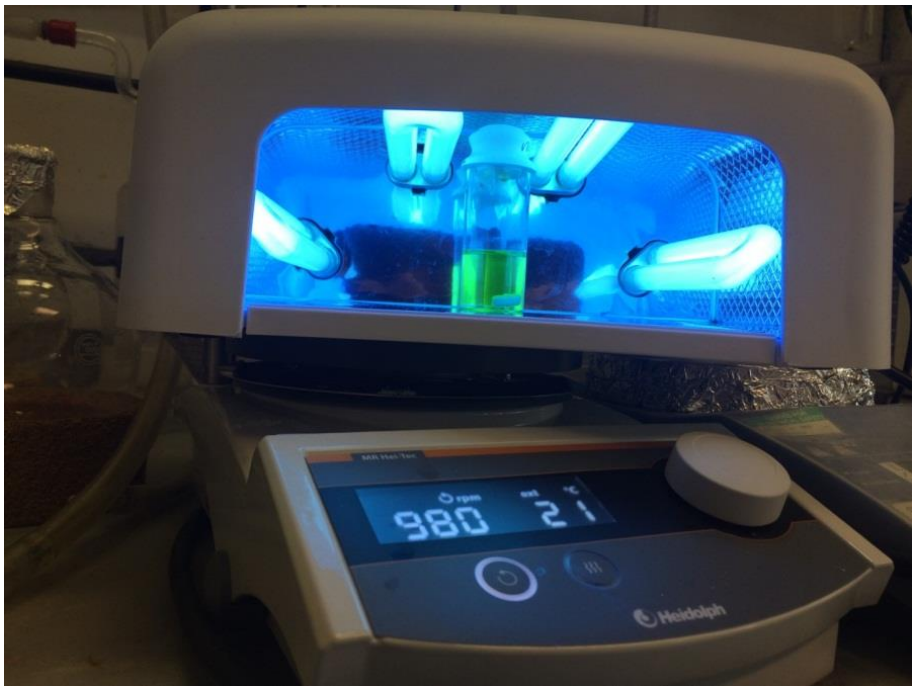

Figure 5.16: Typical set up for photo-induced homopolymerisation of MA.

5.4.3 General procedures

General procedure for the photo-induced polymerisation of MA

Filtered MA (2 mL, 22.2 mmol, 50 eq), EBiB (65 μL, 0.44 mmol, 1 eq), $CuBr_2$ (2.0 mg, 8.8 μmol, 0.02 eq), Me_6-Tren (14 μL, 53.0 μmol, 0.12 eq) and DMSO (2 mL) were added to a septum sealed vial and degassed by purging with nitrogen for 15 min. Polymerisation commenced upon addition of the degassed reaction mixture to the UV lamp. Samples were taken periodically and conversions were measured using ^{1}H NMR and SEC analysis.

General procedure for *in-situ* chain extension reactions

General procedure for MA homopolymerisation was followed. After 90 min a 1 : 0.5 mixture of degassed MA (100 eq) or $PEGA_{480}$ (20 eq) and DMSO was added to the reaction mixture *via* degassed syringe. Samples were taken periodically and conversions were measured using ^{1}H NMR and SEC analysis.

5.4.4 Characterisation

Poly(ethyl acrylate)

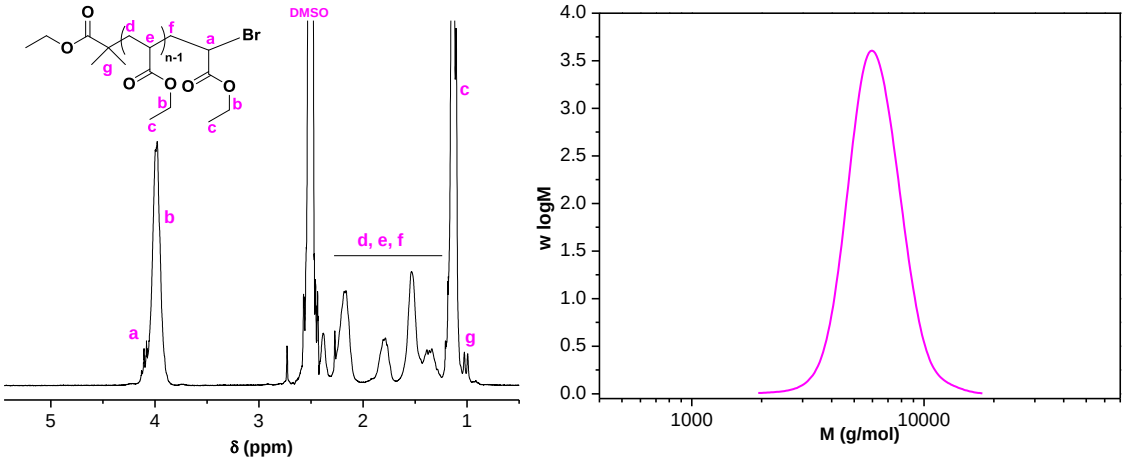

Figure 5.17: (left) ^{1}H NMR spectrum of **poly(ethyl acrylate)** obtained from UV experiment: [$CuBr_2$]/[Me_6-Tren]/[EBiB]/[EA] polymerisation mixture in DMSO (50:50 *v/v* monomer/solvent) at ambient temperature. (right) **:** Molecular weight distribution of **poly(ethyl acrylate)** M_n= 5900 g/mol; $Đ$ =1.07; 97% conversion. [EA]:[EBiB]:[$CuBr_2$]:[Me_6-Tren] = [50]:[1]:[0.02]:[0.12]. DMSO solvent 50% *v/v*.

Poly(*n*-butyl acrylate)

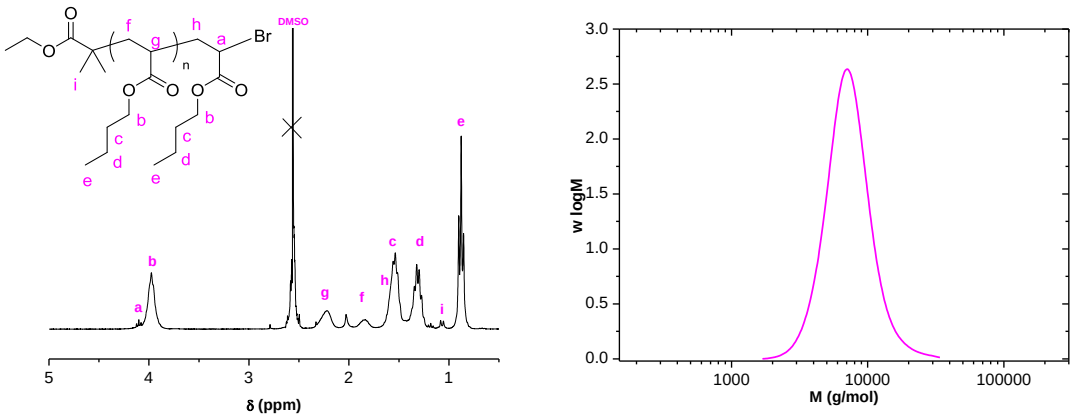

Figure 5.18: (left) ^{1}H NMR spectrum of **poly(butyl acrylate)** obtained from UV experiment: [$CuBr_2$]/[Me_6-Tren]/[EBiB]/[*n*BA] polymerisation mixture in DMSO (50:50 *v/v* monomer/solvent) at ambient temperature. (right) Molecular weight distribution of **poly(butyl acrylate)** M_n= 6800 g/mol; $Đ$ =1.16; 97% conversion. [*n*BA]:[EBiB]:[$CuBr_2$]:[Me_6-Tren] = [50]:[1]:[0.02]:[0.12]. DMSO solvent 50% *v/v*.

Poly(*tert*-butyl acrylate)

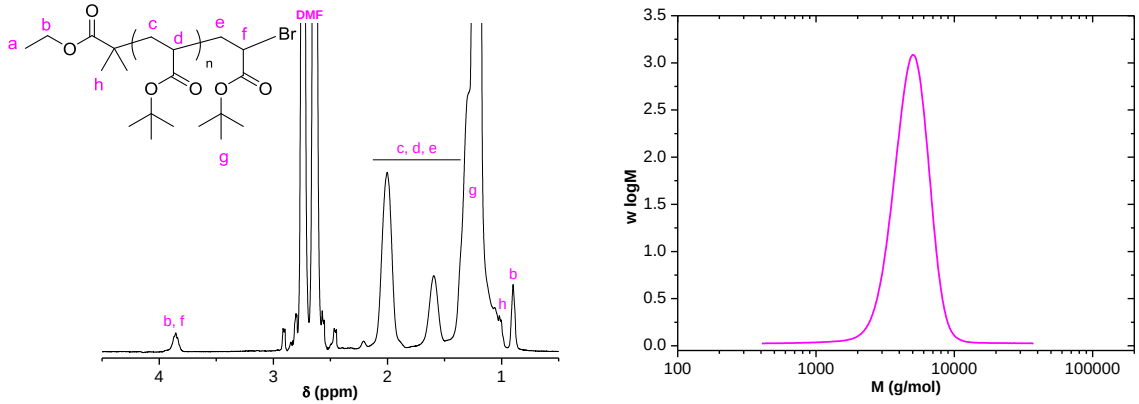

Figure 5.19: (left) ^{1}H NMR spectrum of **poly(*tert*-butyl acrylate)** obtained from UV experiment: [$CuBr_2$]/[Me_6-Tren]/[EBiB]/[*t*BA] polymerisation mixture in DMF (50:50 *v/v* monomer/solvent) at ambient temperature.
(right) Molecular weight distribution of **poly(*tert*-butyl acrylate)** M_n= 4500 g/mol; $Đ$ =1.10; 96% conversion. [*t*BA]:[EBiB]:[$CuBr_2$]:[Me_6-Tren] = [50]:[1]:[0.02]:[0.12]. DMF solvent 50% *v/v*.

Poly(ethylene glycol methyl ether acrylate)

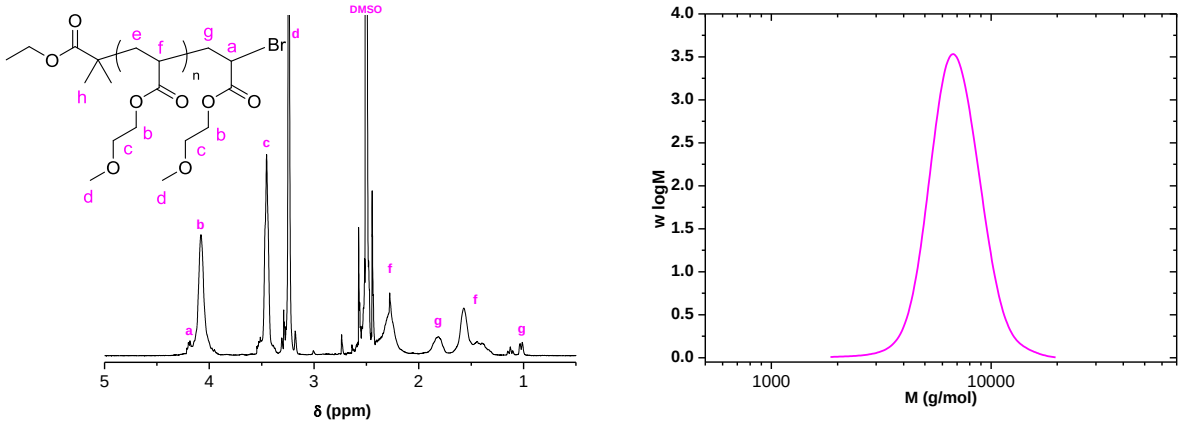

Figure 5.20: (left) ^{1}H NMR spectrum of **poly(ethylene glycol methyl ether acrylate)** obtained from UV experiment: [$CuBr_2$]/[Me_6-Tren]/[EBiB]/[EGA] polymerisation mixture in DMSO (50:50 *v/v* monomer/solvent) at ambient temperature.
(right) Molecular weight distribution of **poly(ethylene glycol methyl ether acrylate)** M_n= 6600 g/mol; $Đ$ =1.07; 97% conversion. [EGA]:[EBiB]:[$CuBr_2$]:[Me_6-Tren] = [50]:[1]:[0.02]:[0.12]. DMSO solvent 50% *v/v*.

Poly[poly(ethylene glycol) methyl ether acrylate]

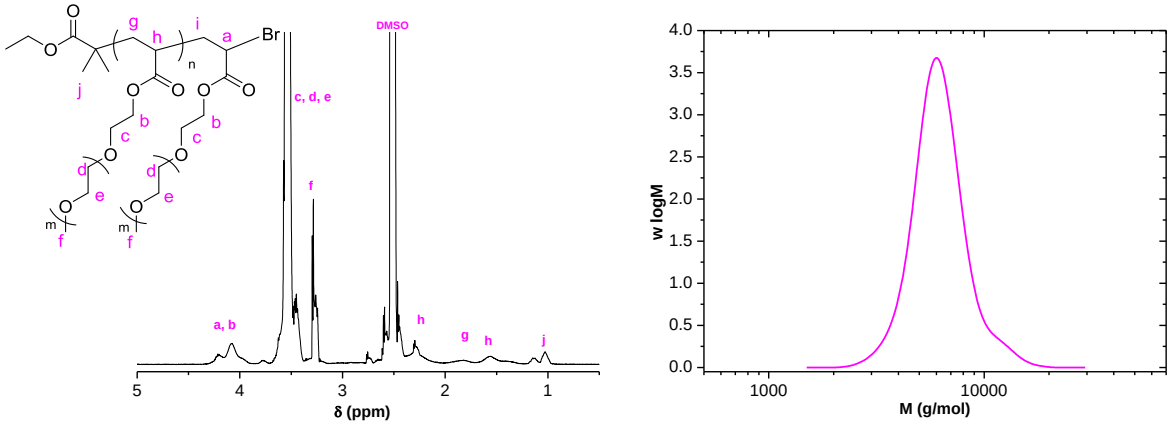

Figure 5.21: (left) ^{1}H NMR spectrum of **poly[poly(ethylene glycol) methyl ether acrylate]** obtained from UV experiment: [$CuBr_2$]/[Me_6-Tren]/[EBiB]/[PEGA] polymerisation mixture in DMSO (50:50 *v/v* monomer/solvent) at ambient temperature.
(right) Molecular weight distribution of **poly[poly(ethylene glycol) methyl ether acrylate]** M_n= 6000 g/mol; $Đ$ =1.09; 92% conversion. [PEGA]:[EBiB]:[$CuBr_2$]:[Me_6-Tren] = [20]:[1]:[0.02]:[0.12]. DMSO solvent 50% *v/v*.

Poly(methyl methacrylate)

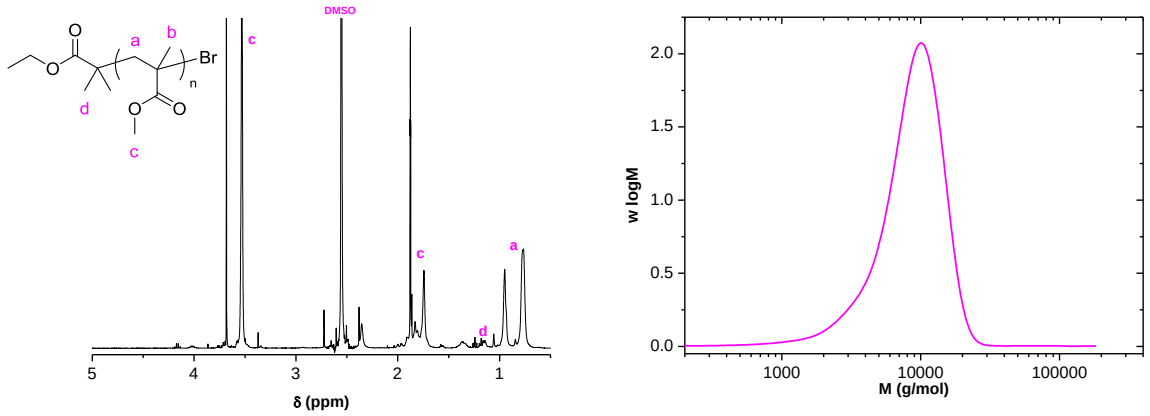

Figure 5.22: (left) ^{1}H NMR spectrum of **poly(methyl methacrylate)** obtained from UV experiment: [$CuBr_2$]/[Me_6-Tren]/[EBiB]/[MMA] polymerisation mixture in DMSO (50:50 *v/v* monomer/solvent) at ambient temperature.
(right) Molecular weight distribution of **poly(methyl methacrylate)** M_n= 7400 g/mol; $Đ$ =1.29; 78% conversion. [MMA]:[EBiB]:[$CuBr_2$]:[Me_6-Tren] = [50]:[1]:[0.02]:[0.12]. DMSO solvent 50% *v/v*.

Polystyrene

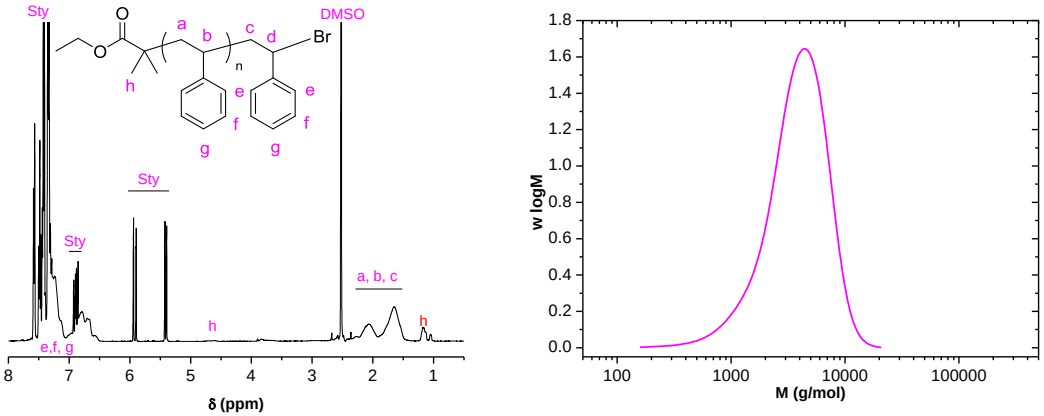

Figure 5.23: (left) ^{1}H NMR spectrum of **polystyrene** obtained from UV experiment: [$CuBr_2$]/[Me_6-Tren]/[EBiB]/[St] polymerisation mixture in DMSO (50:50 *v/v* monomer/solvent) at ambient temperature. (right) Molecular weight distribution of **polystyrene** M_n= 3200 g/mol; $Đ$ =1.42; 40% conversion. [St]:[EBiB]:[$CuBr_2$]:[Me_6-Tren] = [50]:[1]:[0.02]:[0.12]. DMSO as solvent 50% *v/v*.

Using 2-bromo-2-methyl-propionic acid 2-(2-hydroxy-ethoxy)-ethyl ester initiator (2)

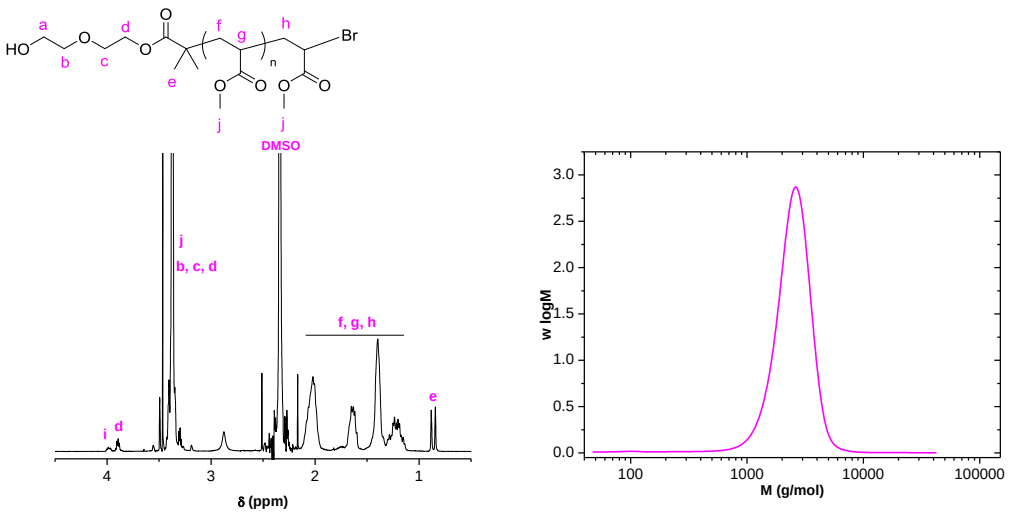

Figure 5.24: (left) ^{1}H NMR spectrum of poly(methyl acrylate) obtained from photo-mediated polymerisation: [MA]:[2]:[$CuBr_2$]:[Me_6-Tren] = [25]:[1]:[0.02]:[0.12] in DMSO (50:50 *v/v* monomer/solvent).
(right) Molecular weight distribution of poly(methyl acrylate) obtained from photo-mediated polymerisation: [MA]:[2]:[$CuBr_2$]:[Me_6-Tren] = [25]:[1]:[0.02]:[0.12] in DMSO (50:50 *v/v* monomer/solvent). M_n=2400 g/mol; $Đ$ =1.11; 92% conversion.

Using 1,2-dihydroxypropane-3-oxy-(2-bromo-2-methylpropioyl) (3) as initiator

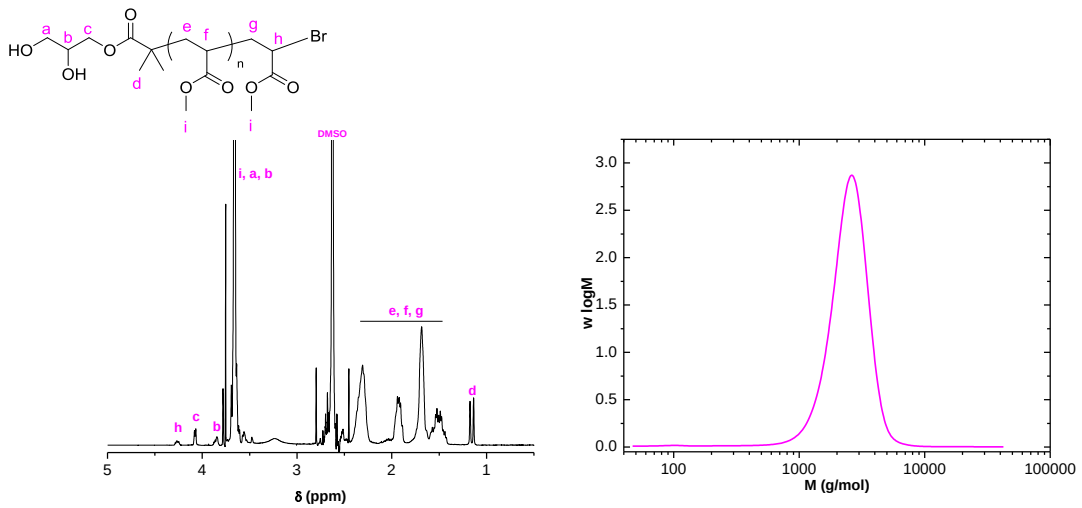

Figure 5.25 (left) ^{1}H NMR spectrum of poly(methyl acrylate) obtained from photo-mediated polymerisation: [MA]:[3]:[$CuBr_2$]:[Me_6-Tren] = [25]:[1]:[0.02]:[0.12] in DMSO (50:50 *v/v* monomer/solvent).
(right) Molecular weight distribution of poly(methyl acrylate) obtained from photo-mediated polymerisation: [MA]:[3]:[$CuBr_2$]:[Me_6-Tren] = [25]:[1]:[0.02]:[0.12] in DMSO (50:50 *v/v* monomer/solvent). M_n = 2300g/mol; $Đ$ =1.15; 93% conversion.

5.5 References

1. H. Fischer, *Macromolecules*, 1997, **30**, 5666-5672.
2. H. Fischer, *J. Polym. Sci., Part A: Polym. Chem.*, 1999, **37**, 1885-1901.
3. H. Fischer, *Chem. Rev.*, 2001, **101**, 3581-3610.
4. G. Lligadas and V. Percec, *J. Polym. Sci., Part A: Polym. Chem.*, 2008, **46**, 6880-6895.
5. B. M. Rosen, X. Jiang, C. J. Wilson, N. H. Nguyen, M. J. Monteiro and V. Percec, *J. Polym. Sci., Part A: Polym. Chem.*, 2009, **47**, 5606-5628.
6. N. H. Nguyen and V. Percec, *J. Polym. Sci., Part A: Polym. Chem.*, 2011, **49**, 4227-4240.
7. M. E. Levere, N. H. Nguyen, X. Leng and V. Percec, *Polym. Chem.*, 2013, **4**, 1635-1647.
8. N. H. Nguyen, H.-J. Sun, M. E. Levere, S. Fleischmann and V. Percec, *Polym. Chem.*, 2013, **4**, 1328-1332.
9. N. V. Tsarevsky, W. A. Braunecker and K. Matyjaszewski, *J. Organomet. Chem.*, 2007, **692**, 3212-3222.
10. F. A. Leibfarth, K. M. Mattson, B. P. Fors, H. A. Collins and C. J. Hawker, *Angew. Chem., Int. Ed.*, 2013, **52**, 199-210.
11. M. Tanabe, G. W. M. Vandermeulen, W. Y. Chan, P. W. Cyr, L. Vanderark, D. A. Rider and I. Manners, *Nat. Mater.*, 2006, **5**, 467-470.
12. S. Yamago and Y. Nakamura, *Polymer*, 2013, **54**, 981-994.

13. J. Rzayev and J. Penelle, *Macromolecules*, 2002, **35**, 1489-1490.
14. J. Rzayev and J. Penelle, *Angew. Chem., Int. Ed.*, 2004, **43**, 1691-1694.
15. A. J. D. Magenau, N. C. Strandwitz, A. Gennaro and K. Matyjaszewski, *Science*, 2011, **332**, 81-84.
16. C. Decker, *Prog. Polym. Sci.*, 1996, **21**, 593-650.
17. M. A. Tasdelen, M. Uygun and Y. Yagci, *Macromol. Rapid Commun.*, 2011, **32**, 58-62.
18. B. P. Fors and C. J. Hawker, *Angew. Chem., Int. Ed.*, 2012, **51**, 8850-8853.
19. J. E. Poelma, B. P. Fors, G. F. Meyers, J. W. Kramer and C. J. Hawker, *Angew. Chem., Int. Ed.*, 2013, **52**, 6844-6848.
20. D. Konkolewicz, K. Schröder, J. Buback, S. Bernhard and K. Matyjaszewski, *ACS Macro Lett.*, 2012, **1**, 1219-1223.
21. M. A. Tasdelen, M. Uygun and Y. Yagci, *Macromol. Chem. Phys.*, 2010, **211**, 2271-2275.
22. M. A. Tasdelen, M. Uygun and Y. Yagci, *Macromol. Chem. Phys.*, 2011, **212**, 2036-2042.
23. M. A. Tasdelen, M. Ciftci and Y. Yagci, *Macromol. Chem. Phys.*, 2012, **213**, 1391-1396.
24. O. S. Taskin, G. Yilmaz, M. A. Tasdelen and Y. Yagci, *Polym. Int.*, 2014, **63**, 902-907.
25. K. Matyjaszewski, W. Jakubowski, K. Min, W. Tang, J. Huang, W. A. Braunecker and N. V. Tsarevsky, *Proc. Natl. Acad. Sci.*, 2006, **103**, 15309-15314.
26. W. Jakubowski and K. Matyjaszewski, *Angew. Chem., Int. Ed.*, 2006, **118**, 4594-4598.
27. J. Mosnáček and M. Ilčíková, *Macromolecules*, 2012, **45**, 5859-5865.
28. J. Yan, B. Li, F. Zhou and W. Liu, *ACS Macro Lett.*, 2013, **2**, 592-596.
29. J. A. Burns, C. Houben, A. Anastasaki, C. Waldron, A. A. Lapkin and D. M. Haddleton, *Polym. Chem.*, 2013, **4**, 4809-4813.
30. Y.-h. Yu, X.-h. Liu, D. Jia, B.-w. Cheng, F.-j. Zhang, P. Chen and S. Xie, *Polymer*, 2013, **54**, 148-154.
31. Y.-H. Yu, X.-H. Liu, D. Jia, B.-W. Cheng, Y.-L. Ren, F.-J. Zhang, H.-N. Li, P. Chen and S. Xie, *J. Polym. Sci., Part A: Polym. Chem.*, 2013, **51**, 1690-1694.
32. H. Tang, Y. Shen, B.-G. Li and M. Radosz, *Macromol. Rapid Commun.*, 2008, **29**, 1834-1838.
33. J. F. Weiss, G. Tollin and J. T. Yoke, *Inorg. Chem.*, 1964, **3**, 1344-1348.
34. H. Dong and K. Matyjaszewski, *Macromolecules*, 2008, **41**, 6868-6870.
35. A. James Grice, PhD Thesis, University of Warwick, 2010.
36. A. Anastasaki, V. Nikolaou, Q. Zhang, J. Burns, S. R. Samanta, C. Waldron, A. J. Haddleton, R. McHale, D. Fox, V. Percec, P. Wilson and D. M. Haddleton, *J. Am. Chem. Soc.*, 2013, **136**, 1141-1149.
37. C. Boyer, A. Atme, C. Waldron, A. Anastasaki, P. Wilson, P. B. Zetterlund, D. Haddleton and M. R. Whittaker, *Polym. Chem.*, 2013, **4**, 106-112.

38. C. Waldron, A. Anastasaki, R. McHale, P. Wilson, Z. Li, T. Smith and D. M. Haddleton, *Polym. Chem.*, 2014, **5**, 892-898.
39. J. Tom, B. Hornby, A. West, S. Harrisson and S. Perrier, *Polym. Chem.*, 2010, **1**, 420-422.
40. X.-f. Zhang, Y. Wu, J. Huang, X.-l. Miao, Z.-b. Zhang and X.-l. Zhu, *Chinese Journal of Polymer Science*, 2013, **31**, 702-712.
41. M. W. Jones, R. A. Strickland, F. F. Schumacher, S. Caddick, J. R. Baker, M. I. Gibson and D. M. Haddleton, *Chem. Commun.*, 2012, **48**, 4064-4066.
42. S. Perrier, S. P. Armes, X. S. Wang, F. Malet and D. M. Haddleton, *J. Polym. Sci., Part A: Polym. Chem.*, 2001, **39**, 1696-1707.
43. Q. Zhang, P. Wilson, Z. Li, R. McHale, J. Godfrey, A. Anastasaki, C. Waldron and D. M. Haddleton, *J. Am. Chem. Soc.*, 2013, **135**, 7355-7363.
44. J. L. Kurz, R. Hutton and F. H. Westheimer, *J. Am. Chem. Soc.*, 1961, **83**, 584-588.
45. W. J. Lautenberger, E. N. Jones and J. G. Miller, *J. Am. Chem. Soc.*, 1968, **90**, 1110-1115.
46. H. Ishibashi, S. Haruki, M. Uchiyama, O. Tamura and J.-i. Matsuo, *Tetrahedron Lett.*, 2006, **47**, 6263-6266.
47. A. J. Clark, S. R. Coles, A. Collis, D. R. Fullaway, N. P. Murphy and P. Wilson, *Tetrahedron Lett.*, 2009, **50**, 6311-6314.
48. H. Ishibashi, M. Sasaki and T. Taniguchi, *Tetrahedron*, 2008, **64**, 7771-7773.
49. A. Goto, T. Suzuki, H. Ohfuji, M. Tanishima, T. Fukuda, Y. Tsujii and H. Kaji, *Macromolecules*, 2011, **44**, 8709-8715.
50. A. Ohtsuki, A. Goto and H. Kaji, *Macromolecules*, 2012, **46**, 96-102.
51. A. Goto, A. Ohtsuki, H. Ohfuji, M. Tanishima and H. Kaji, *J. Am. Chem. Soc.*, 2013, **135**, 11131-11139.

Chapter 6

Expanding the Scope of the Photo-induced Living Radical Polymerisation of Acrylates in the presence of $CuBr_2$ and Me_6-Tren

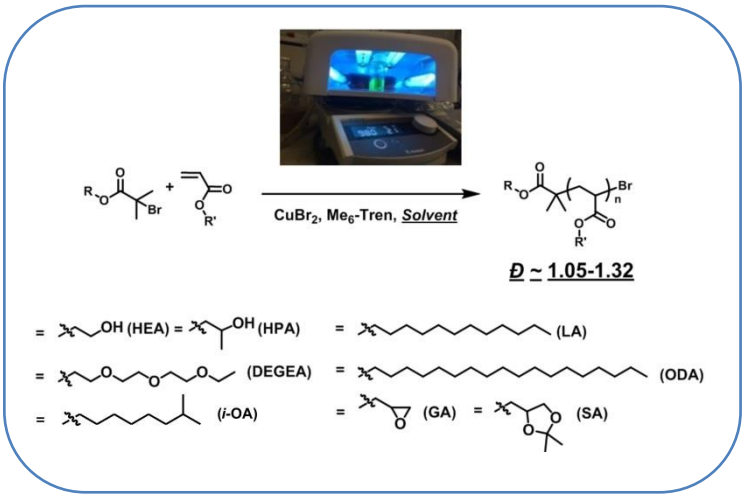

Photo-induced living radical polymerisation of acrylates is achieved upon UV irradiation (λ_{max} ≈ 360 nm) in the presence of an aliphatic tertiary amine ligand (Me_6-Tren) in the presence of low concentrations of $CuBr_2$, yielding poly(acrylates) with near - perfect retention of end-group fidelity. The effect of the nature of the solvent on the rate of polymerisation was investigated in order to expand the scope and identify the limitations of the system. Subsequently, a range of acrylic monomers containing hydrophobic and hydrophilic substituents have been screened, including lauryl acrylate, octadecyl acrylate and diethyleneglycol ethyl ether acrylate, all of which present low dispersities (Đ ≈ 1.1) at very high conversions. Functional monomers, including glycidyl acrylate and solketal acrylate, were also found to be tolerant to the photo-mediated reaction. Finally, solketal acrylate was copolymerised with methyl acrylate which, following deprotection of the pendant ketal group, furnished an amphiphilic diblock copolymer.

6.1 Introduction

In chapter 5 the efficacious photo-activated living polymerisation of acrylates mediated by $CuBr_2$ in the presence of an excess of aliphatic tertiary amine ligands was thoroughly investigated, presenting an outstanding degree of control (~1.10) and very high end-group fidelity[1]. Reaction rates were fast compared to related systems (>95% conversion was achieved in 80 minutes) and temporal control was possible during polymerisation *via* intermittent light and dark reactions. Furthermore, when *α*-hydroxy and *vic*-diol functionalities were incorporated into alkyl halide initiators with retention of control epitomised by the low dispersities achieved. The use of different solvents, including DMSO, MeOH, MeCN and DMF, was briefly probed to demonstrate the polymerisation of short chain alkyl acrylates, in addition to poly(ethylene glycol) methyl ether acrylate ($PEGA_{480}$).

In this chapter, an expansion of the scope of this photo-mediated living radical polymerisation is presented. The use of different solvents was further investigated, and several solvents are shown to be suitable for photo-mediated LRP. Notably, water was found to be an exception, exhibiting poor molecular weight distribution control. The number of available solvents enables polymerisation of a range of monomers, including functional acrylates, (glycidyl acrylate and solketal acrylate), increasingly hydrophobic acrylates (*iso*-octyl acrylate, lauryl acrylate and stearyl acrylate) and thermoresponsive acrylates (diethylene glycol ethyl ether acrylate). Photo-mediated polymerisation was exploited to synthesise well-defined block copolymers (poly(MA)-*b*-(SA)) in a one-pot process, which were rendered amphiphilic upon deprotection of the solketal diol.

6.2 Results and Discussion

Initially, various solvents were screened to ascertain their compatibility with the photo-mediated process. Methyl acrylate (MA) was selected as the model monomer and subjected to previously reported polymerisation conditions with [MA]/[I]/[$CuBr_2$]/[Me_6-Tren] = [50]/[1]/[0.02]/[0.12]. Alcohols were found to be compatible with this technique, although a slower rate of polymerisation was observed relative to DMSO. For example, when ethanol (EtOH) was employed as solvent, a significantly lower conversion (38 %) was obtained in 90 minutes as compared to > 95 % in DMSO. Likewise, in isopropanol (IPA) conversion was limited within a 90 min reaction time (4 %). However, both EtOH and IPA resulted in full conversion (> 99 %) after 16 hours, with low dispersity values obtained from SEC analysis ($Đ$ = 1.08 and 1.16, respectively, Section 6.4.4, Figure 6.4). Fluorinated alcohols, including 2,2,2-trifluoroethanol (TFE) and 2,2,3,3-tetrafluoropropanol (TFP), have recently been reported as good solvents for SET-LRP as catalyzed by Cu(0) wire[2-5]. These solvents possess interesting properties, such as considerably higher melting points and lower boiling temperatures, strong H-bond donor properties and acidic character compared to non-fluorinated analogues. Under photo-mediated polymerisation conditions, TFE gave rise to 54 % conversion after 90 minutes while TFP exhibited a suppression in the rate (3% in 90 minutes), which is in line with the analogous non-fluorinated alcohols (EtOH, IPA). Nevertheless, full conversion (> 99 %) was again obtained within 16 hours, and low dispersities were retained ($Đ$ < 1.10, Section 6.4.4, Figure 6.5).

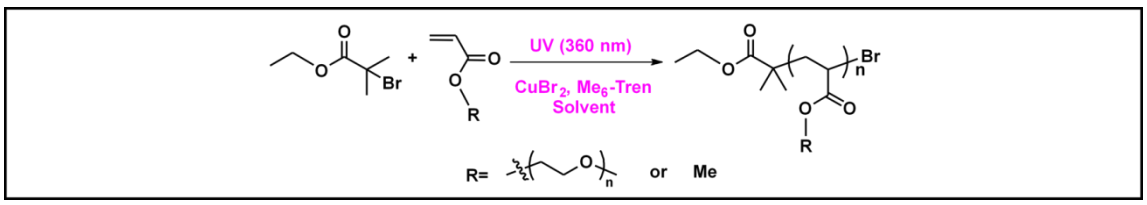

Scheme 6.1: Photo-induced polymerisation of PEG acrylate or methyl acrylate in various solvents

Full dissolution of monomer is an important consideration for maintaining control during the Cu(0)-mediated polymerisation of alkyl acrylates proceeding in both homogeneous and self-generating heterogeneous media[6, 7]. Thus, the polymerisation of MA was investigated in less polar solvents. Polymerisation in toluene was previously reported to proceed with loss of control and furnished polymers with higher dispersities. This was attributed, in part, to the limited solubility of the $CuBr_2$ complexes in toluene. Consequently, mixtures of toluene with methanol or IPA (toluene/alcohol: 4/1) were investigated as an alternative solvent system to satisfy required monomer and $CuBr_2$ solubility. Although relatively slower rates of polymerisation were observed, quantitative yields were obtained without compromising polymerisation control or dispersity ($Đ \sim 1.10$, Section 6.4.4, Figure 6.6). Dioxane and anisole were also utilised as solvents, however, the limited solubility of the $CuBr_2$ complexes again resulted in uncontrolled polymers with dispersities of 2.0 and 1.46 respectively (Section 6.4.4, Figure 6.7).

Finally, water was employed as a solvent for the photo-mediated polymerisation of poly(ethylene glycol) methyl ether acrylate ($PEGA_{480}$). Surprisingly, the aqueous polymerisation of PEGA afforded only poor control over the molecular weight distribution when full conversion was attained (Section 6.4.4, Figure 6.8). However, similar polymerisation in DMSO proceeded with comparable control to that observed during the polymerisation on MA in DMSO (Section 6.4.4, Figure 6.8), indicating that the solvent (H_2O) was responsible for this loss of control. In an attempt to understand this observation a UV-*vis* spectroscopy experiment was performed. A deoxygenated solution of [$CuBr_2$] : [Me_6-Tren] = [1] : [6] to mimic polymerisation conditions in H_2O, revealed the characteristic absorbance at λ_{max} = 950 nm with an additional absorbance at λ = 750 nm both attributed to the d-d transitions of the d^9 Cu^{II}-tertiary amine complex. The mixture was subsequently exposed to UV irradiation for 90 min proceeding with no detectable

decrease in the absorbance. Similar results were observed following irradiation for 24 h, suggesting that Cu^{II} could not be efficiently reduced in aqueous solution (Figure 6.1).

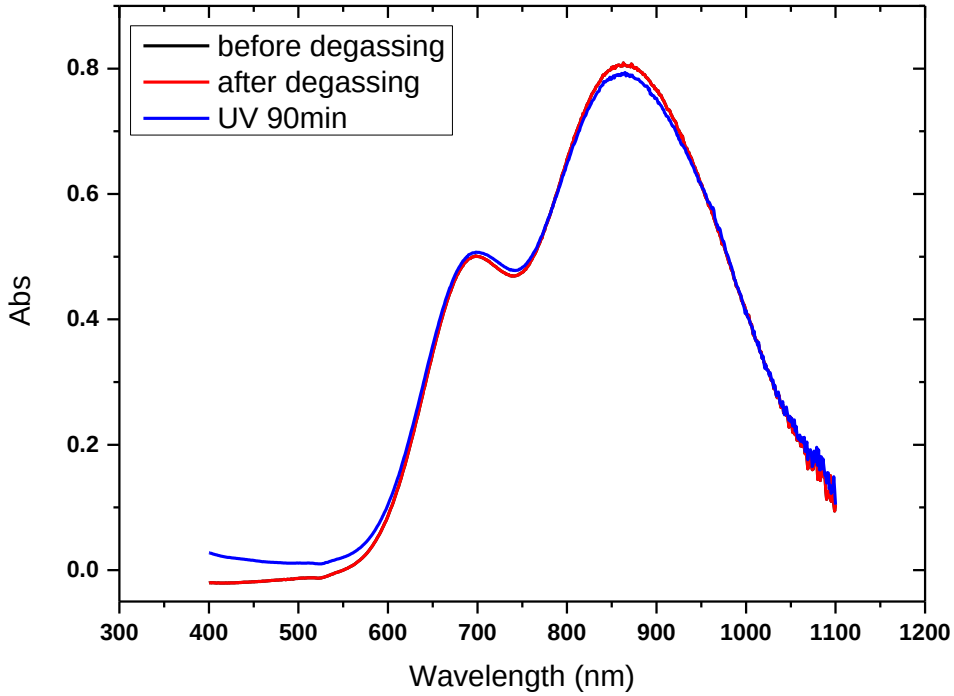

Figure 6.1: UV-vis spectrum of the $CuBr_2$/Me_6-Tren catalyst mixture before (black) and after (red/blue) irradiation at λ_{max}=360 nm.

This is in line with the relative stabilities of Cu^{II} and Cu^{I} amine complexes in H_2O, in which the disproportionation equilibrium is significantly shifted towards the higher oxidation Cu^{II} species ($K_{dis} > K_{com}$).

Nevertheless, for cases where the presence of water is desirable, the polymerisation of $PEGA_{480}$ was screened in mixtures of H_2O : DMSO. In 50% aqueous solution (DMSO : H_2O = 1 : 1) the reaction proceeded with comparable rates to pure DMSO media, furnishing a final polymer with a dispersity of 1.19. Reducing the water content to 25% (DMSO : H_2O = 3 : 1) had no effect on the rate of polymerisation but resulted in an improvement in dispersity (Section 6.4.4, Figure 6.9). The data obtained for the various solvents are summarised in Table 6.1.

Table 6.1: Solvent compatibility study for the photo-mediated polymerisation of MA and PEGA[a]

Solvent	[M][a]	Time [h]	Conv.[b] [%]	$M_{n,th}$ [g mol^{-1}]	$M_{n,SEC}$[c] [g mol^{-1}]	$Đ$
EtOH	MA	1.5	38	4500	2150	1.16
	DP_n = 50	24	99		4200	1.08
IPA		1.5	4		200	1.25
		24	100		3100	1.16
TFE		1.5	54		2000	1.14
		24	99		5200	1.09
TFP		1.5	3		160	1.26
		24	74		7000	1.10
Toluene:MeOH		1.5	8		500	1.22
[4]:[1]		24	100		6300	1.08
Toluene:IPA		1.5	4		300	1.27
[4]:[1]		24	96		6000	1.11
Dioxane		1.5	52		3600	1.91
		24	99		5100	1.99
Anisole		1.5	84		1900	2.27
		24	99		4300	1.46
DMSO	PEGA	1.5	93	5000	6500	1.11
	DP_n = 10	24	99		6900	1.10
H_2O		1.5	95		6600	1.55
		24	99		7900	1.48
DMSO:H_2O		1.5	94		6700	1.21
[1]:[1]		24	99		7200	1.19
DMSO:H_2O		1.5	92		6200	1.12
[3]:[1]		24	99		6900	1.12

[a] [I] : [Cu^{II}] : [Me_6-Tren] = [1] : [0.02] : [0.12] in (50%, *v/v*) solvent. [b]Determined by ^{1}H NMR. [c]Determined by $CHCl_3$ or DMF SEC analysis

In an attempt to expand the scope of this photo-induced system, 2-hydroxyethyl acrylate (HEA) was polymerised using DMSO as solvent using the following reaction conditions: [M]/[I]/[$CuBr_2$]/[Me_6-Tren] = [20]/[1]/[0.02]/[0.12]. The polymerisation proceeds rapidly with near-quantitative monomer conversion (> 97 %) achieved within 90 minutes, as determined by ^{1}H NMR analysis. SEC analysis revealed a symmetrical, monomodal molecular weight distribution with low dispersity ($Đ$ = 1.10) with no observable evidence of high or low molecular weight termination events (Section 6.4.4, Figure 6.10). 2-Hydroxypropyl acrylate (HPA) was polymerised under the same conditions and high conversion was attained within 90 minutes (92%). A slight deviation in

polymerisation control was represented by a broader molecular weight distribution by SEC ($Đ$ = 1.30, Section 6.4.4, Figure 6.11). Diethylene glycol ethyl ether acrylate (DEGEEA) forms thermoresponsive homopolymers with an LCST of ~ 13 °C[8]. As such, it has previously been incorporated into block copolymer compositions to tune the cloud point or phase transition temperature for higher order assembled structures. Pleasingly, DEGEEA was found to be compatible with the photo-mediated reaction conditions, yielding a well-controlled polymer with a final dispersity = 1.13 (Section 6.4.4, Figure 6.12).

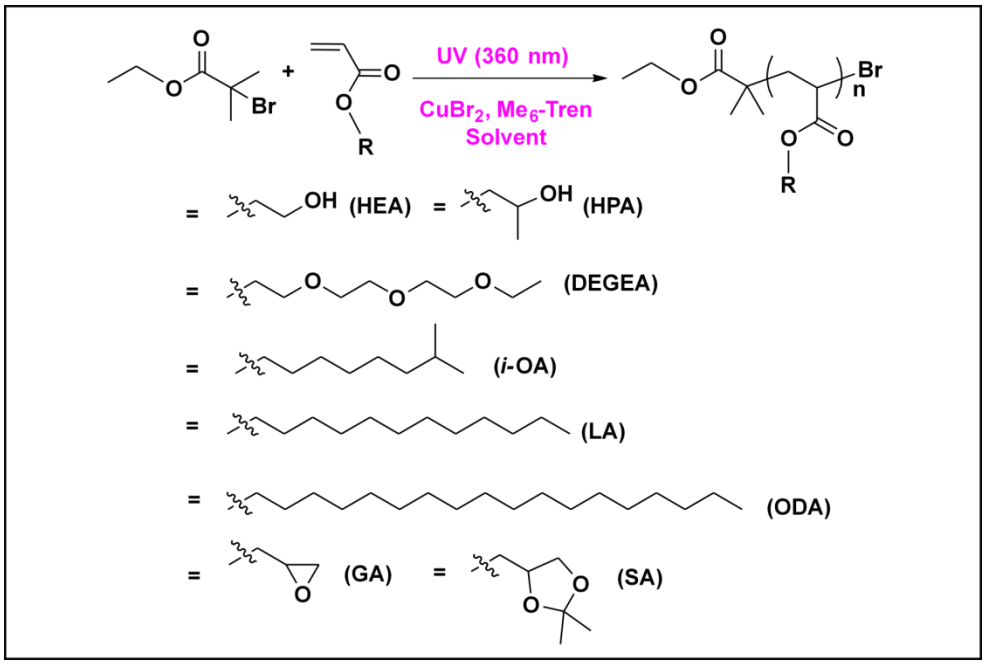

Scheme 6.2: Photo-mediated polymerisation of eight acrylate monomers [I] : [Cu^{II}] : [Me_6-Tren] = [1] : [0.02] : [0.12] in (50%, *v/v*) solvent.

The photo-induced living radical polymerisation of monomers with increasingly hydrophobic acrylates was also investigated. Lauryl acrylate (LA) is insoluble in DMSO and although it has previously been polymerised in this solvent system, discrepancies in molecular weight data and high dispersity values were reported, indicative of a poorly controlled system[6]. The importance of monomer solubility in Cu-mediated polymerisation was reported previously[6, 7], thus, IPA was initially employed as solvent for the polymerisation of LA, with 83% conversion being obtained within 3.5 h with a dispersity

of 1.18. Quantitative conversion was attained within 10 h, furnishing a well-controlled polymer ($Đ$ = 1.21, Section 6.4.4, Figure 6.14). The polymerisation of LA in IPA has been reported to proceed in a self-generating biphasic system without detrimental effect on the polymerisation. This was replicated in the photo-mediated reaction, whereby interruption of the agitation imposed upon the reaction medium resulted in phase separation, yielding a polymer-rich lower phase and a catalyst-rich upper phase. Repeating the polymerisation in a toluene/MeOH (4 : 1) solvent system, to retain homogeneity throughout the reaction, resulted in quantitative conversion (> 99 %) within 12 hours. Crucially, the homogeneity retained throughout the reaction appeared to confer a greater degree of control ($Đ$ = 1.07, Section 6.4.4, Figure 6.13) than that observed in the self-generating biphasic system. The photo-mediated polymerisation of *n*BA in DMSO was recently reported[1] to also proceed in self-generated biphasic media, furnishing poly(*n*BA) with a dispersity = 1.16 (Section 6.4.4, Figure 6.16). We were interested to see whether repeating this polymerisation in a homogeneous system had any effect on the final polymer obtained in accordance with the poly(LA) system. Using DMF as solvent, thus retaining monomer (*n*BA), $CuBr_2$ and propagating polymer in solution, again resulted in narrower dispersities ($Đ$ = 1.06, Section 6.4.4, Figure 6.15) at full conversion (> 99 %). The similarity of the phase data for LA and *n*BA implies that under photo-mediated conditions, homogeneity is preferable, conferring maximal control over the polymerisation reactions. Consequently, to complete the investigation of hydrophobic acrylates, photo-mediated polymerisations of *iso*-octyl (*i*OA) and octadecyl (stearyl, ODA) acrylate were performed in toluene/MeOH (4 : 1) and toluene/IPA (4 : 1) solvent systems respectively. Very high conversions (> 99 %) were achieved within 10 hours for both monomers and the anticipated control over the reaction was confirmed by SEC, yielding dispersity values of 1.17 and 1.10 respectively (Section 6.4.4, Figure 6.17-6.18).

The preparation of functional scaffolds is highly desirable and the incorporation of reactive functional groups can facilitate post-polymerisation modification reactions en route to introducing functionality not necessarily compatible with the selected polymerisation protocol[9, 10]. Glycidyl acrylate (GA), containing pendant epoxy functionality, was synthesised following a standard literature procedure[11, 12], interestingly although glycidyl methacrylate is commercially available the acrylate is not. The epoxide functional group is susceptible to nucleophilic ring-opening attack by amine, thiol and carboxylic acid functional groups[13]. Indeed this has been exploited to furnish various functional linear and hyperbranched polymers, including (block) copolymers, and more recently sequence controlled multi-block glycopolymers[11, 14, 15]. Subjected to photo-mediated polymerisation conditions in DMSO, GA was completely consumed within 90 min, providing well-controlled poly(GA) ($Đ$ = 1.19, Section 6.4.4, Figure 6.19).

Table 6.2: Photo-mediated polymerisation of nine acrylate monomers [I] : [Cu^{II}] : [Me_6-Tren] = [1] : [0.02] : [0.12] in (50%, *v/v*) solvent. [a] Determined by ^{1}H NMR. [b] Determined by $CHCl_3$ SEC analysis

[M]	Solvent	[M]/ [I]	Time [h]	Conv.[a] [%]	$M_{n,th}$ [g mol^{-1}]	$M_{n,SEC}$ [b] [g mol^{-1}]	$Đ$
HEA	DMSO	20	1.5	98	2300	4500	1.10
HPA		20	1.5	92	2600	6200	1.32
ODA	Tol/IPA	15	1.5	4	4800	150	1.10
	[4] : [1]		10	99		4500	
LA	IPA	50	3.5	83		9900	1.18
			16	100	12900	10300	1.21
	Tol/MeOH		7	88		8000	1.05
	[4] : [1]		24	99		11400	1.07
***n*BA**	DMF	50	10	99	6400	6700	1.06
	DMSO		1.5	97		6800	1.16
DEG	DMSO	20	1.5	80	4300	4100	1.10
			17	99		4800	1.13
GA		20	1.5	99	2600	2900	1.19
SA		100	1.5	80	18600	11500	1.10
			10	99		16000	1.07
***i*OA**	Tol/MeOH	25	1.5	3	4600	100	1.17
	[4] : [1]		10	100		2800	

[a]Determined by ^{1}H NMR. [b]Determined by $CHCl_3$ SEC analysis.

Solketal acrylate (SA) contains a ketal protected *vic*-diol pendant functionality which can implement a hydrophobic-hydrophilic switch, *via* ketal deprotection under acidic conditions. Homopolymerisation of SA was complete (> 99 %) within 10 hours and comparable control was retained ($Đ$ = 1.10, Section 6.4.4, Figure 6.20) compared to that observed for poly(MA). To evaluate the integrity of the ω-Br chain end of the functional poly(SA) homopolymer, a second aliquot of deoxygenated SA in DMSO was injected into the unpurified reaction mixture. Excellent control was observed as the molecular weight distribution shifted completely to higher molecular weight, with minimal detectable termination during the initial homopolymerisation, and low dispersities were retained ($Đ$ = 1.08, Figure 6.2).

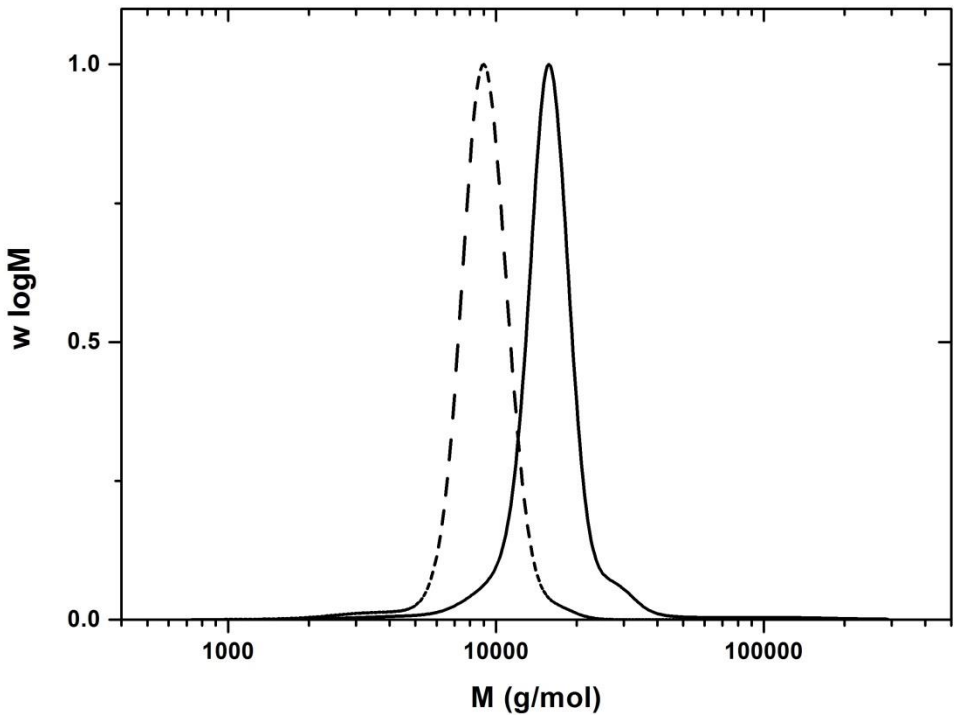

Figure 6.2: *In situ* chain extension of poly(SA) [SA]:[EBiB]: [$CuBr_2$]: [Me_6-Tren]= [50] : [1] : [0.02] : [0.12], DMSO (50% *v/v*). Block copolymerisation achieved by addition of SA (25 eq) in DMSO (50% *v/v*).

The hydrophobic-hydrophilic switch was utilised during the one-pot synthesis of an amphiphilic diblock copolymer. Initially poly(MA) was synthesised by photo-mediated polymerisation in DMSO, providing a macroinitiator with optimum ω-Br chain-end

fidelity (95 % conv., 4700 g/mol, $Đ$ = 1.06). Without isolation or purification of the macroinitiator, a deoxygenated solution of SA in DMSO was injected into the reaction mixture and subjected to photo-mediated polymerisation. Within 24 h, a well-defined poly(MA)-*b*-(SA) diblock copolymer was obtained (99 %, $Đ$ = 1.07, Figure 6.3). Hydrolysis of the pendant ketal protecting groups unmasked the hydrophilic *vic*-diol groups, conferring amphiphilic character on the diblock copolymer.

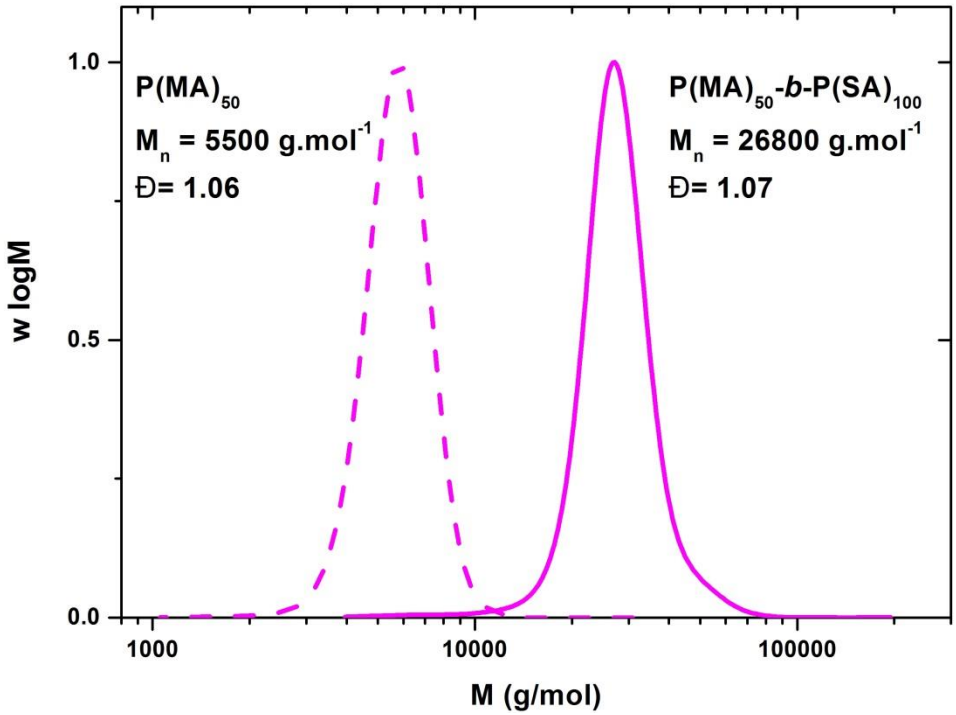

Figure 6.3: Block copolymerisation from a PMA macroinitiator. Initial conditions for block copolymerisation: [MA]:[EBiB]: [$CuBr_2$]: [Me_6-Tren]= [50] : [1] : [0.02] : [0.12], DMSO (50% *v/v*). Block copolymerisation achieved by addition of SA (100 eq) in DMSO (50% *v/v*).

6.3 Conclusions

The scope of photo-mediated living radical polymerisation in the presence of $CuBr_2$ and Me_6-Tren has been expanded to include a range of hydrophilic, hydrophobic and functional acrylates. An investigation into solvent compatibility proved to be particularly instructive for increasingly hydrophobic acrylates that have been shown to polymerise in both homogeneous and self-generating biphasic systems. Optimal control was conferred

when homogeneity of the monomer, $CuBr_2$ and propagating polymer was retained throughout the polymerisation. Epoxide and ketal-protected *vic*-diol functional groups were shown to be compatible with the reaction conditions. The protected *vic*-diol functional group presents the possibility of a hydrophilic-hydrophobic switch which was exploited upon copolymerisation with MA to prepare an poly(MA)-*b*-(SA) di-block copolymer.

6.4 Experimental

6.4.1 Materials

All materials were purchased from Sigma Aldrich or Fisher Scientific unless otherwise stated. Copper(II) bromide ($CuBr_2$) and ethyl 2-bromoisobutyrate (EBiB) were used as received. All monomers were passed through a basic Al_2O_3 column prior to use. Tris-(2-(dimethylamino)ethyl)amine (Me_6-Tren) was synthesised according to a previously reported literature[16]. Solketal acrylate was synthesised according to a reported procedure[17] and distilled under reduced pressure (45°C, 10^{-1} mbar) to yield a colourless liquid. GA was also synthesised following a literature protocol[11] and a flash column chromatography was utilised to obtain a colourless liquid.

6.4.2 Apparatus

^{1}H NMR spectra were recorded on Bruker DPX-300 and DPX-400 spectrometers using deuterated solvents obtained from Aldrich. Chemical shifts are given in ppm downfield from the internal standard tetramethylsilane. Size exclusion chromatography (SEC) measurements were conducted using an Agilent 1260 SEC-MDS fitted with differential refractive index (DRI), light scattering (LS) and viscometry (VS) detectors equipped with 2 × PLgel 5 mm mixed-D columns (300 × 7.5 mm), 1 × PLgel 5 mm guard column (50 × 7.5 mm) and autosampler.. All samples were passed through a 0.45 μm

PTFE filter before analysis. The mobile phase was chloroform with 2% triethylamine eluent at a flow rate of 1.0 mL min^{-1}. SEC data were analysed using Cirrus v3.3 software with calibration curves produced using Varian Polymer laboratories Easi-Vials linear PMMA standards (200-4.7 × 10^5 g mol^{-1}). UV/Vis spectra were recorded on a Agilent Technologies Cary 60 UV-Vis spectrophotometer in the range of 200-1100 nm using a cuvette with 10 mm optical length. The photolysis source of UV light was a UV nail gel curing lamp (available on ebay from a range of suppliers) (λ_{max} ~ 360 nm) equipped with four 9 W bulbs.

6.4.3 General procedures

General procedure for photo-induced polymerisation.

Filtered monomer (DP_n eq), EBiB (1 eq), $CuBr_2$ (0.02 eq), Me_6-Tren (0.12 eq) and DMSO (2 mL) were added to a septum sealed vial and degassed by purging with nitrogen for 15 min. Polymerisation commenced upon exposure of the degassed reaction mixture to the UV lamp. Samples were taken periodically and conversions measured using ^{1}H NMR and SEC analysis.

General procedure for *in-situ* chain extension reactions.

Filtered MA (1 mL, 11.1 mmol, 50 eq), EBiB (32 μL, 0.22 mmol, 1 eq), $CuBr_2$ (1.0 mg, 4.4 μmol, 0.02 eq), Me_6-Tren (7 μL, 22.0 μmol, 0.12 eq) and DMSO (1 mL) were added to a septum-sealed vial and degassed by purging with nitrogen for 15 min. Polymerisation commenced upon exposure of the degassed reaction mixture to the UV lamp. After 90 min a 1: 0.5 mixture of degassed SA (100 eq) and DMSO was added to the reaction mixture *via* degassed syringe. Samples were taken periodically and conversions were measured using ^{1}H NMR and SEC analysis.

6.4.4 Characterisation

Isopropanol (IPA) **Ethanol (EtOH)**

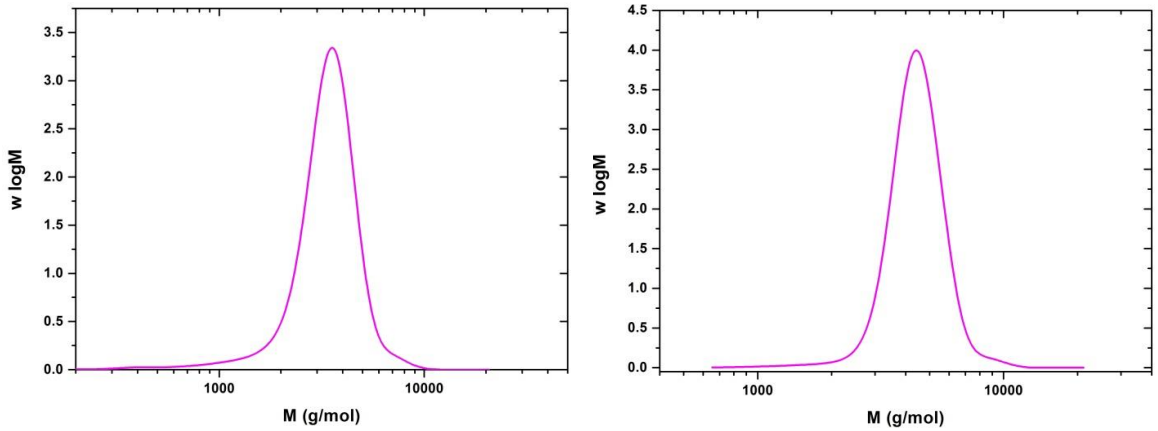

Figure 6.4: (right) Molecular weight distribution of poly(methyl acrylate) M_n = 4200 g/mol; $Đ$ = 1.08; 99% conversion. [MA]:[EBiB]:[$CuBr_2$]:[Me_6-Tren] = [50]:[1]:[0.02]:[0.12]. **EtOH** 50% *v/v*.
(left) Molecular weight distribution of poly(methyl acrylate) M_n = 3100 g/mol; $Đ$ = 1.16; 100% conversion. [MA]:[EBiB]:[$CuBr_2$]:[Me_6-Tren] = [50]:[1]:[0.02]:[0.12]. **IPA** 50% *v/v*.

Tetrafluoroethanol (TFE) **Tetrafluoropropanol (TFP)**

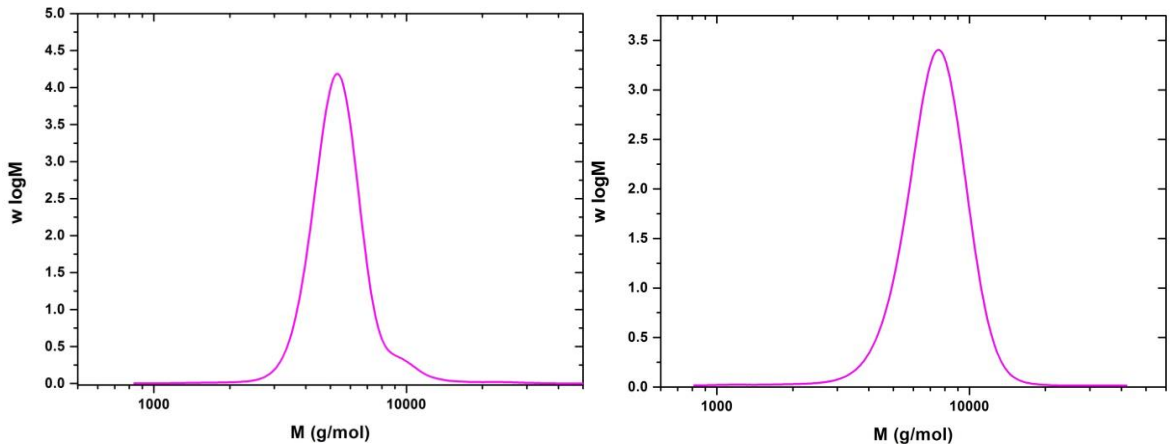

Figure 6.5: (left) Molecular weight distribution of poly(methyl acrylate) M_n = 5200 g/mol; $Đ$ = 1.09; 100% conversion. [MA]:[EBiB]:[$CuBr_2$]:[Me_6-Tren] = [50]:[1]:[0.02]:[0.12]. **TFE** 50% *v/v*.
(right) Molecular weight distribution of poly(methyl acrylate) M_n = 7000 g/mol; $Đ$ = 1.10; 74% conversion. [MA]:[EBiB]:[$CuBr_2$]:[Me_6-Tren] = [50]:[1]:[0.02]:[0.12]. **TFP** 50% *v/v*.

Toluene-methanol **Toluene-IPA**

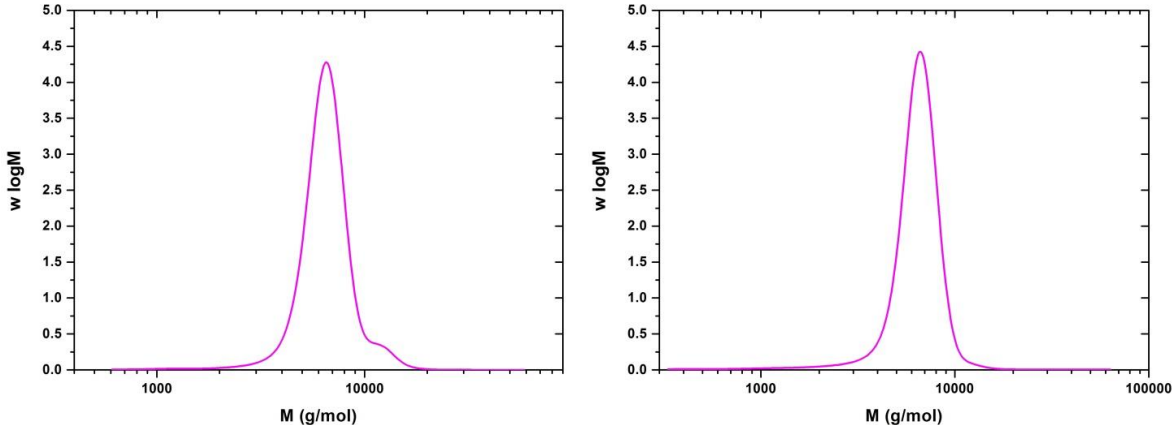

Figure 6.6: (left) Molecular weight distribution of poly(methyl acrylate) M_n = 6300 g/mol; $Đ$ = 1.08; 100% conversion. [MA]:[EBiB]:[$CuBr_2$]:[Me_6-Tren] = [50]:[1]:[0.02]:[0.12]. **Tol/MeOH [4]:[1]** 50% *v/v*.
(right) Molecular weight distribution of poly(methyl acrylate) M_n = 6000 g/mol; $Đ$ = 1.11; 96% conversion. [MA]:[EBiB]:[$CuBr_2$]:[Me_6-Tren] = [50]:[1]:[0.02]:[0.12]. **Tol/IPA [4]:[1]** 50% *v/v*.

Dioxane **Anisole**

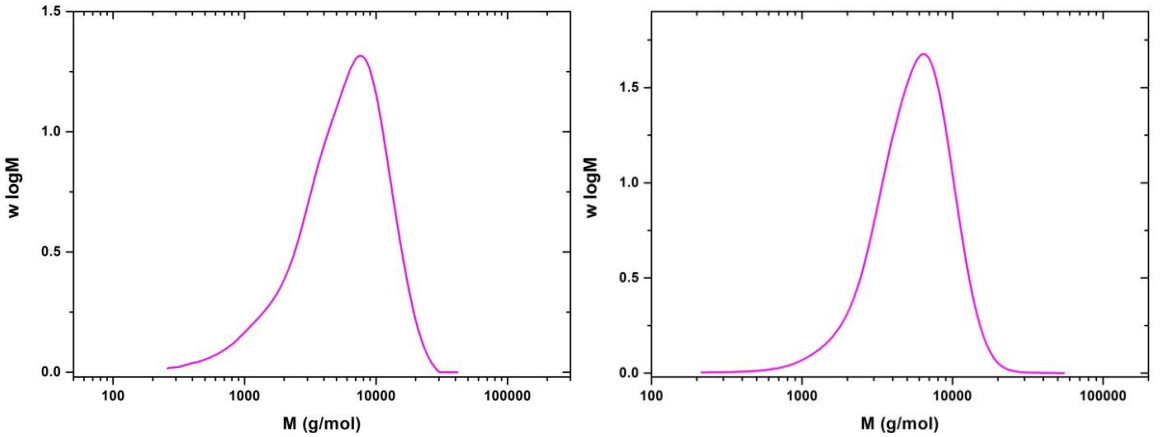

Figure 6.7: (left) Molecular weight distribution of poly(methyl acrylate) M_n = 5100 g/mol; $Đ$ = 2.00; 99% conversion. [MA]:[EBiB]:[$CuBr_2$]:[Me_6-Tren] = [50]:[1]:[0.02]:[0.12]. **Dioxane** 50% *v/v*.
(right) Molecular weight distribution of poly(methyl acrylate) M_n = 4300 g/mol; $Đ$ = 1.46; 99% conversion. [MA]:[EBiB]:[$CuBr_2$]:[Me_6-Tren] = [50]:[1]:[0.02]:[0.12]. **Anisole** 50% *v/v*.

Water (H_2O) **Dimethyl Sulfoxide (DMSO)**

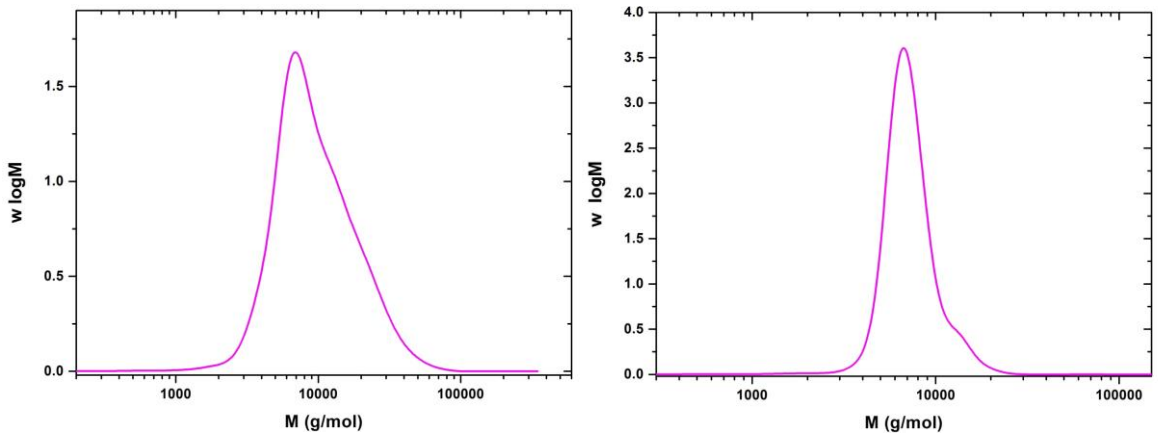

Figure 6.8: (left) Molecular weight distribution of poly($PEGA_{480}$) M_n = 7900 g/mol; $Đ$ = 1.48; 99% conversion. [PEGA]:[EBiB]:[$CuBr_2$]:[Me_6-Tren] = [10]:[1]:[0.02]:[0.12]. **H_2O** 50% *v/v*.
(right) Molecular weight distribution of poly($PEGA_{480}$) M_n = 6900 g/mol; $Đ$ = 1.10; 99% conversion. [PEGA]:[EBiB]:[$CuBr_2$]:[Me_6-Tren] = [10]:[1]:[0.02]:[0.12]. **DMSO** 50% *v/v*

H_2O:DMSO=[1:1] **H_2O:DMSO=[1:3]**

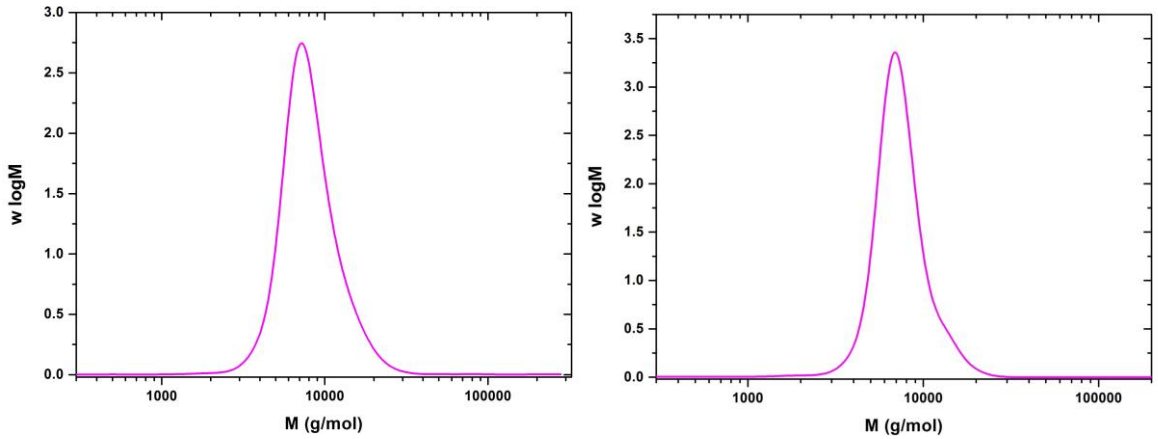

Figure 6.9: (left) Molecular weight distribution of poly($PEGA_{480}$) M_n = 7200 g/mol; $Đ$ = 1.19; 99% conversion. [PEGA]:[EBiB]:[$CuBr_2$]:[Me_6-Tren] = [10]:[1]:[0.02]:[0.12]. **DMSO-H_2O [1]:[1]** 50% *v/v*
(right) Molecular weight distribution of poly($PEGA_{480}$) M_n = 6900 g/mol; $Đ$ = 1.12; 99% conversion. [PEGA]:[EBiB]:[$CuBr_2$]:[Me_6-Tren] = [10]:[1]:[0.02]:[0.12]. **DMSO-H_2O [3]:[1]** 50% *v/v*.

Poly(hydroxyethyl acrylate)

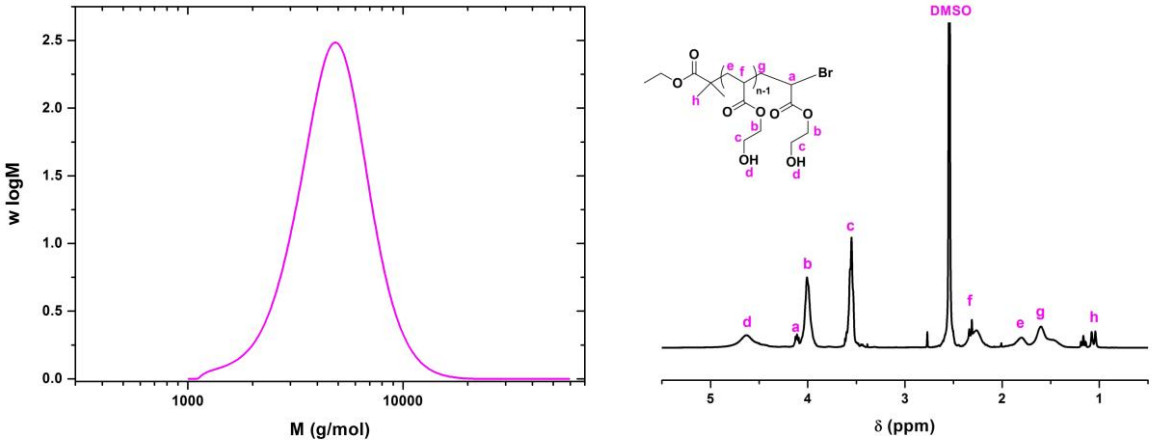

Figure 6.10: (left) Molecular weight distribution of **poly(2-hydroxyl acrylate)** M_n = 4500 g/mol; $Đ$ = 1.10; 98% conversion. [HEA]:[EBiB]:[$CuBr_2$]:[Me_6-Tren] = [20]:[1]:[0.02]:[0.12] in DMSO 50% *v/v*.
(right) ^{1}H NMR spectrum of **poly(2-hydroxyethyl acrylate)** obtained from UV experiment: [$CuBr_2$]/[Me_6-Tren]/[EBiB]/[HEA] polymerisation mixture in DMSO (50:50 *v/v*).

Poly(2-hydroxypropyl acrylate)

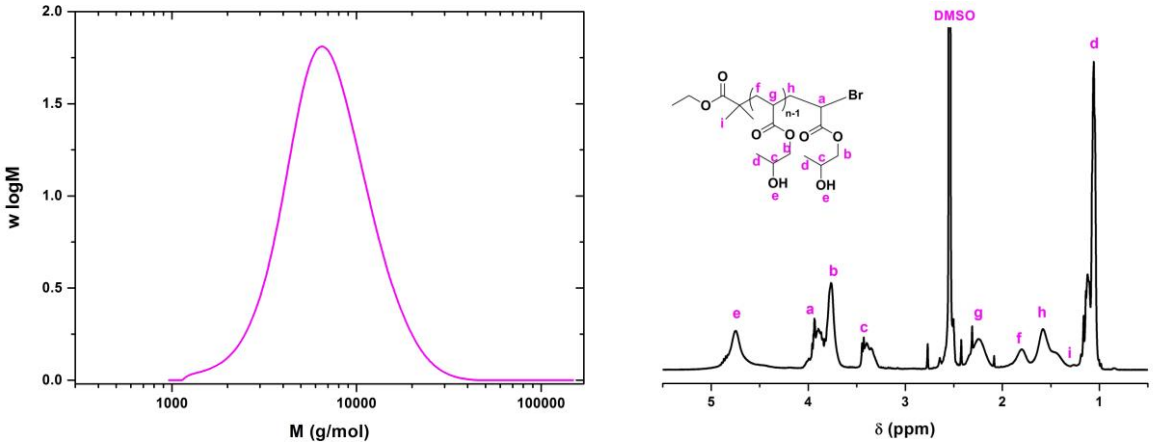

Figure 6.11: (left) Molecular weight distribution of **poly(2-hydroxypropyl acrylate)** M_n= 6200 g/mol; $Đ$ = 1.32; 92% conversion. [HPA]:[EBiB]:[$CuBr_2$]:[Me_6-Tren] = [20]:[1]:[0.02]:[0.12] in DMSO 50% *v/v*.
(right) ^{1}H NMR spectrum of **poly(2-hydroxypropyl acrylate)** obtained from UV experiment: [$CuBr_2$]/[Me_6-Tren]/[EBiB]/[HPA] polymerisation mixture in DMSO (50:50 *v/v*).

Poly(diethylene glycol methyl ethyl acrylate)

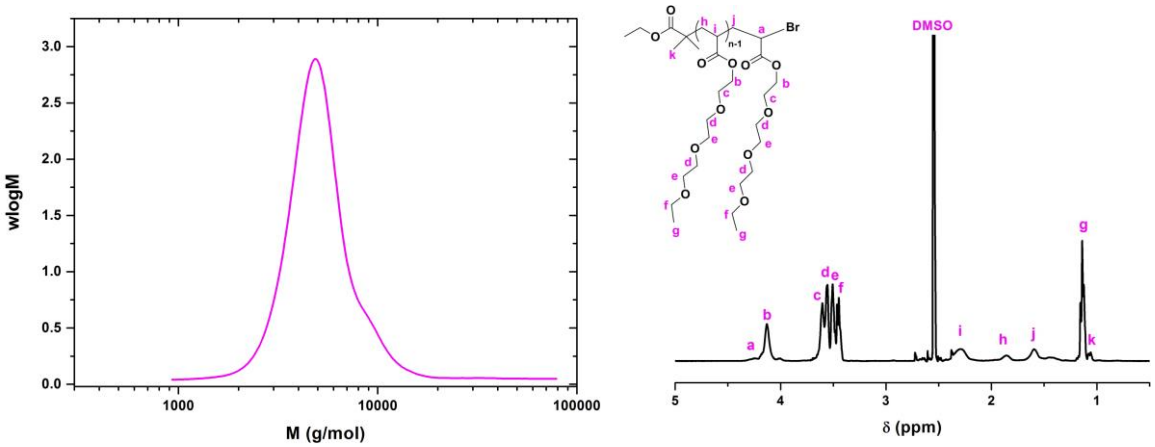

Figure 6.12: (left) Molecular weight distribution of **poly(diethylene glycol methyl ethyl acrylate)** M_n = 4800 g/mol; $Đ$ = 1.13; 99% conversion. [DEG]:[EBiB]:[$CuBr_2$]:[Me_6-Tren] = [20]:[1]:[0.02]:[0.12] in DMSO 50% *v/v*.
(right) ^{1}H NMR spectrum of **poly(diethylene glycol methyl ethyl acrylate)** obtained from UV experiment: [$CuBr_2$]/[Me_6-Tren]/[EBiB]/[DEG] polymerisation mixture in DMSO (50:50 *v/v* monomer/solvent).

Poly(lauryl acrylate) in toluene-MeOH (4:1)

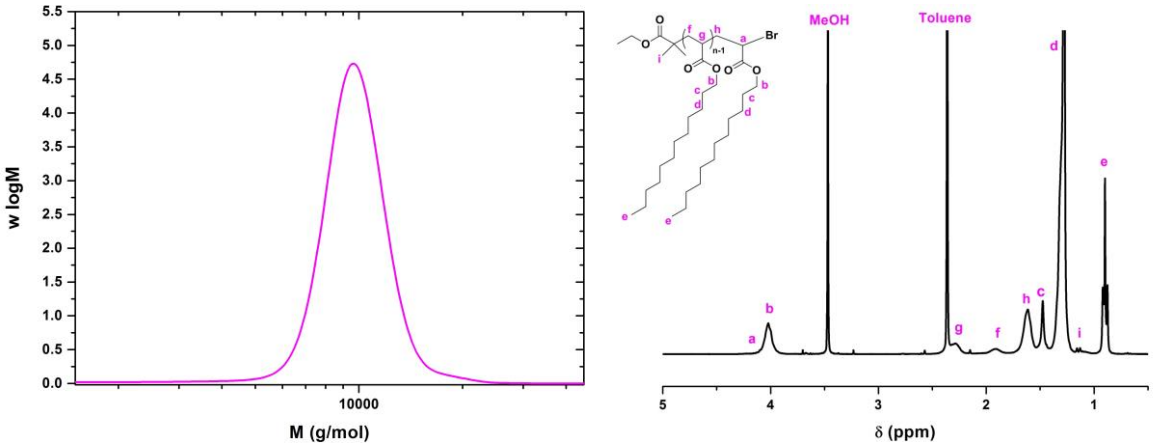

Figure 6.13: (left) Molecular weight distribution of **poly(lauryl acrylate)** M_n = 10300 g/mol; $Đ$ = 1.07; 99% conversion. [LA]:[EBiB]:[$CuBr_2$]:[Me_6-Tren] = [50]:[1]:[0.02]:[0.12]. Toluene-MeOH [4]:[1] 50% *v/v*.
(right) ^{1}H NMR spectrum of **poly(lauryl acrylate)** obtained from UV experiment: [$CuBr_2$]/[Me_6-Tren]/[EBiB]/[LA] polymerisation mixture in Toluene-MeOH [4] : [1] (50:50 *v/v*).

Poly(lauryl acrylate) in IPA

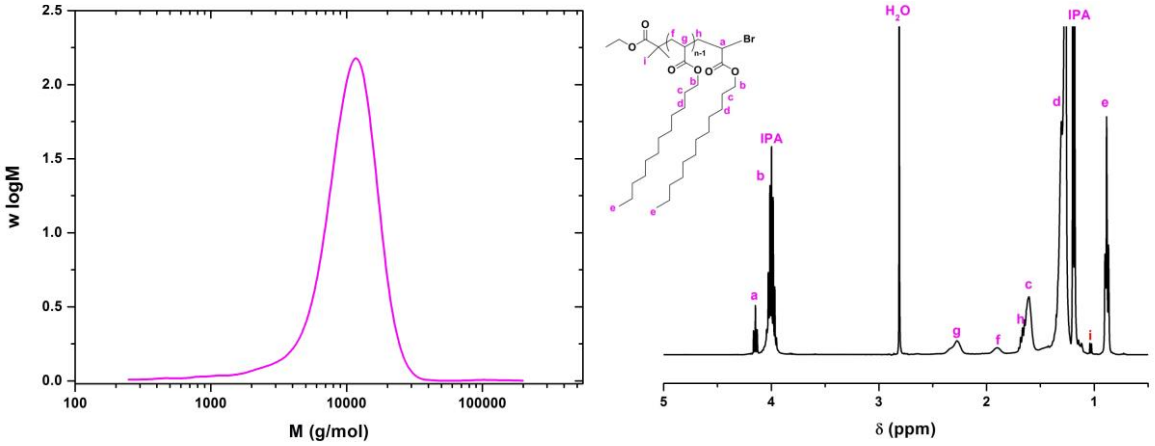

Figure 6.14: (left) Molecular weight distribution of **poly(lauryl acrylate)** M_n = 11400 g/mol; $Đ$ = 1.21; 100% conversion. [LA]:[EBiB]:[$CuBr_2$]:[Me_6-Tren] = [50]:[1]:[0.02]:[0.12]. IPA 50% *v/v*.
(right) ^{1}H NMR spectrum of **poly(lauryl acrylate)** obtained from UV experiment: [$CuBr_2$]/[Me_6-Tren]/[EBiB]/[LA] polymerisation mixture in IPA (50:50 *v/v*).

Poly(*n*-butyl acrylate) in DMF

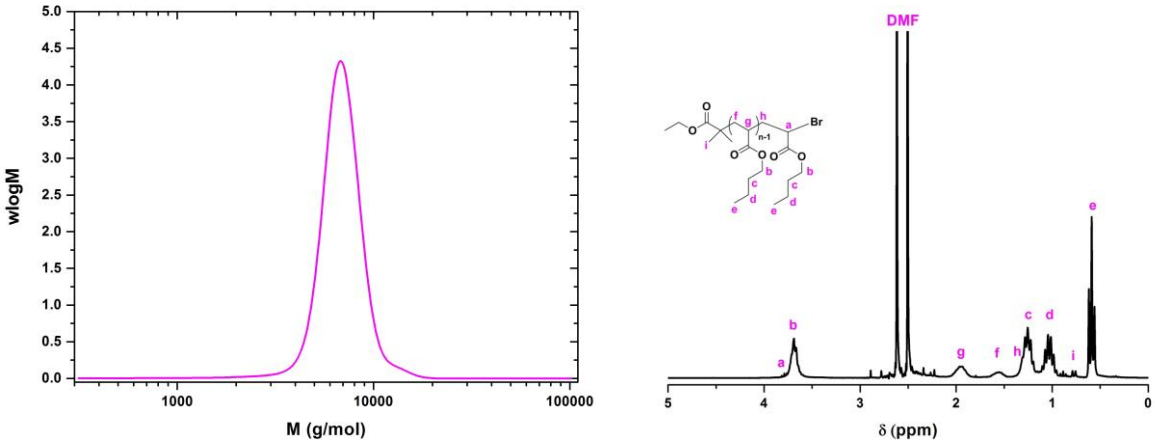

Figure 6.15: (left) Molecular weight distribution of **poly(*n*-butyl acrylate)** M_n = 6700 g/mol; $Đ$ = 1.06; 99% conversion. [*n*BA]:[EBiB]:[$CuBr_2$]:[Me_6-Tren] = [50]:[1]:[0.02]:[0.12]. DMF 50% *v/v*.
(right) ^{1}H NMR spectrum of **poly(*n*-butyl acrylate)** obtained from UV experiment: [$CuBr_2$]/[Me_6-Tren]/[EBiB]/[*n*BA] polymerisation mixture in DMF (50:50 *v/v*).

Poly(*n*-butyl acrylate) in DMSO

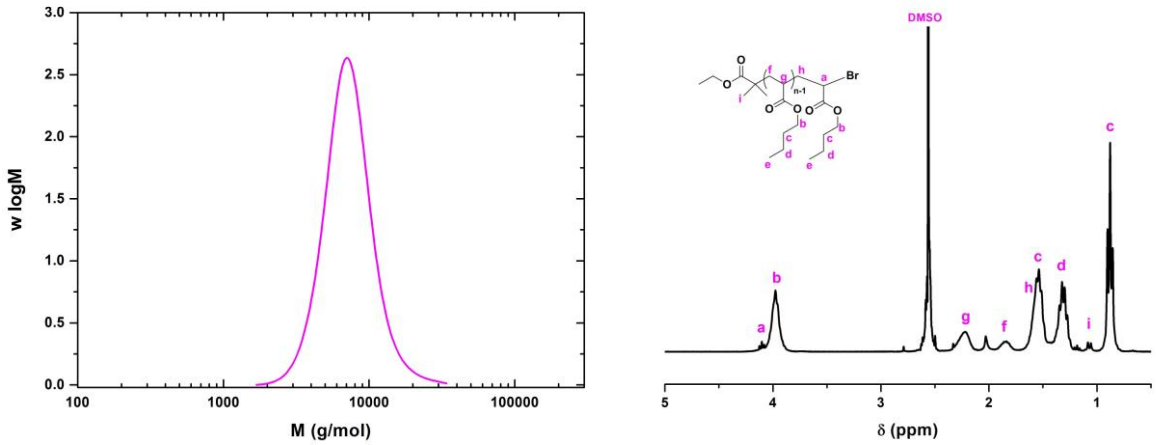

Figure 6.16: (left) Molecular weight distribution of **poly(*n*-butyl acrylate)** M_n = 6800 g/mol; $Đ$ = 1.16; 97% conversion. [*n*BA]:[EBiB]:[$CuBr_2$]:[Me_6-Tren] = [50]:[1]:[0.02]:[0.12]. DMSO 50% *v/v*.
(right) ^{1}H NMR spectrum of **poly(*n*-butyl acrylate)** obtained from UV experiment: [$CuBr_2$]/[Me_6-Tren]/[EBiB]/[*n*BA] polymerisation mixture in DMSO (50:50 *v/v*).

Poly(isooctyl acrylate)

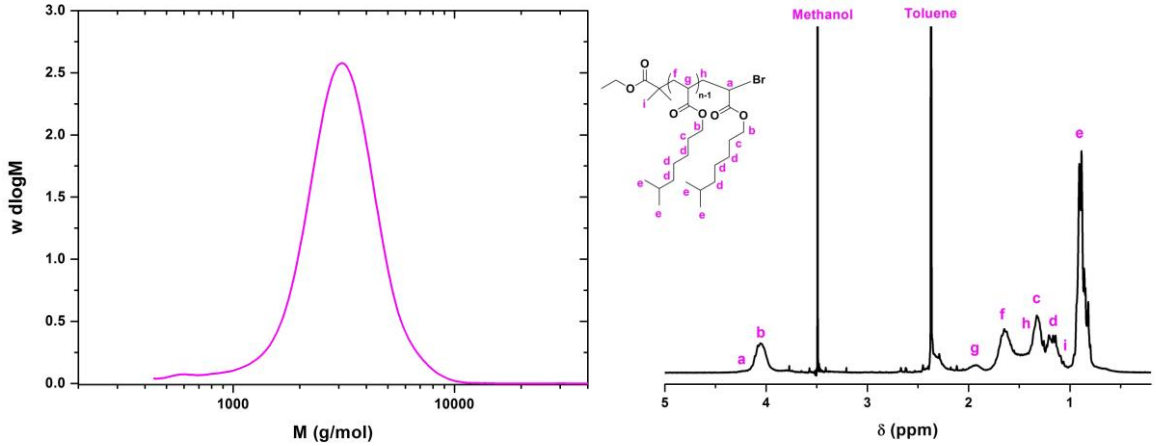

Figure 6.17: (left) Molecular weight distribution of **poly(isooctyl acrylate)** M_n = 2800 g/mol; $Đ$ = 1.17; 100% conversion. [iOA]:[EBiB]:[$CuBr_2$]:[Me_6-Tren] = [25]:[1]:[0.02]:[0.12]. toluene-MeOH [4]:[1] 50% *v/v*.
(right) ^{1}H NMR spectrum of **poly(isooctyl acrylate)** obtained from UV experiment: [$CuBr_2$]/[Me_6-Tren]/[EBiB]/[iOA] polymerisation mixture in toluene-MeOH [4] : [1] (50:50 *v/v*).

Poly(octadecyl acrylate)

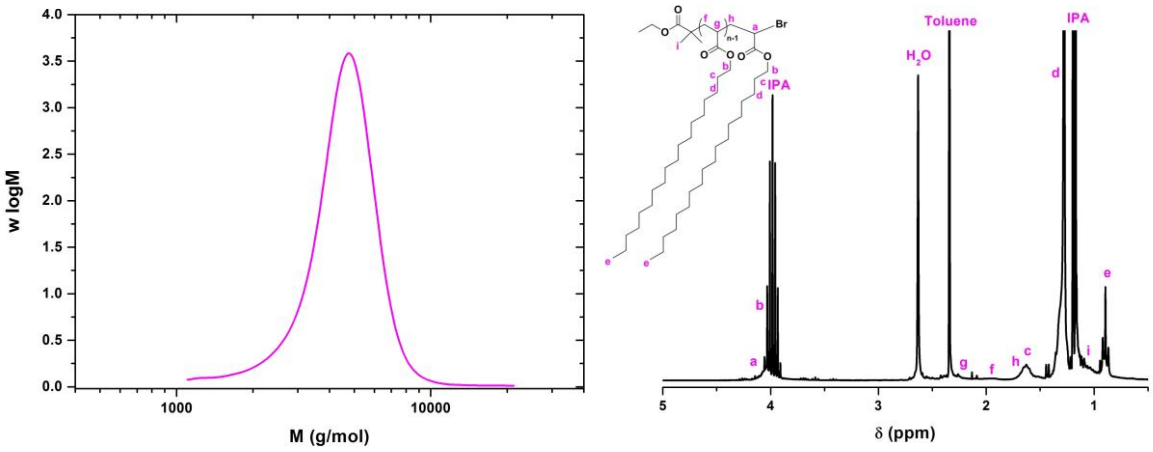

Figure 6.18: (left) Molecular weight distribution of **poly(octadecyl acrylate)** M_n = 4500 g/mol; $Đ$ = 1.10; 99% conversion. [OA]:[EBiB]:[$CuBr_2$]:[Me_6-Tren] = [15]:[1]:[0.02]:[0.12]. toluene-IPA [4]:[1] 50% *v/v*.
(right) ^{1}H NMR spectrum of **poly(octadecyl acrylate)** obtained from UV experiment: [$CuBr_2$]/[Me_6-Tren]/[EBiB]/[OA] polymerisation mixture in toluene-IPA [4]:[1] (50:50 *v/v*).

Poly(glycidyl acrylate)

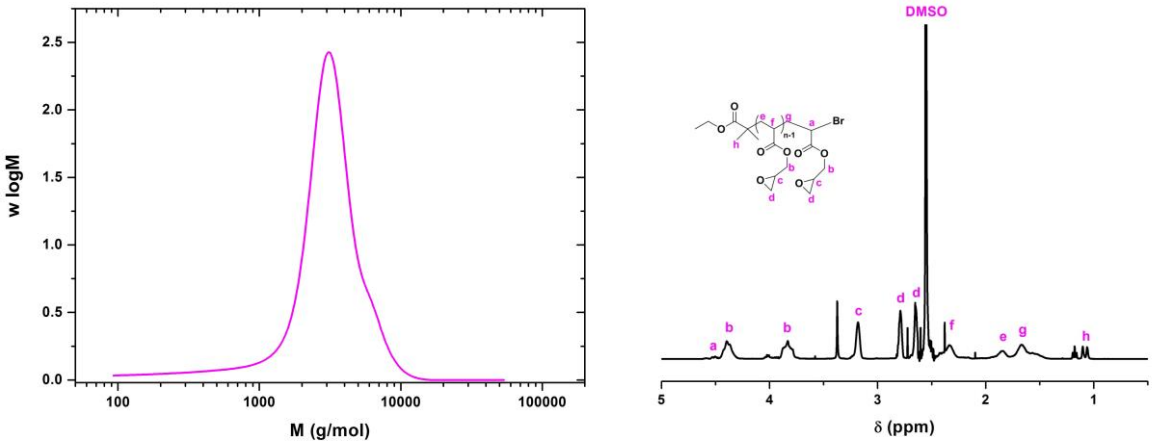

Figure 6.19: (left) Molecular weight distribution of **poly(glycidyl acrylate)** M_n = 2900 g/mol; $Đ$ = 1.19; 99% conversion. [GA]:[EBiB]:[$CuBr_2$]:[Me_6-Tren] = [20]:[1]:[0.02]:[0.12]. DMSO 50% *v/v*.
(right) ^{1}H NMR spectrum of **poly(glycidyl acrylate)** obtained from UV experiment: [$CuBr_2$]/[Me_6-Tren]/[EBiB]/[GA] polymerisation mixture in DMSO (50:50 *v/v*).

Poly(solketal acrylate)

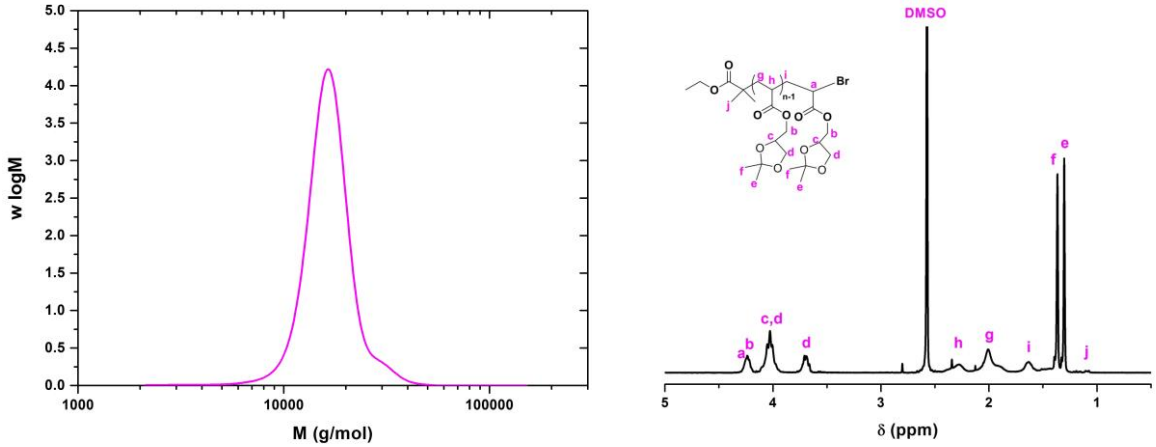

Figure 6.20: (left) Molecular weight distribution of **poly(solketal acrylate)** M_n = 16000 g/mol; $Đ$ = 1.07; 99% conversion. [SA]:[EBiB]:[$CuBr_2$]:[Me_6-Tren] = [100]:[1]:[0.02]:[0.12]. DMSO 50% *v/v*.
(right) ^{1}H NMR spectrum of **poly(solketal acrylate)** obtained from UV experiment: [$CuBr_2$]/[Me_6-Tren]/[EBiB]/[SA] polymerisation mixture in DMSO (50:50 *v/v*).

6.5 References

1. A. Anastasaki, V. Nikolaou, Q. Zhang, J. Burns, S. R. Samanta, C. Waldron, A. J. Haddleton, R. McHale, D. Fox, V. Percec, P. Wilson and D. M. Haddleton, *J. Am. Chem. Soc.*, 2013, **136**, 1141-1149.
2. S. R. Samanta, H.-J. Sun, A. Anastasaki, D. M. Haddleton and V. Percec, *Polym. Chem.*, 2014, **5**, 89-95.
3. S. R. Samanta, A. Anastasaki, C. Waldron, D. M. Haddleton and V. Percec, *Polym. Chem.*, 2013, **4**, 5563-5569.
4. S. R. Samanta, M. E. Levere and V. Percec, *Polym. Chem.*, 2013, **4**, 3212-3224.
5. S. R. Samanta, A. Anastasaki, C. Waldron, D. M. Haddleton and V. Percec, *Polym. Chem.*, 2013, **4**, 5555-5562.
6. C. Boyer, A. Atme, C. Waldron, A. Anastasaki, P. Wilson, P. B. Zetterlund, D. Haddleton and M. R. Whittaker, *Polym. Chem.*, 2013, **4**, 106-112.
7. A. Anastasaki, C. Waldron, V. Nikolaou, P. Wilson, R. McHale, T. Smith and D. M. Haddleton, *Polym. Chem.*, 2013, **4**, 4113-4119.
8. C. Boyer, M. R. Whittaker, K. Chuah, J. Liu and T. P. Davis, *Langmuir*, 2009, **26**, 2721-2730.
9. M. A. Gauthier, M. I. Gibson and H.-A. Klok, *Angew. Chem., Int. Ed.*, 2009, **48**, 48-58.

10. K. A. Günay, P. Theato and H.-A. Klok, *J. Polym. Sci., Part A: Polym. Chem.*, 2013, **51**, 1-28.
11. Q. Zhang, A. Anastasaki, G.-Z. Li, A. J. Haddleton, P. Wilson and D. M. Haddleton, *Polym. Chem.*, 2014, **5**, 3876-3883.
12. M. Benaglia, A. Alberti, L. Giorgini, F. Magnoni and S. Tozzi, *Polym. Chem.*, 2013, **4**, 124-132.
13. R. Barbey and H.-A. Klok, *Langmuir*, 2010, **26**, 18219-18230.
14. K. A. McEwan, S. Slavin, E. Tunnah and D. M. Haddleton, *Polym. Chem.*, 2013, **4**, 2608-2614.
15. J. S. Basuki, L. Esser, H. T. T. Duong, Q. Zhang, P. Wilson, M. R. Whittaker, D. M. Haddleton, C. Boyer and T. P. Davis, *Chem. Sci.*, 2014, **5**, 715-726.
16. M. Ciampolini and N. Nardi, *Inorg. Chem.*, 1966, **5**, 41-44.
17. K. Oguchi, K. Sanui, N. Ogata, Y. Takahashi and T. Nakada, *Polym. Eng. Sci.*, 1990, **30**, 449-452.

Chapter 7

Photo-induced Sequence-control *via* One Pot Living Radical Polymerisation of Acrylates

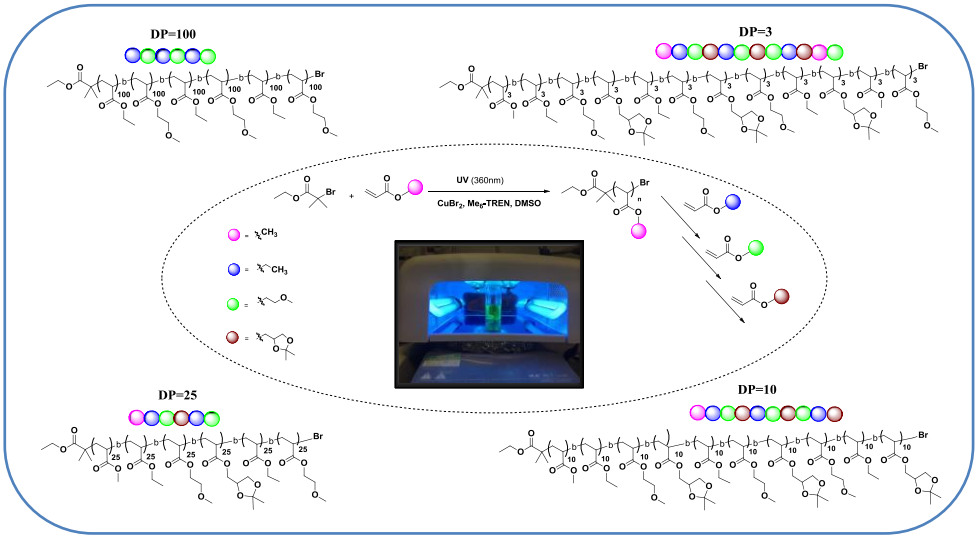

The ability to regulate the activation and deactivation steps via an external stimulus has always been a challenge in polymer chemistry. In an ideal photo-mediated system, whereby quantitative monomer conversion and optimum end-group fidelity can be maintained, precise control over the polymer composition and microstructure would be a significant breakthrough. Herein, we report for the first time, a versatile, simple and inexpensive method that allows the synthesis of sequence-controlled multiblock copolymers in a one-pot polymerisation at room temperature. In the absence of a conventional photo-redox catalyst and dye-sensitisers, low concentrations of $CuBr_2$ in synergy with Me_6-Tren can mediate acrylate block copolymerisation under UV irradiation ($\lambda_{max} \approx 360$ nm). Four different acrylate monomer units were alternated in various combinations within the polymeric sequence to mimic the 4 base pairs of DNA, illustrating the potential of the technique. Narrow dispersed undecablock copolymers were obtained ($Đ < 1.2$) with quantitative conversion achieved between the iterative monomer additions. The effect of the chain length was also investigated and higher molecular weight multiblock copolymers could also be obtained. This new approach offers a versatile and relatively cheap platform for the preparation of high-order multiblock functional materials with additional applications arising from the precise spatiotemporal "on/off" control and resolution when desired.

7.1 Introduction

A perpetual challenge in polymer science is the effective control over the molecular weight, dispersity and end-group functionality, towards the synthesis of materials with ever increasing precise control over macromolecular compositions and architectures. More recently, this improved level of control has been extended to discrete sequences or blocks within polymer molecules. The evolution of controlled living radical polymerisation (CLRP) methods including reversible addition-fragmentation chain transfer polymerisation (RAFT)[1], nitroxide-mediated radical polymerisation (NMP)[2], as well as atom transfer radical polymerisation (ATRP)[3-5] and single electron transfer living radical polymerisation (SET-LRP)[6, 7] has significantly contributed to this rapidly emerging field.

An ambitious target is developing synthetic procedures capable of replicating, or approaching, the precision over monomer sequence exhibited by natural polymers such as nucleic acids, carbohydrates, peptides and proteins. These remarkable and complicated structures are capable of storing an abundance of information and are efficiently constructed by cellular organelles such as the nucleus and ribosome. The ability to mimic these precise structures in synthetic polymers would be beneficial in many applications within nanomedicine and nanotechnology, whereby a high level of monomer sequence control confers the potential for molecular targeting, recognition and biocatalysis, as well as molecular information storage. However, as synthetic chemists we are currently still far away from the sophistication and complexity of the cell in the macromolecular 'tool kit' and as such comparable synthetic analogues have not yet been realised. Nevertheless, over the last 30-40 years notable progress has been made to harness the potential of step-growth and chain-growth polymerisation methods in order to gain synthetic control over the polymer primary sequence[8-13]. Chain-growth polymerisation has seen a number of

approaches explored, including single monomer addition[14], tandem monomer addition and modification[15, 16], kinetic control, solution and segregated templating[17].

The implementation of single monomer addition *via* radical chain-growth polymerisation techniques is challenging given the reactive nature of the radical intermediates involved. This has stimulated the development of synthetic methods focusing on controlling the sequence of multiple discrete regions within the overall macromolecular structure. Whilst this does sacrifice the ability to obtain the control attained by nature, it allows for functional domains which are often sufficient for specific applications. Whittaker and co-workers exploited the degree of control and end-group retention available from Cu(0)-mediated living radical polymerisation to report the first example of a one-pot synthesis of multiblock copolymers *via* iterative monomer addition[18-20]. Multiblock (up to decablock) copolymers containing discrete block lengths (2-10) in linear and star architectures were reported. However, a limitation of this exemplary work was recognised during the synthesis of linear decablock copolymers, whereby molecular weight distributions were found to gradually increase, indicative of the accumulation of terminated chains. The same technique was employed to synthesise a number of multiblock glycopolymers with a high degree of monomer sequence control in various compositions containing mannose, glucose, and fucose moieties in the presence and absence of spacer comonomers[21, 22]. Higher molecular weight multiblocks with narrower dispersities have also been attained[23] but the yield of the intermediate blocks was often < 95%, thus compromising the integrity of the multiblock structures (See Chapter 4).

More recently, Perrier and co-workers reported the synthesis of multi-block copolymers comprising acrylamide monomer units using an optimised RAFT approach, achieving up to an icosa-block (20 block) copolymer in both organic (dioxane) and aqueous media[24-27]. However, the high temperature (65-70 ˚C) required for the

polymerisation reaction potentially limits the possibility of simultaneous biological modifications. This has been addressed by the use of the *fac*-[Ir(ppy)$_3$] photoredox catalyst, previously employed by Hawker[28] *et al.* to induced photo-mediated ATRP of methacrylates. Boyer[29] *et al.* have reported RAFT polymerisation of activated and unactivated vinyl monomers at ambient temperature, highlighting the utility of the photoredox catalysis *via* recycling for chain extension and multiblock copolymerisation experiments.

In this chapter, the Cu-mediated photo-polymerisation of acrylates to prepare multi-block copolymers, up to a dodecablock (12 blocks), containing repeat units composed of four alternating monomer sequences whilst maintaining narrow dispersities ($Đ$ < 1.2) is reported. In the absence of a photoredox catalyst and dye-sensitisers, careful optimisation of the polymerisation conditions provides access to a range of single-block chain lengths (DP$_n$ = 3, 10, 25 and 100) all of which present narrow dispersities at high conversions (> 99%) upon iterative monomer addition without the need for rigorous degassing procedures. The monomer sequence can also be varied to illustrate the versatility of the technique, showing little ill effects in either the polymerisation rate or the final dispersity. Importantly, under UV irradiation (λ_{max} = 360 nm) in a jacketed cell, with a steady flow of cold water to maintain a constant, sub-ambient internal temperature, the polymerisation can proceed with equal efficiency, enabling a potential transition to biological applications. Finally, this photo-mediated approach confers the potential of spatiotemporal control when desired, simply by switching "on" and "off" the system upon demand.

7.2 Results and Discussion

7.2.1 Block copolymer synthesis; initial attempts

In chapters 5 and 6, it has been demonstrated that excellent end-group fidelity could be attained during the photo-mediated living radical polymerisation of acrylates in the presence of low concentrations of $CuBr_2$ and aliphatic tertiary amine ligands (Me_6-Tren)[30-32]. The remarkable degree of control obtained during both homo and block copolymerisations motivated further investigation into the scope of the system in pursuit of acrylic multiblock copolymers, with good sequential control over discrete block compositions, synthesised *via* a photo-mediated approach at ambient temperature in a one-pot process without intermediate purification steps and in the absence of potentially costly additives such as photo-redox catalysts, initiators and dye sensitisers.

Initially, the synthesis of a model decablock homopolymer poly(MA-*b*-MA-*b*-MA-*b*-MA-*b*-MA-*b*-MA-*b*-MA-*b*-MA-*b*-MA-*b*-MA) was attempted *via* sequential addition of individual aliquots of MA employing an initial feed ratio of $[I]_0 : [CuBr_2]_0 : [Me_6\text{-Tren}]_0 = [1] : [0.02] : [0.12]$ in DMSO 50% (*v/v*). Each block was designed to be $DP_n = 3$ in order to facilitate electrospray mass-spectrometry (ESI-MS) analysis and demonstrate the versatility as well as the high efficiency of this technique. Under the aforementioned conditions, the first PMA block was obtained at full conversion within 10 h with a dispersity = 1.25 (Figure 7.1, Table 7.1 entry 1).

Table 7.1: Summary of the investigation towards optimising the polymerisation [a] Final conversion by ^{1}H NMR; [b] $CHCl_3$; the following was added upon each iteration [c] MA and DMSO (2 : 1 *v/v*); [d] neat MA upon every 2nd iteration; [e] as (c) with $CuBr_2$/Me_6-Tren ([0.02] : [0.12] w.r.t. $[I]_0$) every 4th iteration; [f] as (c) with $CuBr_2$/Me_6-Tren ([0.02] : [0.12] w.r.t. $[I]_0$) every 2nd iteration; [g] as (c) with $CuBr_2$/Me_6-Tren ([0.02] : [0.12] w.r.t. $[I]_0$) every 3rd iteration.

Entry	Conditions	No of Cycles	Conversion[a] (%)	$M_{n,th}$ (g/mol)	$M_{n,SEC}$[b] (g/mol)	$Đ$
1[c]	No additional $CuBr_2$/Me_6-Tren	7	96	2800	4700	1.18
2[d]	No additional solvent upon every 2nd iteration	9	95	3400	8000	1.35
3[e]	$CuBr_2$/Me_6-Tren upon every 4th addition	8	96	2300	8400	1.09
4[f]	$CuBr_2$/Me_6-Tren upon every 2nd addition	10	90	2600	6200	1.59
5[g]	$CuBr_2$/Me_6-Tren upon every 3rd addition	11	99	4300	7000	1.19

[a]Determined by ^{1}H NMR. [b]Determined by $CHCl_3$ SEC analysis.

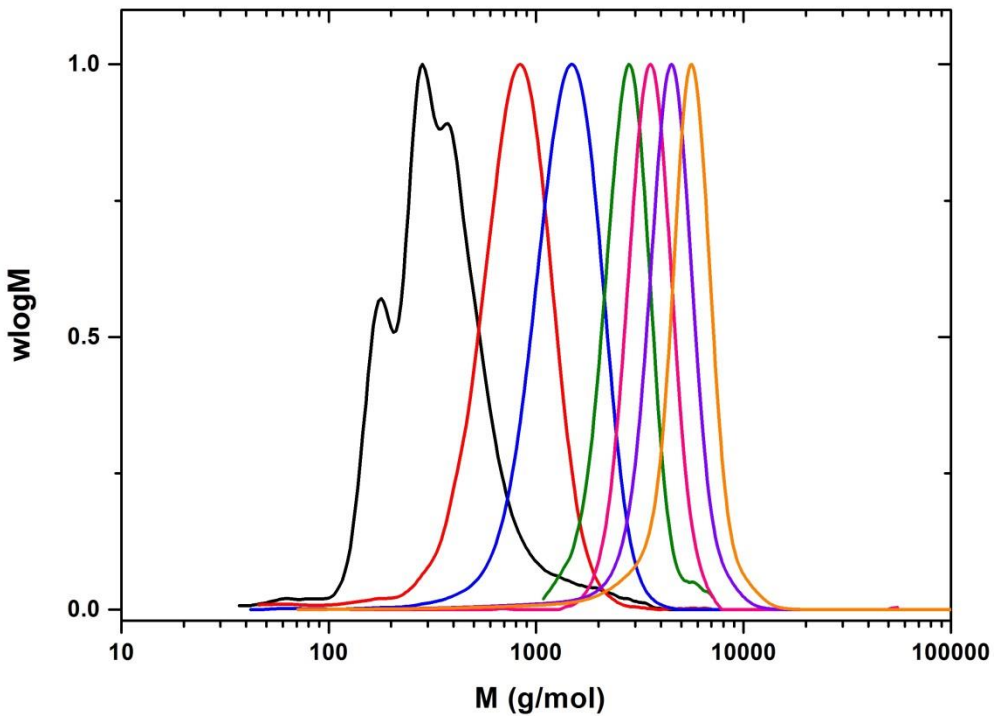

Figure 7.1: Molecular weight distributions for successive cycles during synthesis of heptablock homopolymer (DP_n=3) in DMSO and ^{1}H NMR spectra showing the monomer conversion for each cycle. *No additional $CuBr_2$/Me_6-Tren was added.*

This relatively broad dispersity was attributed to the low molecular weight of the polymer. The absence of termination events during homopolymerisation should maximise the end-group fidelity of the final polymer and facilitate efficient *in situ* chain extension. Indeed, upon addition of the second aliquot of MA in DMSO (2 : 1 *v/v*), high conversion was attained within 12 h (>99% conversion), revealing a symmetrical SEC chromatogram without any visible trace of low or high molecular weight shoulders, which would indicate potential termination events. This process was repeated several times with SEC analysis of the molecular weight distributions confirming the successful chain extensions as manifested by clear shifts to higher molecular weights after each addition (Figure 7.1). However, the time required to achieve quantitative conversion increased upon each monomer addition with the 7th block achieving 96% yield only after a total time of 48 h (Section 7.4.4, Table 7.3 and Figure 7.13) Although narrow dispersities ($Đ$ < 1.18) were maintained, following addition of an eighth aliquot of MA, little, if any, monomer consumption was observed over the course of 48 h, indicating that the rate of polymerisation had become close to zero. This is most likely due to an accumulated loss of end-group fidelity over the course of the reaction.

7.2.2 Optimisation studies; effect of varying the [MA], [$CuBr_2$] and [Me_6-Tren]

In an attempt to optimise the reaction conditions, it was speculated that an increase in the polymerisation rate could circumvent the accumulated termination enabling synthesis of higher order multiblock copolymers. Accordingly, the polymerisation concentration was increased by injecting monomer in the absence of additional solvent upon every 2nd iterative addition (Table 7.1, entry 2). Initially, a faster reaction rate was observed, accompanied by an observable increase in viscosity. Following addition of the 9th aliquot of MA, stirring was completely retarded as a result of the increase in the

solution viscosity. This translated into a loss of control, as indicated by the broader molecular weight distributions ($Đ$ > 1.3, Figure 7.2) observed by SEC. Nevertheless, very high conversions were achieved in every cycle and the preceding heptablock copolymer presented a narrow final dispersity ($Đ$ = 1.15, Section 7.4.4, Table 7.4).

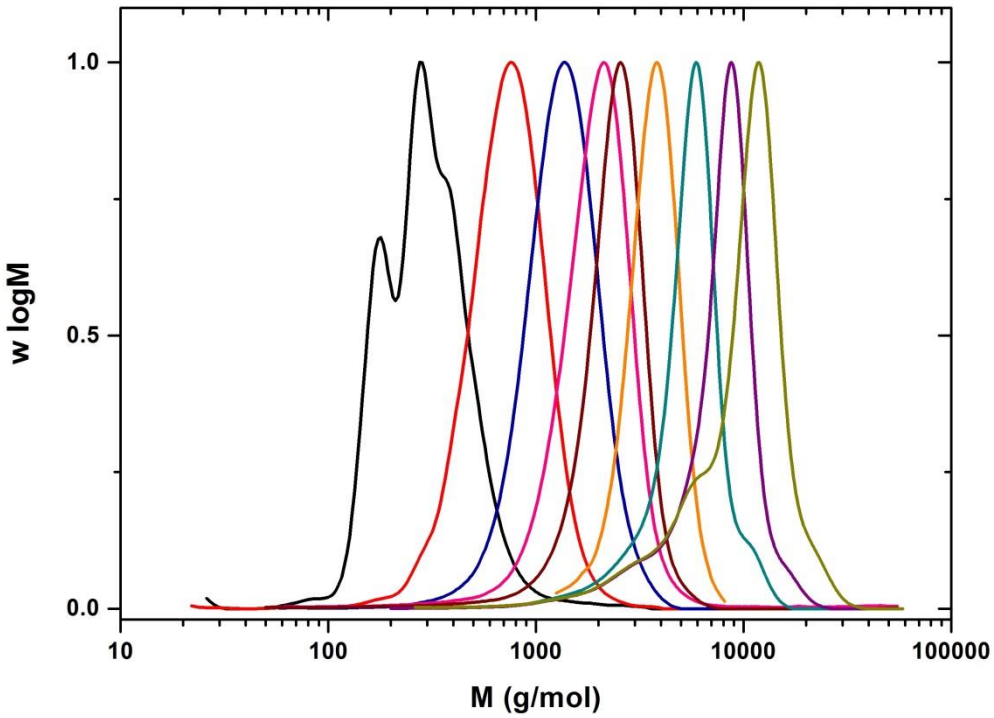

Figure 7.2: Molecular weight distributions for successive cycles during the synthesis of pseudo heptablock homopolymer (DP_n=3) obtained from UV experiment: [MA]:[EBiB]:[$CuBr_2$]:[Me_6-Tren] = [2]:[1]:[0.02]:[0.12] in DMSO. *No additional solvent was added upon every 2nd iteration.*

In an attempt to further increase the reaction rate a fresh solution of $CuBr_2$/Me_6-Tren in DMSO ([0.02] : [0.12] with respect to $[I]_0$) was fed into the polymerisation mixture, once every four monomer additions. This allowed an octablock copolymer to be obtained with narrow molecular weight distributions ($Đ$ < 1.10, Figure 7.3, Section 7.4.4, Table 7.5) at very high conversions. Further chain extension was found to be significantly slower and the polymerisation eventually stopped with no recognisable increase in molecular weight observed according to SEC.

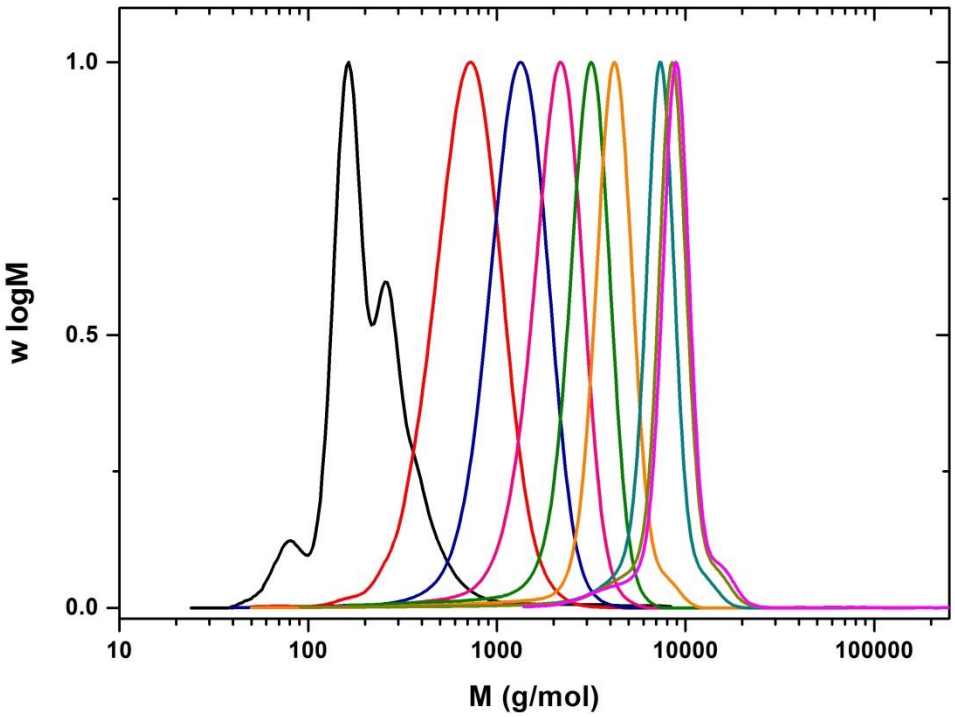

Figure 7.3: Molecular weight distributions for successive additions and ^{1}H NMR in $CDCl_3$ during the synthesis of multiblock homopolymers (DP_n=3 per block) in DMSO with MA, DMSO and *$CuBr_2$/Me_6-Tren upon every 4th iteration.*

Encouraged by these initial findings, we subsequently decided to feed the polymerisation with additional $CuBr_2$ and Me_6-Tren once every three monomer additions (Figure 7.4). High monomer conversions were attained at each iteration as confirmed by ^{1}H NMR (Figure 7.4b) and a well-defined pseudo-undecablock homopolymer was obtained with low dispersity ($Đ \leq 1.20$, Figure 7.4a). High resolution electrospray ionisation mass spectroscopy (HR-ESI-MS) analysis was employed to verify the end-group fidelity of the intermediate block homopolymers. As expected by the successful chain extensions, a gradual increase in the molecular weight was observed from block 1 to block 5 with the MALDI spectrum presenting two main polymer peak distributions (Figure 7.4c). The first polymer peak distribution corresponds to PMA initiated by initiator (EBiB) and terminated by a bromine atom. The second main peak distribution also reveals initiation from the EBiB fragment. However, this time chlorine is at the terminus of the polymer

chains as indicated by the characteristic isotopic splitting pattern (Section 7.4.4, Figure 7.14). This is attributed to halogen exchange[33] that probably occurs due to several dilutions of the samples with deuterated chloroform (^{1}H NMR analysis) or chloroform eluent (SEC analysis) prior to performing the HR-ESI-MS analysis.

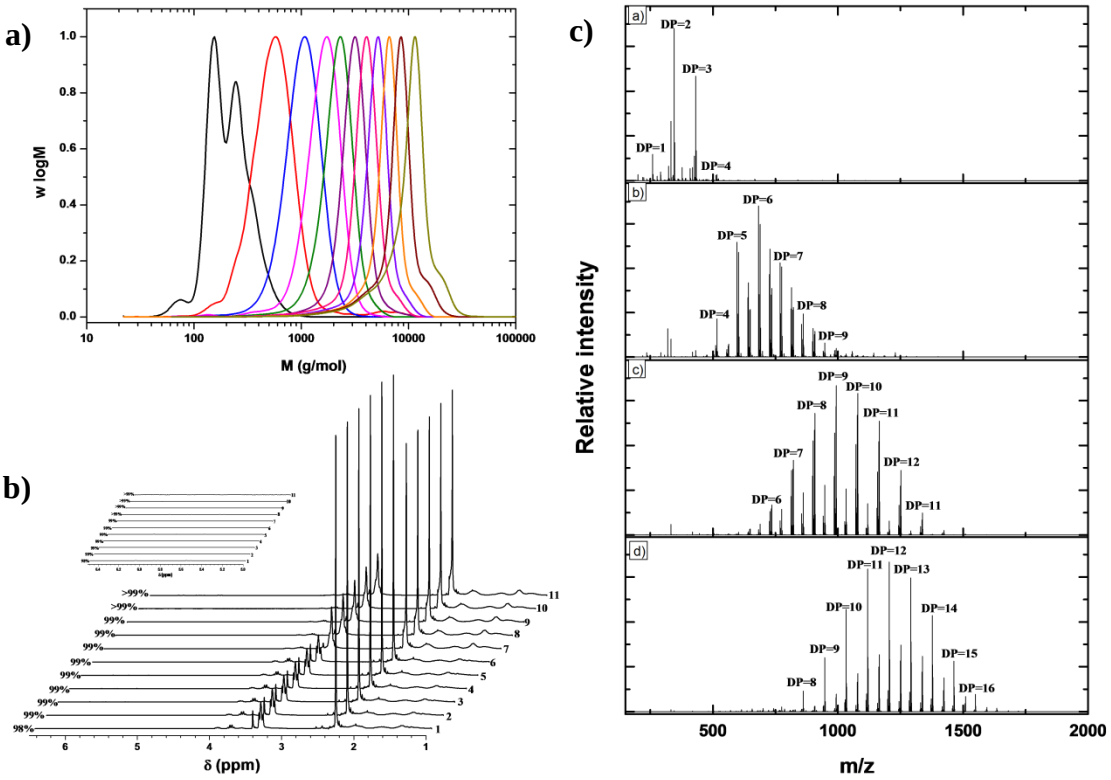

Figure 7.4: a) Molecular weight distributions by $CHCl_3$ SEC, b) ^{1}H NMR in $CDCl_3$ c) HR-ESI-MS for successive cycles during the synthesis of multiblock homopolymers (DP_n = 3 per block) in DMSO. *A fresh solution of [$CuBr_2$]:[Me_6-Tren] =[0.02]:[0.12], was added together with the monomer upon every 3rd addition.*

Further chain extensions resulted in broader molecular weight distributions. Nevertheless, a dodecablock homopolymer could be achieved with a relatively low final dispersity ($Đ$ = 1.30, Section 7.4.4, Table 7.6 and Figure 7.15).

Increasing the frequency of catalyst feed to every other monomer addition resulted in significant loss of control for the final decapolymer ($Đ$ ~ 1.6, Section 7.4.4, Table 7.7), characterised by significant low molecular weight tailing in SEC (Figure 7.5). This is in

agreement with previously reported results that indicated that even small changes in the ligand concentration can dramatically affect the end-group fidelity of the polymer chains due to chain transfer to the ligand and *via* quaternisation reactions[34]. Figure 7.6 summarises the investigation that was conducted towards optimising the polymerisation.

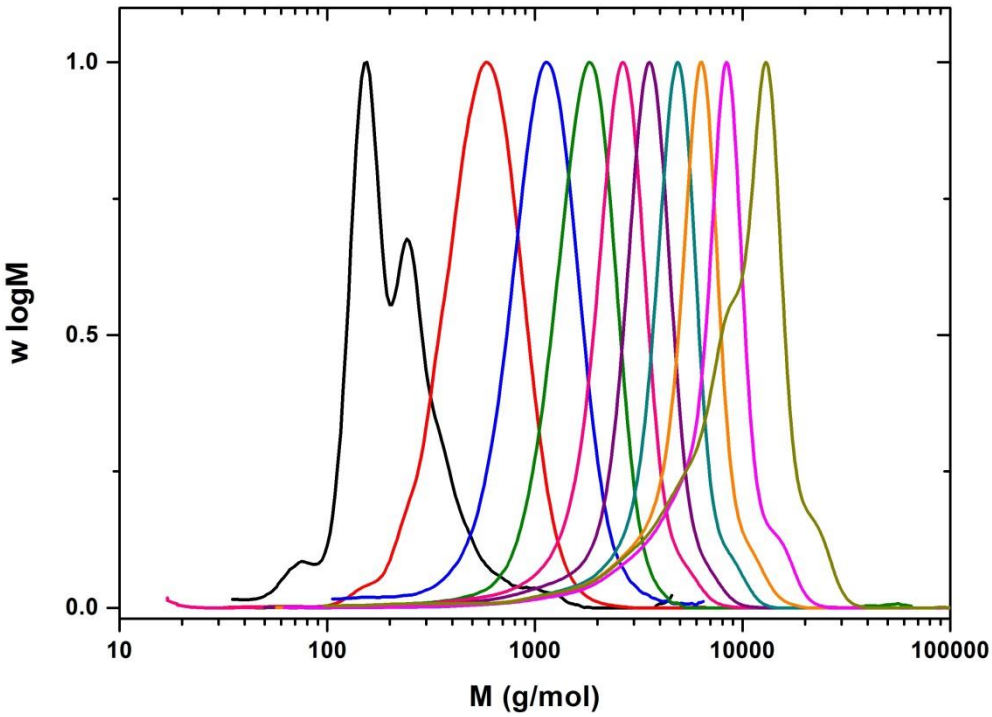

Figure 7.5: Molecular weight distributions for successive additions and ^{1}H NMR in $CDCl_3$ during the synthesis of multiblock homopolymers (DP_n=3 per block) in DMSO with *additional $CuBr_2$/Me_6-Tren upon every 2nd iteration.*

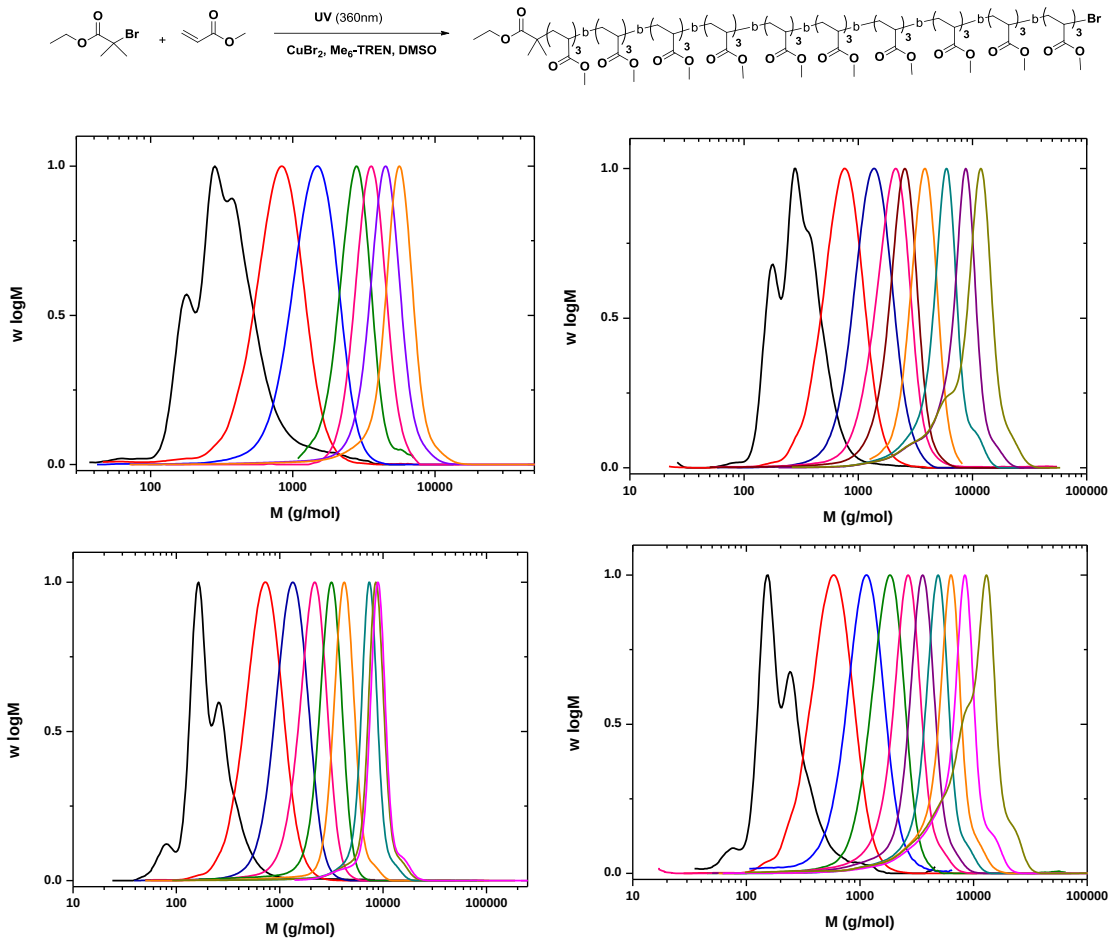

Figure 7.6: Molecular weight distributions for successive additions during the synthesis of multiblock homopolymers (DP_n = 3 per block) in DMSO with a) MA and DMSO (2 : 1 *v/v*) b) MA (neat) upon every 2nd iteration c) Additional $CuBr_2$/Me_6-Tren upon ([0.02] : [0.12] w.r.t. [I]0) every 4th monomer addition, d) Additional $CuBr_2$/Me_6-Tren ([0.02] : [0.12] w.r.t. [I]0) upon every 2nd monomer addition.

Control experiments, in which $CuBr_2$ (Figure 7.7, Section 7.4.4, Table 7.8) or Me_6-Tren (Figure 7.7, Section 7.44, Table 7.9) was added were also conducted, resulting in extremely slow polymerisation rates and significant termination events and respectively. Thus, the addition of both $CuBr_2$ and Me_6-Tren is required in order to maintain high end-group fidelity and pushing the polymerisation further. In our original publication introducing photo-mediated polymerisation in the presence of $CuBr_2$ and Me_6-Tren we proposed that the presence of free ligand was crucial for initiation and subsequent reactivation of dormant chains. These new data imply that the excess ligand, present in the initial feed ratio, is gradually consumed during the polymerisation and must be replenished to maintain activity and acceptable reaction rates.

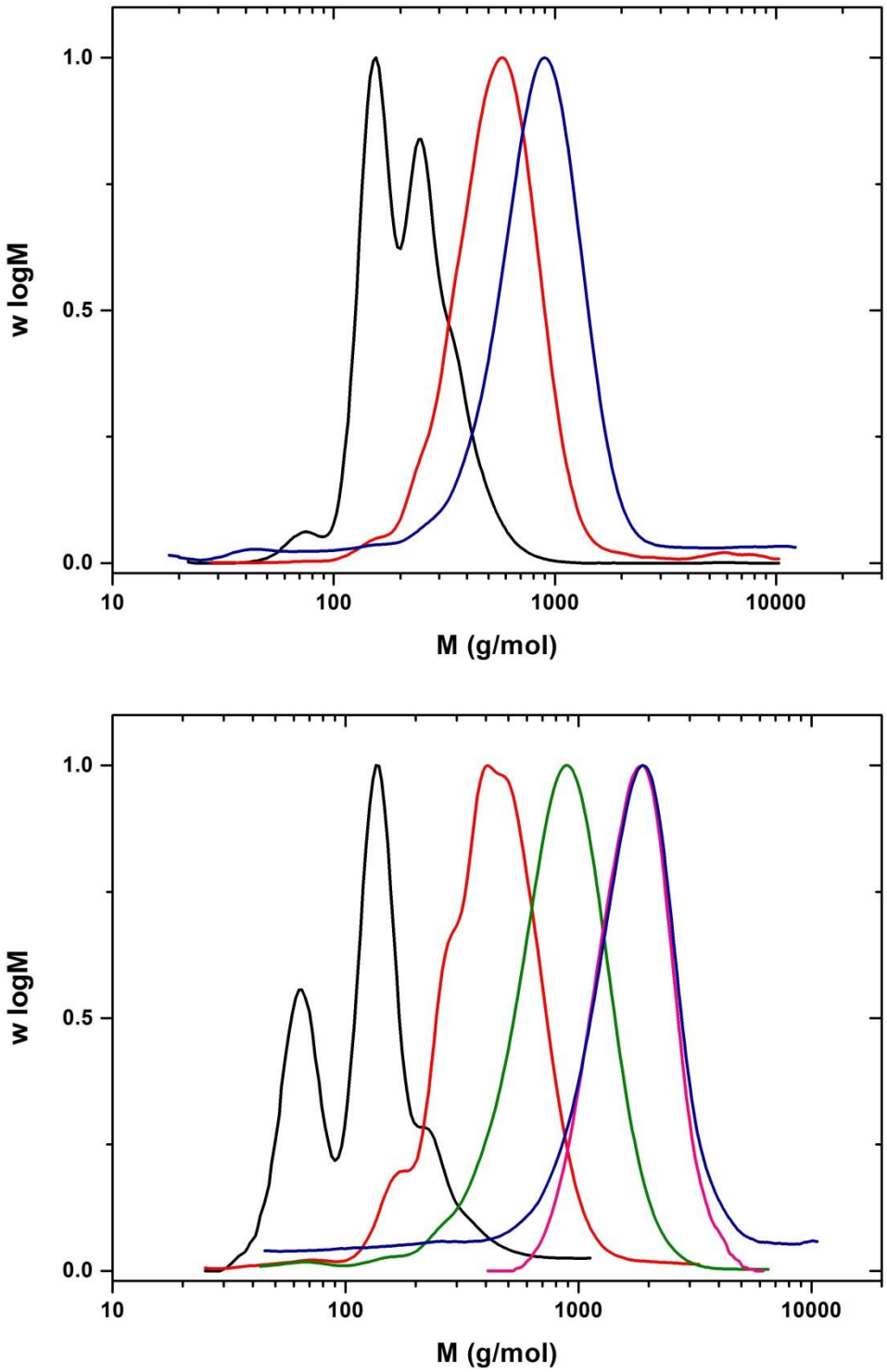

Figure 7.7: Molecular weight distributions for successive cycles during synthesis of triblock homopolymer DP_n=3 (top graph) and pentablock homopolymer DP_n=3 (bottom graph) in DMSO. A fresh solution of [$CuBr_2$] = [0.02] or [Me_6-Tren] = [0.12] in DMSO was added respectively together with the monomer *upon every 2nd addition.*

An increase in the polymerisation rate could alternatively be achieved by reducing the concentration of Cu(Me_6-Tren)Br_2 in the initial feed ratio ([Cu(Me_6-Tren)Br_2] =

[$CuBr_2$] = [0.02]). Thus, the initial feed ratio was modified to $[I]_0$: [$CuBr_2$] : [Me_6-Tren] = [1] : [0.01] : [0.12] and, considering that the best results obtained thus far were achieved by feeding additional $CuBr_2$ and Me_6-Tren upon every three iterations of monomer addition, an identical approach was adopted. Although faster polymerisation kinetics were observed (Section 7.4.4, Table 7.10), the dispersities of the polymers obtained were noticeably higher compared with those when higher amounts of copper were employed, indicating that a higher ratio of deactivator is essential for achieving optimum control over the molecular weight distributions (Figure 7.8).

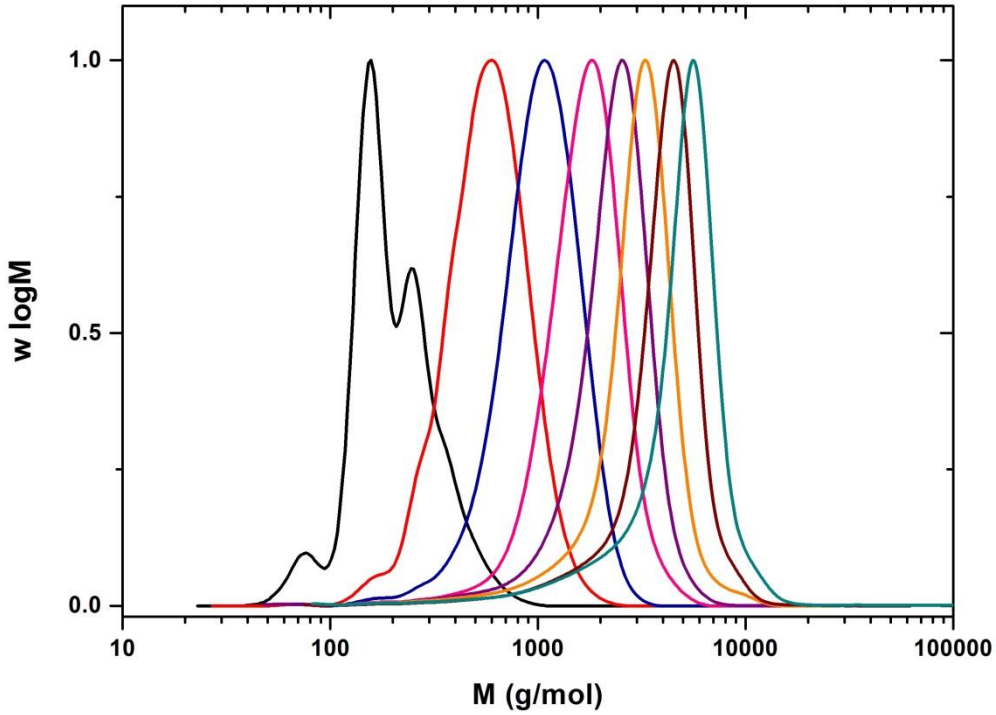

Figure 7.8: Molecular weight distributions and ^{1}H NMR in $CDCl_3$ for successive cycles during synthesis of octablock homopolymer DP_n=3 in DMSO. *A fresh solution of [$CuBr_2$]:[Me_6-Tren] =[0.01]:[0.12], was added together with the monomer upon every 3rd addition.*

7.2.3 Sequence-controlled multiblock copolymers

Having optimised the reaction conditions using methyl acrylate (MA), we were interested in applying them to construct more complex multiblock compositions. Thus, a family of 4 monomers was employed including alkyl acrylates; MA and ethyl acrylate

(EA), a short PEG containing acrylate; ethylene glycol methyl ether acrylate (EGA) and a protected functional monomer; solketal acrylate (SA). An initial feed ratio of $[M]_0$: $[I]_0$: $[CuBr_2]_0$: $[Me_6\text{-Tren}]_0$ = [3] : [1] : [0.02] : [0.12] was employed with iterative additions (DP_n = 3) consisting of [M]/[DMSO] = 2 : 1 *v/v* with an additional feed of $[CuBr_2]$: $[Me_6\text{-Tren}]$ = [0.02] : [0.12], with respect to $[I]_0$, every three iterations. Despite the inclusion of different monomers, the final dispersity of the multiblock copolymer was not compromised, presenting extremely narrow molecular weight distributions for an undecablock copolymer ($Đ$ < 1.20, Figure 7.9, Section 7.4.4 Table 7.11), combined with near-quantitative conversions during each iterative monomer addition (Figure 7.10).

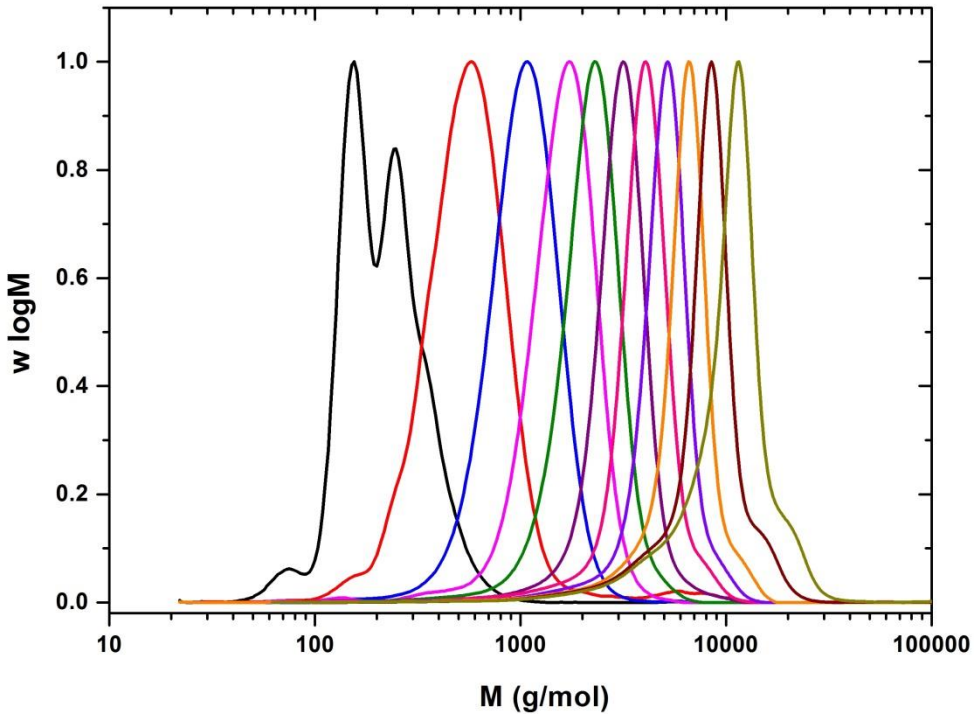

Figure 7.9: Molecular weight distributions for successive cycles during synthesis of undecablock copolymer DP_n=3 in DMSO. *A fresh solution of $[CuBr_2]$:$[Me_6\text{-Tren}]$ =[0.02]:[0.12], was added together with the monomer upon every 3rd addition.*

Sequence control was achieved by alternating the order of monomer addition during the polymerisation reaction. Pleasingly, each of the acrylate monomers was found to support propagation, enabling the desired manipulation of the monomer sequence to

yield a well-defined multiblock copolymer poly(MA_3-*b*-EA_3-*b*-EGA_3-*b*-SA_3-*b*-MA_3-*b*-EGA_3-*b*-EA_3-*b*-SA_3-*b*-EA_3-*b*-MA_3-*b*-SA_3).

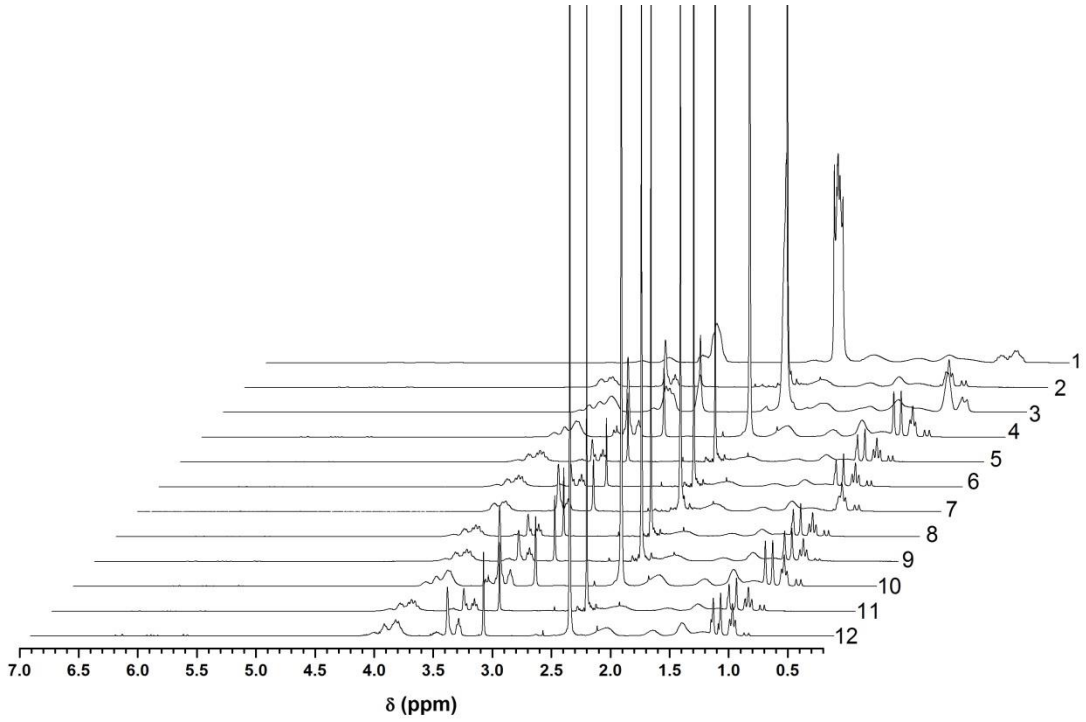

Figure 7.10: ^{1}H NMR spectra showing the monomer conversion for each cycle during synthesis of the dodecablock multiblock copolymer (DP_n=3) obtained from UV experiment: [MA]:[EBiB]:[$CuBr_2$]:[Me_6-Tren] = [2]:[1]:[0.02]:[0.12] in DMSO. *A fresh solution of [$CuBr_2$]:[Me_6-Tren] =[0.02]:[0.12], was added together with the monomer upon every 3rd addition.*

Attempts to extend the sequence beyond the undecablock resulted in an increase in dispersity (*Đ* = 1.39, Figure 7.11 and Section 7.4.4, Table 7.11). Nevertheless, this represents an excellent example of sequence design within a multiblock copolymer composition, illustrating the robustness of the system and hinting at the potential for mass information storage in the guise of functional monomer side chains.

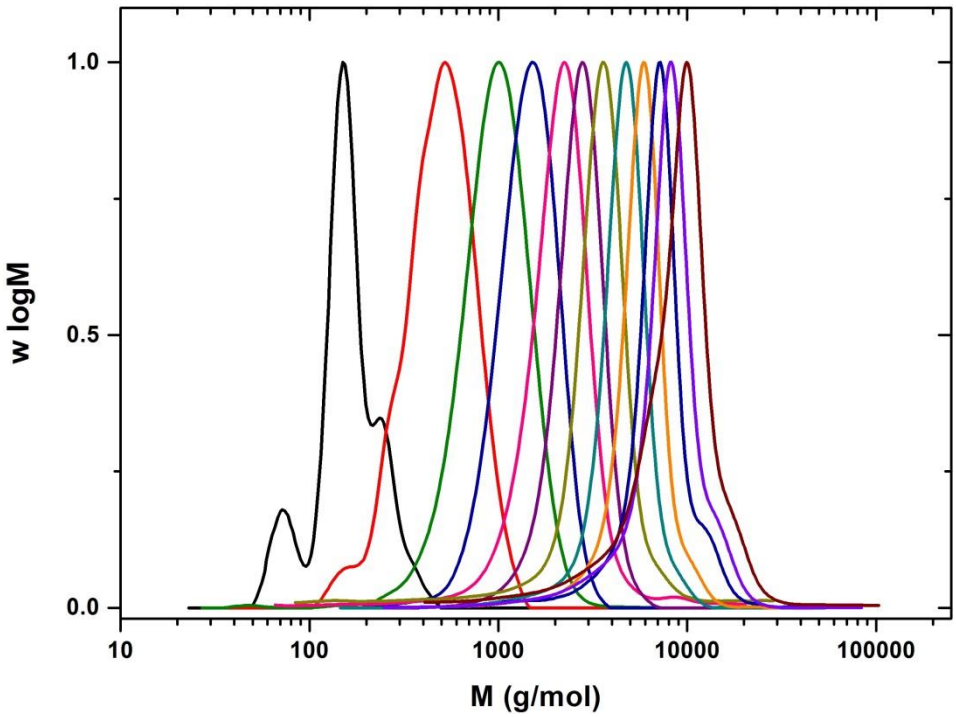

Figure 7.11: Molecular weight distributions for successive cycles during synthesis of dodecablock copolymer DP_n=3 in DMSO. *A fresh solution of [$CuBr_2$]:[Me_6-Tren] =[0.02]:[0.12], was added together with the monomer upon every 3rd addition.*

7.2.4 Increasing block chain length; higher molecular weight multiblock copolymers

We were interested to see if this photo-mediated process could support the multiblock copolymerisation of higher molecular weight block lengths. Thus, a multiblock copolymer composed of 10 repeat units per block was attempted. Under the previously optimised polymerisation conditions ($[I]_0$: $[CuBr_2]_0$: $[Me_6\text{-Tren}]_0$ = [1] : [0.02] : [0.12]), including an additional $CuBr_2$/Me_6-Tren feed every three iterations, a well-defined heptablock copolymer with a target block length of DP_n = 10 was attained with a narrow final dispersity ($Đ$ ~ 1.15, Figure 7.12 and Section 7.4.4, Table 7.12).

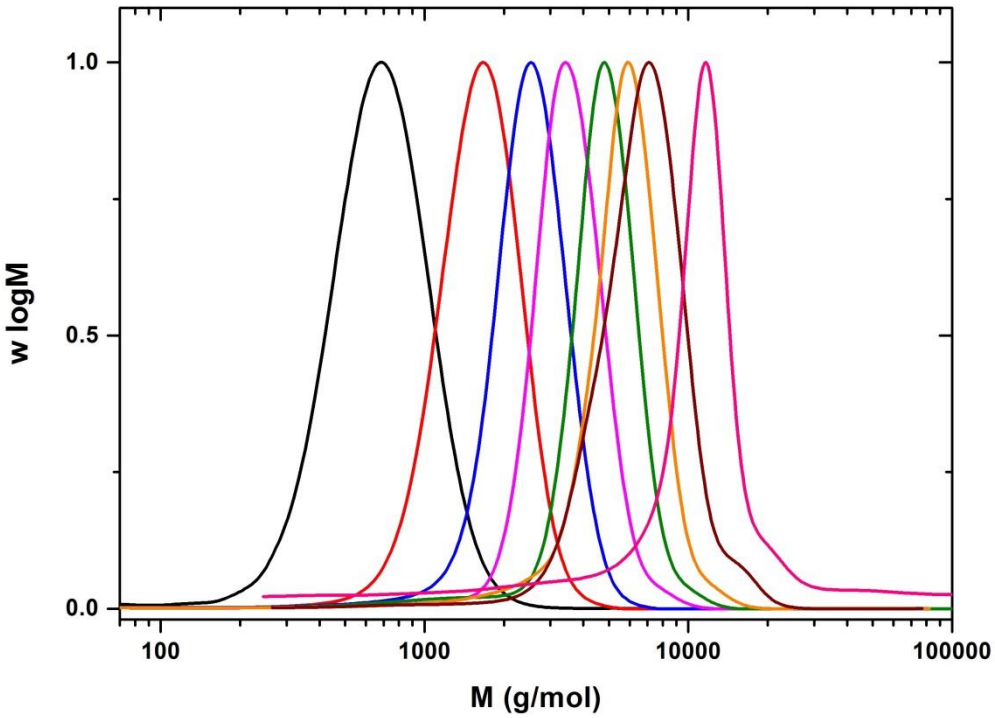

Figure 7.12: Molecular weight distributions for successive cycles during synthesis of octablock copolymer DP_n=10 in DMSO at ambient temperature**.** *A fresh solution of [$CuBr_2$]:[Me_6-Tren] =[0.02]:[0.12], was added together with the monomer upon every 3rd addition.*

Increasing the frequency of the $CuBr_2$/Me_6-Tren feed to every 2nd monomer addition, resulted in an improvement in the control leading to the heptablock copolymer (*Đ* = 1.11, Figure 7.13). Consequently, an additional chain extension was possible, furnishing an octablock copolymer with final dispersity = 1.10 (Figure 7.13 and Section 7.4.4, Table 7.13). Further attempts to reduce the dispersities or extend the 'livingness' of the system beyond an octablock were unsuccessful. Increasing the catalyst feed frequency to every addition (Figure 7.14 and Section 7.44, Table 7.14) and reducing the [$CuBr_2$] feed concentration (Figure 7.15 and Section 7.4.4, Table 7.15) resulted in significantly higher dispersities (*Đ* > 1.3) in the latter stages of the polymerisations.

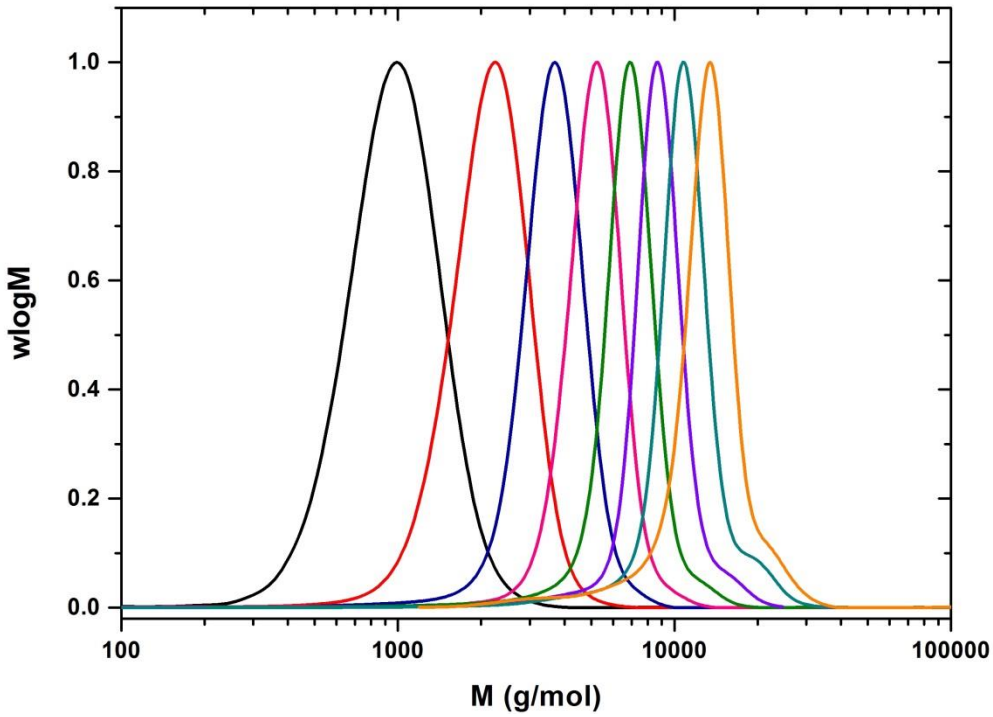

Figure 7.13: Molecular weight distributions for successive cycles during synthesis of octablock copolymer DP_n=10 in DMSO**.** *A fresh solution of [$CuBr_2$]:[Me_6-Tren] =[0.02]:[0.12], was added together with the monomer upon every 2nd addition.*

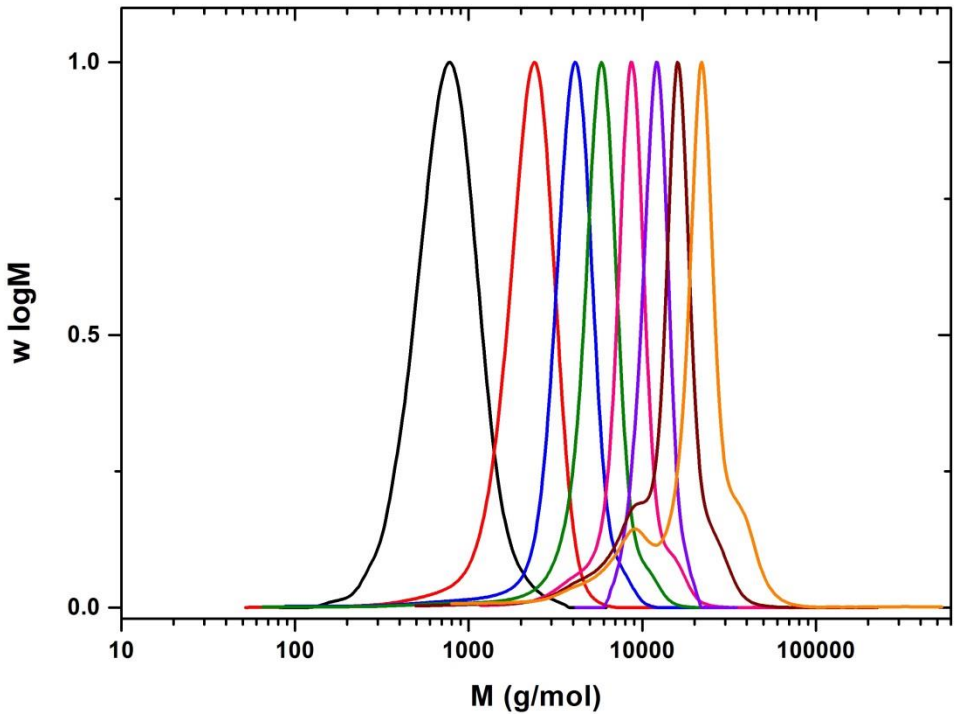

Figure 7.14: Molecular weight distributions for successive cycles during synthesis of octablock copolymer DP_n=10 in DMSO at ambient temperature**.** *A fresh solution of [$CuBr_2$]:[Me_6-Tren] =[0.02]:[0.12], was added together with the monomer upon every addition.*

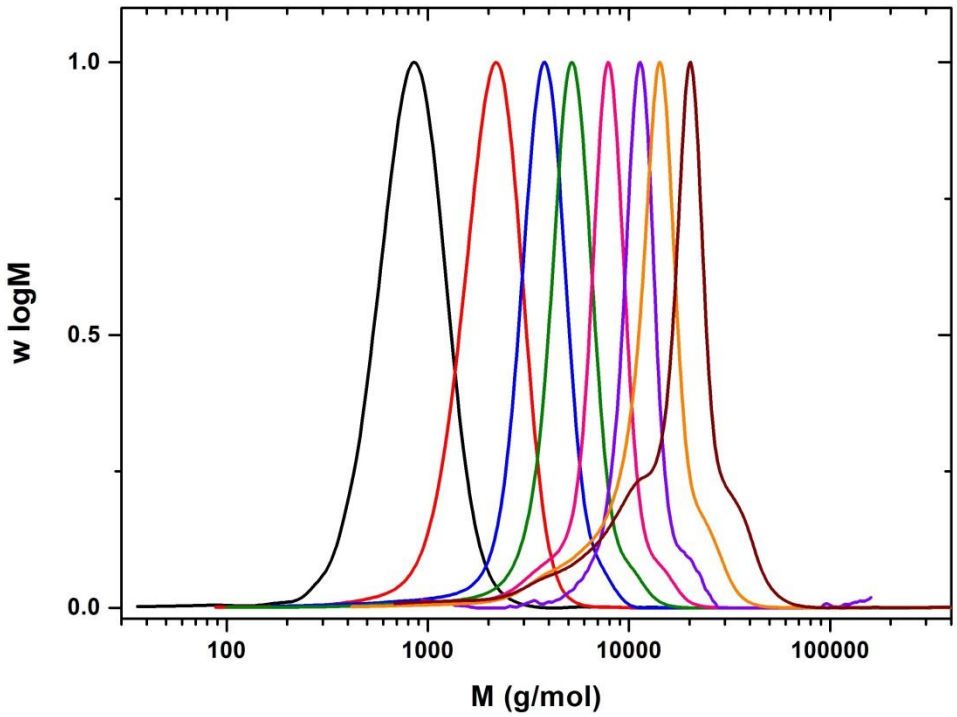

Figure 7.15: Molecular weight distributions for successive cycles during synthesis of octablock copolymer DP_n=10 in DMSO at ambient temperature *A fresh solution of [$CuBr_2$]:[Me_6-Tren] =[0.01]:[0.12], was added together with the monomer upon every addition.*

Higher molecular weight multiblock copolymers are of interest due to the potential applications that arise from the combination of monomers with different physicochemical properties, confined within block sequences. These systems can undergo self-assembly and phase separation on the micrometer and nanometer scale, forming higher-ordered structures[35-37]. Thus, we were inspired to investigate the potential for higher molecular weight multiblock copolymer synthesis under photo-mediated conditions. When each block was composed of 25 repeat units (DP_n = 25), an initial feed ratio of $[M]_0$: $[I]_0$: $[CuBr_2]_0$: $[Me_6\text{-Tren}]_0$ = [25] : [1] : [0.02] : [012] with additional $CuBr_2$ and Me_6-Tren fed into the polymerisation every other iteration furnished a hexablock copolymer with low dispersity ($Đ$ = 1.15) and high conversions (>97%) maintained throughout (Figure 7.16 and Section 7.4.4, Table 7.16).

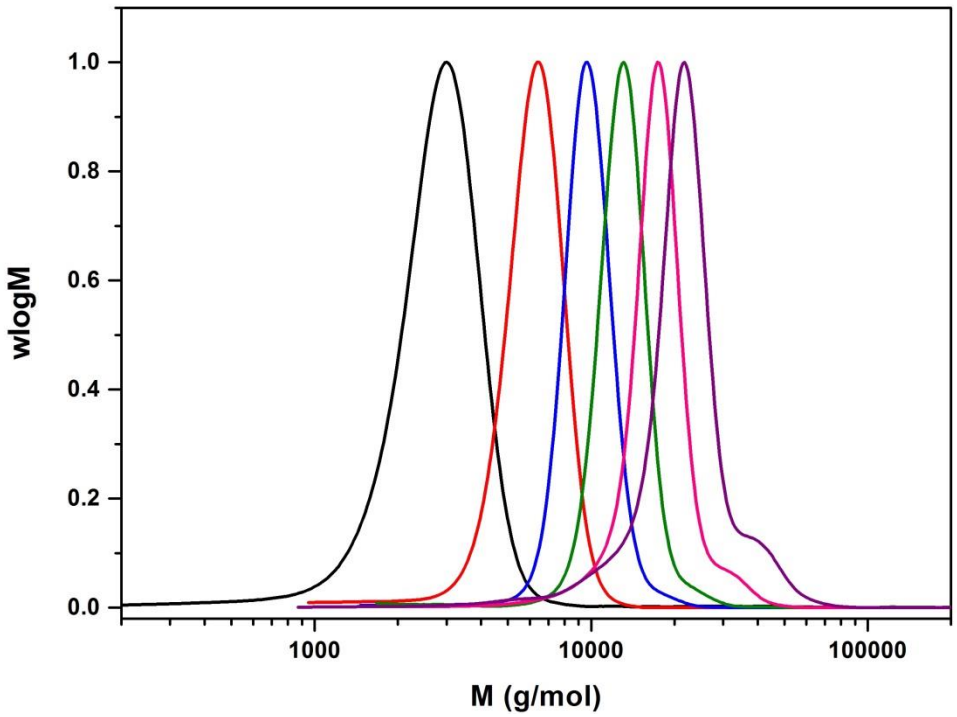

Figure 7.16: Molecular weight distributions for successive cycles during synthesis of hexablock copolymer DP_n=25 in DMSO. *A fresh solution of [$CuBr_2$]:[Me_6-Tren] =[0.02]:[0.12], was added together with the monomer upon every 2nd addition.*

Identical conditions were subsequently applied for a multiblock copolymerisation with block chain lengths of DP_n = 100 ($[M]_0$: $[I]_0$: $[CuBr_2]_0$: $[Me_6\text{-Tren}]_0$ = [100] : [1] : [0.02] : [012]). Initial homopolymerisation of MA presented a low dispersity and high conversion (97 %, $Đ$ = 1.05). Four subsequent additions of monomer again resulted in high conversions (> 97%), presenting a relatively low final dispersity ($Đ$ = 1.21, Figure 7.17) of the corresponding pentablock. However, upon addition of a 6th and final aliquot of monomer, conversion was limited 84% conversion and an increase in dispersity was observed ($Đ$ = 1.33, Figure 7.17 and Section 7.4.4, Table 7.17). Nevertheless, a well-controlled hexablock copolymer was attained with a relatively narrow final dispersity and molecular weight of ≈ 100 kDa. The optimum polymerisation data for the multiblock copolymers are presented and summarised in Figure 7.18 and Table 7.2.

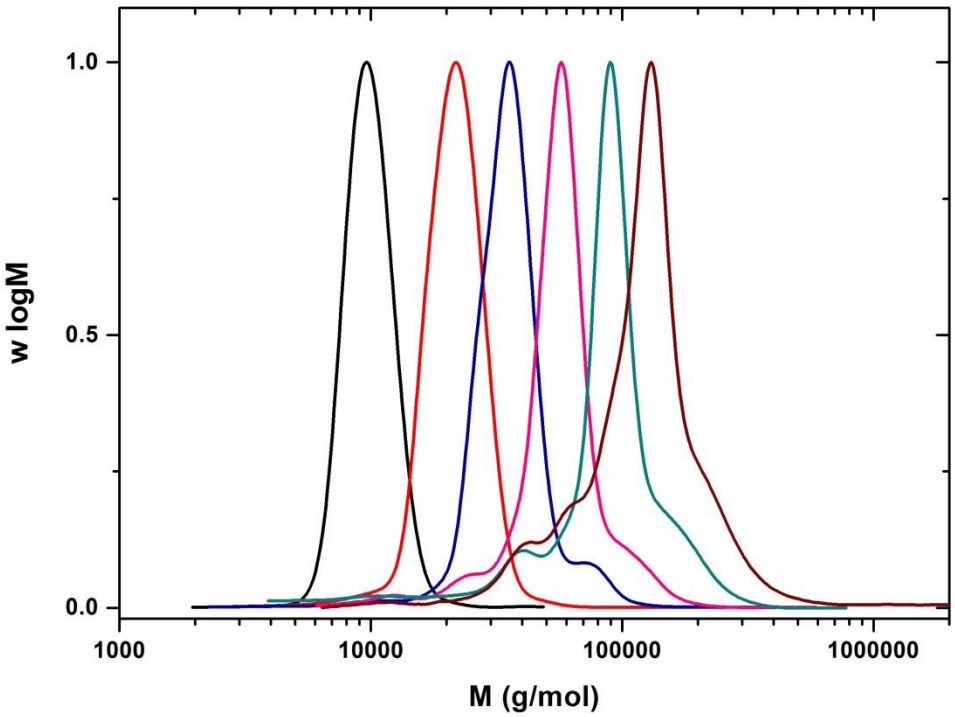

Figure 7.17: Molecular weight distributions for successive cycles during synthesis of hexablock copolymer DP_n=25 in DMSO. *A fresh solution of [$CuBr_2$]:[Me_6-Tren] =[0.02]:[0.12], was added together with the monomer upon every 2nd addition.*

Table 7.2: Summary of the multiblock copolymers synthesised in this study.

Multiblock copolymer	Conversion (%)	$M_{n,th}$ (g.mol^{-1})	$M_{n,SEC}$ (g.mol^{-1})	$Đ$
DP_n = 3 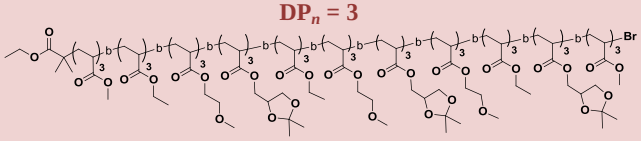	99	4500	7000	1.19
DP_n = 10 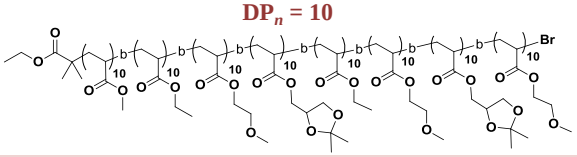	99	11200	12400	1.10
DP_n = 25 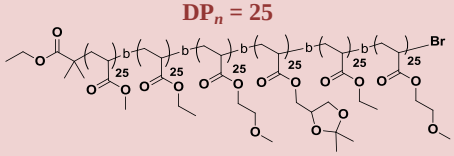	99	18200	19900	1.15
DP_n = 100 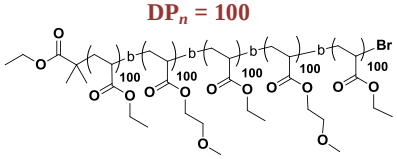	98	56200	80000	1.21

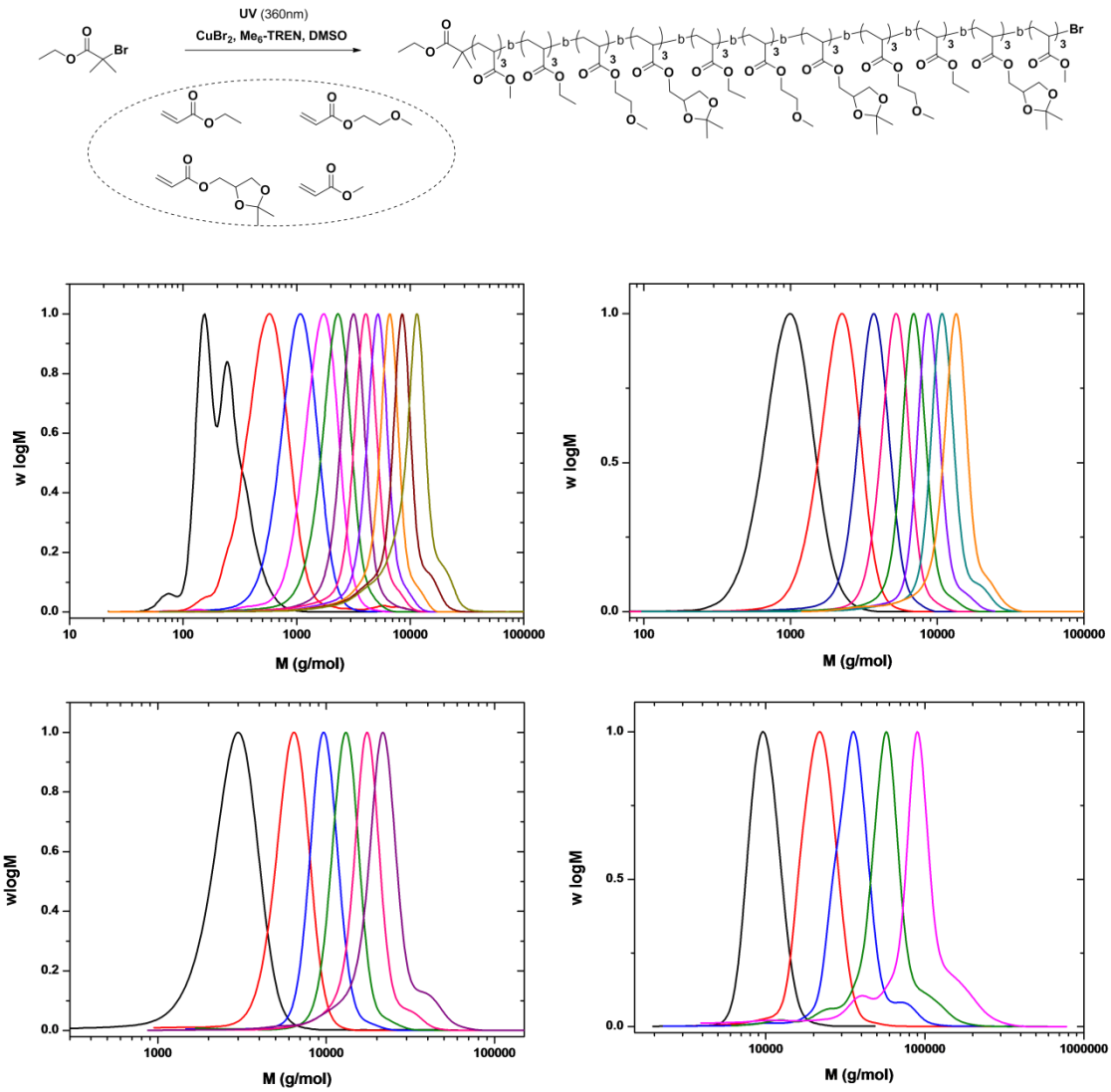

Figure 7.18: Molecular weight distributions for successive cycles during the synthesis of a) an undecablock copolymer (DP_n = 3 per block); b) an octablock copolymer (DP_n = 10 per block); c) a hexablock block copolymer (DP_n = 25 per block); d) a pentablock copolymer (DP_n = 100 per block) in DMSO. Monomers A,B,C,D were alternated during the synthesis.

Considering the radical nature of the polymerisation, termination, either due to radical coupling events or adventitious side reactions, occurs at each iteration and has a deleterious effect on the end-group fidelity of polymer chains. This is best illustrated by plotting the evolution of molecular weight with each addition of monomer (Figure 7.19-7.22). Ideally the M_n should increase linearly with little deviation from $M_{n,th}$ which is indeed the case with DP_n = 10/25 sequential monomer feeds (Figure 7.19-7.20). The high

degree of end-group retention is confirmed by close agreement between $M_{n,th}$ and $M_{n,SEC}$ for the final polymers (Table 7.2).

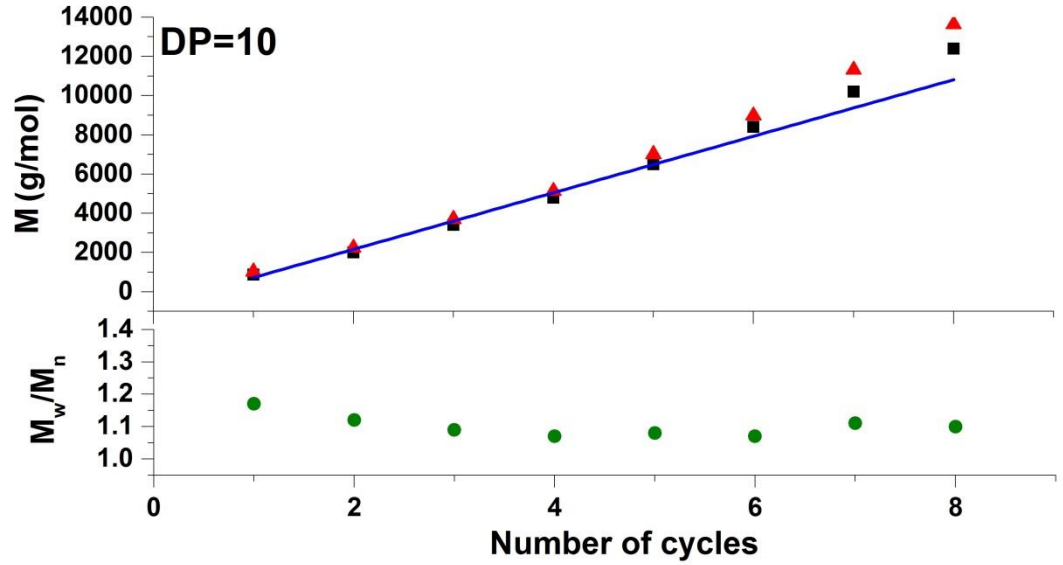

Figure 7.19: Evolution of theoretical (blue straight line) and experimental molecular weight M_n (■) and M_w (▲) determined by SEC and M_w/M_n (●) versus the number of cycles during synthesis of octablock copolymer DP_n=10 in DMSO at ambient temperature. A fresh solution of [$CuBr_2$]:[Me_6-Tren] =[0.02]:[0.12], was added together with the monomer upon every 2nd addition.

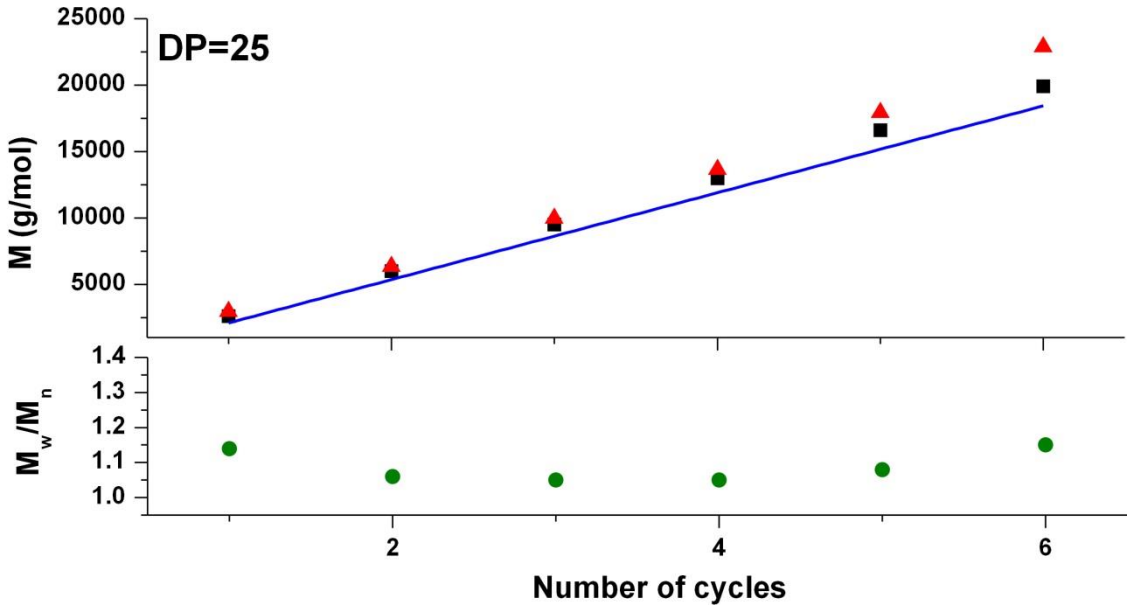

Figure 7.20: Evolution of theoretical (blue straight line) and experimental molecular weight M_n (■) and M_w (▲) determined by SEC and M_w/M_n (●) versus the number of cycles during synthesis of hexablock copolymer DP_n=25 in DMSO at ambient temperature. A fresh solution of [$CuBr_2$]:[Me_6-Tren] =[0.02]:[0.12], was added together with the monomer upon every 2nd addition.

The deviation in final molecular weight data observed at higher and lower DP_n monomer feeds can be better understood with examination of the related evolution of molecular weight. At lower DP_n (DP_n = 3, Figure 7.21), good agreement between $M_{n,th}$ and $M_{n,SEC}$ is maintained up to a heptablock copolymer, comparable to the data obtained for DP_n = 10/25. Deviations in the molecular weight data are shown to occur after this point, probably as a consequence of increased reaction times, resulting in increased termination and adventitious side reactions. Conversely, when targeting DP_n = 100, deviations from linearity are evident after only two chain extension events (Figure 7.22). Loss of end-group fidelity in this case has a much more drastic effect on M_n considering that there are fewer chains from the outset, and a relatively high concentration of monomer is added with each iteration. The sensitivity of the higher molecular weight system is accentuated in blocks 4, 5 and 6 (Figure 7.22) and translates to a significant deviation in $M_{n,th}$ and $M_{n,SEC}$ of the final polymer (Table 7.2).

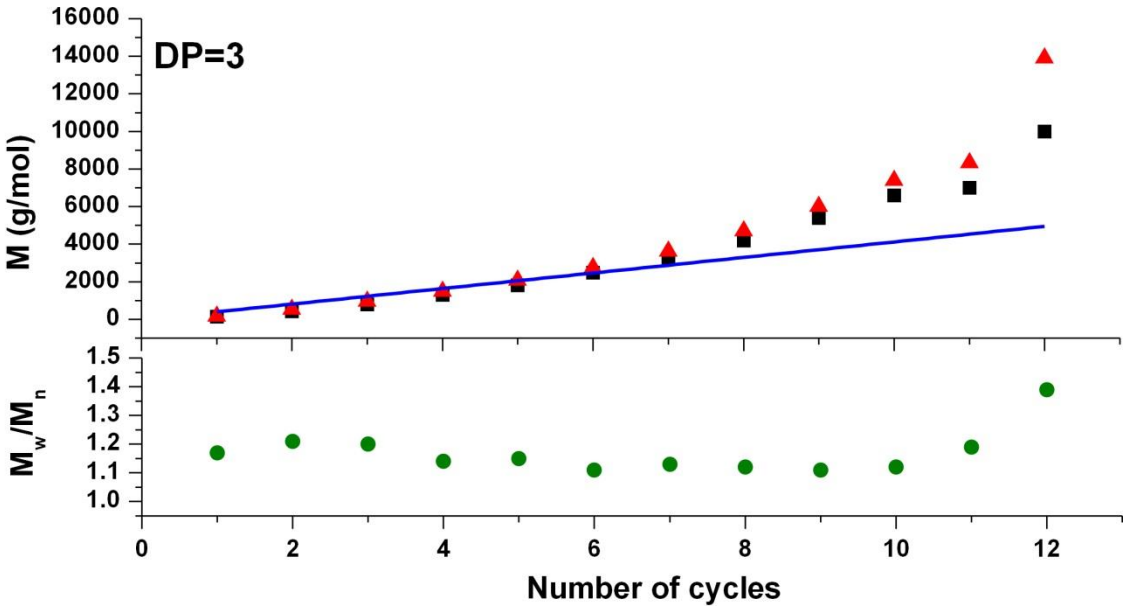

Figure 7.21: Evolution of theoretical (blue straight line) and experimental molecular weight M_n (■) and M_w (▲) determined by SEC and M_w/M_n (●) versus the number of cycles during synthesis of dodecablock homopolymer DP_n=3 in DMSO at ambient temperature. A fresh solution of [$CuBr_2$]:[Me_6-Tren] =[0.02]:[0.12], was added together with the monomer upon every 3rd addition.

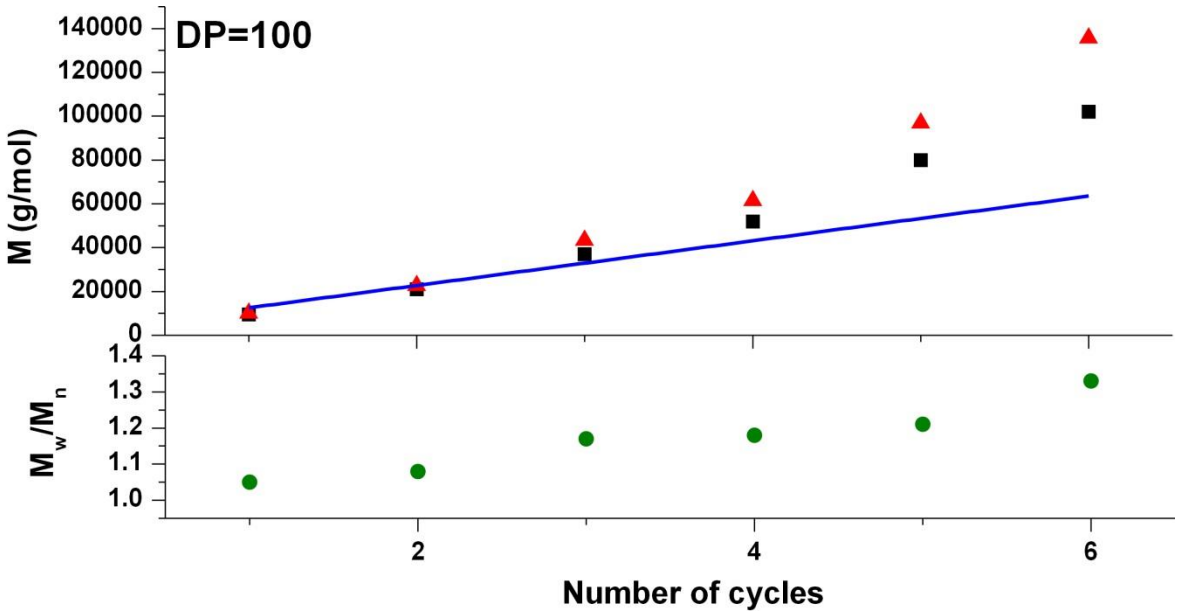

Figure 7.22: Evolution of theoretical (blue straight line) and experimental molecular weight M_n (■) and M_w (▲) determined by SEC and M_w/M_n (●) versus the number of cycles during synthesis of hexablock copolymer DP_n=100 in DMSO at ambient temperature. A fresh solution of [$CuBr_2$]:[Me_6-Tren] =[0.02]:[0.12], was added together with the monomer upon every 2nd addition.

Nevertheless, such high molecular weight multiblock copolymers have not yet been reported in the literature and we believe that our approach paves the way for the design and synthesis of a new class of functional polymeric materials.

7.3 Conclusion

In summary, this chapter reports the synthesis of high-order acrylic multiblock copolymers composing of four different repeat units which have been alternated in various combinations in order to illustrate the versatility and the robustness of the technique. High conversions (>97%) were obtained throughout the polymerisations while the possibility to perform the reactions at ambient temperature expands the scope of the multiblock copolymers to include biological applications, where milder reaction conditions are frequently required. Narrow dispersity multiblock copolymers were obtained (typically $Đ$ < 1.20) while the effect of the chain length was also investigated. Under carefully optimised conditions higher molecular weight copolymers could also be obtained ($M_{n,SEC} \approx$

100 kDa). Importantly, this approach utilises an inexpensive catalyst ($CuBr_2$) in low concentration in conjunction with tertiary amines and can be carried out under very low intensity/power light. The amines are consumed by a photo-reduction in the polymerisation requiring replenishing through a feed process to maintain the polymerisation rates. The end-group fidelity and very low rates of termination are quite remarkable and allow for multi-block polymers where the DP_n of each block can be quite low or quite high resulting in a very versatile polymerisation process.

7.4 Experimental

7.4.1 Materials

All materials were purchased from Sigma Aldrich or Fisher Scientific unless otherwise stated. Copper (II) bromide ($CuBr_2$) and ethyl 2-bromoisobutyrate (EBiB) were used as received. All monomers were passed through a basic Al_2O_3 chromatography column prior to use. Tris-(2-(dimethylamino)ethyl)amine (Me_6-Tren) was synthesised according to previously reported literature. Solketal acrylate was synthesised according to a reported procedure and distilled under reduced pressure (45°C, 10^{-1} mbar) to yield a colourless liquid.

7.4.2 Apparatus

1H NMR spectra were recorded on Bruker DPX-250 or DPX-300 spectrometers using deuterated chloroform ($CDCl_3$) obtained from Aldrich. Chemical shifts are given in ppm downfield from the internal standard tetramethylsilane. Size exclusion chromatography (SEC) measurements were conducted using an Agilent 1260 SEC-MDS fitted with differential refractive index (DRI), light scattering (LS) and viscometry (VS) detectors equipped with 2 × PLgel 5 mm mixed-D columns (300 × 7.5 mm), 1 × PLgel 5 mm guard column (50 × 7.5 mm) and autosampler. Narrow linear poly(methyl

methacrylate) standards in range of 200 to 1.0×10^6 g·mol^{-1} were used to calibrate the system. All samples were passed through a 0.45 μm PTFE filter before analysis. The mobile phase was chloroform with 2% triethylamine eluent at a flow rate of 1.0 mL/min. SEC data was analysed using Cirrus v3.3 software with calibration curves produced using Varian Polymer laboratories Easi-Vials linear poly(methyl methacrylate) standards (200-4.7×10^5 g/mol). ESI-ToF spectra were recorded on Bruker MicroTOF .Samples were loaded by direct infusion at a flow rate of 240 μL/hr in MeOH:H_2O. The source of UV light was a UV nail gel curing lamp (available online from a range of suppliers) (λ_{max} ~ 360 nm) equipped with four 9W bulbs.

7.4.3 General procedures

Filtered monomer (DP_n eq), EBiB (1 eq), $CuBr_2$ (0.02 eq), Me_6-Tren (0.12 eq) and DMSO (2 mL) were added to a septum-sealed vial and degassed by purging with nitrogen for 15 min. Polymerisation commenced upon addition of the degassed reaction mixture to the UV lamp. Samples were taken periodically and conversions were measured using ^{1}H NMR and SEC analysis.

For the iterative chain extensions, an aliquot of a degassed monomer (DP_n eq), in DMSO (50% v/v) was added via a nitrogen-purged syringe and again the solution was allowed to polymerise in the lamp. When required (according to guidelines within the chapter), a fresh solution of $CuBr_2$ (0.02 eq), Me_6-Tren (0.12 eq) in DMSO was fed together with the monomer *via* a nitrogen-purged syringe. The above polymerisation extension protocol was repeated as required.

7.4.4 Characterisation

Scheme 7.1: Synthesis of **multiblock homopolymers or copolymers DP$_n$=3** by sequential addition of monomers without intermediate purification.

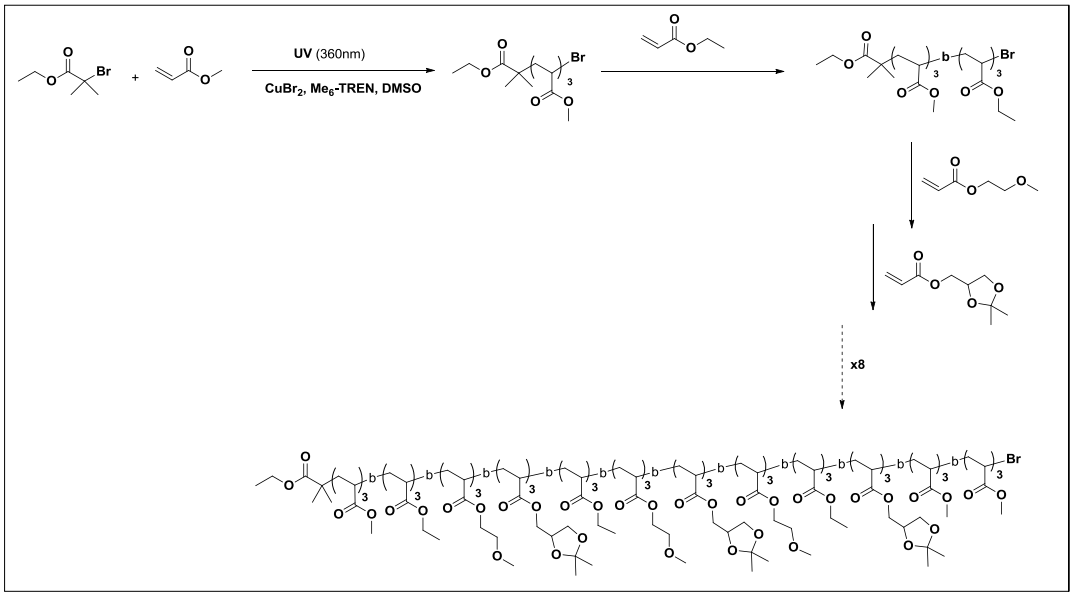

Table 7.3: Characterisation data for the synthesis of the pseudo heptablock homopolymer (DP$_n$=3) obtained from UV experiment: [MA]:[EBiB]:[CuBr$_2$]:[Me$_6$-Tren] = [2]:[1]:[0.02]:[0.12] in DMSO. *No additional CuBr$_2$/Me$_6$-Tren were added.*

Cycle	Multiblock homopolymer composition	Time (h)	Monomer conversion[a] (%)	$M_{n,th}$ [g mol^{-1}]	$M_{n,SEC}$ [b] [g mol^{-1}]	$Đ$
1	Poly(MA$_3$)	12	99	450	300	1.39
2	Poly(MA$_3$-MA$_3$)	12	100	710	700	1.19
3	Poly(MA$_3$-MA$_3$-MA$_3$)	12	100	970	1300	1.17
4	Poly(MA$_3$-MA$_3$-MA$_3$-MA$_3$)	15	98	1230	2600	1.09
5	Poly(MA$_3$-MA$_3$-MA$_3$-MA$_3$-MA$_3$)	18	100	1500	3400	1.07
6	Poly(MA$_3$-MA$_3$-MA$_3$-MA$_3$-MA$_3$-MA$_3$)	26	99	1750	4000	1.10
7	Poly(MA$_3$-MA$_3$-MA$_3$-MA$_3$-MA$_3$ -MA$_3$-MA$_3$)	48	96	2010	4700	1.18

[a]Determined by ^{1}H NMR. [b]Determined by CHCl$_3$ SEC analysis.

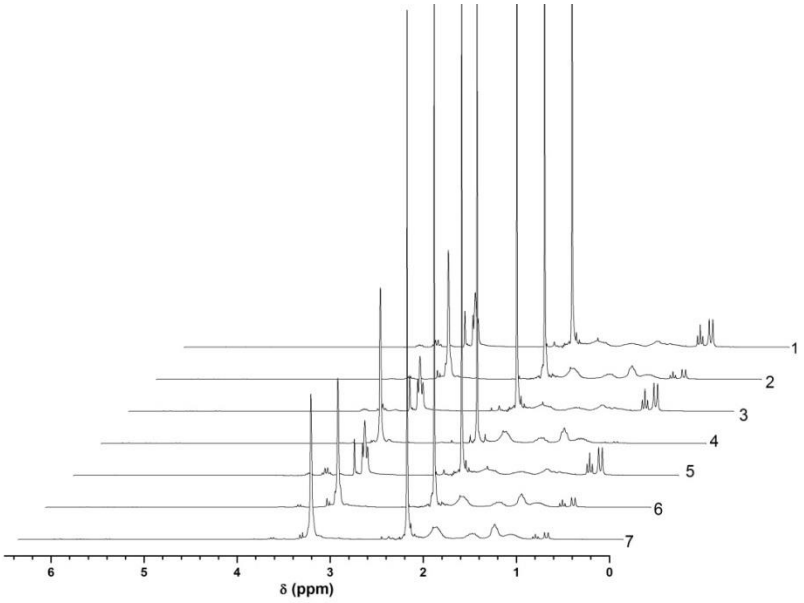

Figure 7.23: ^{1}H NMR spectra showing the monomer conversion for each cycle during synthesis of the pseudo heptablock homopolymer(DP_n=3) obtained from UV experiment: [MA]:[EBiB]:[$CuBr_2$]:[Me_6-Tren] = [2]:[1]:[0.02]:[0.12] in DMSO. *No additional $CuBr_2$/Me_6-Tren were added.*

Table 7.4: Characterisation data for the synthesis of the nonablock homopolymer obtained from UV experiment. Initial feed ratio = [MA]:[EBiB]:[$CuBr_2$]:[Me_6-Tren] = [3]:[1]:[0.02]:[0.12] in DMSO. *No additional solvent was added upon every 2nd iterative addition.*

Cycle	Multiblock copolymer composition	Time (h)	Monomer conversion[a] (%)	$M_{n,th}$ [g mol^{-1}]	$M_{n,SEC}$[b] [g mol^{-1}]	$Đ$
1	Poly(MA_3)	12	100	450	260	1.26
2	Poly(MA_3-MA_3)	12	100	710	650	1.23
3	Poly(MA_3-MA_3-MA_3)	12	100	970	1200	1.20
4	Poly(MA_3-MA_3-MA_3-MA_3)	12	100	1230	1800	1.18
5	Poly(MA_3-MA_3-MA_3-MA_3-MA_3)	12	100	1500	2400	1.12
6	Poly(MA_3-MA_3-MA_3-MA_3-MA_3-MA_3)	12	99	1750	3400	1.10
7	Poly(MA_3-MA_3-MA_3-MA_3-MA_3- MA_3-MA_3)	12	99	2010	5100	1.15
8	Poly(MA_3-MA_3-MA_3-MA_3-MA_3- MA_3-MA_3-MA_3)	12	99	2270	6100	1.33
9	Poly(MA_3-MA_3-MA_3-MA_3-MA_3- MA_3-MA_3-MA_3-MA_3)	14	95	2530	8000	1.35

[a]Determined by ^{1}H NMR. [b]Determined by $CHCl_3$ SEC analysis.

Table 7.5: Characterisation data for the synthesis of the pseudo nonablock copolymer (DP_n=3) obtained from UV experiment. Initial feed ratio = [MA]:[EBiB]:[$CuBr_2$]:[Me_6-Tren] = [3]:[1]:[0.02]:[0.12] in DMSO. Additional [$CuBr_2$]:[Me_6-Tren] =[0.02]:[0.12], was added together with the monomer *upon every 4th addition.*

Cycle	Multiblock copolymer composition	Time (h)	Monomer conversion[a] (%)	$M_{n,th}$ [g mol^{-1}]	$M_{n,SEC}$[b] [g mol^{-1}]	$Đ$
1	Poly(MA_3)	12	>99	450	180	1.30
2	Poly(MA_3-MA_3)	12	>99	710	610	1.23
3	Poly(MA_3-MA_3-MA_3)	12	97	970	1200	1.16
4	Poly(MA_3-MA_3-MA_3-MA_3)	15	96	1230	1800	1.16
5	Poly(MA_3-MA_3-MA_3-MA_3-MA_3)	12	95	1500	2800	1.09
6	Poly(MA_3-MA_3-MA_3-MA_3-MA_3-MA_3)	13	99	1750	4000	1.08
7	Poly(MA_3-MA_3-MA_3-MA_3-MA_3-MA_3-MA_3)	16	97	2010	6900	1.08
8	Poly(MA_3-MA_3-MA_3-MA_3-MA_3-MA_3-MA_3-MA_3)	24	96	2270	7900	1.09
9	Poly(MA_3-MA_3-MA_3-MA_3-MA_3-MA_3-MA_3-MA_3-MA_3)	48	50	2530	8400	1.09

[a]Determined by ^{1}H NMR. [b]Determined by $CHCl_3$ SEC analysis.

Table 7.6: Characterisation data for the synthesis of the dodecablock homopolymer obtained from UV experiment. Initial feed ratio = [MA]:[EBiB]:[$CuBr_2$]:[Me_6-Tren] = [3]:[1]:[0.02]:[0.12] in DMSO. *A fresh solution of [$CuBr_2$]:[Me_6-Tren] =[0.02]:[0.12], was added together with the monomer upon every 3rd addition.*

Cycle	Multiblock copolymer composition	Time (h)	Monomer conversion[a] (%)	$M_{n,th}$ [g mol^{-1}]	$M_{n,SEC}$[b] [g mol^{-1}]	$Đ$
1	Poly(MA_3)	12	>99	450	190	1.23
2	Poly(MA_3-MA_3)	12	>99	710	480	1.24
3	Poly(MA_3-MA_3-MA_3)	12	99	970	920	1.19
4	Poly(MA_3-MA_3-MA_3-MA_3)	12	>99	1230	1400	1.16
5	Poly(MA_3-MA_3-MA_3-MA_3-MA_3)	12	98	1500	1900	1.15
6	Poly(MA_3-MA_3-MA_3-MA_3-MA_3-MA_3)	12	99	1750	2800	1.13
7	Poly(MA_3-MA_3-MA_3-MA_3-MA_3-MA_3-MA_3)	12	99	2010	3600	1.13
8	Poly(MA_3-MA_3-MA_3-MA_3-MA_3-MA_3-MA_3-MA_3)	14	97	2270	4600	1.12
9	Poly(MA_3-MA_3-MA_3-MA_3-MA_3-MA_3-MA_3-MA_3-MA_3)	16	99	2530	5700	1.10
10	Poly(MA_3-MA_3-MA_3-MA_3-MA_3-MA_3-MA_3-MA_3-MA_3-MA_3)	17	98	2790	7100	1.19
11	Poly(MA_3-MA_3-MA_3-MA_3-MA_3-MA_3-MA_3-MA_3-MA_3-MA_3-MA_3)	24	98	3050	9000	1.20
12	Poly(MA_3-MA_3-MA_3-MA_3-MA_3-MA_3-MA_3-MA_3-MA_3-MA_3-MA_3-MA_3)	30	95	3310	11800	1.30

[a]Determined by ^{1}H NMR. [b]Determined by $CHCl_3$ SEC analysis.

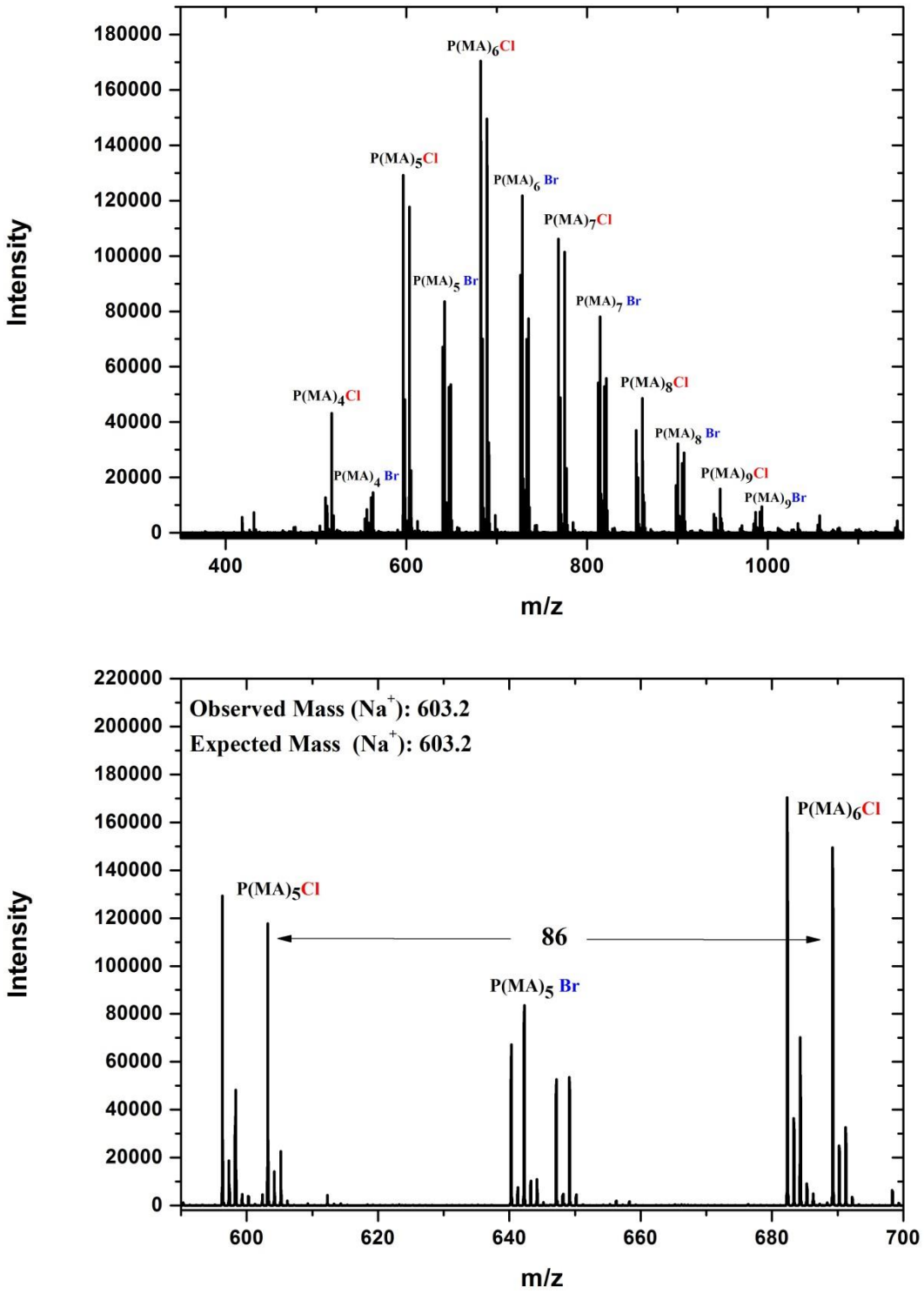

Figure 7.14: ESI-MS spectra of the 2nd block (top) obtained during the synthesis of dodecablock homopolymer (DP_n=3) in DMSO. Zoom of the same spectrum (bottom). *A fresh solution of [$CuBr_2$]:[Me_6-Tren] =[0.02]:[0.12], was added together with the monomer upon every 3rd addition.*

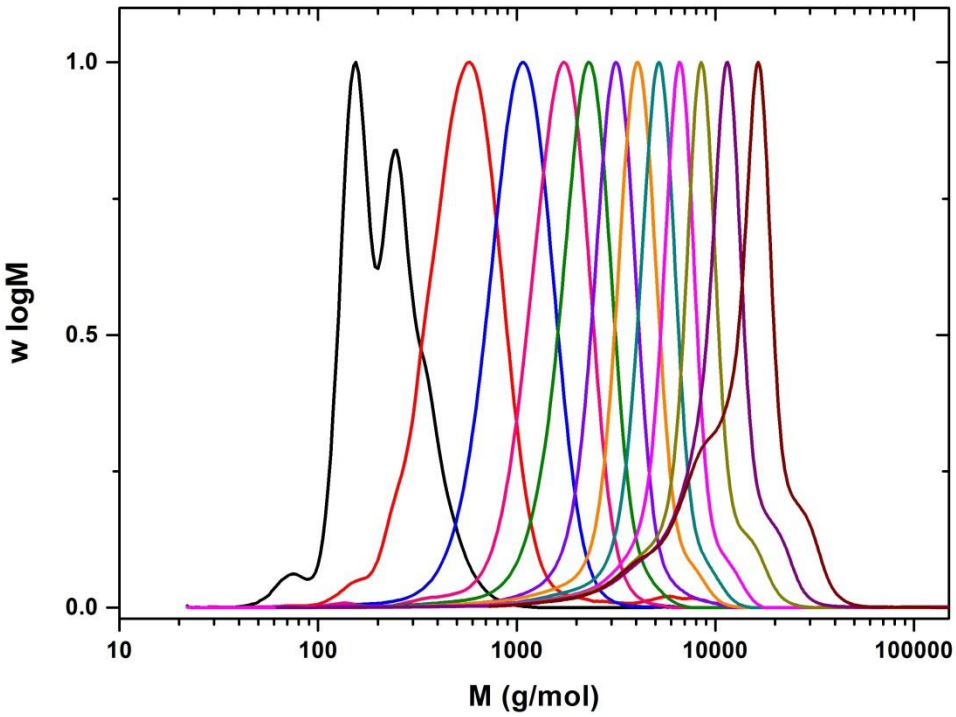

Figure 7.15: Molecular weight distributions for successive cycles during synthesis of dodecablock homopolymer (DP_n=3) in DMSO at ambient temperature. *A fresh solution of [$CuBr_2$]:[Me_6-Tren] =[0.02]:[0.12], was added together with the monomer upon every 3rd addition.*

Table 7.7: Characterisation data for the synthesis of decablock homopolymer obtained from UV experiment. Initial feed ratio = [MA]:[EBiB]:[$CuBr_2$]:[Me_6-Tren] = [3]:[1]:[0.02]:[0.12] in DMSO. *A fresh solution of [$CuBr_2$]:[Me_6-Tren] =[0.02]:[0.12], was added together with the monomer upon every 2nd addition.*

Cycle	Multiblock copolymer composition	Time (h)	Monomer conversion[a] (%)	$M_{n,th}$ [g mol^{-1}]	$M_{n,SEC}$[b] [g mol^{-1}]	Đ
1	Poly(MA_3)	12	100	450	180	1.26
2	Poly(MA_3-MA_3)	12	99	710	490	1.23
3	Poly(MA_3-MA_3-MA_3)	12	100	970	1000	1.18
4	Poly(MA_3-MA_3-MA_3-MA_3)	12	99	1230	1500	1.16
5	Poly(MA_3-MA_3-MA_3-MA_3-MA_3)	12	99	1500	2000	1.20
6	Poly(MA_3-MA_3-MA_3-MA_3-MA_3-MA_3)	12	97	1750	2800	1.22
7	Poly(MA_3-MA_3-MA_3-MA_3-MA_3-MA_3-MA_3)	12	96	2010	4000	1.18
8	Poly(MA_3-MA_3-MA_3-MA_3-MA_3-MA_3-MA_3-MA_3)	12	96	2270	4900	1.23
9	Poly(MA_3-MA_3-MA_3-MA_3-MA_3-MA_3-MA_3-MA_3-MA_3)	14	95	2530	5900	1.32
10	Poly(MA_3-MA_3-MA_3-MA_3-MA_3-MA_3-MA_3-MA_3-MA_3-MA_3)	24	89	2790	6200	1.59

[a]Determined by ^{1}H NMR. [b]Determined by $CHCl_3$ SEC analysis.

Table 7.8: Characterisation data for the synthesis of the triblock homopolymer obtained from UV experiment. Initial feed ratio = [MA]:[EBiB]:[$CuBr_2$]:[Me_6-Tren] = [3]:[1]:[0.02]:[0.12] in DMSO. *A fresh solution of [$CuBr_2$] = [0.02] was added together with the monomer upon every 2nd addition*

Cycle	Multiblock copolymer composition	Time (h)	Monomer conversion[a] (%)	$M_{n,th}$ [g mol^{-1}]	$M_{n,SEC}$[b] [g mol^{-1}]	Đ
1	Poly(MA_3)	12	99	450	200	1.23
2	Poly(MA_3-MA_3)	12	99	710	500	1.24
3	Poly(MA_3-MA_3-MA_3)	19	97	970	700	1.23
4	Poly(MA_3-MA_3-MA_3-MA_3)	48	0	970	700	1.23

. [a]Determined by ^{1}H NMR. [b]Determined by $CHCl_3$ SEC analysis.

Table 7.9: Characterisation data for the synthesis of the pentablock homopolymer obtained from UV experiment. Initial feed ratio = [MA]:[EBiB]:[$CuBr_2$]:[Me_6-Tren] = [3]:[1]:[0.02]:[0.12] in DMSO. *A fresh solution of [Me_6-Tren] = [0.12], was added together with the monomer upon every 2nd addition.*

Cycle	Multiblock copolymer composition	Time (h)	Monomer conversion[a] (%)	$M_{n,th}$ [g mol^{-1}]	$M_{n,SEC}$[b] [g mol^{-1}]	$Đ$
1	Poly(MA_3)	12	99	450	105	1.45
2	Poly(MA_3-MA_3)	12	99	710	355	1.34
3	Poly(MA_3-MA_3-MA_3)	12	99	970	680	1.25
4	Poly(MA_3-MA_3-MA_3-MA_3)	12	99	1230	1500	1.15
5	Poly(MA_3-MA_3-MA_3-MA_3-MA_3)	12	100	1500	1560	1.35

[a]Determined by ^{1}H NMR. [b]Determined by $CHCl_3$ SEC analysis.

Table 7.10: Characterisation data for the synthesis of the octablock homopolymer obtained from UV experiment. Initial feed ratio = [MA]:[EBiB]:[$CuBr_2$]:[Me_6-Tren] = [3]:[1]:[0.01]:[0.12] in DMSO. *A fresh solution of [$CuBr_2$]:[Me_6-Tren] =[0.01]:[0.12], was added together with the monomer upon every 3rd addition.*

Cycle	Multiblock copolymer composition	Time (h)	Monomer conversion[a] (%)	$M_{n,th}$ [g mol^{-1}]	$M_{n,SEC}$[b] [g mol^{-1}]	$Đ$
1	Poly(MA_3)	12	100	450	200	1.25
2	Poly(MA_3-MA_3)	12	99	710	500	1.24
3	Poly(MA_3-MA_3-MA_3)	12	100	970	900	1.23
4	Poly(MA_3-MA_3-MA_3-MA_3)	12	99	1230	1500	1.21
5	Poly(MA_3-MA_3-MA_3-MA_3-MA_3)	12	100	1500	2000	1.23
6	Poly(MA_3-MA_3-MA_3-MA_3-MA_3-MA_3)	12	99	1750	2500	1.29
7	Poly(MA_3-MA_3-MA_3-MA_3-MA_3- MA_3-MA_3)	13	98	2010	3500	1.22
8	Poly(MA_3-MA_3-MA_3-MA_3-MA_3- MA_3-MA_3-MA_3)	15	95	2270	3800	1.37

[a]Determined by ^{1}H NMR. [b]Determined by $CHCl_3$ SEC analysis.

Table 7.11: Characterisation data for the synthesis of the dodecablock copolymer obtained from UV experiment. Initial feed ratio = [MA]:[EBiB]:[$CuBr_2$]:[Me_6-Tren] = [3]:[1]:[0.02]:[0.12] in DMSO. *A fresh solution of [$CuBr_2$]:[Me_6-Tren] =[0.02]:[0.12], was added together with the monomer upon every 3rd addition.*

Cycle	Multiblock copolymer composition	Time (h)	Monomer conversion[a] (%)	$M_{n,th}$ [g mol^{-1}]	$M_{n,SEC}$[b] [g mol^{-1}]	$Đ$
1	Poly(MA_3)	12	99	450	144	1.17
2	Poly(MA_3-EA_3)	12	99	760	430	1.21
3	Poly(MA_3-EA_3-EGA_3)	12	98	1150	800	1.20
4	Poly(MA_3-EA_3-EGA_3-SA_3)	12	99	1700	1300	1.14
5	Poly(MA_3-EA_3-EGA_3-SA_3-EA_3)	12	98	2000	1800	1.15
6	Poly(MA_3-EA_3-EGA_3-SA_3-EA_3-EGA_3)	12	96	2400	2480	1.11
7	Poly(MA_3-EA_3-EGA_3-SA_3-EA_3-EGA_3-SA_3)	12	96	3000	3200	1.13
8	Poly(MA_3-EA_3-EGA_3-SA_3-EA_3-EGA_3-SA_3-EGA_3)	12	96	3400	4200	1.12
9	Poly(MA_3-EA_3-EGA_3-SA_3-EA_3-EGA_3-SA_3-EGA_3-EA_3)	15	97	3600	5400	1.11
10	Poly(MA_3-EA_3-EGA_3-SA_3-EA_3-EGA_3-SA_3-EGA_3-EA_3-SA_3)	19	99	4200	6600	1.12
11	Poly(MA_3-EA_3-EGA_3-SA_3-EA_3-EGA_3-SA_3-EGA_3-EA_3-SA_3-MA_3)	24	99	4500	7000	1.19
12	Poly(MA_3-EA_3-EGA_3-SA_3-EA_3-EGA_3-SA_3-EGA_3-EA_3-SA_3-MA_3-EGA_3)	48	92	4900	10000	1.39

[a]Determined by ^{1}H NMR. [b]Determined by $CHCl_3$ SEC analysis.

Scheme 7.2: Synthesis of **multiblock copolymers DP$_n$=10** by sequential addition of monomers without intermediate purification.

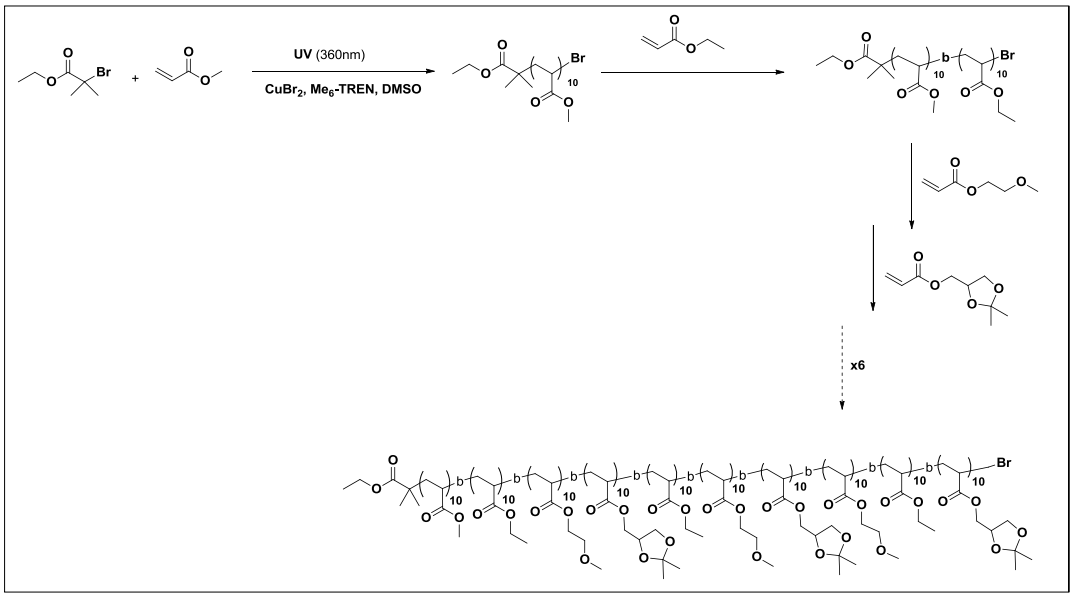

Table 7.12: Characterisation data for the synthesis of the octablock copolymer obtained from UV experiment. Initial feed ratio = [MA]:[EBiB]:[$CuBr_2$]:[Me_6-Tren] = [10]:[1]:[0.02]:[0.12] in DMSO. *A fresh solution of [$CuBr_2$]:[Me_6-Tren] =[0.02]:[0.12], was added together with the monomer upon every 3rd addition.*

Cycle	Multiblock copolymer composition	Time (h)	Monomer conversion[a] (%)	$M_{n,th}$ [g mol^{-1}]	$M_{n,SEC}$ [b] [g mol^{-1}]	$Đ$
1	Poly(MA_{10})	2	99	1060	600	1.24
2	Poly(MA_{10}-EA_{10})	6	99	2100	1500	1.15
3	Poly(MA_{10}-EA_{10}-EGA_{10})	12	100	3400	2300	1.15
4	Poly(MA_{10}-EA_{10}-EGA_{10}-SA_{10})	12	97	5200	3300	1.12
5	Poly(MA_{10}-EA_{10}-EGA_{10}-SA_{10}-EA_{10})	12	99	6200	4000	1.19
6	Poly(MA_{10}-EA_{10}-EGA_{10}-SA_{10}-EA_{10}-EGA_{10})	14	99	7600	5000	1.17
7	Poly(MA_{10}-EA_{10}-EGA_{10}-SA_{10}-EA_{10}-EGA_{10}-SA_{10})	16	98	9400	6000	1.15
8	Poly(MA_{10}-EA_{10}-EGA_{10}-SA_{10}-EA_{10}-EGA_{10}-SA_{10}-EGA_{10})	24	97	11200	8000	1.35

[a]Determined by ^{1}H NMR. [b]Determined by $CHCl_3$ SEC analysis.

Table 7.13: Characterisation data for the synthesis of the octablock copolymer obtained from UV experiment. Initial feed ratio = [MA]:[EBiB]:[$CuBr_2$]:[Me_6-Tren] = [10]:[1]:[0.02]:[0.12] in DMSO. *A fresh solution of [$CuBr_2$]:[Me_6-Tren] =[0.02]:[0.12], was added together with the monomer upon every 2nd addition.*

Cycle	Multiblock copolymer composition	Time (h)	Monomer conversion[a] (%)	$M_{n,th}$ [g mol^{-1}]	$M_{n,SEC}$[b] [g mol^{-1}]	$Đ$
1	Poly(MA_{10})	2	99	1060	880	1.17
2	Poly(MA_{10}-EA_{10})	6	99	2100	2000	1.12
3	Poly(MA_{10}-EA_{10}-EGA_{10})	12	100	3400	3400	1.09
4	Poly(MA_{10}-EA_{10}-EGA_{10}-SA_{10})	12	97	5200	4800	1.07
5	Poly(MA_{10}-EA_{10}-EGA_{10}-SA_{10}-EA_{10})	12	95	6200	6500	1.08
6	Poly(MA_{10}-EA_{10}-EGA_{10}-SA_{10}-EA_{10}-EGA_{10})	14	99	7600	8400	1.07
7	Poly(MA_{10}-EA_{10}-EGA_{10}-SA_{10}-EA_{10}-EGA_{10}-SA_{10})	16	98	9400	10200	1.11
8	Poly(MA_{10}-EA_{10}-EGA_{10}-SA_{10}-EA_{10}-EGA_{10}-SA_{10}-EGA_{10})	24	99	11200	12400	1.10

[a]Determined by ^{1}H NMR. [b]Determined by $CHCl_3$ SEC analysis.

Table 7.14: Characterisation data for the synthesis of the octablock copolymer obtained from UV experiment. Initial feed ratio = [MA]:[EBiB]:[$CuBr_2$]:[Me_6-Tren] = [10]:[1]:[0.02]:[0.12] in DMSO. *A fresh solution of [$CuBr_2$]:[Me_6-Tren] =[0.02]:[0.12], was added together with the monomer upon every addition.*

Cycle	Multiblock copolymer composition	Time (h)	Monomer conversion[a] (%)	$M_{n,th}$ [g mol^{-1}]	$M_{n,SEC}$[b] [g mol^{-1}]	$Đ$
1	Poly(MA_{10})	2	100	1060	700	1.22
2	Poly(MA_{10}-EA_{10})	6	100	2100	2000	1.17
3	Poly(MA_{10}-EA_{10}-EGA_{10})	12	100	3400	3800	1.10
4	Poly(MA_{10}-EA_{10}-EGA_{10}-SA_{10})	12	99	5200	5200	1.13
5	Poly(MA_{10}-EA_{10}-EGA_{10}-SA_{10}-EA_{10})	12	97	6200	8000	1.11
6	Poly(MA_{10}-EA_{10}-EGA_{10}-SA_{10}-EA_{10}-EGA_{10})	14	99	7600	11500	1.05
7	Poly(MA_{10}-EA_{10}-EGA_{10}-SA_{10}-EA_{10}- EGA_{10}-SA_{10})	16	97	9400	10800	1.29
8	Poly(MA_{10}-EA_{10}-EGA_{10}-SA_{10}-EA_{10}- EGA_{10}-SA_{10}-EGA_{10})	24	99	11200	15900	1.36

[a]Determined by ^{1}H NMR. [b]Determined by $CHCl_3$ SEC analysis.

Table 7.15: Characterisation data for the synthesis of the octablock copolymer obtained from UV experiment. Initial feed ratio = [MA]:[EBiB]:[$CuBr_2$]:[Me_6-Tren] = [10]:[1]:[0.01]:[0.12] in DMSO. *A fresh solution of [$CuBr_2$]:[Me_6-Tren] =[0.01]:[0.12], was added together with the monomer upon every addition.*

Cycle	Multiblock copolymer composition	Time (h)	Monomer conversion[a] (%)	$M_{n,th}$ [g mol^{-1}]	$M_{n,SEC}$[b] [g mol^{-1}]	$Đ$
1	Poly(MA_{10})	2	100	1060	800	1.19
2	Poly(MA_{10}-EA_{10})	6	99	2100	1800	1.19
3	Poly(MA_{10}-EA_{10}-EGA_{10})	12	100	3400	3500	1.11
4	Poly(MA_{10}-EA_{10}-EGA_{10}-SA_{10})	12	99	5200	4600	1.15
5	Poly(MA_{10}-EA_{10}-EGA_{10}-SA_{10}-EA_{10})	12	97	6200	7100	1.12
6	Poly(MA_{10}-EA_{10}-EGA_{10}-SA_{10}-EA_{10}-EGA_{10})	14	99	7600	10000	1.10
7	Poly(MA_{10}-EA_{10}-EGA_{10}-SA_{10}-EA_{10}-EGA_{10}-SA_{10})	16	99	9400	10500	1.32
8	Poly(MA_{10}-EA_{10}-EGA_{10}-SA_{10}-EA_{10}-EGA_{10}-SA_{10}-EGA_{10})	24	99	11200	14000	1.36

[a]Determined by ^{1}H NMR. [b]Determined by $CHCl_3$ SEC analysis.

Scheme 7.3: Synthesis of **multiblock copolymers DP$_n$=25** by sequential addition of monomers without intermediate purification.

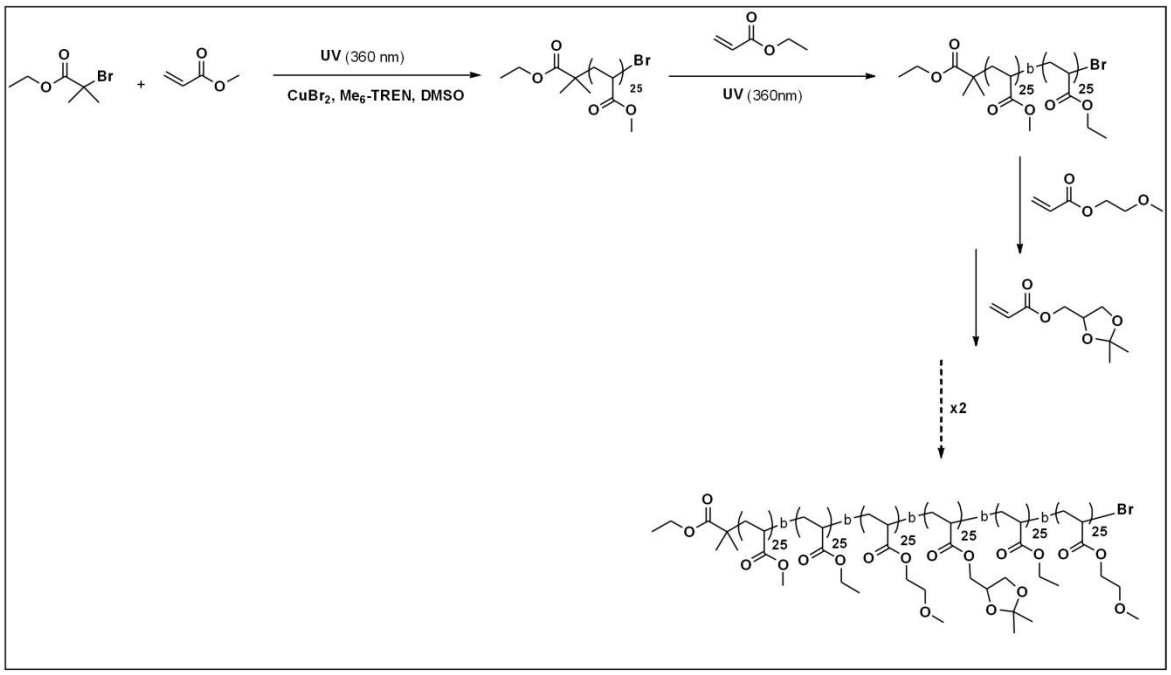

Table 7.16: Characterisation data for the synthesis of the hexablock copolymer obtained from UV experiment. Initial feed ratio = [MA]:[EBiB]:[$CuBr_2$]:[Me_6-Tren] = [25]:[1]:[0.02]:[0.12] in DMSO at ambient temperature. *A fresh solution of [$CuBr_2$]:[Me_6-Tren] =[0.02]:[0.12], was added together with the monomer upon every 2nd addition.*

Cycle	Multiblock copolymer composition	Time (h)	Monomer conversion[a] (%)	$M_{n,th}$ [g mol^{-1}]	$M_{n,SEC}$[b] [g mol^{-1}]	$Đ$
1	Poly(MA_{25})	2	99	2400	2600	1.14
2	Poly(MA_{25}-EA_{25})	4	99	4900	6000	1.06
3	Poly(MA_{25}-EA_{25}-EGA_{25})	7	98	8200	9500	1.05
4	Poly(MA_{25}-EA_{25}-EGA_{25}-SA_{25})	8	99	12700	13000	1.05
5	Poly(MA_{25}-EA_{25}-EGA_{25}-SA_{25}-EA_{25})	12	97	15200	16600	1.08
6	Poly(MA_{25}-EA_{25}-EGA_{25}-SA_{25}-EA_{25}-EGA_{25})	20	99	18200	19900	1.15

[a]Determined by ^{1}H NMR. [b]Determined by $CHCl_3$ SEC analysis.

Scheme 7.4: Synthesis of **multiblock copolymers DP$_n$=100** by sequential addition of monomers without intermediate purification.

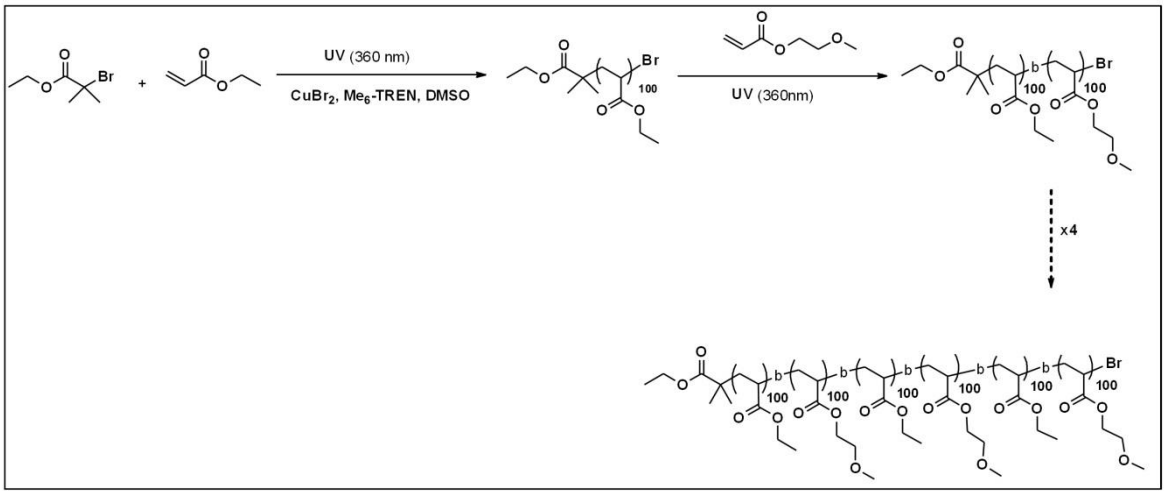

Table 7.17: Characterisation data for the synthesis of the hexablock copolymer obtained from UV experiment. Initial feed ratio = [MA]:[EBiB]:[$CuBr_2$]:[Me_6-Tren] = [100]:[1]:[0.02]:[0.12] in DMSO. *A fresh solution of [$CuBr_2$]:[Me_6-Tren] =[0.02]:[0.12], was added together with the monomer upon every 2nd addition.*

Cycle	Multiblock copolymer composition	Time (h)	Monomer conversion[a] (%)	$M_{n,th}$ [g mol^{-1}]	$M_{n,SEC}$[b] [g mol^{-1}]	$Đ$
1	Poly(EA_{100})	3	98	10200	9600	1.05
2	Poly(EA_{100}-$OEGMA_{100}$)	8	99	23200	21000	1.08
3	Poly(EA_{100}-$OEGMA_{100}$-EA_{100})	12	98	33200	37000	1.17
4	Poly(EA_{100}-$OEGMA_{100}$-EA_{100}-$OEGMA_{100}$)	15	99	46200	52000	1.18
5	Poly(EA_{100}-$OEGMA_{100}$-EA_{100}-$OEGMA_{100}$- EA_{100})	24	97	56200	80000	1.21
6	Poly(EA_{100}-$OEGMA_{100}$-EA_{100}-$OEGMA_{100}$- EA_{100})	48	85	59200	102000	1.33

[a]Determined by ^{1}H NMR. [b]Determined by $CHCl_3$ SEC analysis.

7.5 References

1. G. Moad, E. Rizzardo and S. H. Thang, *Aust. J. Chem.*, 2012, **65**, 985-1076.
2. C. J. Hawker, A. W. Bosman and E. Harth, *Chem. Rev.*, 2001, **101**, 3661-3688.
3. M. Kato, M. Kamigaito, M. Sawamoto and T. Higashimura, *Macromolecules*, 1995, **28**, 1721-1723.
4. J.-S. Wang and K. Matyjaszewski, *J. Am. Chem. Soc.*, 1995, **117**, 5614-5615.
5. D. M. Haddleton, C. B. Jasieczek, M. J. Hannon and A. J. Shooter, *Macromolecules*, 1997, **30**, 2190-2193.
6. V. Percec, T. Guliashvili, J. S. Ladislaw, A. Wistrand, A. Stjerndahl, M. J. Sienkowska, M. J. Monteiro and S. Sahoo, *J. Am. Chem. Soc.*, 2006, **128**, 14156-14165.
7. B. M. Rosen and V. Percec, *Chem. Rev.*, 2009, **109**, 5069-5119.
8. N. Badi and J.-F. Lutz, *Chem. Soc. Rev.*, 2009, **38**, 3383-3390.
9. M. Ouchi, N. Badi, J.-F. Lutz and M. Sawamoto, *Nat. Chem.*, 2011, **3**, 917-924.
10. J.-F. Lutz, M. Ouchi, D. R. Liu and M. Sawamoto, *Science*, 2013, **341**, 628-637.
11. M. Ouchi, T. Terashima and M. Sawamoto, *Chem. Rev.*, 2009, **109**, 4963-5050.
12. M. Minoda, M. Sawamoto and T. Higashimura, *Macromolecules*, 1990, **23**, 4889-4895.

13. J.-F. Lutz, *Polym. Chem.*, 2010, **1**, 55-62.
14. J. Vandenbergh, G. Reekmans, P. Adriaensens and T. Junkers, *Chem. Commun.*, 2013, **49**, 10358-10360.
15. K. Nakatani, T. Terashima and M. Sawamoto, *J. Am. Chem. Soc.*, 2009, **131**, 13600-13601.
16. K. Nakatani, Y. Ogura, Y. Koda, T. Terashima and M. Sawamoto, *J. Am. Chem. Soc.*, 2012, **134**, 4373-4383.
17. R. McHale, J. P. Patterson, P. B. Zetterlund and R. K. O'Reilly, *Nat. Chem.*, 2012, **4**, 491-497.
18. A. H. Soeriyadi, C. Boyer, F. Nyström, P. B. Zetterlund and M. R. Whittaker, *J. Am. Chem. Soc.*, 2011, **133**, 11128-11131.
19. C. Boyer, A. Derveaux, P. B. Zetterlund and M. R. Whittaker, *Polym. Chem.*, 2012, **3**, 117-123.
20. C. Boyer, A. H. Soeriyadi, P. B. Zetterlund and M. R. Whittaker, *Macromolecules*, 2011, **44**, 8028-8033.
21. Q. Zhang, A. Anastasaki, G.-Z. Li, A. J. Haddleton, P. Wilson and D. M. Haddleton, *Polym. Chem.*, 2014, **5**, 3876-3883.
22. Q. Zhang, J. Collins, A. Anastasaki, R. Wallis, D. A. Mitchell, C. R. Becer and D. M. Haddleton, *Angew. Chem., Int. Ed.*, 2013, **52**, 4435-4439.
23. A. Anastasaki, C. Waldron, P. Wilson, C. Boyer, P. B. Zetterlund, M. R. Whittaker and D. Haddleton, *ACS Macro Lett.*, 2013, **2**, 896-900.
24. P. B. Zetterlund, G. Gody and S. Perrier, *Macromol. Theory Simul.*, 2014, **23**, 331-339.
25. G. Gody, T. Maschmeyer, P. B. Zetterlund and S. Perrier, *Macromolecules*, 2014, **47**, 3451-3460.
26. G. Gody, T. Maschmeyer, P. B. Zetterlund and S. Perrier, *Macromolecules*, 2014, **47**, 639-649.
27. G. Gody, T. Maschmeyer, P. B. Zetterlund and S. Perrier, *Nat. Commun.*, 2013, **4**, 2505-2514
28. B. P. Fors and C. J. Hawker, *Angew. Chem., Int. Ed.*, 2012, **51**, 8850-8853.
29. J. Xu, K. Jung, A. Atme, S. Shanmugam and C. Boyer, *J. Am. Chem. Soc.*, 2014, **136**, 5508-5519.
30. A. Anastasaki, V. Nikolaou, Q. Zhang, J. Burns, S. R. Samanta, C. Waldron, A. J. Haddleton, R. McHale, D. Fox, V. Percec, P. Wilson and D. M. Haddleton, *J. Am. Chem. Soc.*, 2013, **136**, 1141-1149.
31. J. A. Burns, C. Houben, A. Anastasaki, C. Waldron, A. A. Lapkin and D. M. Haddleton, *Polym. Chem.*, 2013, **4**, 4809-4813.

32. A. Anastasaki, V. Nikolaou, A. Simula, J. Godfrey, M. Li, G. Nurumbetov, P. Wilson and D. M. Haddleton, *Macromolecules*, 2014, **47**, 3852-3859.
33. D. M. Haddleton, A. M. Heming and D. Kukulj, *Chem. Commun.*, 1998, **16**, 1719-1720.
34. A. Anastasaki, C. Waldron, P. Wilson, R. McHale and D. M. Haddleton, *Polym. Chem.*, 2013, **4**, 2672-2675.
35. A. O. Moughton, M. A. Hillmyer and T. P. Lodge, *Macromolecules*, 2011, **45**, 2-19.
36. G. Pasparakis, N. Krasnogor, L. Cronin, B. G. Davis and C. Alexander, *Chem. Soc. Rev.*, 2010, **39**, 286-300.
37. J. Rodríguez-Hernández, F. Chécot, Y. Gnanou and S. Lecommandoux, *Prog. Polym. Sci.*, 2005, **30**, 691-724.

Chapter 8

Conclusions and Future Outlook

The aim of this work was initially to investigate the potential of Cu(0)-mediated living radical polymerisation and push the system to its limits in order to maximise the livingness, as manifested by high end-group fidelity.

Initially, the ligand and the catalyst concentration had to be optimised in order to suppress termination and side reactions, such as chain transfer, bimolecular termination and quarternisation. Very hydrophobic monomers such as lauryl acrylate were found to be compatible with SET-LRP conditions when the solvent was carefully tuned, presenting very high end-group functionality which allowed successful post-polymerisation modifications. Exploiting this high livingness even at quantitative monomer conversion, high molecular weight multiblock copolymers were subsequently synthesised presenting narrow dispersity values and good agreement between theoretical and experimental molecular weight. Although a well-defined hexablock homopolymer was successfully obtained, the technique could not be successfully extended to different monomers.

In the second part of this thesis, the photo-induced living radical polymerisation of acrylates in the absence of conventional photoinitiators or dye sensitisers has been realised in "daylight" and is enhanced upon irradiation with UV radiation (λ_{max} ~ 360 nm). In the presence of low concentrations of copper(II) bromide and an aliphatic tertiary ligand (Me_6-Tren), near-quantitative monomer conversion (>95%) was obtained within 80 min, yielding poly(acrylates) with dispersities as low as 1.05 and excellent end-group fidelity (<99%). The versatility of the technique was demonstrated by polymerisation of methyl acrylate to a range of chain lengths (DP_n = 25-800), and a number of (meth)acrylate

monomers including macromonomer poly(ethylene glycol) methyl ether acrylate ($PEGA_{480}$), tert-butyl acrylate (*t*BA) and methyl methacrylate (MMA), as well as styrene (Sty). Moreover, hydroxyl and *vic*-diol functional initiators were shown to be compatible with the polymerisation conditions, forming *α*,*ω*-heterofunctional poly(acrylates) with unparalleled efficiency and control. The control retained during polymerisation was confirmed by MALDI-ToF-MS and exemplified by *in situ* chain extension upon sequential monomer addition, furnishing higher molecular weight polymers with an observed reduction in dispersity ($Đ$ = 1.03). Similarly, efficient one-pot diblock copolymerisation by sequential addition of ethylene glycol methyl ether acrylate (EGA) and $PEGA_{480}$ to a poly(methyl) acrylate (PMA) macroinitiator without prior work-up or purification is also presented. Minimal polymerisation in the absence of light confers temporal control and suggests potential application at one of the frontiers of material chemistry, whereby precise spatiotemporal control "on/off" control and resolution is desirable. The scope of this technique was subsequently expanded to include more monomers and solvents but also to identify the limitations of the system.

Finally, the high end-group fidelity obtained *via* this polymerisation protocol was utilised in order to synthesise multiblock acrylic copolymers in a one-pot polymerisation reaction. Four different acrylic monomers were alternated in various combinations within the polymer composition illustrating the potential of the technique. Narrow disperse undecablock copolymers were obtained ($Đ$ < 1.20) with quantitative conversions being achieved between the iterative monomer additions. The effect of chain length was also investigated allowing for higher molecular weight multiblock copolymers to be obtained. This approach offers a versatile and inexpensive platform for the preparation of high-order multiblock functional materials with additional applications arising from the precise spatiotemporal "on/off" control and resolution when desired.

The current status of copper-mediated living radical polymerisation enables us to design and synthesise functional materials in various architectures and compositions. We now look to apply these protocols to more biologically relevant systems. For instance, we can fine tune the sequences of sugars in glycopolymers evaluating their binding efficiency and immunogenicity. Alternatively, we envisage directing these domains to self-assemble into well-defined highly-ordered structures with precise size and shape, capable of expressing chemical functionality to fulfil a predefined purpose. The possibilities are really endless and we are limited only by our own imagination.